UNIVERSITY OF COPENHAGEN
FACULTY OF HEALTH AND MEDICAL SCIENCES

Epigenetic and gene expression profiling of the human ovarian follicles with the significance of age and ovarian reserve

PhD thesis by Kristina Wendelboe Olsen

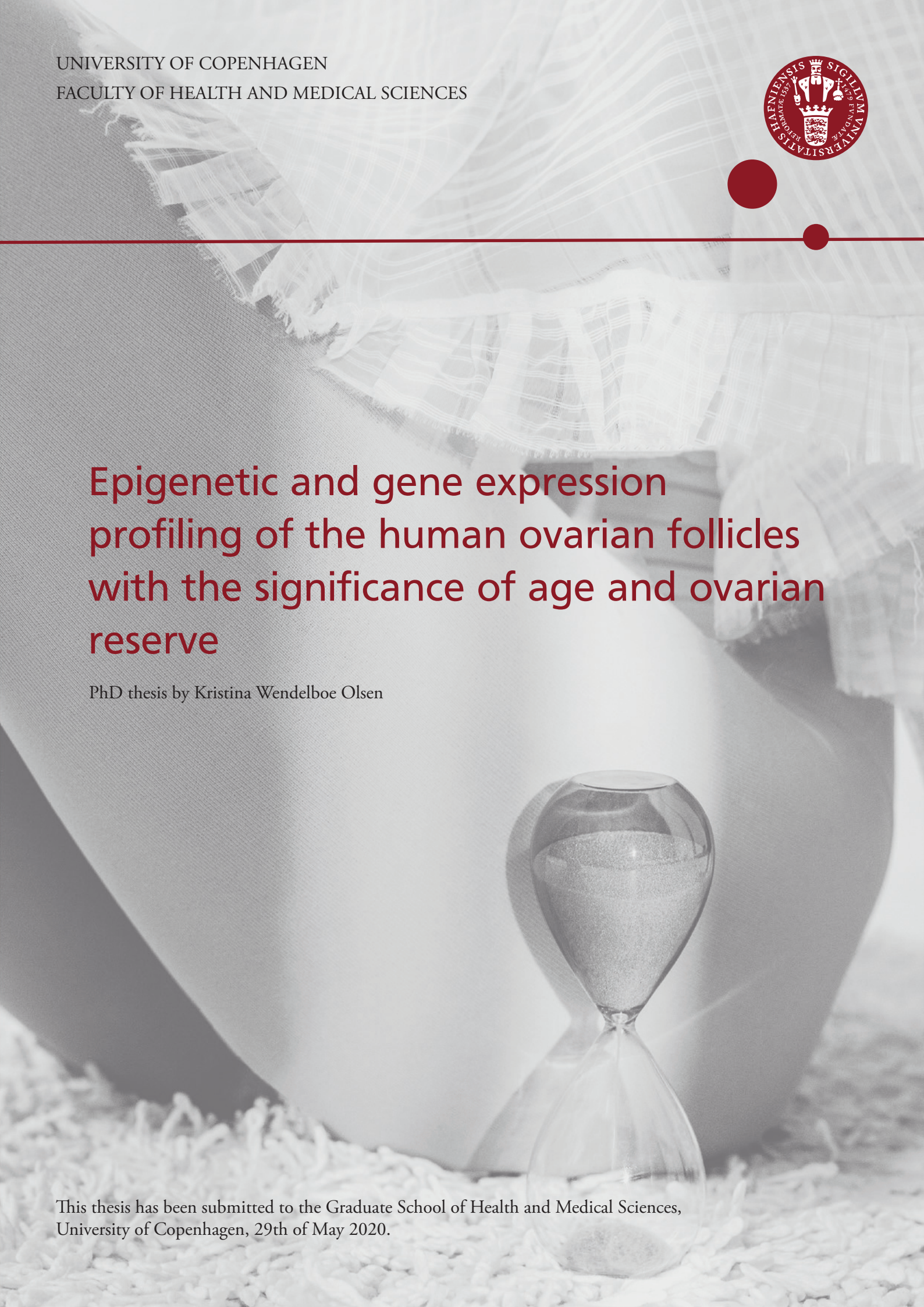

This thesis has been submitted to the Graduate School of Health and Medical Sciences, University of Copenhagen, 29th of May 2020.

Department of Obstetrics and Gynaecology, Copenhagen University Hospital, Herlev,
Borgmester Ib Juuls Vej 9, 2730 Herlev, Denmark.
E-mail: kristina.wendelboe.olsen.01@regionh.dk, kwo@sund.ku.dk, kristinawo@hotmail.com

Photographer
www.miajorgensen.com

This thesis is dedicated to the memory of

a brilliant scientist and loving person,

Agnieszka K. Warzecha,

who I started this journey with.

I will never forget you.

Author

Kristina Wendelboe Olsen, MSc
Fertility Clinic, Department of Obstetrics and Gynaecology
Copenhagen University Hospital Herlev, Denmark

DNRF Center for Chromosome Stability
Department of Cellular and Molecular Medicine
Faculty of Health and Medical Sciences
University of Copenhagen, Denmark

Academic Supervisors

Marie Louise Grøndahl, PhD, DMSc
Fertility Clinic, Department of Obstetrics and Gynaecology
Copenhagen University Hospital Herlev, Denmark.

Professor **Eva R. Hoffmann,** PhD
DNRF Center for Chromosome Stability
Department of Cellular and Molecular Medicine
Faculty of Health and Medical Sciences
University of Copenhagen, Denmark.

Rehannah Borup Helweg-Larsen, MSc, PhD
DNRF Center for Chromosome Stability
Department of Cellular and Molecular Medicine
Faculty of Health and Medical Sciences
University of Copenhagen, Denmark.

Professor **Sven O. Skouby,** MD, DMSc
Fertility Clinic, Department of Obstetrics and Gynaecology
Copenhagen University Hospital Herlev, Denmark.

Department of Clinical Medicine
Faculty of Health and Medical Sciences
University of Copenhagen, Copenhagen, Denmark.

Assessment committee

Associate Professor **Morten Scheibye-Knudsen,** MD**,** DMSc
Center for Healthy Aging
Department of Cellular and Molecular Medicine
Faculty of Health and Medical Sciences
University of Copenhagen, Denmark.

Associate Professor **Anders Lade Nielsen,** MSc, PhD
Department of Biomedicine, Faculty of Health
Aarhus University, Denmark.

Professor **Stephen Franks,** MD, FRCP, FMedSci
Faculty of Medicine, Department of Metabolism, Digestion and Reproduction
Imperial College London, United Kingdom.

Preface

This thesis is based on research conducted at the Fertility Clinic at Herlev Hospital and at the Center for Chromosome Stability at the University of Copenhagen between March 2016 and May 2020. During this period, I was employed at the Department of Obstetrics and Gynaecology, Herlev Hospital, and a member of the Hoffmann group at Center for Chromosome Stability, University of Copenhagen, which specifically works with chromosome dynamics in germline. I was enrolled as a PhD student at the Graduate School of Cellular and Genetic Medicine, University of Copenhagen.

The study is part of the ReproUnion program, supported by the Interreg program for Øresund-Kattegat-Skagerak, which was supported by EU funds, the Capital Region of Denmark, Region Zealand, Region Skåne and Ferring Pharmaceutical Company. In addition, the study is supported by the Department of Obstetrics and Gynaecology at Herlev Hospital and the Danish National Research Foundation (DNRF) along with the Center for Chromosome Stability.
The funders had no role in the study design, data collection, data interpretation or reporting.

"*Even miracles take a little time.*"
- Cinderella's Fairy Godmother

Table of content

Acknowledgement

My four years engagement to this PhD study has been a life-changing experience and I would like to thank the people who have helped and contributed to the work, resulting in this thesis. I also want to express my gratitude for getting the opportunity to do a PhD project within the area of reproduction.

First, I would like to thank my supervisors, Marie Louise Grøndahl, Rehannah Borup-Helweg Larsen and Professor Sven O. Skouby for believing in me and giving me the opportunity to do this exciting project after only a short job interview back in January 2016. Marie Louise, thank you for being a great inspiration and for our many (many) meetings. I have learned a lot from you and admire you immensely (both as a person and a scientist). Thanks to you and Christian for opening your home in Cambridge to me, when I was working at Babraham Institute for three weeks in 2017. Rehannah, thank you for good advices and discussions regarding scientific and private matters and for opening my eyes to the importance of bioinformatics. Thank you for always being understanding; it has been a pleasure to accompany you at our journey at CCS. Marie Louise and Rehannah, I hope I still can be part of some of your frequent coffee meetings. Sven, thank you for your academic guidance and for facilitating the possibilities for my research. I would also like to thank my supervisor Professor Eva R. Hofmann, which lab I joined in January 2017. I have learned so much from you regarding science but also about life and how to balance it. You are a great inspiration and I admire your drive and courage, and your fight for women in science. I am truly honoured to be working with all four of you.

I thank the ReproUnion, the Department of Obstetrics and Gynaecology, Herlev Hospital and Center for Chromosome Stability (CCS), University of Copenhagen for funding this project.

Furthermore, I extend my gratitude to former and present employees at the Fertility Clinic at Herlev Hospital and to members of the Hoffmann group at CCS. A special thanks to Malene Fynbo, Hanne Udengaard and Mette Villads Nielsen for helping me with the recruitment of participants and collection of samples. Another special thanks to Vallari Shukla, Ajuna Azad, Amruta Shrikhande and Andy Chi Ho Chan for helping me with practical and scientific matters. Particularly, I want to express my appreciation and thank Jenny Gruhn for reviewing this thesis. Thank you, Miya Kudo Høffding, for our many talks about life in science and life in general.

Thanks to Gavin Kelsey for letting me be a part of your lab at Babraham Institute and for our continuing collaboration. Thanks to Erika Herrera, who kindly helped me in the lab and included me in the social things.

Thanks to Juan Castillo Fernandez for a close collaboration on our methylation manuscripts. You have been patient with my never-ending flow of questions about bioinformatics.

I also would like to thank former and present PhD students from Runddyssen 13. We have indeed had many unforgettable moments in our little house. A special thanks to Maria Buhl Borgstrøm for many talks in our small kitchen. You have made my last year as a PhD student much more fun and I have enjoyed all your good advice and support. Also, a special thanks to my PhD buddy Agnieszka K. Warzecha, who this thesis is dedicated to. She was the most inspiring, generous and kind person, I have ever known.

Thank you Mia Linnea Jørgensen for making the beautiful cover photo for this thesis.

Finally, I would like to thank all my family and friends. You have been my door to the outside world in busy times and reminded me of what is important in life. Thank you for always being there for me. However, I also want to apologies all my female friends, which I might have caused any stress with facts about female reproductive ageing from time to time.
A great thanks to my parents who have helped taking care of my children in busy times. A special thanks to my sister Rebecca who, as the only other scientist in our family, has been listening to many frustrations and worries, but also sharing my enthusiasm, when even small things succeed. My deepest thank to the love of my life, my husband Jón, who always believed in me. I cannot describe how lucky I feel I am; to have your support and love. I am so grateful that you always have been ready to listen to me babble on about my project, even though you are not into science. And thank you for taking so good care of our children, when I have been away. Arthúr and Sóllilja, I love you.

Frederiksberg, 2020
Kristina Wendelboe Olsen

Manuscripts

This thesis is based on the following manuscripts:

Paper I

K. W. Olsen, J. Castillo-Fernandez, A. Zedeler, N. C. Freiesleben, M. Bungum, A. C. Chan, A. Cardona, J. R. B. Perry, S. O. Skouby, R. Borup, E. R. Hoffmann, G. Kelsey[3,9], M. L. Grøndahl. **A distinctive epigenetic ageing profile in human granulosa cells.** *Accepted by Human Reproduction the 17th of March 2020.*

Paper II

K. W. Olsen, J. Castillo-Fernandez, A. C. Chan, N. C. Freiesleben, A. Zedeler, M. Bungum, A. Cardona, J. R. B. Perry, S. O. Skouby, R. Borup, E. R. Hoffmann, G. Kelsey, M. L. Grøndahl. **Identification of a unique epigenetic profile in women with diminished ovarian reserve.** *Submitted to Fertility and Sterility the 20th of May 2020.*

Paper III

K. W. Olsen, V. Shukla, A. Azad, S. O. Skouby, M. L. Grøndahl, R. Borup, E. R. Hoffmann. **Gene expression profile of human metaphase II oocytes in relation to age by single cell RNA sequencing.** *In preparation.*

No conflict of interest is declared by the authors of the included manuscripts.

During my PhD study, I also co-authored the following manuscripts:

L. Borgwardt, K. W. Olsen, M. Rossing, R. Borup Helweg-Larsen, M. Toftager, A. Pinborg, J. Bogstad, K. Løssl, A. Zedeler, M.L. Grøndahl. **Rare genetic variants suggest dysregulation of signaling pathways in low and high-risk patients developing severe ovarian hyperstimulation syndrome.** *Submitted to Journal of Assisted Reproduction and Genetics.*

K. W. Olsen, J. Gruhn, E. R. Hoffmann, M. L. Grøndahl. **Processing of single human IVF/IVM oocytes for RNA sequencing.** *Protocol Exchange*. *Published online May 2020.*

Abbreviations

5-mc	5-methylcytosine
AMH	Anti-Müllerian hormone
ART	Assisted reproductive technology
ATP	Adenosine triphosphate
bFGF	Basic fibroblast growth factor
BMP	Bone morphogenetic protein
CpG	Cytosine-phosphate-guanine
DMRs	Differentially methylation regions
DNAmTL	DNA methylation-based telomere length predictor
DOR	Diminished ovarian reserve
EDTA	Ethylenediaminetetraacetic acid
EGF	Epidermal growth factor
eIF4E	Eukaryotic translation initiation
ELOVL2	ELOVL fatty acid elongase 2
ERK5	Extracellular signal regulated kinase 5
ESR1	Oestrogen receptor 1
FDR	False discovery rate
FGF-2	Fibroblast growth factor 2
FHL2	Four and a half LIM domains 2
FMR1	Fragile X mental retardation 1
FOX12	Forkhead box 12
FOXL2	Forkhead box protein L2
FOXO	Forkhead box
FSH	Follicle stimulating hormone
FSHR	Follicle stimulating hormone receptor
GDF9	Growth differential factor 9
GnRH	Gonadotrophin-releasing hormone
GV	Germinal vesicle
ICSI	intracytoplasmic sperm injection
IL-6	Interleukin 6
IL-β	Interleukin 1 beta
IVF	In vitro fertilisation
KGF	Keratinocyte growth factor
LH	Luteinizing hormone
LIF	Leukemia inhibitory factor
MAR	Medically assisted reproduction
MI	Metaphase I
MII	Metaphase II
OA-1	Ocular albinism type 1
P27	Cyclin-dependent kinase inhibitor 27
PCOS	Polycystic ovary syndrome
PCR	Polymerase chain reaction
PENK	Proenkephalin
PTEN	Phosphatase and tensin homolog
scRNA-seq	Single cell RNA sequencing
SLC38A3	Solute carrier family 38 member 3
SNP	Single nucleotide polymorphism
TGF-β	Transforming growth factor beta
TNF-α	Tumour necrosis factor alpha
TORC1	CREB regulated transcription coactivator 1
WGBS	Whole-genome bisulfite sequencing

English summary

Advanced reproductive age is a major risk factor for infertility, pregnancy loss and children born with congenital diseases. This is mainly due to an increasing number of abnormal chromosomes numbers (aneuploidies) in the oocytes with increasing age. Why women have a decreasing fertility with advanced reproductive age and why, unlike other species, women lose their fertility completely, when entering menopause, are not fully understood.

One of the hallmarks of ageing is epigenetic alterations, which includes alterations in DNA methylation. Data from methylation arrays have shown that some tissue types have an accelerated epigenetic age compared with the chronological age of the tissue. Whether the human ovarian follicles have a different epigenetic profile, and whether there exists underlying epigenetic mechanism of the female reproductive function remains to be fully elucidated.

The aim of the present PhD project was to describe the DNA methylation profile of the human ovarian follicle cells (mural granulosa cells) with the effect of age and ovarian reserve, and to identify any potential age-related changes in the gene expression of the human oocyte. The material (mural granulosa cells, leukocytes and oocytes) in these studies was donated by 121 women undergoing fertility treatment at three fertility clinics at university hospitals and one private clinic.

The first and second paper describes our findings from methylation data from 118 leukocyte samples and 63 mural granulosa cell samples. We found, that leukocytes follow the chronological age of the women, while mural granulosa cells have a very young DNA methylation age when estimated with well-known age predictors. This indicates that mural granulosa cells have a distinctive methylation profile compared to other somatic cell types. This resulted in the development of a Granulosa Cell clock, able to predict the age of both the mural granulosa cells and the leukocytes. Further investigations showed a higher number of epimutations and differential methylated regions (DMR) in mural granulosa cells with advanced reproductive age, suggesting that their function is affected by age, which, however speculative, could contribute to the age-related decline in oocyte competences. Genes with a key function in the development of the ovarian follicle were represented in the age-DMRs. Predicted telomere lengths were found to be unaffected by age (Paper I).

We showed in paper II, that mural granulosa cells from women with diminished ovarian reserve have an altered DNA methylation profile compared to age-matched women with normal ovarian reserve. A higher number of epimutations and a greater variability in DNA methylation were present in the mural granulosa cells from these women, which were similar to the changes we found in women with advanced reproductive age. These changes were not seen in leukocytes. Furthermore, we found an increased

predicted telomere length in both leukocytes and mural granulosa cells from women with diminished ovarian reserve.

The third paper describes our findings from a small pilot study with single cell RNA sequencing (scRNA-seq) data from eleven metaphase II oocytes. The gene expression showed 315 differential expressed genes between women with young and advanced reproductive age. Genes (n = 187) involved in cell cycle, microtubule-based process and mitotic nuclear division were downregulated in the older metaphase II oocytes, while genes (n = 128) involved in mitochondrial organization, oxidative phosphorylation and adenosine triphosphate (ATP) metabolic process were upregulated in these oocytes.

This thesis adds novel insights to the understanding of female reproductive ageing, which might be valuable for future advances in reproductive medicine.

Dansk resumé

For kvinder i den fødedygtige alder er en fremskreden alder en stor risikofaktor for infertilitet, graviditetstab og fødsel af børn med medfødte sygdomme. Dette er hovedsageligt på grund af en øget forekomst af fejl i antallet af kromosomer (aneuploidi) i æggene ved stigende alder. Hvorfor kvinder har dette fald i fertiliteten med alderen, og hvorfor kvinder, i modsætning til andre arter, fuldstændig mister deres fertilitet i forbindelse med overgangsalderen, er endnu uklart.
Et af kendetegnene ved aldring er epigenetiske ændringer, hvilket inkluderer ændringer i DNA methyleringen. Data fra methyleringsarrays har vist, at visse væv har en accelereret epigenetisk alder sammenlignet med den kronologiske alder af vævet. Om follikler fra kvinders æggestokke har en anderledes epigenetisk profil, og om der er underliggende epigenetiske mekanismer for den kvindelige reproduktive funktion og aldring er endnu ikke klarlagt.

Formålet med dette Ph.d.-projekt var at beskrive methyleringsprofilen af humane follikelceller (granulosaceller) fra ovariet med fokus på effekten af kvindens alder og ovariereserve, samt at identificere aldersrelaterede ændringer i genekspressionen i det humane æg. Materialet (granulosaceller, leukocytter og æg) til disse studier blev doneret af i alt 121 kvinder i fertilitetsbehandling på tre klinikker på universitetshospitaler og én privat fertilitetsklinik.
Artikel I og II beskriver vores fund fra methyleringsdata fra 118 leukocytprøver samt 63 granulosacelleprøver. Vi viste, at leukocytternes epigenetiske alder følger kvindernes kronologiske alder, mens granulosacellerne har en meget ung DNA methyleringsalder, når vi beregner den med kendte alders-prædiktorer. Dette indikerer, at granulosaceller har en karakteristisk methyleringsprofil sammenlignet med andre somatiske celler. Vi udviklede derefter en Granulosacelle-klokke, som er i stand til at bestemme alderen på både granulosaceller og leukocytter. Yderligere analyse viste et højere antal epimutationer og differentiel methylerede regioner i granulosaceller ved stigende alder, hvilket tyder på at funktionen af folliklens celler er påvirket af alder, som omend en smule spekulativt, kunne tænkes at være medvirkende til det aldersafhængige fald i æggets evne til at etablere en graviditet og fødsel af et rask barn. Gener med central funktion for ovariets follikeludvikling var repræsenteret i de alders påvirkede regioner. Beregnet telomerlængde i granuloscellerne var derimod aldersuafhængig (Artikel I).
I artikel II viste vi, at hos kvinder med en lav ovariereserve i forhold til deres alder, har granulosacellerne en ændret DNA methyleringsprofil sammenlignet med kvinder med normal ovariereserve på samme alder. Hos disse kvinder fandt vi også højere antal epimutationer og en større variabilitet i DNA methyleringen i granulosacellerne, hvilket lignede den ændring, vi så i kvinder med høj reproduktivalder. Det viste sig kun i

granulosaceller og ikke i leukocytterne, til gengæld fandt vi en højere estimeret værdi for telomerlængden i både leukocytter og granulosaceller fra kvinder med en lav ovariereserve.

Den tredje artikel beskriver vores fund fra et lille pilotforsøg med enkeltcelle RNA-sekventering (scRNA-seq) af elleve metafase II æg. Genexpressionen viste 315 differentielt udtrykte gener mellem kvinder med lav og høj reproduktiv alder. Gener (n = 187) som er involveret i cellecyklus, mikrotubuli-baserede processer og mitotisk celledeling var nedreguleret i de ældre æg, mens gener (n= 128), som er involveret i mitokondriel organisation, oxidativ fosforylering og adenosin trifosfat (ATP) metaboliske processer var opreguleret i disse æg.

Denne afhandling bidrager med ny viden til forståelsen af kvindelig reproduktivaldring, som kan vise sig at være værdifuld for kommende fremskridt i reproduktionsmedicin.

1. Introduction

Presently, around 9.8% of Danish children are born after medically assisted reproduction (MAR) (The Danish Fertility Society 2019)[1]. Despite this accessibility of MAR and a desire for growing families (only 2.5% of couples do not want children) (Leridon and Slama 2008), the fertility rate (number of children born per woman) (Broekmans *et al.* 2009) in Denmark is only 1.7 (Statistics Denmark 2019). As follows, 20% of men and 12% of women are childless at 50 years of age (Statistics Denmark 2016).

One likely contributing factor to the decline in fertility rate is the age-related decrease in female fecundity (the ability to produce offspring) which is exacerbated by the current trend of having children later in life (OECD Family Database 2018). This is seen in the increasing age of first-time mothers in Denmark, from 23.1 years in 1960 compared to 29.3 years in 2018 (Statistics Denmark 2018); therefore, giving women a shorter time to have their desired number of children (Vassard *et al.* 2016). This has contributed to a growing number of involuntary childless couples and a growing need for MAR (The Danish Fertility Society 2019; Leridon and Slama 2008).
Consequently, there is a need for a better understanding of the complex cellular mechanisms involved in the ageing of the ovarian follicles in order to provide future strategies for prevention and/or treatment of the age-related female infertility.

[1] In 2018: 3999 children born after IVF/ICSI treatment. 2020 children born after IUI treatment.

2. Background

2.1 Female reproduction

The human ovary is an extraordinary organ which serves as a reservoir for the female gametes and at maturity as a factory of steroid sex hormones. It is well known that female fecundity decreases with increasing chronological age. This has been shown in historical studies (Spira 1988; Wood 1989) as well as in contemporary population studies (Abma *et al.* 1997) and reports on age-dependent success rates in MAR (Templeton A *et al.* 1996; Nyboe Andersen *et al.* 2009). Females are born with all the oocytes they will ever have. With increasing age, the human ovarian reserve (the number of primordial follicles) is reduced by a process known as follicular atresia; starting with 1-2 million primordial follicles at birth (Markström *et al.* 2002) which declines to below 1000 at the time of menopause (Faddy and Gosden 1996). In addition to this decline in oocyte numbers, the competence of the oocytes to establish a viable pregnancy declines primary due to a significant increased prevalence of aneuploidy in the metaphase II (MII) oocytes with advancing reproductive age (Fragouli *et al.* 2011).

2.1.1 Reproductive lifespan

A woman's reproductive life starts with the onset of menarche, which is the most detectable indicator of puberty (Chen *et al.* 2018) and terminates at menopause, which for most women are around the age of 51 years (Treloar 1981; te Velde and Pearson 2002; Depmann *et al.* 2016). An approximately 5–14% of women experience early menopause, before the age of 45 years (Jacobsen *et al.* 1999; Jacobsen *et al.* 2004; Vegetti *et al.* 2000), and 1-2% before the age of 40 years (Coulam *et al.* 1986; Vegetti *et al.* 2000). Natural fertility terminates around ten years before menopause (te Velde and Pearson 2002), which for a number of women results in the need for MAR to achieve pregnancy when they are in their late-twenties or early to mid-thirties.

2.1.2 Folliculogenesis

Folliculogenesis is the development and maturation of the ovarian follicle. It is a long and continuous process due to a constant recruitment of primordial follicles (*initial recruitment*) independent of follicle stimulating hormone (FSH), resulting in an ovary that at any given time contains follicles in multiple different stages of development (McGee and Hsueh 2000). In the presence of FSH, a number of growing follicles start developing (*cyclic recruitment*), of which only one becomes the dominant follicle that is ovulated in response to luteinizing hormone (LH) (McGee and Hsueh 2000). In women with a normal

menstrual cycle, the dominant follicle has been suggested to be recruited from the primordial follicle stage up to one year earlier (Conti and Chang 2016; Gougeon 1986).

The primordial follicles

The primordial follicles are produced during foetal development around gestational week 18-22 (Wallace and Kelsey 2010) and no further production of oocytes will occur later on. This dogma has been challenged in mice studies, which suggest the existence of putative germline stem cells originating from bone marrow and peripheral blood, potentially having the capability of regenerating oocytes (Johnson *et al.* 2004). However, no reproducible evidence exists and the theory about neo-oogenesis remains controversial (Celik *et al.* 2011).

Primordial follicles are oocytes arrested in prophase of meiosis I surrounded by a single layer of flattened pre-granulosa cells (Li and Chian 2017). The number of initial primordial follicles is essential and is referred to as the woman's ovarian reserve, which represents her reproductive potential. Foetal ovaries contain a maximum of 6 million primordial follicles that after atresia is reduced to 1-2 million at birth and about 300,000 at the onset of puberty (Li and Chian 2017). This massive amount of atresia, combined with continuous recruitment and loss of primordial follicles (Richardson *et al.* 1987), accelerates the decline in fertility seen in most women around the age 37 (Faddy *et al.* 1992).

Recruitment of the primordial follicles

When a follicle grows during the initial recruitment, changes are seen in both the oocyte (growth) and the surrounding pre-granulosa cells (proliferation, differentiation and growth). Only a limited number of primordial follicles will be recruited at a time, while the rest of the follicles will remain resting for months or even decades until they enter a cycle of recruitment (McGee and Hsueh 2000). The mechanisms holding, protecting and activating the primordial follicles still remain unclear.

Mouse models have shown that the PTEN-PI3K-AKT pathway in oocytes is involved in the primordial follicle activation during initial recruitment (Hsueh *et al.* 2015). Oocytes in resting follicles are also metabolically active and transcribing genes essential for oogenesis (mouse: (Gallardo *et al.* 2007), human: (Markholt *et al.* 2012)). Possible oocyte candidates involved in activation of the initial recruitment include the kit ligand, fibroblast growth factor 2 (FGF-2), keratinocyte growth factor (KGF), leukemia inhibitory factor (LIF), bone morphogenetic protein (BMP)-4/7/15 and growth differential factor 9 (GDF-9), while the suppressors embrace the phosphatase and tensin homolog (PTEN), CREB regulated transcription coactivator 1 (TORC1),

forkhead Box I2 O3a (FOXO3a), forkhead box 12 (Fox12), cyclin-dependent kinase inhibitor 27 (p27), LIM homeobox 8 (LHX8), forkhead box protein L2 (FOXL2) and anti-Müllerian hormone (AMH) (Ernst *et al.* 2017).

The cascade in which the follicles can be activated includes the suppression of forkhead box O3 (FOXO3), which normally functions by preventing the initial recruitment of follicles (Pelosi *et al.* 2013). This suppression occurs by a series of upstream events starting with the activation of the receptor tyrosine kinases (RTKs), which stimulate the phosphoinositide 3-kinase (PI3K) activity, leading to activation of protein kinase B (AKT) (Hsueh *et al.* 2015). The activated AKT then migrates to the nucleus and inhibit the FOXO3 activity (Hsueh *et al.* 2015). Furthermore, $FOXO3^{-/-}$ mice have shown early depletion of ovarian follicles due to a global follicular activation (Castrillon *et al.* 2003).

Primary follicles

The transition from primordial follicle to primary follicle includes both growth of the oocyte and the proliferation of the granulosa cells (Li and Chian 2017). The granulosa cells surrounding the oocyte proliferate from around 30 pre-granulosa cells in the primordial follicle (Westergaard *et al.* 2007) to an estimate of 60 million mural granulosa cells in the fully mature follicle (McNatty *et al.* 1979) where they support the ovulation of the cumulus embedded oocyte.

The beginning of the primordial to primary transition is characterized by the granulosa cells changing their morphology from a squamous to cuboidal shape (Gougeon and Chainy 1987; Gougeon 1996). Cultured ovarian granulosa cells undergo morphologically changes in response to FSH (Lawrence *et al.* 1979). A recent transcriptomics study found differences between pre-granulosa cells and maturing granulosa cells from primordial and primary follicles, respectively (Ernst *et al.* 2018). Interestingly, Ernst *et. al.* found an enrichment in STAT3 and CREB signalling, which is known to be of importance in FSH induced regulation, in granulosa cells from primordial and primary follicles (Ernst et al. 2018). However, Ernst and colleagues failed to show an increase in FSH receptor (*FSHr*) expression between the two stages and hence could not confirm previous report of primary follicle developing FSHr (Oktay *et al.* 1997). The role of FSH in the initial follicle growth still remains unclear.

In the primordial to primary transition, the genome of the oocyte is activated and genes are transcribed (Li and Chian 2017). A recent study comparing the transcriptomes of human oocytes from primordial and primary follicles, highlighted genes and pathways differentially expressed between the two developmental stages and are, therefore, potentially involved in the early stages of human oogenesis (Ernst *et al.* 2017).

The Hippo signalling pathway functions as a regulator of tissue growth and was found to be significantly enriched in oocytes from primary follicles (Ernst *et al.* 2017). There was a similar increase in the activity of the extracellular signal regulated kinase 5 (ERK5) signalling pathway of meiotic and mitotic cell division between the two developmental stages (Maciejewska Z *et al.* 2011; Ernst *et al.* 2017). Furthermore, *FOXO3A* was found to be specific to the primary stage oocytes, while *FOXO1* was seen in the nucleus of oocytes from primordial follicles and was suggested to function in parallel as a downstream effector of the PTEN pathway in the activation/dormancy of the primordial follicles (Ernst *et al.* 2017). The gene, eukaryotic translation initiation 4E (*eIF4E*), which functions in mRNA translation and processes of meiosis, was found in the cytoplasm of oocytes from primary oocytes (Henderson *et al.* 2009) and is significantly increased during the transition from primordial follicle to primary follicle (Ernst *et al.* 2017).
The zona pellucida, a glycoprotein polymer extracellular matrix, will at this stage be formed around the oocyte separating it from the surrounding granulosa cells (Conti and Chang 2016).

Secondary follicles

The secondary follicle is characterized by two or more layers of cuboidal granulosa cells (Conti and Chang 2016), and the development of the theca externa and interna, that run around the entire basal lamina of the follicle. The theca cells are endocrine cells that produce androgens later in folliculogenesis in response to LH, which are subsequently converted to oestrogens by aromatase within the granulosa cells (Conti and Chang 2016). During the development of the theca layer two capillary vascular networks will be formed through angiogenesis in order to sustain the ovarian follicles changing needs for hormones and nutrients to and from the follicle (Brown and Russell 2014).

The secondary and small antral follicles (≤ 4 mm in diameter) are also characterized by having the highest expression level of AMH during follicular development (Weenen *et al.* 2004), which clinically, therefore, are used as a biomarker of the functional ovarian reserve (Anderson 2012).

Antral follicles

In the late state of the secondary follicle, fluid begins to accumulate between some of the granulosa cells to form the antrum (Erickson 2000). To become a tertiary follicle, the volume of the antrum increases, the granulosa cells and theca cells continue to undergo mitosis, and the follicle diameter increases to 400 µm (Erickson 2000). The growth of the follicle is now primarily depended on the availability of the gonadotrophins (Li and Chian 2017), and they can be visualized by ultrasonography. Subsequently, with the

formation of the antrum the granulosa cells differentiate morphologically and functionally into two cell types: cumulus granulosa cells (cumulus cells) and mural granulosa cells (Diaz *et al.* 2006; Eppig 2001).

The granulosa and cumulus cells are specialized cells essential for the developing oocyte. Through close bi-directional communication via a network of receptors, growth factors and gap junctions, granulosa and cumulus cells provide many functions for the growing oocyte. This include the exchange of signaling molecules, providing nutrition (Brower and Schultz 1982; Khamsi and Roberge 2001), transporting macromolecules (Rossello *et al.* 2009; Macaulay *et al.* 2014), and producing sex steroid hormones and growth factors necessary throughout folliculogenesis (Edson *et al.* 2009). All of the support provided to the oocyte during folliculogenesis allows the oocyte to grow from 35 µm in diameter to its full size (≈120 µm in diameter) at the antral stage (Conti and Chang 2016).

The ovulating follicle

After the onset of puberty, a limited number of antral follicles further develop during each menstrual cycle in preparation for ovulation. One follicle becomes dominant by day 3-5 in the cycle (the other follicles will undergo atresia) and transforms into the pre-ovulatory follicle within 14 days of the follicular phase of the menstrual cycle. This pre-ovulatory follicle is then ready to burst and excrete the cumulus-oocyte-complex into the ovarian duct for fertilisation (Li and Chian 2017). The mid-cycle LH surge ensures granulosa cells and cumulus cell signalling to the oocyte to trigger the resumption of meiosis and the expansion of cumulus cells enclosing the oocyte in preparation for fertilisation (Chen *et al.* 1993). The LH induced change in mural granulosa cells ensures both ovulation, as well as the shift from producing primarily oestrogen to progesterone. These progesterone producing granulosa cells, together with the theca cells, forming the corpus luteum together after ovulation (Regan *et al.* 2018; Abedel-Majed *et al.* 2019).

Follicular atresia

Follicular atresia is an apoptotic breakdown of ovarian follicles, which occurs, at all stages throughout folliculogenesis and eliminates more than 90% of the follicles entering into the growth phase (Gougeon 1986). Only a limited number of the follicles at the early antral stage will be rescued from undergoing atresia by survival factors (e.g. LH, FSH) and only 300-400 will be selected and ovulated for potential fertilisation during a woman's reproductive lifetime (Townson and Combelles 2012; Faddy MJ *et al.* 1992; Markström *et al.* 2002). The reduction in the number of follicles is a hormonally regulated process, achieved primarily with apoptosis of the granulosa cells (Hsueh *et al.* 1994; Zhou *et al.* 2019). Follicular atresia is regulated by a combination of endocrine factors (e.g. FSH, LH), paracrine factors insulin-like

growth factor I (IGF-I), epidermal growth factor (EGF), basic fibroblast growth factor (bFGF), activin and interleukin 1β (IL-1β), atherogenic factors tumour necrosis factor α (TNF-α), gonadotrophin-releasing hormone (GnRH), androgens, Interleukin 6 (IL-6) and free radicals (Kaipia and Hsueh 1997). However, most inhibitors of atresia in the later phase of folliculogenesis are regulated by FSH and LH, since sufficient level of FSH is critical for the survival of the follicles and LH is necessary for the ovulation (Markström *et al.* 2002).

2.1.3 Anti-Müllerian hormone

In females, AMH is produced by the granulosa cells of preantral and small antral follicles (Weenen *et al.* 2004). AMH is a glycoprotein hormone and part of the transforming growth factor-β (TGF-β) superfamily (Cate *et al.* 1986). Expression levels of AMH are linked to specific stages of folliculogenesis and is seen to increase throughout early primary follicles development and reduces again in the large antral follicle (8-10 mm in diameter) (Andersen *et al.* 2010). AMH is suggested to be a gatekeeper of the initial recruitment of primordial follicles into the growing pools of follicles (Durlinger *et al.* 2002). It has also been suggested that AMH is regulator of follicular atresia by decreasing the sensitivity of the follicles to FSH and thereby inhibit the growth of the follicles (Seifer and Merhi 2014). Moreover AMH expression levels are low or absent in atretic follicles (Durlinger *et al.* 2002).

AMH is generally accepted as a serum biomarker to reflect the *functional ovarian reserve,* as it is only produced by the growing follicles (Anderson 2012). Moreover, the AMH levels are used to identify women at risk for developing ovarian hyperstimulation syndrome in connection with controlled ovarian stimulation for assisted reproductive technology (ART) treatment. Clinically, serum AMH can be used in the diagnosis of polycystic ovary syndrome (PCOS) (Pigny *et al.* 2003; Dewailly *et al.* 2011), oligomenorrhea (Li *et al.* 2011), premature ovarian insufficiency (Knauff *et al.* 2009) and granulosa cell carcinoma (La Marca and Volpe 2007). Finally, the molecular function of AMH is suggested to be involved in the ovarian dysfunction observed in women with PCOS (highly elevated AMH expression) (Catteau-Jonard *et al.* 2007).

2.1.4 Meiosis

At the time of completed fertilisation, oocytes and sperm cells are both haploid, thus allowing them to be combined to form a diploid zygote. Meiosis I is initiated in the female gonad during foetal development, beginning with the replication of chromosomes in interphase to form homologous chromosome pairs. During prophase, the homologous chromosomes from maternal and paternal origin exchange genetic information by forming crossovers (homologous recombination sites) to increase genetic diversity and to

create the necessary homolog interactions to assist in chromosome segregation later in meiosis (Coop and Przeworski 2007; Baudat *et al.* 2013; Hassold and Hunt 2001). The oocytes arrest in the dictyate stage (end of prophase) and by the time of birth are all surrounded by pre-granulosa cells forming the primordial follicles (Hassold and Hunt 2001). As primordial follicles are recruited periodically after the onset of puberty, the oocyte chromosomes decondense and the DNA is transcribed to overcome growth requirements and to stock up RNAs and proteins needed in early embryonic development (Macaulay *et al.* 2011). The resumption of meiosis I induced by the mid-cycle LH surge allows for the completion of the first meiotic division just before ovulation (Hassold and Hunt 2001). This division is characterised by the segregation of homologous chromosomes, followed by an asymmetrical division of the cytoplasm and the formation of two daughter cells: a metaphase II oocyte (secondary oocyte) and the first polar body (MacLennan *et al.* 2015). Oocytes are then briefly arrested in metaphase II until meiotic resumption is triggered by fertilisation. The sperm cell specific phospholipase C-Zeta (Saleh *et al.* 2020) induces the resumption of meiosis, thereby initiating the degradation of centromeric cohesion, segregation of sister chromatids (Herbert *et al.* 2015; Hauf and Watanabe 2004; Page and Hawley 2003) and the extrusion of the second polar body.

2.1.5 Oocyte competency

The age of a woman is the most predictive parameter for her chance to conceive (Menken *et al.* 1986). This is, as described in section 1.1, due to a decline in the quantity and quality of oocytes. The competences of the oocyte to mature correctly and develop declines with increasing age, primarily a decline in the ability to complete the first and second meiotic divisions leading to an increase in aneuploidy (Franasiak *et al.* 2014). Female age has been shown to influence the transcriptome of *in vivo* matured human MII oocytes, specifically transcripts of genes central to spindle organisation and DNA repair that could directly impact chromosome missegregation rates (Grøndahl *et al.* 2010). A recent study showed that aneuploidy are not only increased in oocytes from women of advanced reproductive age (> 33 years), but also in oocytes from very young women (< 20 years) (Gruhn *et al.* 2019). This is suggested to reflect two different evolutionary pathways that respectively protect the woman from pregnancy and birth before her body is fully developed (Huseynov *et al.* 2016; Kumar *et al.* 2007; Kim *et al.* 2012; Zelazowski *et al.* 2017) and later in life, where the woman instead should focus on her grandchildren (the Grandmother Hypothesis) to ensure the survival of her genes through the younger generations (Hawkes *et al.* 1998; O'Connell *et al.* 1999; Kim *et al.* 2012; Kim *et al.* 2014).

A major change in the cytoplasmic organization and functional activity occurs during oogenesis where, for example, the number of mitochondria increases (Darbandi *et al.* 2016) and the transcription and translational activity are changing to store mRNA and proteins to be used later in the oocyte development, at fertilisation and during embryogenesis (Miyara *et al.* 2003; Grøndahl *et al.* 2013; Macaulay *et al.* 2011). The oocyte provides important signals for follicular development, however, the supported provided by the granulosa and cumulus cells is necessary to secure optimal growth and maturation (Monniaux 2016).

2.1.6 Cumulus and granulosa cells

Cumulus and granulosa cells are highly specialized cells having close communication with the oocyte. They support the oocyte with nutrition and trafficking macromolecules through a network of receptors and gap junctions (Grøndahl *et al.* 2012). Furthermore, the cumulus and granulosa cells produce growth factors (e.g. inhibins, activins, EGFs and insulin-like growth factors) and hormones (e.g. AMH, estradiol and progesterone) essential for folliculogenesis, oogenesis and ovulation (Monniaux 2016). During the antral stage of the folliculogenesis the granulosa cells upregulate the sensitivity to FSH, which stimulates the recruitment and growth to the final ovulating follicle (Hsueh *et al.* 2015). The gene expression of cumulus and granulosa cells change during late folliculogenesis (Grøndahl *et al.* 2011), as well as during ovulation (Wissing *et al.* 2014). Poulsen and co-workers described two waves of changes in the gene expression profile in human granulosa cells, from women undergoing ovarian stimulation, between ovulation induction and oocyte retrieval 36 hours later, involving upregulated genes enriching inflammation, angiogenesis, intracellular matrix and growth factors, whereas down regulated genes enriched cell cycle and proliferation (Poulsen *et al.* 2020). Likewise, cumulus and granulosa cells showed unique gene expression profiles in the human pre-ovulatory follicles (Grøndahl *et al.* 2012). Cumulus cells and granulosa cells are easily isolated and collected as a biproduct of oocyte retrieval during *in vitro* fertilisation (IVF)/intracytoplasmic sperm injection (ICSI) treatment, making them an optimal resource for studying follicular health and female fertility.

2.1.7 Diminished ovarian reserve

Diminished ovarian reserve (DOR) is defined as a reduced number of primordial follicles compared to other age matched women (Levi *et al.* 2001; Pastore *et al.* 2012; May-Panloup *et al.* 2012; Gleicher *et al.* 2009b; Greene *et al.* 2014). DOR can be both *physiological* due to advanced reproductive age and *pathological* due to an autoimmune, idiopathic or iatrogenic disease (Sun *et al.* 2008; Fusco *et al.* 2011; Greene *et al.* 2014). In the case of pathological DOR, the prematurely lower number of follicles can either be a smaller pool of primordial follicles developed during embryonic development, abnormal follicular development, increased

follicular atresia (e.g. seen in Turner's Syndrome) or a defect in the communication between the oocyte and granulosa cells (Greene *et al.* 2014). It is suggested that a minor percentage of women with pathological DOR has a genetic aetiology, which might also be associated with early/premature menopause and premature ovarian insufficiency (Pastore *et al.* 2012; Persani *et al.* 2010; Torgerson *et al.* 1997). Gene mutations or polymorphisms associated with DOR have been found in example fragile X mental retardation 1 (*FMR1*) (Barasoain *et al.* 2013; Pastore *et al.* 2012; Welt *et al.* 2004; Gleicher *et al.* 2009a), *GDF9* (Wang *et al.* 2013; Wang *et al.* 2010), *FSHR* (Sheikhha *et al.* 2011; Livshyts *et al.* 2009) and oestrogen receptor 1 (*ESR1*) (Livshyts *et al.* 2013; M'Rabet *et al.* 2012).

Clinical assessment of DOR includes serum AMH (< 0.1 ng/ml ≈ 7.14 pmol/L) and FSH (> 10 IU/L) levels as well as ultrasound guided antral follicle count as indicators for the condition (Centers for Disease Control and Prevention 2015). However, no ideal test to evaluate the ovarian reserve exist and the clinical diagnosis of DOR is not standardised nor specific (Pastore *et al.* 2017).

2.2 DNA methylation

2.2.1 The structure and establishment of DNA methylation

DNA methylation is an epigenetic process where a methyl group (CH_3) is added to the DNA. This modification influences many physiological and pathological processes such as genomic imprinting, X-chromosome inactivation, embryonic development, ageing and carcinogenesis (Wilson *et al.* 2012; Jones 2012). The most common type of DNA methylation is 5-methylcytosine (5-mC), where a methyl group is attached to the 5^{th} atom in a six-atom ring. DNA methylation provides the instructions for how and when DNA is read, and thereby controls the transcription (reviewed in (Dor and Cedar 2018)). DNA methylation in gametes is erased prior to implantation of the embryo and new methylation patterns are established during embryonic development (Smith *et al.* 2012; Smith *et al.* 2014). This epigenetic reprogramming starts with *de novo* methylation of the entire genome in early embryogenesis, excluding a large group of cytosine-phosphate-guanine (CpG) sites primarily, located in promotors of housekeeping gene, that are protected and remain unmethylated (Cedar and Bergman 2012). This process is followed by changes in the methylome (the set of DNA methylation modifications in the genome) after implantation, which are characterized by being both tissue- and gene-specific (Cedar and Bergman 2012). DNA methylation continues to undergo programmed variations after birth in response to environmental inputs, which can affect ageing and predispose to various diseases (Dor and Cedar 2018).

2.2.2 Detection of DNA methylation

Bisulfite sequencing is the gold standard for detection of DNA methylation, as it gives both quantitative and qualitative information about the DNA methylation status at a single base-pair resolution. The method was developed by Frommer and colleagues in 1992 (Frommer *et al.* 1992) and it is based on treatment of the DNA with sodium bisulfite to distinguish between unmethylated and methylated cytosines. Upon sodium bisulfite treatment unmethylated cytosines are converted into uracil (Figure 1A) and methylated cytosines, which are immune to this conversion, remain as cytosines (Figure 1B). This allows the methylated cytosines to be distinguished from the unmethylated cytosines via subsequent PCR amplification and sequencing, where uracil is converted into thymine and the methylated cytosines remain.

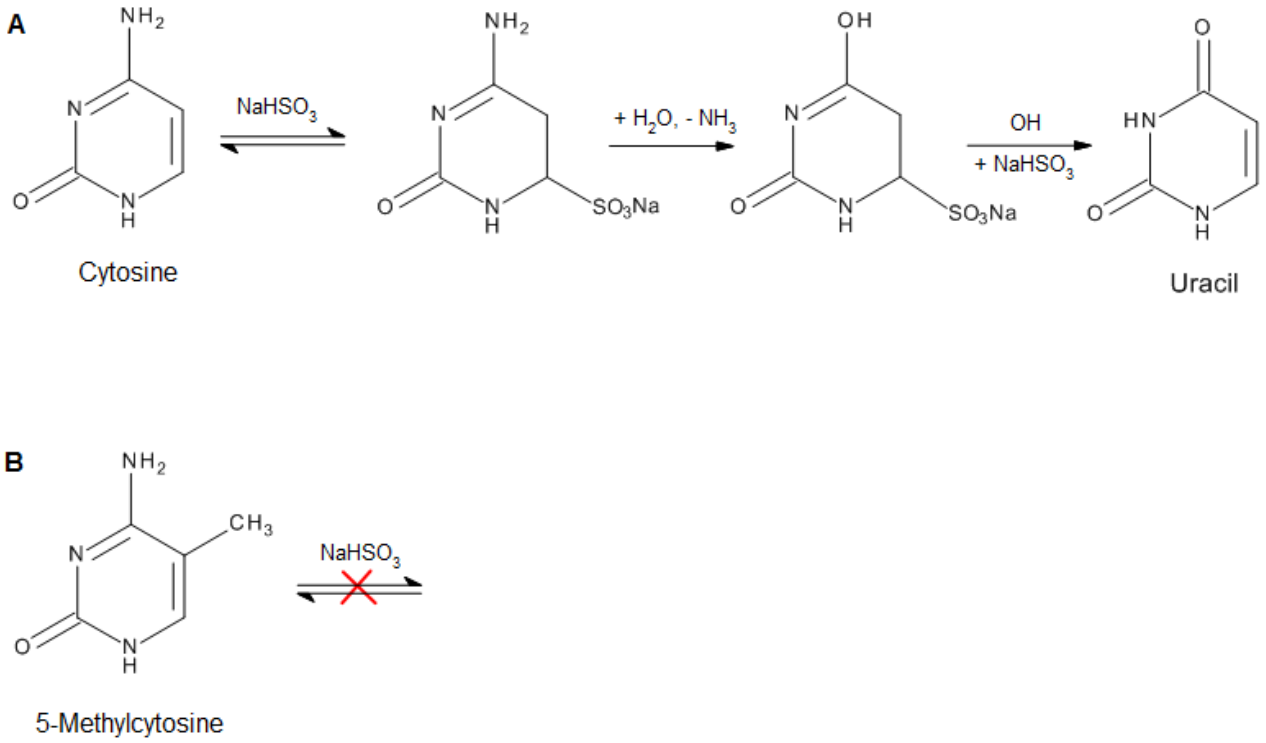

Figure 1 A. The chemical reaction of the unmethylated cytosine been converted to uracil through a bisulfite-catalytic reaction. **B.** Methylated cytosines are protected from this chemical reaction and stays as cytosines. Figure is created with ChemDraw.

2.2.3 DNA methylation aberrations and differentially methylated regions

Epigenetic aberrations (or epimutations) are stable changes in the DNA methylation profile, which can affect gene expression without changing the DNA sequence (Maslov and Vijg 2009). They are a result of errors occurring during DNA damage repair or DNA replication, which are likely to contribute to a decline in the affected tissue's functionality and to increase the incidence of disease such as cancer (Maslov and Vijg

2009). Epimutations are increasing during ageing (Maslov and Vijg 2009), likewise are some differentially methylated regions (DMRs) found to be associated with age. DMRs contain clusters of differentially methylated CpG sites and differ between phenotype (Peters *et al.* 2015). DMRs can be found throughout the genome but have been identified especially in promotors regions and within the body of genes as well as in intergenic regulatory regions (Suzuki and Bird 2008; Jones and Baylin 2002; Aran *et al.* 2011; Bert *et al.* 2013; Spilianakis *et al.* 2005; Peters *et al.* 2015). Genes within age associated DMRs have been found to be associated with age-related diseases such as cancer, Alzheimer's disease, cardiovascular disease, type-2 diabetes (Xiao *et al.* 2015).

2.2.4 DNA methylation and ageing

Ageing can be defined as a decline in a set of multiple essential physiological functions leading to an increase in age-specific mortality rate and a decrease in age-specific reproductive rate (Flatt 2012). Epigenetic alterations are one of the nine hallmarks of ageing as defined by Lopéz-Otín *et al.* (Lopéz-Otín *et al.* 2013). The dramatic epigenetic changes observed in the early development are programmed and necessary (Jung and Pfeifer 2015), but the changes in DNA methylation during ageing can negatively affect gene expression levels, e.g. decreasing expression of DNA repair genes or anti-inflammatory genes (Jung and Pfeifer 2015). A study comparing the DNA methylation profile of newborns and centenarians, shows that newborns have much more homogeneous profiles compared to centenarians. This indicates that the methylome is continuously changing over our lifetime, specifically seen as primarily decreasing DNA methylation levels and a reduced correlation in the methylation status to the surrounding CpGs with advanced age (Heyn *et al.* 2012). Methylation levels changes over time and may been maintained under genetic control (Bjornsson *et al.* 2008). The first gene found to be hypermethylated with increasing age was the gene encoding the oestrogen receptor in the colon (Issa *et al.* 1994). This raised the idea of whether it is possible to develop an epigenetic age predictor from the methylation data of specific genes (Jung and Pfeifer 2015).

2.3 Age predictors

The first multi-tissue age predictor was developed by Steve Horvath in 2013 using *in silico* analysis of 7844 samples from 82 individual public available data sets. Horvath used these 82 individuals to assess DNA methylation in 51 different cell and tissue types using the Illumina 27K and 450K array platforms (Horvath 2013). Thirty-nine datasets were used for constructing the age predictor, while the rest were used for validation or other purposes, such as an estimate of the DNA methylation age (epigenetic age based on CpG methylation) of embryonic stem cells (Horvath 2013).

A transformed version of chronological age (a weighted average of methylation levels is transformed to an - DNA methylation age estimate using a calibration function) was applied to the training datasets to select the CpGs of importance for the age prediction, using a penalized regression model (Horvath 2013). The challenge with the development of a multi-tissue predictor is that the DNA methylation pattern differs a lot across cell and tissue types, as well as in early versus later life (Horvath and Raj 2018). To overcome this issue, a high number of CpGs needed to be included to make the predictor accurate enough to fulfil these criteria.

Horvath found 353 key CpG sites that must be included in his predictor in order to reach the highest age correlation between DNA methylation age and chronological age (measured by the Pearson correlation coefficient) (Horvath 2013). Out of the 353 CpGs, 193 CpGs are located in poised promoters (bivalent; both gene activation and gene repression activity) and the methylation state is positively correlated with age, while the remaining 160 are negatively correlated to state of methylation and located in weak promotors or in strong enhancers (Horvath 2013). A great proportion of the 353 CpGs is located near genomic sites that are already known to control expression of genes involved in development and differentiation (Horvath 2013).

The multi-tissue age predictor stands out from other epigenetics clocks by its high accuracy in children, its homogeneity of age estimates across tissues in the same individual (Horvath *et al.* 2015b), that it can be applied on human foetal tissue to determine gestational age (Knight *et al.* 2016; Spiers *et al.* 2015) and can also predict the age of chimpanzees tissue (Horvath 2013). Accordingly, the predictor does not reflect the proliferative history of the cells, since the same methylation age is found in both high and low proliferative tissue (e.g. blood and brain tissue, respectively) in the same individual (Horvath 2013; Horvath *et al.* 2015b). Equally important is that the predictor is compatible with different platforms, such as microarrays, pyrosequencing, quantitative PCR and next generation sequencing due to its robustness against missing data points (Horvath and Raj 2018). For example, the predictor is trained with methylation data from the Illumina 27K and 450K arrays, but it still performs well with the EPIC array regardless the absence of 17 clock CpGs (Horvath 2013; Horvath and Raj 2018). However, the predictor also has its limitations; it does not work on sperm cells and the DNA methylation age of certain tissues (e.g. normal female breast tissue, spleen, cerebellum, oesophagus, jejunum and pancreas) is higher (or lower) compared with the DNA methylation age of the blood or the chronological age of the individual (Horvath 2013; Sehl *et al.* 2017). It remains unclear why the predictor does not perform well with certain tissues.

Horvath was the first to discover that the rate in which DNA methylation changes, also referred to as the "ticking rate" of the age predictor, is faster during growth and development (Horvath 2013; Binder *et al.* 2018). They also determined that the age predictor may reflect the innate ageing process that is under genetic control more than the adaptive ageing process, as shown by a weak association with lifestyle factors and inflammatory markers (Quach *et al.* 2017).

2.3.1 Age acceleration

To determine whether a given tissue has a higher (older) or lower (younger) DNA methylation age (Figure 2), the *average age acceleration* can be calculated as the average difference between the DNA methylation age and the chronological age (Horvath 2013). When applying the multi-tissue predictor or any other epigenetic clock to data of the general population outliers are expected to occur. This will result in either positive age acceleration (older DNA methylation age) or negative age acceleration (younger DNA methylation age (sometimes also referred to as *deceleration*)), suggesting that the underlying tissue ages either faster or slower than expected based on the chronological age (Horvath and Raj 2018).

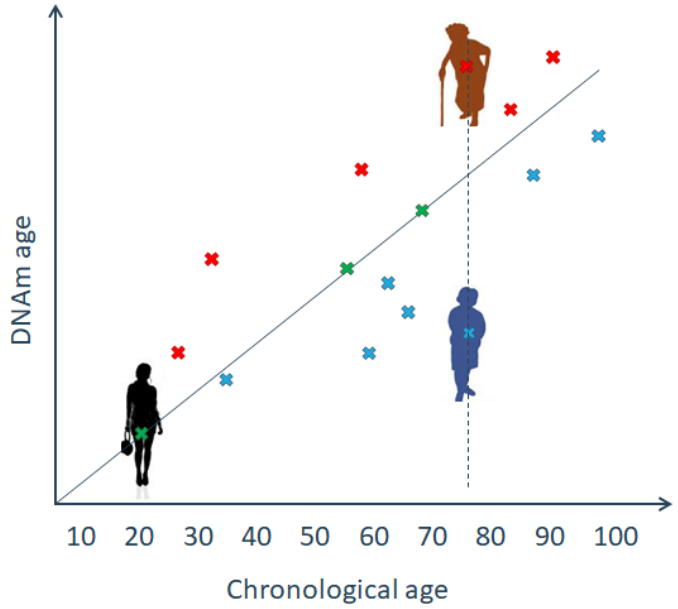

Figure 2 Normally the DNA methylation (DNAm) age follows chronological age (line, green), However the DNAm age can also be higher (red) or lower (blue) than the chronological age. Figure is created in PowerPoint.

After Steve Horvath published his age predictor in 2013, several studies have shown associations between age acceleration and different pathologic and physiologic conditions. For example, a positive age acceleration in cord blood from newborns is associated with higher fat mass, taller heights throughout

childhood and adolescence, and correlation with certain markers of pubertal timing, such as female breast density and age at menarche (Simpkin *et al.* 2017; Binder *et al.* 2018).
Age acceleration is also associated with certain diseases including Down syndrome (Horvath *et al.* 2015a), Parkinson's Disease (Horvath and Ritz 2015) and obesity (Quach *et al.* 2017; Levine *et al.* 2018). In addition, an increased DNA methylation age in blood is correlated with certain type of cancers (Horvath 2013; Levine *et al.* 2015; Dugue *et al.* 2018), cardio-vascular diseases (Roetker *et al.* 2018) and can predict all-cause of mortality in later life (Marioni *et al.* 2015).

2.3.2 Other age predictors

As a results of Horvath's multi-tissue age predictor multiple epigenetic clocks have since been developed. In the same year (2013), the Hannum clock was developed with data from whole blood but was also able to predict age in multiple tissues (Hannum *et al.* 2013). The year after in 2014, Weidner and colleagues published an age predictor for blood using only three CpG sites (Weidner *et al.* 2014). Two years later a group in Italy presented an age predictor using methylation levels at ELOVL fatty acid elongase 2 (*ELOVL2*), four and a half LIM domains 2 (*FHL2*), and proenkephalin (*PENK*) genes from human teeth DNA (Giuliani *et al.* 2016). In 2018, the DNA methylation PhenoAge epigenetic biomarker of ageing for lifespan and health span (Levine *et al.* 2018) and the Skin & Blood clock specialized to be used in fibroblasts, endothelia, skin, salvia and blood samples (Horvath *et al.* 2018) were published. Whether these methylation changes at specific CpGs (clock CpGs) are driving ageing or are consequences of the ageing process remain unclear (Fransquet *et al.* 2019).

2.3.3 Measurement and analysis of DNA methylation

To fully understand the function of DNA methylation in various diseases and in the healthy body, it requires that we can measure the DNA methylation profile across larger portions of the genome. The gold standard for DNA methylation analysis is whole genome bisulfite sequencing (WGBS), since it can provide a full map of the approximately 28 million CpG methylations sites in the human genome (Pidsley *et al.* 2016). However, it is a very expensive method and it requires special technical expertise to be able to process the high amount of data. Instead many researchers prefer to use a microarray, as it is less technically difficult and cheaper. In 2016, Illumina's EPIC array superseded the Infinium HumanMethylation450 as the primary microarray platform for DNA methylation analysis, as it contains 93.3% of the probes from HumanMethylation450 array plus additional probes (Pidsley *et al.* 2016; Illumina 2015). The EPIC array covers more than 863 thousand CpG loci and almost 300 non-CpG sites (Pidsley *et al.* 2016) and provides single-base methylation information for the covered sites.

2.4 DNA methylation age in female reproduction

DNA methylation age has been measured in several reproductive tissues and DNA methylation age acceleration has been associated with several reproductive life events. DNA methylation age acceleration in young girls was significantly associated with a decreased time to menarche (Binder *et al.* 2018). Likewise, positive age acceleration is associated with early menopause (Levine *et al.* 2016). Additionally, the natural onset of menopause itself can act to accelerate DNA methylation age (Levine *et al.* 2016), which then correlates with the increased risk of age-related morbidity and mortality in postmenopausal women (Ossewaarde *et al.* 2005; Finch 2014).
Finally, the number of pregnancies can also affect DNA methylation age acceleration, with an increase in the DNA methylation age associated with each pregnancy (Ryan *et al.* 2018).

In a variety of reproductive tissues, the DNA methylation age is found not to be correlated with the chronological age. This applies for the uterine endometrium, which has a significantly older DNA methylation age (Olesen *et al.* 2018), and with cumulus cells that have a significantly younger DNA methylation age compared with chronological age (Morin *et al.* 2018). Placental tissue was also found not to correlate well with chronological age; however, placental predictors for gestational age have been developed (Mayne *et al.* 2016; Lee *et al.* 2019a). This has revealed that the predicted DNA methylation gestational age in placenta from early-onset preeclampsia patients is accelerated compared with placenta from healthy women (Mayne *et al.* 2016).

2.5 Telomere length variations in ageing

Telomeres are repetitive nucleotide sequences (TTAGGG) at the ends of the chromosomes that protect the chromosomes from degradation rearrangements, end-to-end fusions and chromosome loss during the mitotic divisions (Siderakis and Tarsounas 2007). During the divisions, telomeres are shortened, while telomerase aims counteracting this to maintain the telomeres (Lee *et al.* 2019b). However, despite the activity of telomerase the length of the telomeres will be shortened as a result of DNA replication, oxidative stress, senescence (the state which cells can no longer divide) and ageing (Sanders and Newman 2013). The length will therefore decrease significantly from birth (11-15 kb) to advanced age (~4 kb) (Okuda 2002; Bischoff *et al.* 2012; Kimura *et al.* 2008). The length of the telomeres is therefore considered as an accurate predictor of a given cells ability to replicate and as a biomarker of human ageing (Olovnikov 1996; Mather *et al.* 2011).

Telomere length is normally measured by quantitative PCR and the length reported as a ratio in relation to a standard DNA reference. Several recent studies have associated telomere length with reproductive events. In 2016, the telomere length in granulosa cells determined in women with premature ovarian insufficiency and showed a significantly shorter length compared with healthy controls (Xu *et al.* 2017a). Another recent study found that telomere length in cumulus cells were shorter than telomere length from whole blood cells within the same women (Morin *et al.* 2018). In addition, the telomere length of leukocytes in parous women compared with nulliparous women was shown to be in average 116 base pair shorter for each parity (Pollack *et al.* 2018). Finally, shorter leukocyte telomeres in both male and female partner are associated with idiopathic recurrent pregnancy loss (Thilagavathi *et al.* 2013).

2.5.1 Prediction of telomere length

In 2019, a new DNA methylation-based telomere length estimator was published by Lu and colleagues (Lu *et al.* 2019). This estimator (DNAmTL) was developed from blood samples and is based on 140 CpGs. For leukocytes the DNAmTL association with age is stronger than the measured telomere length association (Lu *et al.* 2019). Moreover, the DNAmTL was shown to be better to predict time-to-death, time to coronary heart disease or time to heart failure than the measured telomere length (Lu *et al.* 2019). Finally, longer DNAmTL was associated with a higher age at menopause, physical activity and healthy diet, which makes it an attractive molecular biomarker of ageing due to its greater sensitivity to age-related conditions and lifestyle (Lu *et al.* 2019).

3. Aim and Objectives

The primary aim of this thesis was to increase our knowledge of age and ovarian reserve and epigenetics involved in the somatic cells of the ovary and blood cells of otherwise healthy women of reproductive age. This knowledge could potentially contribute to the development of a future biomarker for the timing of the loss of fertility, thus allowing women to make informed reproductive decisions. The secondary aim was to identify maternal genes that change with women age using gene expression studies of single human oocytes.

The objectives were:

1. To compare the DNA methylation age of leukocytes and mural granulosa cells with the chronological age of the women.
2. To investigate differences in the DNA methylation profile of leukocytes and mural granulosa cells between women of young (< 30 years) or advanced reproductive age (≥ 40 years).
3. To investigate whether the ovarian reserve influences the DNA methylation age of leukocytes and mural granulosa cells from healthy women of reproductive age.
4. To identify differences in the DNA methylation profile between women with a high, normal or diminished ovarian reserve.
5. To identify genes in MII oocytes that change with reproductive women's age.
6. To consider the possibility of developing a biomarker for ovarian ageing or age-related infertility.

4. Materials and Methods

4.1 Study design

This PhD study is based on prospectively collected material from a multicentre cohort of women undergoing fertility treatment with all the analyses performed retrospectively at the end of recruitment. Buffy coat, plasma, mural granulosa cells, cumulus cells and follicular fluid were collected from all participants. Furthermore, women with more than eight oocytes after retrieval had the opportunity to donate one oocyte.

4.2 The participating women

The women participating in the study underwent fertility treatment (IVF or ICSI) during the period from September 2016 to March 2019 at the fertility clinics at Copenhagen University Hospitals, Herlev Hospital and Hvidovre Hospital, Stork IVF clinic and Center for Reproductive Medicine (RMC) at Skåne University Hospital, Sweden.

Newly referred women at the clinics were screened together with women entering their second or third ovarian stimulation cycle. The women consented to participate after receiving oral and written information. All women were treated with GnRH antagonist protocol for controlled ovarian stimulation. Women were included regardless of their age and AMH level.

Women with PCOS, endometrioses stage III-IV, ovarian cysts on day 1 of stimulation, dysregulated thyroid disease, severe comorbidity (insulin-dependent diabetes mellitus, non-insulin diabetes mellitus, gastrointestinal-, cardio-vascular-, pulmonary, liver or kidney disease) were excluded from the study.

4.2.1 Treatment protocol

The women were treated with a standard GnRH antagonist protocol according to the clinic's guidelines. The initiation of the controlled ovarian stimulation started at day 2 or 3 of the woman's menstrual cycle with recombinant FSH (Bemfola®; Gedeon Richter, Denmark. Gonal-f®; Merck-Serono, Denmark. Pergoveris®, Merck-Serono, Denmark) or urinary derived human menopausal gonadotropin (Menopur®; Ferring Pharmaceuticals, Denmark) for 8-12 days. From day 5 or 6, the women were additionally treated daily with a GnRH antagonist (Orgalutran®; MSD, Denmark). An ovulation trigger of recombinant human chorionic gonadotropin (Ovitrelle®; Merck-Serono, Denmark) or a GnRH agonist (Gonapeptyl®; Ferring

Pharmaceuticals, Denmark) was administered 36 hours before oocyte retrieval for the final follicle maturation and ovulation induction, when the leading follicles reached a diameter of >16 mm.

4.3 The collection of samples

4.3.1 Blood

Two 6 ml peripheral blood samples were collected in ethylenediaminetetraacetic acid (EDTA) tubes during one of the routine ultrasound scan visits in the clinics before the day of the oocyte retrieval. Within one hour of the blood samples being drawn, they were centrifuged at 2000 g at 4°C in 20 minutes to divide the blood into three sections: plasma, buffy coat and erythrocytes. Plasma was transferred to cryovials (377267, Nunc™, Thermo Fisher Scientific™, Denmark) and stored at -80°C in the research biobank for potential later analysis. The buffy coat containing the leukocytes was transferred to cryovials and stored at -80°C for analysis of the DNA methylation profile. The erythrocytes were discarded.

4.3.2 Mural granulosa cells

Mural granulosa cells (estimated cell count per follicle: 100,000 – 1,000,000) were collected simultaneously with the oocyte retrieval by manually isolating blood-free cell aggregates from the follicular fluid. They were washed (10% phosphate-buffered saline (AM9625, Invitrogen™, Thermo Fisher Scientific™, Denmark), sterile water, 1% polyvinyl alcohol (341584, Sigma-Aldrich, Denmark)) followed by centrifugation for 10 minutes at 300 g. The sediment containing the mural granulosa cells was isolated and transferred to a 0.2 ml tube (AB0620, Thermo Fisher Scientific™, USA), snap frozen in liquid nitrogen, and stored at -80°C until analysis. At the same time the cell aggregates were classified as low, medium and high, which indicated which samples individually had a sufficient number of cells/DNA for the later DNA methylation analysis.

4.3.3 Cumulus cells

Cumulus cells (estimated cell count: 500) from four cumulus-oocyte-complexes were mechanically removed (18G needles) and washed twice in washing solution (see 4.3.2), transferred with 5 µl to a 0.2 ml tube, snap frozen in liquid nitrogen, and stored at -80°C in the research biobank within 30 minutes after the oocyte retrieval.

4.3.4 Follicular fluid

Follicular fluid from 4-6 follicles was collected per woman. Immediately after granulosa cell collection, the follicular fluid was centrifuged at 300 g for 10 minutes. The supernatant was transferred and split into three cryovials and stored at -80°C in the research biobank.

4.3.5 Oocytes

The procedure is thoroughly described in the protocol published in Protocol Exchange (Olsen *et al.* 2020c). For ethical reasons only women with more than eight oocytes retrieved had the opportunity to donate an oocyte. Within 30 minutes after oocyte retrieval, the donated oocyte underwent an enzymatic treatment to remove the remaining cumulus cells in 50 µl of hyaluronidase (15115001, SynVitro™ Hyadase, Origio, Denmark), after which it was washed in two 50 µl droplets of washing solution (see 4.3.2). Each oocyte was checked for nuclear maturation (germinal vesicle (GV), metaphase I (MI) or metaphase (MII)) and morphology, then briefly incubated in Tyrode's solution (10605000A, Acidified Tyrodes Solution, Origio, Denmark) to remove the zona pellucida. The zona free oocyte was then washed in two droplets of washing solution. The oocytes were transferred with 2 µl washing solution to a 0.2 ml tube, flash frozen in liquid nitrogen and stored at -80°C in the research biobank until the single cell RNA sequencing analysis.

4.4 Ethics

All human materials were donated under approval from The Scientific Ethical Committee of the Capital Region, Denmark (ethical approval number: H-16027088) and the Danish Data Protection Agency (ID-nr.: HGH-2016_086). The Swedish samples were approved by The Regional Ethical Committee of Lund (registration no: 2017/220).

All samples were anonymized, and no person identifiable data remained on the samples. The study was conducted in accordance with the Helsinki Declaration II and all participants gave informed consent before the inclusion in the study. Furthermore, women donating an oocyte were compensated with an additional ART cycle if pregnancy was not achieved within the three cycles, covered by the Danish national health insurance system.

4.5 Methodology

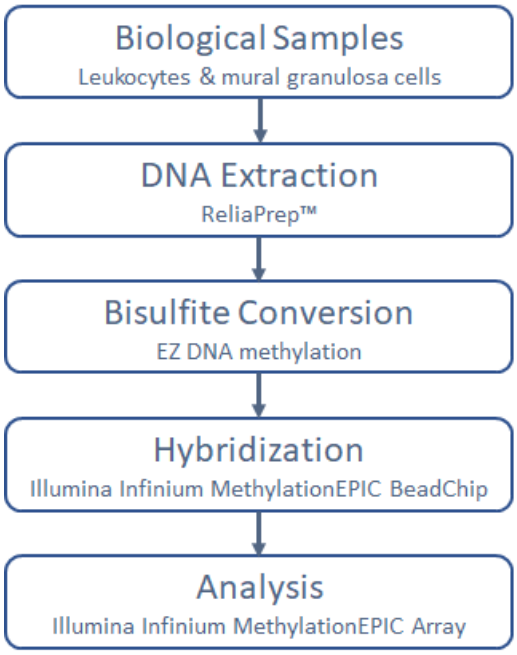

Figure 3 Flow chart describing the methodology.

4.5.1 Selection and preparation of the tested samples

Samples from the 119 women (56 women with only leukocytes, 1 woman with only mural granulosa cells and 62 women with both cell types) analysed in this study were chosen to represent all the included participating women with a diversity in their age and AMH level (Tables I and II (Paper I) and Tables I and SII (Paper II)). Only mural granulosa cells from women with medium or high numbers of cell aggregates were chosen to be analysed to ensure enough DNA input for the later analysis.

4.5.2 DNA isolation

A minimum of 250 ng of DNA was required for the EPIC array analysis therefore, the mural granulosa cells were pooled from several follicles from both ovaries. The leukocytes were collected from the buffy coat fraction derived from 12 ml of peripheral blood. DNA isolation from mural granulosa cells and buffy coat was performed by the Human Genotyping Facility of the Genetic Laboratory of the Department of Internal Medicine, Erasmus MC, the Netherlands. DNA from 1 ml buffy coat and one 0.2 ml tube of pooled mural granulosa cells was isolated with the ReliaPrep™ Large Volume HT gDNA Isolation kit (A2751, Promega, Wisconsin, USA) according to the manufacturer's instructions (Promega 2018). The isolation was performed using the Tecan Freedom EVO®-HSM Workstation.

4.5.3 DNA methylation analysis

After DNA isolation, a total of 500 ng DNA per sample was used for further analysis. The bisulfite conversion was performed using the Zymo EZ-96 DNA methylation kit (Zymo Research, Irvine, CA, USA) (Zymo Research 2019). After the bisulfite conversion, the samples were hybridized to the Infinium Methylation EPIC array, according to the protocol of the manufacturer (Illumina 2015). The genome-wide methylation levels were measured using the Illumina Infinium MethylationEPIC BeadChip (Illumina Inc., San Diego, CA) (Illumina 2015).

4.6 Data analysis

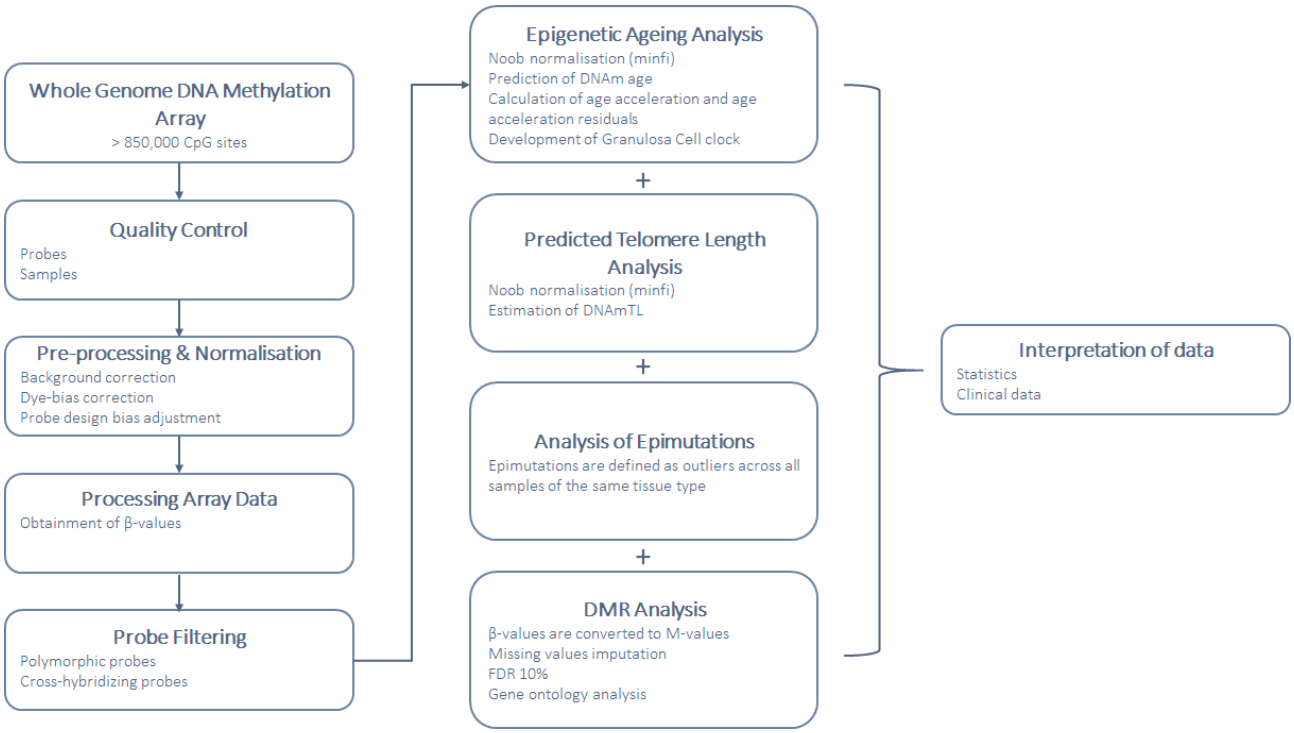

Figure 4 Flow chart of the data processing.

4.6.1 Data processing

Initially, the quality of DNA methylation data was controlled using the control single nucleotide polymorphism (SNP) probes on the array, confirming that the samples were matched correctly. The data was pre-processed and normalised with a background correction using the exponential-normal mixture distribution (ENmix) method using out-of-band type I probe intensities to model the background noise (Xu *et al.* 2016). Furthermore, a dye-bias correction was performed using the regression on logarithm of internal control probes (RELIC) method (Xu *et al.* 2017b). Bias in the probe design was adjusted for by

applying the regression on correlated probes (RCP) method (Niu *et al.* 2016). To obtain methylation β-values from the dataset, i.e. the estimated ratio of intensities between methylated and total (methylated + unmethylated) intensities, the data was processed in R (R Core Team 2016) using the ENmix package (Niu *et al.* 2016). Polymorphic and cross-hybridising probes, defined as probes containing SNPs at the interrogated CpG site and probes mapping to multiple regions, respectively, were filtered using the DMRcate package (Peters *et al.* 2015). Signals from the array with a detection p-value above $1x10^{-6}$ and a number of beads below three, were labelled as missing. CpG sites with missing data in more than five percent of the samples were excluded, as well as samples with missing data in more than five percent of the CpGs.

According to the ENmix quality control function, samples identified with outlier values in bisulfite intensity, total intensity, or β-value distribution were also excluded. Fifty-nine mural granulosa samples remain for the analysis after the quality control together with all 118 samples of leukocytes.

4.6.2 Epigenetic ageing analysis

The first step of the epigenetic ageing analysis was a normal-exponential (noob) normalisation performed in minfi (Aryee *et al.* 2014) to obtain β-values. Afterwards the DNA methylation age was estimated with Horvath's multi-tissue age predictor (Horvath 2013) and the Skin & Blood clock (Horvath *et al.* 2018) using the DNA Methylation Age Calculator (https://dnamage.genetics.ucla.edu/home). The two cell types, mural granulosa cells and leukocytes, were analysed separately. For the further analysis the age acceleration difference was defined as the difference between DNA methylation age and chronological age, while age acceleration residuals were defined as the residuals of DNA methylation age regressed on chronological age.

4.6.3 The Granulosa Cell clock

We developed a Granulosa Cell clock, which correlates with chronological age to estimate the DNA methylation age in mural granulosa cells. By adding the DNA methylation data from 27 mural granulosa cell samples from women with normal AMH level to a subset (n = 621) of the samples used to train the Skin & Blood clock (Horvath *et al.* 2018), we were able to build the clock as described by Steve Horvath and colleagues (Horvath *et al.* 2018). The shared CpG sites (n = 452,567) between the Illumina 450K and EPIC methylation arrays were regressed with a transformed version of chronological age, which had a logarithmic dependence until the age of 20 and linear dependence afterwards. An elastic regression model was used (10-fold cross validation to select lambda) to automatically select the 296 CpG sites included in

the clock. Subsequently, the clock was tested with the remaining 32 mural granulosa cells samples and 118 leukocytes samples, that were not part of the training dataset.

4.6.4 Predicted telomere length

As with the estimation of DNA methylation age, we used the DNA Methylation Age Calculator (https://dnamage.genetics.ucla.edu/home) for the prediction of the DNAmTL. The estimated measures of the telomere length are outputs in which higher values indicates longer telomeres (Lu *et al.* 2019).

4.6.5 Analysis of the accumulation of DNA methylation aberrations (epimutations)

Aberrations in the DNA methylation, which we chose to define as epimutations as also previously described by Gentilini and co-workers (Gentilini *et al.* 2015), were defined as outliers of all samples across the same tissue type. The methylation β-values greater than or less than three time the interquartile range from the upper or lower quartiles, respectively, were used to define the epimutations.

4.6.6 Differentially methylated regions analysis

To study the association between the DNA methylation and ageing we performed an epigenome-wide association study (EWAS) of chronological age. We did an identification of the differentially methylated regions (DMR) in the extremes of our samples (women < 30 years (n = 19) and women ≥ 40 years (n = 6)) by using the DMRcate package (Peters *et al.* 2015). The gene ontology (GO) analysis was performed in R (R Core Team 2016) using the missMethyl package (Phipson *et al.* 2015). Methylation β-values were converted to M-values through a logistic transformation. Missing data were imputed to the mean across all samples of the same cell type and false discovery rate (FDR) was set at 10%. To study the association between differentially methylated regions and AMH level and/or ovarian reserve group, we compared DOR or high ovarian reserve samples to normal controls. We were underpowered to detect genome-wide significant signals with a moderate effect size, due to a limited sample size.

4.6.7 Differential variability analysis of DNA methylation

The DNA methylation variations at each CpG site were tested using the missMethyl package (Phipson *et al.* 2015). In order to identify regions containing multiple neighbouring CpG sites that show evidence of differential variability, we used the DMRcate package in R (R Core Team 2016) allowing for at least two repeated CpG sites. Again β-values were converted to M-values and FDR was set at 5%. All missing data were, as with the DMRs, calculated to the mean across all samples of the same tissue type.

The missMethyl package (Phipson *et al.* 2015) in R (R Core Team 2016) were also used for the GO analysis accounting for the different number of probes per gene in the array.

4.7 Single cell RNA sequencing

The cDNA was prepared with SMART-Seq v4 Ultra Low Input RNA kit (TaKaRa, CA, USA) through a workflow of lysis, first strand synthesis and cDNA amplification. The Nextera XT DNA Library Preparation kit (FC-131-1024, Illumina, CA, USA) was used to construct the libraries from the cDNA. AMPure XP beads (A63880, Beckman Coulter, IN, USA) was used for purifying the cDNA and the libraries.

4.7.1 Library preparation

The cells were lysed individually at room temperature for 5 minutes directly in the collection tubes. A mixture of 1 µl lysis buffer containing RNase inhibitor and nuclease water up to a volume of 11.5 µl was added to each sample tube. For the first strand synthesis 1.5 µl of 3' SMART-Seq CDS Primer II A (TaKaRa, CA, USA) was added and shortly incubated at 72°C (for 3 minutes). A master mix of SMART-Seq v4 Oligonucleotide and SMARTScribe Reverse Transcriptase was added to each sample and the samples were placed on a thermal cycler and run through the program specified by the manufacturer. The cDNA was then amplified with PCR Primer A and SeqAmp DNA polymerase for 15 cycles on the thermal cycler according to the protocol. The cDNA was purified by AMPure XP beads (A63880, Beckman Coulter, IN, USA) with 50 µl AMPure XP beads per sample, two washes with 80% chilled ethanol and the cDNA eluted with 13 µl Elution buffer. At last, the cDNA was quantified on the Qubit Fluorometer (Q33216, Qubit® 3.0 Fluorometer, Thermo Fisher Scientific™, Denmark) using dsDNA High Sensitivity Assay kit (Q32851, Thermo Fisher Scientific™, Denmark).

4.7.2 Library construction

For the tagmentation of the cDNA, Amplicon Tagment mix and Tagmentation DNA buffer were incubated together with 1 µl of each 0.2 ng/µl sample (Nextera XT DNA Library, FC-131-1024, Illumina, CA, USA). This tagmented DNA was enriched by a final PCR reaction during which the unique indexes were added, thus allowing for the pooling of individual libraries. The PCR product was purified with AMPure XP beads (A63880, Beckman Coulter, IN, USA) in a 1:0.6 ratio, washed and eluted with 18 µl Elution buffer. The final library was again quantified with the Qubit Fluorometer High Sensitivity Assay kit and the Bioanalyzer High Sensitivity DNA kit (5067-4626, Agilent Technologies, CA, USA). Finally, 1.5 picomolar (pm) of the pooled libraries were sequenced at the Illumina NextSeq550 (Illumina, CA, USA) at the Biotech Research & Innovation Centre, University at Copenhagen, Copenhagen, Denmark.

4.7.3 Gene expression profiling

The data processing from the single cell RNA sequencing (scRNA-seq) is thoroughly described in paper III and is based on the protocol from Sankar et al. (Sankar *et al.* 2020).

The data was transformed and multiplexed to generate one set of paired fastq files per sample, which subsequently went through quality control and filtering to remove low quality reads and bases, and adaptor sequences. Then, the data was aligned to a human reference genome and new generated files were sorted, indexed and transformed before they were normalized and downsampled.

The 11 MII samples were divided into two age groups (< 35 years (n = 8), > 36 years (n = 3)) and a differential expression analysis was made followed by a principal component analysis (PCA) and hierarchical cluster in R (R Core Team 2016). A functional enrichment analysis was performed on the differentially expressed genes by using Molecular Signatures Database (https://www.gsea-msigdb.org/gsea, Broad Institute, San Diego, CA, USA).

4.8 Statistical analysis

In papers I and II, the difference between age groups and ovarian reserve groups were tested by a one-way ANOVA and a Wilcoxon test post hoc was used to compare epimutation rates between the cell types.

A Fisher's exact test was used in paper I to test the enrichments of gene categories. A Kruskal-Wallis test was used to compare epimutation rates, DNAmTL and age acceleration in paper II. The association between AMH levels and DNAmTL was tested with linear regression analysis. The Pearson coefficient was used to estimate the accuracy of the different clocks, together with the median error (the absolute difference between DNA methylation age and chronological age). The value of $p < 0.05$ was considered statistically significant.

The age of the women used in our analysis was determined at the time of oocyte retrieval and the subgrouping of women by ovarian reserve status was based on data from Lee et al. (Lee *et al.* 2012). Women with the lowest age-related AMH level (5^{th} and 10^{th} percentiles) were categorised as DOR, women with the medium age-related AMH level (25^{th} to 75^{th} percentile) were categorised as 'normal' and women with the largest age-related AMH level (> 90^{th} percentile) were categorised as 'high'.

In paper I, we tested if adjustment for AMH (in the age acceleration analysis) influence the results, but we found no effect. Neither found we any association between FSH dose and the results. As a result, no adjustments were included in the analysis.

In paper II, we adjusted for age in the age acceleration and DNAmTL analyses.

In paper III, the difference between the two age groups was tested according to the DeSeq2 dispersion model and Benjamini-Hochberg adjusted *p*-values of the Wald DESeq2 performs an internal normalisation that corrects for library size and RNA composition bias. During the normalisation process, the count measure, for a gene in each sample, is divided by its geometric mean across all samples. The median of these ratios in a given sample is the normalizing size factor for that sample. Rlog transformation of count data to log2 scale was performed and the differential analyses was performed by estimating a dispersion (variance) value for each gene by fitting a negative binomial generalized linear model followed by the Wald test for significance testing of differences in expression between the age groups.
A gene is differentially expressed if Benjamini-Hochberg adjusted p-values < 0.05 by the Wald test and a FC > 1.5 (Love *et al.* 2014). Functional enrichments were determined by the one-sided version of Fisher's exact test with $p < 0.001$ and q-value < 0.05.

5. Summary of the results

Over a 2.5-year period we recruited 211 women (four were later excluded) to the study, the majority (n = 170) were included at the Fertility Clinic at Herlev Hospital and 13, 18 and 10 women were included at Hvidovre Hospital, RMC and the private clinic Stork IVF, respectively. The cohort was in average 33.9 years old with an AMH level at 20.6 pmol/L including 51 women with diminished ovarian reserve (Table 1). Approximately 25% of the women were infertile due to female factor, which for most of the participants were due to advanced reproductive age.

Only women from the Fertility Clinic at Herlev Hospital had the opportunity to donate an oocyte along with their granulosa cell and leukocyte samples. A total of 29 oocytes were collected (GV: 1, MI: 4, MII: 22), two oocytes were unfortunately lost or lysed.

The dataset used in paper I and II is a subset of this cohort and includes 119 women and two different cell types (mural granulosa cells (n = 63) and leukocytes (n = 118)). The women in the studied group were selected in the spring of 2018 to represent the range of included women regarding both age and AMH level. Samples of mural granulosa cells were chosen to ensure a sufficient number of cells for the further analysis. Besides the total FSH dose received during treatment, no difference in the clinical and demographic data were found between the cohort and the study group (Table I).

5.1 Paper I: A distinctive epigenetic ageing profile in human granulosa cells.

In the first paper we showed that mural granulosa cells have a distinctive epigenetic ageing profile compared with leukocytes from the same woman. Adjustments for AMH did not affect the results and were therefore not included in the final analysis.

The DNA methylation age in the mural granulosa cells was considerably younger (average: 2.7 years) than both the chronological age (average: 33.9 years) and the DNA methylation age of the leukocytes (average: 33.0 years) (Figure 5). This resulted in the development of a Granulosa Cell clock able to predict the chronological age of the mural granulosa cells (average: 32.4 years) and the leukocytes (average: 38.8 years) within our sample population. In order to study various aspects of the ageing process, we investigated the number of epimutations in the two cell types. We found that the number of epimutations was increased with increasing reproductive age, and that mural granulosa cells had a significantly higher number of epimutations compared to leukocytes (p = 0.0026).

Table I. Demographic and clinical characteristics of the participant population from all recruited women in Denmark and from the study group used in paper I and II.

	Study group (Paper I and II)	**Subgroup** (not incl. in paper I and II)	**All recruited women in Denmark**	**One-way ANOVA**
Number	119	72	191	-
Age at oocyte retrieval (years)	33.9 ± 4.7	33.9 ± 4.2	33.9 ± 4.5	0.9338
AMH (pmol/L)	23.5 ± 20.9	16.4 ± 12.9	20.6 ± 18.5	0.0117
Ovarian reserve category				
- DOR	28	23	51	-
- Normal	65	44	109	-
- High	26	5	31	-
Primary cause of infertility				
- Male factor	34	17	51	-
- Female factor	28	18	46	-
- Unexplained	39	19	58	-
- Other causes*	18	18	36	-
FSH (IU/L)	7.8 ± 6.4	7.8 ± 6.5	7.8 ± 6.4	0.9839
LH (IU/L)	7.1 ± 6.9	6.5 ± 7.1	6.9 ± 6.9	0.6912
LH/FSH ratio	1.04 ± 0.8	0.8 ± 0.5	1.0 ± 0.7	0.2058
Prolactin (IU/L)	295 ± 135	264 ± 149	282 ± 141	0.2949
TSH (IU/L)**	1.7 ± 0.8	0.9 ± 1.0	1.0 ± 1.0	0.0870
Total FSH dose (IU)	1853 ± 970	2500 ± 1113	2144 ± 1083	6×10^{-5}
Stimulation duration (days)	9.5 ± 2.7	9.8 ± 2.6	9.6 ± 2.7	0.3518
Cycle Characteristics				
No. of oocytes	8.1 ± 5.3	7.4 ± 5.1	7.9 ± 5.2	0.3207
No. of 2PN zygotes	4.2 ± 3.4	3.7 ± 2.9	4.1 ± 3.2	0.2499
No. of clinically usable embryos	2.3 ± 2.5	1.9 ± 0.6	2.3 ± 2.3	0.1183
Utilization rate***	0.6 ± 0.3	0.6 ± 0.4	0.6 ± 0.4	0.7793

Mean ± standard deviation.

*Single women and women with a female partner.

**Baseline measurement.

*** No. of clinically useable embryos divided by the no. of 2PN zygotes.

Another biomarker of ageing is the length of the telomeres. We found the DNAmTL was unaffected by age (cor = -0.1, $p = 0.47$) in the mural granulosa cells. In the leukocytes, however, we found a negative correlation with the woman's age (cor = -0.62, $p = 4.0 \times 10^{-14}$). When studying the relationship between DNA methylation and ageing we identified DMRs associated with age almost exclusively in the mural granulosa cells (n = 335) (leukocytes, n = 1). After performing a GO analysis, we found that the 335 DMRs had a significant enrichment for genes involved in RNA processing (45 genes, $p = 3.96 \times 10^{-08}$) and gene expression (152 genes, $p = 2.3 \times 10^{-06}$). The most significant signals in the epialleles were; *VTRNA2-1*, *ZFP57* and the *AMH* gene. By investigating these different characteristics of the DNA methylation profile, we may have

identified unique aspects of ageing within the mural granulosa cells. We can only speculate, that the age-associated epigenetic changes (the higher number of epimutations and age-DMRs) in the somatic cells of the follicle affect their function and thereby their support of the oocyte.

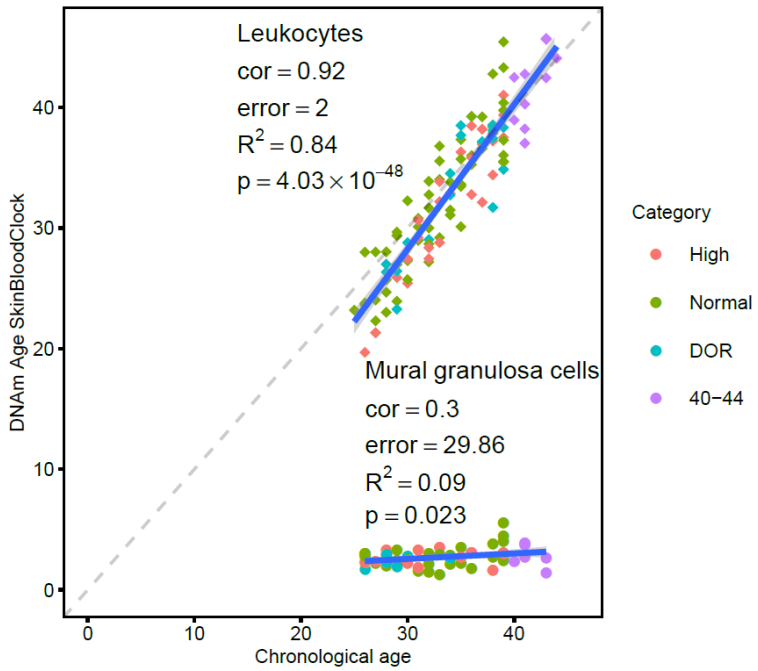

Figure 5 DNA methylation age in leukocytes and mural granulosa cells. Ovarian reserve categories are defined as 'High' (red), 'Normal' (green), 'Diminished ovarian reserve (DOR)' (blue) and advanced reproductive age (40-44 years) (purple). Figure 1A from paper I (Olsen *et al.* 2020b).

5.2 Paper II: Identification of a unique epigenetic profile in women with diminished ovarian reserve.

In the second paper we showed that DNA methylation profiles from mural granulosa cells from women with DOR are different compared to women with a normal or high ovarian reserve. We found greater differential variability in the DNA methylation profile of mural granulosa cells from women with DOR when compared with women with a normal ovarian reserve (4,199 CpGs) and relatively smaller differential variability in mural granulosa cells between 'high' and 'normal' (447 CpGs) (FDR < 0.05) (Figure 6). Only few signals were detected in the DNA methylation variability analysis between the leukocytes from the three levels of ovarian reserve and no overlaps with the signals in mural granulosa cells were found. Interestingly, the greater variability observed in mural granulosa cells of the DOR group was found in genes with central function in ovarian folliculogenesis such as *AMH* and *IGF2*, among others. The variable CpGs in the DOR group enriched the regions of H3K27me3, which is a chromatin modification associated with heritable gene silencing (Simon and Kingston 2009) and suggested to be inhibited in response to hCG stimulation (Okada

et al. 2016; Maekawa *et al.* 2016). This finding may reflect an altered effect of LH on the mural granulosa cells in the follicle in women with DOR. Furthermore, we found a higher number of epimutations in the DOR group exclusively in mural granulosa cells, but not in the leukocytes.

The analysis on the telomere length and AMH level category, revealed a significantly higher DNAmTL in the DOR group in both the mural granulosa cells and in the leukocytes compared with the 'normal' and 'high' group ('normal' group: leukocytes: $p = 0.008$, mural granulosa cells: $p = 0.0001$; 'high' group: leukocytes: $p = 0.028$, mural granulosa cells: $p = 0.013$).

Women with DOR have a distinctive DNA methylation profile in their mural granulosa cells compared to women with a higher AMH level. The same does not apply for leukocytes. We suggest that the unique epigenetic profile found in women with DOR could potential be a future target or biomarker for women with pathological or physiological loss of fertility.

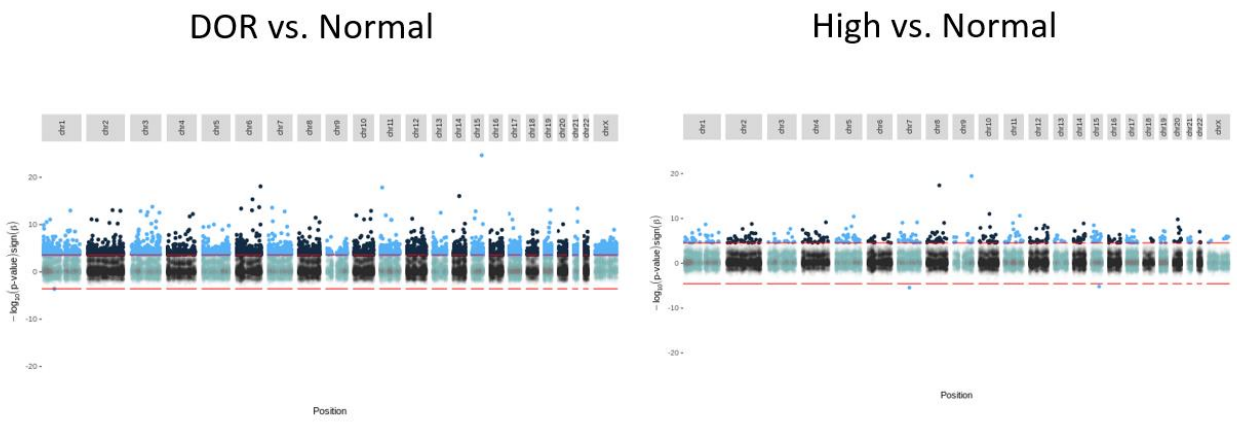

Figure 6 DNA methylation variability in mural granulosa cells. A great variability is found in mural granulosa cells from women with diminished ovarian reserve (DOR) and high ovarian reserve. The variability is, however, more pronounced in the DOR group. Figure 3C and 3D from paper II (Olsen *et al.* 2020a).

5.3 Paper III: Gene expression profile of human metaphase II oocytes in relation to age by single cell RNA sequencing.

The last paper comprises single-cell RNA-sequencing data from eleven MII from the recruited cohort. Here we found 315 differentially expressed genes in the oocytes when comparing women with advanced reproductive age with women of young reproductive age. Of the differentially expressed genes, 187 were downregulated in women with advanced reproductive age. These were characterized by being involved in

cell cycle, mitosis, nuclear division etc (gene examples: *CDC20*, *CHEK1*, *KIEF4*). The last 128 differentially expressed genes, on the other hand, were upregulated in the older MII oocytes and were coding for mitochondrial function, oxidative phosphorylation and metabolic processes (gene examples: *TIMM10*, *NDUFS5*, *ATP5H*).

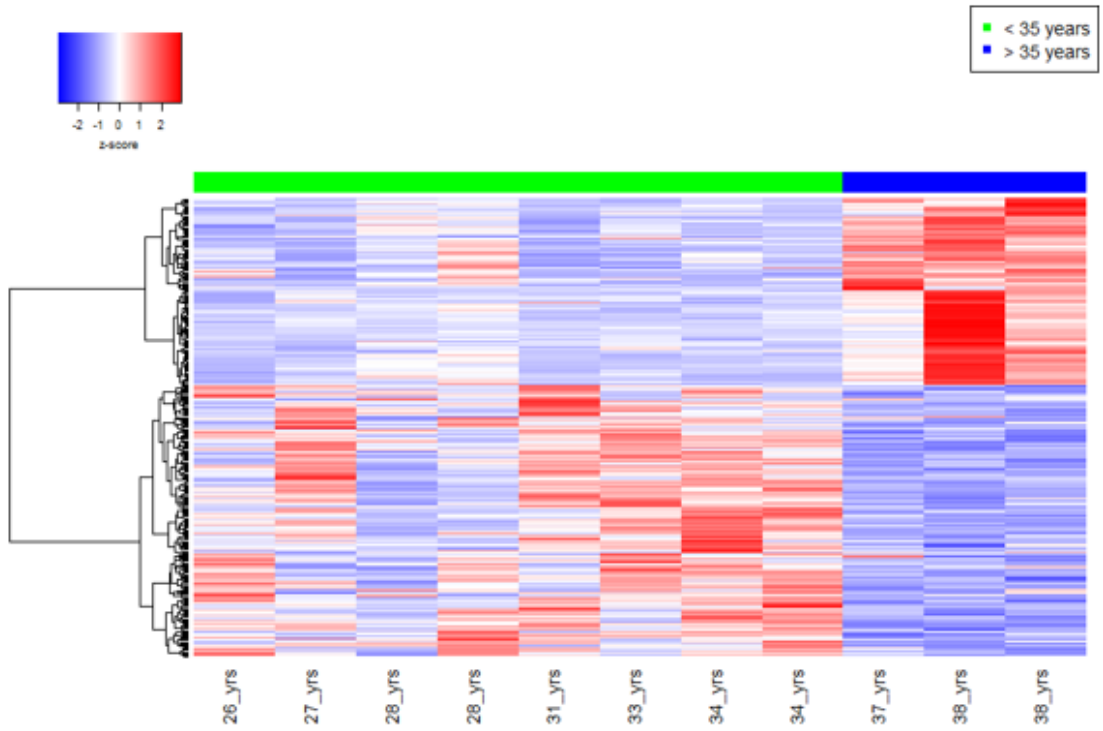

Figure 7 Hierarchical cluster of 315 differentially expressed genes. Upregulated (red) genes in the MII oocytes from women of advanced maternal age is involved in mitochondria organization and function, while downregulated genes (blue) are involved in cell cycle, mitosis and chromosome segregation. Figure 1A from paper III (Olsen *et al.* 2020d).

6. Discussion and future perspectives

In this PhD project we investigated the epigenetic and gene expression profiles of cells from the human ovarian follicle with respect to age and ovarian reserve. A comprehensive discussion of the results is found within the three resulting papers. The following discussion provides a broader evaluation of the methodology, the implications of our findings and directions for future research.

Infertility is not only a biological problem, but also a socioeconomic problem for society in countries where the fertility rate is below a replacement level of 2.1 children per woman (Craig 1994)[2]. With increasing age, female fertility decreases due to a decline in the quantity and quality of the oocytes. Many fertility awareness campaigns have been broadcasted to encourage women to have children at a younger age. But campaigns such as '*Beauty has no age. Fertility does.*' (Fertility day 2016, Italy), '*Advancing age decreases your ability to have children*' (Seattle News and Events, 9 October 2006, USA), '*Have you counted your eggs today*?' (City of Copenhagen and Copenhagen University Hospital, Rigshospitalet, 2015, Denmark) or as Dr Meenakshi Choudhary has expressed it: '*Pick Mr Good Enough!'* (Dr Meenakshi Choudhary, the Ovarian Club annual meeting in Paris 2019) have also provoked many young women who for many reasons may decide to delay childbirth (Nielsen 2015; Sørensen *et al.* 2016). By finding a clinical biomarker for ovarian ageing, it will allow a woman to plan the time for pregnancy according to her own life and her own biology. However, the molecular and cellular mechanisms of ovarian ageing and the age-related decline in female fertility remain unclear (Wang *et al.* 2020) and more research in this subject is therefore needed.

The objectives of this thesis were to investigate the methylation age and methylation profile of mural granulosa cells and leukocytes from women of different ages and different levels of ovarian reserve. Furthermore, we aimed to investigate the gene expression alterations in mature oocytes from reproductively younger and older women undergoing fertility treatment.
To our knowledge, we are the first to analyse the DNA methylation profile in mural granulosa cells from the human ovarian follicle in relation to healthy women's age and detailed ovarian reserve. In addition, we have contributed with knowledge in this new field of identifying age-related differences in the gene expression profile in MII oocytes using scRNA-seq.

[2] Replacement level in Denmark: 1.7 (Statistics Denmark 2019).

6.1 Evaluation of the methodology

6.1.1 Sampling

The samples used in this project were collected from women undergoing ovarian stimulation due to male factor or idiopathic female infertility, as single women, women with a female partner or female factor e.g. tubal factor. However, even though the project was designed to avoid selection bias we cannot exclude that some of these women have an unknown cause of infertility that might influence the data. In contrast to if we had women recruited from outside the fertility clinics with no fertility problems.

One limitation in our study is that we have no data from women in the early end of the female reproductive lifespan. The participants were in the range of 25 to 44 years old. In the Capital Region of Denmark women are in average older when having their first child compared to women outside the Capital Region (30,5 years vs. 28,3 years in Region Zealand (Statistics Denmark 2020)). If we had included a clinic outside the Copenhagen area, we might have been able to include a few young women within the youngest age range. This would have allowed us to include data from women in both ends of the reproductive age range.

We divided the women into subgroups according to their AMH level based on the age-related distribution of AMH levels published by Lee et al. (Lee *et al.* 2012). We defined DOR broadly as the women who had an AMH level below the 10th percentile. For future research it would be interesting to restrict inclusion to women with premature ovarian insufficiency (POI) potentially representing a more uniformly challenged group. The European Society of Human Reproduction and Embryology (ESHRE) guideline from 2016 suggests that the diagnosis criteria of POI are oligo/amenorrhea for at least four months together with an elevated FSH level > 25 IU/l on two occasions more than four weeks apart (ESHRE 2016) in women under the age of 40 years. However, as POI only represents 1% of a population (Krailo and Pike 1983; Cooper *et al.* 2011; Cramer and Xu 1996; Luborsky *et al.* 2003), the patient recruitment and sampling of sufficient number of mural granulosa cells for analysis would be rather challenging.

For DNA methylation analysis of the mural granulosa cells, samples were selected based upon number of cells to ensure a proper yield of DNA to fulfil the requirement for the EPIC array. Even though we aimed to include women representing the whole cohort, we avoided women with very few follicles at oocyte retrieval and therefore had few cells isolated. These samples could instead have been used for single cell bisulfite sequencing, allowing us to represent women with very low ovarian response to controlled ovarian stimulation. During the collection of the mural granulosa cells, we cannot exclude the risk that other cell

types (e.g. blood cells) have been collected together with the granulosa cells. However, we avoid cell aggregates with visible blood clots and previous studies have shown a minimal blood contamination in such granulosa cell samples (Raad *et al.* 2020; Grøndahl *et al.* 2009).

6.1.2 DNA Methylation array vs. Whole genome bisulfite sequencing

The age predictors used in this project (Horvath 2013; Horvath *et al.* 2018) were developed with data from both the Illumina 450K and EPIC platform, which was one of the reasons why we chose the EPIC array for our DNA methylation analysis. However, since the predictors did not work well in mural granulosa cells, it would be interesting to perform a study with WGBS, allowing us to investigate the whole genome methylation ageing profile in more details. Another interesting project would be single cell bisulfite sequencing of the granulosa cells from single follicles in order to compare the DNA methylation profile of the follicles together with the oocyte competence. However, sequencing is still an expensive method, which also requires proper skills to analyse the large amount of data produced. In contrast, the EPIC array is cheaper and provides a lot of information about the methylome, specifically at the promotor sites (Pidsley *et al.* 2016).

6.1.3 Bioinformatic considerations to the EPIC array and the analysis

The development of the EPIC array has allowed for large-scale epigenome-wide studies at single CpG site resolution (Xu *et al.* 2016). The array is based on measuring probe hybridization intensities of bisulfite-converted DNA to estimate the relative number of methylated and unmethylated cytosines at selected loci (Xu *et al.* 2016). However, these quantitative measures are sensitive to variations in the experimental set-up, therefore, a number of different pre-processing methods have to be included to improve the methylation array quality. The initial step in the pre-processing pipeline is the background correction, for our study we used the ENmix method (Xu *et al.* 2016), allowing us to model the methylation signal intensity with a flexible exponential-normal mixture distribution, together with a truncated normal distribution to model background noise (Xu *et al.* 2016). The EPIC array measures the intensities of two different colour channels, which means that there is background noise from the probe around, and the red and green channels will give different intensities. We therefore used RELIC for dye bias correction, which is a method based on properties observed in paired internal normalisation control probes (Xu *et al.* 2017b).

For the probe design bias adjustment, we used RCP, which uses the existing correlation between pairs of nearby Infinium I and II probes to adjust the beta values of all Infinium II probes (Niu *et al.* 2016). Normally, the use of two chemistries (Infinium I and II) increase the CpG coverage across the genome, but the two

different probes also have an unequal dynamic range (Niu *et al.* 2016), thus making the probe adjustment necessary. Both RELIC and RCP are implemented in the ENmix package developed by Xu and colleagues (Xu *et al.* 2016).

After the pre-processing and normalisation, we excluded bad quality samples and bad quality probes based on the number of missing data points (5% cut-off). Probes targeting a CpG that is a SNP were excluded, because the readout would reflect the genetic variation and not the change in methylation. Lastly some probes were excluded because they were found to be non-specific and targeted multiple regions of the genome.

6.1.4 Microarrays vs. Single cell RNA-sequencing

It has previously been technically challenging to study the gene expression profile in a single cell. Additionally, *in vivo* matured MII oocytes from women undergoing fertility treatment are a limited resource for both practical and ethical reasons. For these reasons, previous studies have mainly investigated the gene expression of *in vitro* matured oocytes or GV oocytes. The few studies conducted using single *in vivo* matured MII oocytes (Grøndahl *et al.* 2010; Battaglia *et al.* 2016; Barragan *et al.* 2017; Santonocito *et al.* 2013) show different gene expression profiles in genes involved in cell cycle regulation, chromosome alignment, sister chromatid separation, and oxidative stress. However, these studies are limited by the number of oocytes (as the present study) and/or the technology used (microarray). As sequencing has become cheaper, the use of microarrays has decreased and has shifted towards sequencing. Sequencing is a more sensitive technique and has a much more dynamic range in detecting transcripts. In paper III, we used scRNA-seq, which has the advantage of detecting differences on single cell level and not only in a bulk of cells. Bulk pooled oocytes are often used in studies when multiple oocytes from the same individual are available, as in animal studies or studies connected to ovarian tissue cryopreservation programs. In contrast, since the study in paper III only had one oocyte from each woman, the scRNA-seq allowed us to associate the gene expression with an individual clinical data point. However, our study was a small pilot study and we have therefore not utilized the full potential of the method. But now with our data and the recently published data from Zhang et al. and Barone et al. (Zhang *et al.* 2020; Barone *et al.* 2020) a larger study will be interesting to carry out using the full sequencing potential to investigate the full transcriptome profile of aged MII oocytes.

6.2 Epigenetic ageing

One of the nine hallmarks of ageing is epigenetic alterations (Lopéz-Otín *et al.* 2013). In paper I and II we found a distinctive methylation profile in mural granulosa cells from women of advanced reproductive age and women with DOR when compared with younger women and women with a normal or high ovarian reserve, respectively. Interestingly, differences were found in genes involved in female reproduction (*AMH)*, regulation of cell growth (*VTRNA2-1*), transcriptional regulation of genetic imprinting maintenance (*ZFP57*), and growth-promoting activity (*IGF2*). We also found that the predicted telomere length was unaffected by age in the mural granulosa cells; however, in women with DOR we found higher values of DNAmTL in both leukocytes and mural granulosa cells. We found that the DNA methylation age was very young in mural granulosa cells, which led us to the development of the Granulosa Cell clock. We found no significant differences between the ovarian reserve groups, but using the Granulosa Cell clock a tendency towards an increased age in the leukocytes from high to diminished ovarian reserve was observed. Therefore, future studies with only the most extreme samples (only < 5^{th} percentile age dependent AMH level, or POI) might show an accelerated DNA methylation age.

It might seem counterintuitive to have lower DNA methylation age and a higher epimutation rate in mural granulosa cells. These two outcomes, however, might be associated with different aspects of ageing and influenced by the unique biology of mural granulosa cells and the ovarian follicle. For instance, mural granulosa cells may experience a similar, fixed process of proliferation and expansion once the follicle is activated irrespective of when during the woman's life course it occurs; in contrast, with increasing age, the length of time that the follicle has remained in the dormant state increases. Thus, if telomere length and predicted DNA methylation age are properties associated with the same biological events, these parameters will be similar whatever the chronological age of the donor. The increase in epimutations we observe with age in mural granulosa cells might therefore indicate that these DNA methylation aberrations are accumulating more in the period of extended follicle dormancy. A study from 2015 using Next Generation Sequencing and Reduced Representation Bisulfite Sequencing showed changes in the transcriptome and methylome in mural granulosa cells as the women age and their ovarian function decline (Yu *et al.* 2015). They also found age-related changes in the *AMH* gene, which supports our findings from paper I and II, where we found the *AMH* gene as the second most significant signal in differential methylation regions associated with age in mural granulosa cells. Additionally, in mural granulosa cells from women with DOR the *AMH* gene had a high variability in the DNA methylation.

After the development of the Granulosa Cell clock, we successfully tested it on publicly available DNA methylation data from granulosa cells (Makrinou *et al.* 2019). So, while our clock still needs to be validated on other follicle cell types (e.g. cumulus cells), we are confident that it has potential to be used to study female infertility in subgroups of women (e.g. with POI, PCOS and endometriosis). Future studies are needed to investigate whether such diseases affect the DNA methylation age of the cells within the follicle.

6.3 Gene expression in mature oocytes

Despite the small samples size we were able to detect changes in the gene expression profiles of MII oocytes from women who all had more than eight oocytes retrieved, but who had different chronological age (26-38 years) and a normal ovarian reserve (13-38 pmol/L). We found that 315 genes were differentially expressed, when comparing the young MII oocytes with the older MII oocytes. These genes were primarily involved in cell cycle, mitosis, mitochondria organization and function. Barone and coworkers found 1852 dysregulated genes in MII oocytes from women between < 35 years and ≥ 35 years (Barone *et al.* 2020), while Zhang et al. found 357 differentially expressed genes when comparing oocytes from women ≤ 30 years and ≥ 40 years (Zhang *et al.* 2020). Likewise, our results, they also found these genes associated with cellular processes such as cytoskeleton organization and oxidative stress (Barone *et al.* 2020; Zhang *et al.* 2020). A larger study with more age groups (e.g. 20-25 years, 26-30 years, 31-35, 36-40 and > 40 years) could be interesting to carry out in order to investigate and narrow down, when the change in the expression profile is occurring and to confirm if transcriptome profiling of human MII oocytes can be used as a biomarker for oocyte quality as suggested by Barone and colleagues (Barone *et al.* 2020). However, such a study requires multiple MII oocytes, which unfortunately is a rare resource in human reproduction research.

6.4 Biomarker for ovarian ageing

Since 2011, as a part of a research project, men, women and couples in Copenhagen have had the opportunity to receive fertility counselling at one of the public fertility clinics at the Copenhagen University Hospitals in the Capital Region of Copenhagen. The project has been a success and many single women have participated to get an assessment of their reproductive potential (Sylvest *et al.* 2018; Birch Petersen *et al.* 2015). At the counselling a questionnaire, a transvaginal ultrasound scan and measurement of AMH level combined give the woman an assessment of her fertility. However, these are still just estimates and the need for a more precise biomarker for ovarian ageing is still needed to better forecast a woman's reproductive lifespan. Such a biomarker could very well be an epigenetic biomarker, perhaps used in combination with other markers such as AMH and/or FSH to assess a woman's future fertility.

The development of an epigenetic clock to predict onset of menopause or ovarian ageing is a desirable clinical tool to help women find the best time for pregnancy. Our studies showed, that women with DOR have a higher number of epimutations, greater variability in the DNA methylation profile and higher values of DNAmTL in the mural granulosa cells. A biomarker using mural granulosa cells would be invasive and would therefore only be suitable for women undergoing ART treatment. A biomarker in blood would be easier and more applicable, but further studies are needed to investigate whether the methylation age of leukocytes from women with female infertility is different from healthy women. A case control study performed with healthy women who become mothers spontaneously compared with women having a diagnosis of female infertility could provide insight into any variation in leukocyte methylation patterns that may impact the use of this blood biomarker. On the other hand, the ovary has a special environment and it may not be possible to find a biomarker in the blood that truly reflect the condition of the ovarian follicles. However, a recent study showing a decreased oocyte yield in women undergoing ovarian stimulation having an accelerated epigenetic age of their blood cells (Monseur *et al.* 2020), suggesting that we in the future may be able to help women accessing their reproductive age/potential more precisely by an epigenetic assessment.

6.5 Infertility as biomarker for future health

It has for a long time been debated and suggested that fertility is a marker of longevity and infertility is a risk factor for all-cause mortality later in life (Senapati 2018). Perturbations in female reproduction have shown to be associated with cancer, cardiovascular disease and mortality (Zeng *et al.* 2016).
Equally, abnormal methylation is associated with cancer, neurological and immunological diseases, atherosclerosis and osteoporosis (reviewed in (Ehrlich 2019)). We already know that age is one of the greatest risk factors for morbidity and mortality (Harman 1991) and women with POI have shown to have a greater risk of osteoporosis, cardiovascular disease, immunological diseases and a shorter life expectancy (Podfigurna-Stopa *et al.* 2016; Shuster *et al.* 2010). Already in 1946, case-reports indicated that women with POI have an increased risk of the rare granulosa cell tumours (Rhoads 1946). We can only speculate that the change in the methylated profile with increased age and with DOR plays a role in development of disease later in life. Further follow up studies with women with DOR or register studies showing the health outcomes in infertile women would elucidate whether any initiation of preventive actions is needed as a part of the fertility treatment.

6.6 Limitations

One limitation in this study, is that we had to choose women with enough mural granulosa cells collected to ensure a sufficient amount of DNA for the methylation analysis. The samples included in this study may therefore represent a selected group, since samples from women with very few follicles retrieved and a low number of mural granulosa cells in the follicular fluid were excluded. However, we were still able to include women with diverse AMH level. Originally, we planned to compare the methylation profile of the mural granulosa cells from single follicles, but we had to change our strategy when preliminary experiments showed too low DNA yield. Furthermore, all our samples were collected during ovarian stimulation which may influence DNA methylation; however, we found no correlation between FSH dose and the number of epimutations in the mural granulosa cells, which suggests this was not the case. In paper III, we could for practical and ethical reasons not collect *in vivo* matured oocytes in other set-ups and it is therefore impossible to know whether the gene expression will differ in MII oocytes collected in a natural cycle.
A gene expression analysis of the mural granulosa cells and leukocytes could have been interesting to include to investigate whether the epigenetic changes also have a functional affect. Unfortunately, the number of cells were limited in our mural granulosa cells samples and the whole samples were used for DNA isolation for the EPIC array analysis. An additional analysis was therefore not possible but should be considered to include in future studies.

7. Conclusion

In conclusion, the results of this PhD project describe the DNA methylation profile of leukocytes and mural granulosa cells from healthy women undergoing IVF or ICSI treatment. From a subgroup of these women preliminary data identified differentially expressed genes between young and older MII oocytes involved in cell cycle, mitosis, oxidative phosphorylation and mitochondrial function. To our knowledge, we are the first to perform this analyse with DNA methylation profiling of mural granulosa cells from the human ovarian follicles from healthy women and by adding knowledge of the molecular mechanisms of ovarian ageing, we may have come closer to the development of a biomarker for female reproductive ageing.

The study has revealed that granulosa cells are very different from other somatic cells in the body. Even though we already knew that granulosa cells have a characteristic life cycle with many years or decades of quiescent in the ovary, it was fascination to find that they indeed have a distinctive epigenetic ageing profile and that the methylation profile also differs within women with DOR compared with women with a normal ovarian reserve.

Collectively, the PhD project enlighten our understanding of the genetic and epigenetic ageing process of the cells of the human ovarian follicle.

8. References

Abedel-Majed MA, Romereim SM, Davis JS, and Cupp AS. Perturbations in Lineage Specification of Granulosa and Theca Cells May Alter Corpus Luteum Formation and Function. *Front Endocrinol (Lausanne)* 2019: 832.

Abma JC, Chandra A, Mosher WD, Peterson LS, and Piccinino LJ. Fertility, family planning, and women's health: new data from the 1995 National Survey of Family Growth. *Vital and health statistics. Series 23, Data from the National Survey of Family Growth* 1997.

Andersen CY, Schmidt KT, Kristensen SG, Rosendahl M, Byskov AG, and Ernst E. Concentrations of AMH and inhibin-B in relation to follicular diameter in normal human small antral follicles. *Hum Reprod* 2010; **5**: 1282-1287.

Anderson RA. What does anti-Mullerian hormone tell you about ovarian function? *Clin Endocrinol (Oxf)* 2012; **5**: 652-655.

Aran D, Toperoff G, Rosenberg M, and Hellman A. Replication timing-related and gene body-specific methylation of active human genes. *Hum Mol Genet* 2011; **4**: 670-680.

Aryee MJ, Jaffe AE, Corrada-Bravo H, Ladd-Acosta C, Feinberg AP, Hansen KD, and Irizarry RA. Minfi: A flexible and comprehensive Bioconductor package for the analysis of Infinium DNA methylation microarrays. *Bioinformatics* 2014; **10**: 1363-1369.

Barasoain M, Barrenetxea G, Huerta I, Telez M, Carrillo A, Perez C, Criado B, and Arrieta I. Study of FMR1 gene association with ovarian dysfunction in a sample from the Basque Country. *Gene* 2013; **1**: 145-149.

Barone S, Sarogni P, Valli R, Pallotta MM, Silvia G, Frattini A, Khan AW, Rapalini E, Parri C, and Musio A. Chromosome Missegregation in Single Human Oocytes Is Related to the Age and Gene Expression Profile. *Int J Mol Sci* 2020; **6**.

Barragan M, Pons J, Ferrer-Vaquer A, Cornet-Bartolome D, Schweitzer A, Hubbard J, Auer H, Rodolosse A, and Vassena R. The transcriptome of human oocytes is related to age and ovarian reserve. *Mol Hum Reprod* 2017; **8**: 535-548.

Battaglia R, Vento ME, Ragusa M, Barbagallo D, La Ferlita A, Di Emidio G, Borzi P, Artini PG, Scollo P, Tatone C*, et al.* MicroRNAs Are Stored in Human MII Oocyte and Their Expression Profile Changes in Reproductive Aging. *Biol Reprod* 2016; **6**: 131.

Baudat F, Imai Y, and de Massy B. Meiotic recombination in mammals: localization and regulation. *Nat Rev Genet* 2013; **11**: 794-806.

Bert SA, Robinson MD, Strbenac D, Statham AL, Song JZ, Hulf T, Sutherland RL, Coolen MW, Stirzaker C, and Clark SJ. Regional activation of the cancer genome by long-range epigenetic remodeling. *Cancer Cell* 2013; **1**: 9-22.

Binder AM, Corvalan C, Mericq V, Pereira A, Santos JL, Horvath S, Shepherd J, and Michels KB. Faster ticking rate of the epigenetic clock is associated with faster pubertal development in girls. *Epigenetics* 2018; **1**: 85-94.

Birch Petersen K, Hvidman HW, Sylvest R, Pinborg A, Larsen EC, Macklon KT, Andersen AN, and Schmidt L. Family intentions and personal considerations on postponing childbearing in childless cohabiting and single women aged 35-43 seeking fertility assessment and counselling. *Hum Reprod* 2015; **11**: 2563-2574.

Bischoff C, Graakjaer J, Petersen HC, Jeune B, Bohr VA, Koelvraa S, and Christensen K. Telomere Length Among the Elderly and Oldest-Old. *Twin Research and Human Genetics* 2012; **5**: 425-432.

Bjornsson HT, Sigurdsson MI, Fallin MD, Irizarry RA, Aspelund T, Cui H, Yu W, Rongione MA, Ekstrom TJ, Harris TB*, et al.* Intra-individual change over time in DNA methylation with familial clustering. *JAMA* 2008; **24**: 2877-2883.

Broekmans FJ, Soules MR, and Fauser BC. Ovarian aging: mechanisms and clinical consequences. *Endocr Rev* 2009; **5**: 465-493.

Brower PT and Schultz RM. Intercellular communication between granulosa cells and mouse oocytes: existence and possible role during oocyte growth. *Dev. Biol.* 1982: 144–153.
Brown HM and Russell DL. Blood and lymphatic vasculature in the ovary: development, function and disease. *Hum Reprod Update* 2014; **1**: 29-39.
Castrillon DH, Miao L, Kollipara R, Horner JW, and DePinho RA. Suppression of ovarian follicle activation in mice by the transcription factor Foxo3a. *Science* 2003; **5630**: 215-218.
Cate RL, Mattaliano RJ, Hession C, Tizard R, Farber NM, Cheung A, Ninfa EG, Frey AZ, Gash DJ, Chow EP*, et al.* Isolation of the bovine and human genes for müllerian inhibiting substance and expression of the human gene in animal cells. *Cell* 1986; **5**: 685-698.
Catteau-Jonard S, Pigny P, Reyss AC, Decanter C, Poncelet E, and Dewailly D. Changes in serum anti-mullerian hormone level during low-dose recombinant follicular-stimulating hormone therapy for anovulation in polycystic ovary syndrome. *J Clin Endocrinol Metab* 2007; **11**: 4138-4143.
Cedar H and Bergman Y. Programming of DNA methylation patterns. *Annu Rev Biochem* 2012: 97-117.
Celik O, Celik E, and Turkcuoglu I. Neo-oogenesis: Has its existence been proven? *J Turk Ger Gynecol Assoc* 2011; **4**: 274-276.
Centers for Disease Control and Prevention. Reporting of pregnancy success rates from assisted reproductive technology (ART) programs. *Department of Health and Human Services* 2015.
Chen L, Russell PT, and Larsen WJ. Functional significance of cumulus expansion in the mouse: roles for the preovulatory synthesis of hyaluronic acid within the cumulus mass. *Mol. Reprod. Dev* 1993: 87–93.
Chen X, Liu Y, Sun X, Yin Z, Li H, Liu X, Zhang D, Cheng C, Liu L, Liu F*, et al.* Age at menarche and risk of all-cause and cardiovascular mortality: a systematic review and dose-response meta-analysis. *Menopause* 2018; **6**: 670-676.
Conti M and Chang RJ. Folliculogenesis, Ovulation, and Luteogenesis. Endocrinology: Adult and Pediatric. 2016. pp 2179-2191.e2173.
Coop G and Przeworski M. An evolutionary view of human recombination. *Nat Rev Genet* 2007; **1**: 23-34.
Cooper A, Baker V, Sterling E, Ryan M, Woodruff T, and Nelson L. The time is now for a new approach to primary ovarian insufficiency. *Fertil Steril* 2011; **6**: 1890-1897.
Coulam C, Adamson S, and Annegers J. Incidence of premature ovarian failure. *Obstet Gynecol.* 1986; **4**: 604-606.
Craig J. Replacement Level Fertility and Future Population Growth. *Popul Trends* 1994; **78**: 20-22.
Cramer D and Xu H. Predicting age at menopause. . *Maturitas* 1996; **3**: 319-326.
.
Darbandi S, Darbandi M, Khorshid HR, Sadeghi MR, Al-Hasani S, Agarwal A, Shirazi A, Heidari M, and Akhondi MM. Experimental strategies towards increasing intracellular mitochondrial activity in oocytes: A systematic review. *Mitochondrion* 2016: 8-17.
Depmann M, Broer SL, van der Schouw YT, Tehrani FR, Eijkemans MJ, Mol BW, and Broekmans FJ. Can we predict age at natural menopause using ovarian reserve tests or mother's age at menopause? A systematic literature review. *Menopause* 2016; **2**: 224-232.
Dewailly D, Gronier H, Poncelet E, Robin G, Leroy M, Pigny P, Duhamel A, and Catteau-Jonard S. Diagnosis of polycystic ovary syndrome (PCOS): revisiting the threshold values of follicle count on ultrasound and of the serum AMH level for the definition of polycystic ovaries. *Hum Reprod* 2011; **11**: 3123-3129.
Diaz FJ, O'Brien MJ, Wigglesworth K, and Eppig JJ. The preantral granulosa cell to cumulus cell transition in the mouse ovary: development of competence to undergo expansion. *Dev Biol* 2006; **1**: 91-104.
Dor Y and Cedar H. Principles of DNA methylation and their implications for biology and medicine. *The Lancet* 2018; **10149**: 777-786.
Dugue PA, Bassett JK, Joo JE, Jung CH, Ming Wong E, Moreno-Betancur M, Schmidt D, Makalic E, Li S, Severi G*, et al.* DNA methylation-based biological aging and cancer risk and survival: Pooled analysis of seven prospective studies. *Int J Cancer* 2018; **8**: 1611-1619.

Durlinger AL, Visser JA, and Themmen APN. Regulation of ovarian function: the role of anti-Mullerian hormone. *Reproduction* 2002; **5**: 601-609.
Edson MA, Nagaraja AK, and Matzuk MM. The mammalian ovary from genesis to revelation. *Endocr Rev* 2009; **6**: 624-712.
Ehrlich M. DNA hypermethylation in disease: mechanisms and clinical relevance. *Epigenetics* 2019; **12**: 1141-1163.
Eppig JJ. Oocyte control of ovarian follicular development and function in mammals. *Reproduction* 2001; **6**: 829-838.
Erickson GF. The Graafian Follicle: A Functional Definition. In Adashi, EY (ed) Ovulation: evolving scientific and clinical concepts. 2000. Springer-Verlaag, New York, pp 31-48.
Ernst EH, Franks S, Hardy K, Villesen P, and Lykke-Hartmann K. Granulosa cells from human primordial and primary follicles show differential global gene expression profiles. *Hum Reprod* 2018; **4**: 666-679.
Ernst EH, Grondahl ML, Grund S, Hardy K, Heuck A, Sunde L, Franks S, Andersen CY, Villesen P, and Lykke-Hartmann K. Dormancy and activation of human oocytes from primordial and primary follicles: molecular clues to oocyte regulation. *Hum Reprod* 2017; **8**: 1684-1700.
ESHRE PGDG. ESHRE Guideline: management of women with premature ovarian insufficiency. 2016.
Faddy MJ, Gosden RG, Gougeon A, Richardson SJ, and JF N. Accelerated disappearance of ovarian follicles in mid-life: implications for forecasting menopause. *Human Reproduction* 1992: 1342-1346.
Faddy MJ and Gosden RG. A model conforming the decline in follicle numbers to the age of menopause in women. *Hum. Reprod.* 1996; **7**: 1484-1486.
Faddy MJ, Gosden RG, Gougeon A, Richardson SJ, and Nelson JF. Accelerated disappearance of ovarian follicles in mid-life: implications for forecasting menopause. *Hum Reprod* 1992; **10**: 1342-1346.
Finch CE. The menopause and aging, a comparative perspective. *J Steroid Biochem Mol Biol* 2014: 132-141.
Flatt T. A new definition of aging? *Front Genet* 2012: 148.
Fragouli E, Alfarawati S, Goodall NN, Sanchez-Garcia JF, Colls P, and Wells D. The cytogenetics of polar bodies: insights into female meiosis and the diagnosis of aneuploidy. *Mol Hum Reprod* 2011; **5**: 286-295.
Franasiak JM, Forman EJ, Hong KH, Werner MD, Upham KM, Treff NR, and Scott RT, Jr. The nature of aneuploidy with increasing age of the female partner: a review of 15,169 consecutive trophectoderm biopsies evaluated with comprehensive chromosomal screening. *Fertil Steril* 2014; **3**: 656-663 e651.
Fransquet PD, Wrigglesworth J, Woods RL, Ernst ME, and Ryan J. The epigenetic clock as a predictor of disease and mortality risk: a systematic review and meta-analysis. *Clin Epigenetics* 2019; **1**: 62.
Frommer M, McDonald LE, Millar DS, Collis CM, Watt F, Grigg GW, Molloy PL, and Paul CL. A genomic sequencing protocol that yields a positive display of 5-methylcytosine residues in individual DNA strands. *Proceedings of the National Academy of Sciences* 1992; **5**: 1827-1831.
Fusco F, Paciolla M, Chen E, Li X, Genesio R, Conti A, Jones J, Poeta L, Lioi MB, Ursini MV*, et al.* Genetic and molecular analysis of a new unbalanced X;18 rearrangement: localization of the diminished ovarian reserve disease locus in the distal Xq POF1 region. *Hum Reprod* 2011; **11**: 3186-3196.
Gallardo TD, John GB, Shirley L, Contreras CM, Akbay EA, Haynie JM, Ward SE, Shidler MJ, and Castrillon DH. Genomewide discovery and classification of candidate ovarian fertility genes in the mouse. *Genetics* 2007; **1**: 179-194.
Gentilini D, Garagnani P, Pisoni S, Bacalini MG, Calzari L, Mari D, Vitale G, Franceschi C, and Di Blasio AM. Stochastic epigenetic mutations (DNA methylation) increase exponentially in human aging and correlate with X chromosome inactivation skewing in females. *Aging* 2015; **8**: 568-578.
Giuliani C, Cilli E, Bacalini MG, Pirazzini C, Sazzini M, Gruppioni G, Franceschi C, Garagnani P, and Luiselli D. Inferring chronological age from DNA methylation patterns of human teeth. *Am J Phys Anthropol* 2016; **4**: 585-595.

Gleicher N, Weghofer A, and Barad DH. A pilot study of premature ovarian senescence: I. Correlation of triple CGG repeats on the FMR1 gene to ovarian reserve parameters FSH and anti-Mullerian hormone. *Fertil Steril* 2009a; **5**: 1700-1706.

Gleicher N, Weghofer A, Oktay K, and Barad DH. Is the immunological noise of abnormal autoimmunity an independent risk factor for premature ovarian aging? *Menopause* 2009b; **4**: 760-764.

Gougeon A. Dynamics of follicular growth in the human: a model from preliminary results. *Hum Reprod* 1986; **2**: 81-87.

Gougeon A. Regulation of Ovarian Follicular Development in Primates: Facts and Hypotheses. *Endocrine Reviews* 1996; **2**: 121-155.

Gougeon A and Chainy GB. Morphometric studies of small follicles in ovaries of women at different ages. *J. Reprod Fert* 1987; **2**: 433-442.

Greene AD, Patounakis G, and Segars JH. Genetic associations with diminished ovarian reserve: a systematic review of the literature. *J Assist Reprod Genet* 2014; **8**: 935-946.

Gruhn JR, Zielinska AP, Shukla V, Blanshard R, Capalbo A, Cimadomo D, Nikiforov D, Chan ACH, Newnham LJ, Vogel I*, et al.* Chromosome errors in human eggs shape natural fertility over reproductive life span. *Science* 2019; **6460**: 1466-1469.

Grøndahl ML, Andersen CY, Bogstad J, Borgbo T, Boujida VH, and Borup R. Specific genes are selectively expressed between cumulus and granulosa cells from individual human pre-ovulatory follicles. *Mol Hum Reprod* 2012; **12**: 572-584.

Grøndahl ML, Borup R, Lee YB, Myrhoj V, Meinertz H, and Sorensen S. Differences in gene expression of granulosa cells from women undergoing controlled ovarian hyperstimulation with either recombinant follicle-stimulating hormone or highly purified human menopausal gonadotropin. *Fertil Steril* 2009; **5**: 1820-1830.

Grøndahl ML, Borup R, Vikesa J, Ernst E, Andersen CY, and Lykke-Hartmann K. The dormant and the fully competent oocyte: comparing the transcriptome of human oocytes from primordial follicles and in metaphase II. *Mol Hum Reprod* 2013; **9**: 600-617.

Grøndahl ML, Nielsen ME, Dal Canto MB, Fadini R, Rasmussen IA, Westergaard LG, Kristensen SG, and Yding Andersen C. Anti-Mullerian hormone remains highly expressed in human cumulus cells during the final stages of folliculogenesis. *Reprod Biomed Online* 2011; **4**: 389-398.

Grøndahl ML, Yding Andersen C, Bogstad J, Nielsen FC, Meinertz H, and Borup R. Gene expression profiles of single human mature oocytes in relation to age. *Hum Reprod* 2010; **4**: 957-968.

Hannum G, Guinney J, Zhao L, Zhang L, Hughes G, Sadda S, Klotzle B, Bibikova M, Fan JB, Gao Y*, et al.* Genome-wide methylation profiles reveal quantitative views of human aging rates. *Mol Cell* 2013; **2**: 359-367.

Harman D. The aging process: Major risk factor for disease and death. *PNAS USA* 1991; **12**: 5360-5363.

Hassold T and Hunt P. To err (meiotically) is human: the genesis of human aneuploidy. *Nature reviews. Genetics* 2001; **4**: 280-291.

Hauf S and Watanabe Y. Kinetochore Orientation in Mitosis and Meiosis. *Cell* 2004; **3**: 317-327.

Hawkes K, O'Connell JF, Blurton Jones NG, Alvarez H, and Charnov EL. Grandmothering, menopause, and the evolution of human life histories. *Proc. Natl. Acad. Sci. USA* 1998; **3**: 1336-1339.

Henderson MA, Croniand E, Dunkelbarger S, Contreras V, Strome S, and Keiper BD. A germline-specific isoform of eIF4E (IFE-1) is required for efficient translation of stored mRNAs and maturation of both oocytes and sperm. *J. Cell Sci.* 2009; **10**: 1529-1539.

Herbert M, Kalleas D, Cooney D, Lamb M, and Lister L. Meiosis and maternal aging: insights from aneuploid oocytes and trisomy births. *Cold Spring Harb Perspect Biol* 2015; **4**: a017970.

Heyn H, Li N, Ferreira HJ, Moran S, Pisano DG, Gomez A, Diez J, Sanchez-Mut JV, Setien F, Carmona FJ*, et al.* Distinct DNA methylomes of newborns and centenarians. *PNAS USA* 2012; **26**: 10522-10527.

Horvath S. DNA methylation age of human tissues and cell types. *Genome Biol.* 2013; **10**: R115.

Horvath S, Garagnani P, Bacalini MG, Pirazzini C, Salvioli S, Gentilini D, Di Blasio AM, Giuliani C, Tung S, Vinters HV*, et al.* Accelerated epigenetic aging in Down syndrome. *Aging Cell* 2015a; **3**: 491-495.

Horvath S, Mah V, Lu AT, Woo JS, Choi OW, Jasinska AJ, Riancho JA, Tung S, Coles NS, Braun J*, et al.* The cerebellum ages slowly according to the epigenetic clock. *Aging* 2015b; **5**: 294-306.
Horvath S, Oshima J, Martin GM, Lu AT, Quach A, Cohen H, Felton S, Matsuyama M, Lowe D, Kabacik S*, et al.* Epigenetic clock for skin and blood cells applied to Hutchinson Gilford Progeria Syndrome and ex vivo studies. *Aging* 2018; **7**: 1758-1775.
Horvath S and Raj K. DNA methylation-based biomarkers and the epigenetic clock theory of ageing. *Nat Rev Genet* 2018; **6**: 371-384.
Horvath S and Ritz BR. Increased epigenetic age and granulocyte counts in the blood of Parkinson's disease patients. *Aging* 2015; **12**: 1130-1142.
Hsueh AJ, Kawamura K, Cheng Y, and Fauser BC. Intraovarian control of early folliculogenesis. *Endocr Rev* 2015; **1**: 1-24.
Hsueh AJW, Billig H, and Tsafriri A. Ovarian Follicle Atresia: A Hormonally Controlled Apoptotic Process. *Endocrine Reviews* 1994; **6**: 707–724.
Huseynov A, Zollikofer CP, Coudyzer W, Gascho D, Kellenberger C, Hinzpeter R, and Ponce de Leon MS. Developmental evidence for obstetric adaptation of the human female pelvis. *Proc Natl Acad Sci U S A* 2016; **19**: 5227-5232.
Illumina. Infinium® MethylationEPIC BeadChip. Data sheet: Epigenetics. 2015.
Issa JPJ, Ottaviano YL, Celano P, Hamilton SR, Davidson NE, and Baylin SB. Methylation of the oestrogen receptor CpG island links ageing and neoplasia in human colon. *Nat. Genet.* 1994; **4**: 536-540.
Jacobsen B, Knutsen SF, and Fraser G. Age at natural menopause and total mortality and morbidity from ischaemic heart disease. *J. Clin. Epidemiol.* 1999; **4**: 303-307.
Jacobsen BK, Heuch I, and Kvale G. Age at natural menopause and stroke mortality: cohort study with 3561 stroke deaths during 37-year follow-up. *Stroke* 2004; **7**: 1548-1551.
Johnson J, Canning J, Kaneko T, Pru JK, and Tilly JL. Germline stem cells and follicular renewal in the postnatal mammalian ovary. *Nature* 2004; **6979**: 145-150.
Jones PA. Functions of DNA methylation: islands, start sites, gene bodies and beyond. *Nat Rev Genet* 2012; **7**: 484-492.
Jones PA and Baylin SB. The fundamental role of epigenetic events in cancer. *Nat Rev Genet* 2002; **6**: 415-428.
Jung M and Pfeifer GP. Aging and DNA methylation. *BMC Biol* 2015: 7.
Kaipia A and Hsueh AJW. Regulation of ovarian follicle atresia. *Annual review of physiology* 1997: 349-363.
Khamsi F and Roberge S. Granulosa cells of the cumulus oophorus are different from mural granulosa cells in their response to gonadotrophins and IGF-I. *J. Endocrinol.* 2001; **3**: 565-573.
Kim PS, Coxworth JE, and Hawkes K. Increased longevity evolves from grandmothering. *Proc Biol Sci* 2012; **1749**: 4880-4884.
Kim PS, McQueen JS, Coxworth JE, and Hawkes K. Grandmothering drives the evolution of longevity in a probabilistic model. *J Theor Biol* 2014: 84-94.
Kimura M, Hjelmborg JV, Gardner JP, Bathum L, Brimacombe M, Lu X, Christiansen L, Vaupel JW, Aviv A, and Christensen K. Telomere length and mortality: a study of leukocytes in elderly Danish twins. *Am J Epidemiol* 2008; **7**: 799-806.
Knauff EA, Eijkemans MJ, Lambalk CB, ten Kate-Booij MJ, Hoek A, Beerendonk CC, Laven JS, Goverde AJ, Broekmans FJ, Themmen AP*, et al.* Anti-Mullerian hormone, inhibin B, and antral follicle count in young women with ovarian failure. *J Clin Endocrinol Metab* 2009; **3**: 786-792.
Knight AK, Craig JM, Theda C, Baekvad-Hansen M, Bybjerg-Grauholm J, Hansen CS, Hollegaard MV, Hougaard DM, Mortensen PB, Weinsheimer SM*, et al.* An epigenetic clock for gestational age at birth based on blood methylation data. *Genome Biol* 2016; **1**: 206.
Krailo M and Pike M. Estimation of the distribution of age at natural menopause from prevalence data. *Am J Epidemiol* 1983; **3**: 356-361.
Kumar A, Singh T, Basu S, Pandey S, and Bhargava V. Outcome of teenage pregnancy. *Indian J. Pediatr.* 2007; **10**: 927-931.

La Marca A and Volpe A. The Anti-Mullerian hormone and ovarian cancer. *Hum Reprod Update* 2007; **3**: 265-273.
Lawrence TS, Ginzberg RD, Gilula NB, and Beers WH. Hormonally induced cell shape changes in cultured rat ovarian granulosa cells. *J Cell Biol* 1979; **1**: 21-36.
Lee JE, Park DS, Kim M-L, Yoon BS, Song T, Kim MK, Seong SJ, and Kim Y-J. Age-related distribution of anti-Müllerian hormone levels in 2,879 Korean women with regular menstruation. *Korean J of Obstet Gynecol.* 2012; **12**: 920.
Lee Y, Choufani S, Weksberg R, Wilson SL, Yuan V, Burt A, Marsit C, Lu AT, Ritz B, Bohlin J*, et al.* Placental epigenetic clocks : estimating gestational age using placental DNA methylation levels. *Aging* 2019a; **12**: 4238-4253.
Lee Y, Sun D, Ori APS, Lu AT, Seeboth A, Harris SE, Deary IJ, Marioni RE, Soerensen M, Mengel-From J*, et al.* Epigenome-wide association study of leukocyte telomere length. *Aging* 2019b: 1-19.
Leridon H and Slama R. The impact of a decline in fecundity and of pregnancy postponement on final number of children and demand for assisted reproduction technology. *Hum Reprod* 2008; **6**: 1312-1319.
Levi AJ, Raynault MF, Bergh PA, Drews MR, Miller BT, and Scott RT. Reproductive outcome in patients with diminished ovarian reserve. *Fertil Steril* 2001; **4**: 666-669.
Levine ME, Hosgood HD, Chen B, Absher D, Assimes T, and Horvath S. DNA methylation age of blood predicts future onset of lung cancer in the women's health initiative. *Aging* 2015; **9**: 690-700.
Levine ME, Lu AT, Chen BH, Hernandez DG, Singleton AB, Ferrucci L, Bandinelli S, Salfati E, Manson JE, Quach A*, et al.* Menopause accelerates biological aging. *Proc Natl Acad Sci U S A* 2016; **33**: 9327-9332.
Levine ME, Lu AT, Quach A, Chen BH, Assimes TL, Bandinelli S, Hou L, Baccarelli AA, Stewart JD, Li Y*, et al.* An epigenetic biomarker of aging for lifespan and healthspan. *Aging* 2018; **4**: 573-591.
Li H and Chian R-C. Chapter 2. Follicular Development and Oocyte Growth. Development of In Vitro Maturation for Human Oocytes: Natural and Mild Approaches to Clinical Infertility Treatment. 2017. pp 37-57.
Li HW, Anderson RA, Yeung WS, Ho PC, and Ng EH. Evaluation of serum antimullerian hormone and inhibin B concentrations in the differential diagnosis of secondary oligoamenorrhea. *Fertil Steril* 2011; **3**: 774-779.
Livshyts G, Podlesnaja S, Kravchenko S, and Livshits L. Association of PvuII polymorphism in ESR1 gene with impaired ovarian reserve in patients from Ukraine. *Reprod Biol* 2013; **1**: 96-99.
Livshyts G, Podlesnaja S, Kravchenko S, Sudoma I, and Livshits L. A distribution of two SNPs in exon 10 of the FSHR gene among the women with a diminished ovarian reserve in Ukraine. *J Assist Reprod Genet* 2009; **1**: 29-34.
Lopéz-Otín C, Blasco MA, Partridge L, Serrano M, and Kroemer G. The hallmarks of aging. *Cell* 2013; **6**: 1194-1217.
Love MI, Huber W, and Anders S. Moderated estimation of fold change and dispersion for RNA-seq data with DESeq2. *Genome Biol* 2014; **12**: 550.
Lu AT, Seeboth A, Tsai P-C, Sun D, Quach A, Reiner AP, Kooperberg C, Ferrucci L, Hou L, Baccarelli AA*, et al.* DNA methylation-based estimator of telomere length. *Aging* 2019.
Luborsky J, Meyer P, Sowers M, Gold E, and Santoro N. Premature menopause in a multi-ethnic population study of the menopause transition. *Hum Reprod* 2003: 199-206.
M'Rabet N, Moffat R, Helbling S, Kaech A, Zhang H, and de Geyter C. The CC-allele of the PvuII polymorphic variant in intron 1 of the alpha-estrogen receptor gene is significantly more prevalent among infertile women at risk of premature ovarian aging. *Fertil Steril* 2012; **4**: 965-972 e961-965.
Macaulay A, Scantland S, and Robert C. RNA Processing During Early Embryogenesis: Managing Storage, Utilisation and Destruction. In Grabowski, P (ed) RNA Processing. 2011. IntechOpen.
Macaulay AD, Gilbert I, Caballero J, Barreto R, Fournier E, Tossou P, Sirard MA, Clarke HJ, Khandjian EW, Richard FJ*, et al.* The gametic synapse: RNA transfer to the bovine oocyte. *Biol Reprod* 2014; **4**: 90.

Maciejewska Z, Pascal A, Kubiak JZ, and MA. C. Phosphorylated ERK5/BMK1 transiently accumulates within division spindles in mouse oocytes and preimplantation embryos. *Folia Histochem Cytobiol* 2011: 528–534.

MacLennan M, Crichton JH, Playfoot CJ, and Adams IR. Oocyte development, meiosis and aneuploidy. *Semin Cell Dev Biol* 2015: 68-76.

Maekawa R, Lee L, Okada M, Asada H, Shinagawa M, Tamura I, Sato S, Tamura H, and Sugino N. Changes in gene expression of histone modification enzymes in rat granulosa cells undergoing luteinization during ovulation. *J Ovarian Res* 2016: 15.

Makrinou E, Drong AW, Christopoulos G, Lerner A, Chapa-Chorda I, Karaderi T, Lavery S, Hardy K, Lindgren CM, and Franks S. Genome-wide methylation profiling in granulosa lutein cells of women with polycystic ovary syndrome (PCOS). *Mol Cell Endocrinol* 2019: 110611.

Marioni RE, Shah S, McRae AF, Chen BH, Colicino E, Harris SE, Gibson J, Henders AK, Redmond P, Cox SR*, et al.* DNA methylation age of blood predicts all-cause mortality in later life. *Genome Biol* 2015: 25.

Markholt S, Grøndahl ML, Ernst EH, Andersen CY, Ernst E, and Lykke-Hartmann K. Global gene analysis of oocytes from early stages in human folliculogenesis shows high expression of novel genes in reproduction. *Mol Hum Reprod* 2012; **2**: 96-110.

Markström E, Svensson EC, Shao R, Svanberg B, and Billig H. Survival factors regulating ovarian apoptosis - Dependence on follicle differentiation. *Reproduction* 2002; **1**: 23-30.

Maslov AY and Vijg J. Genome instability, cancer and aging. *Biochim Biophys Acta* 2009; **10**: 963-969.

Mather KA, Jorm AF, Parslow RA, and Christensen H. Is telomere length a biomarker of aging? A review. *J Gerontol A Biol Sci Med Sci* 2011; **2**: 202-213.

May-Panloup P, Ferre-L'Hotellier V, Moriniere C, Marcaillou C, Lemerle S, Malinge MC, Coutolleau A, Lucas N, Reynier P, Descamps P*, et al.* Molecular characterization of corona radiata cells from patients with diminished ovarian reserve using microarray and microfluidic-based gene expression profiling. *Hum Reprod* 2012; **3**: 829-843.

Mayne BT, Leemaqz SY, Smith AK, Breen J, Roberts CT, and Bianco-Miotto T. Accelerated placental aging in early onset preeclampsia pregnancies identified by DNA methylation. *Epigenomics* 2016; **3**: 279-289.

McGee EA and Hsueh AJW. Initial and cyclic recruitment of ovarian follicles. *Endocrine Reviews* 2000; **2**: 200-214.

McNatty KP, SMITH DM, MAKRIS A, OSATHANONDH R, and RYAN KJ. The Microenvironment of the Human Antral Follicle: Interrelationships among the Steroid Levels in Antral Fluid, the Population of Granulosa Cells, and the Status of the Oocyte in Vivo and in Vitro. *The Journal of Clinical Endocrinology & Metabolism* 1979; **6**: 851-860.

Menken J, Trussell J, and Larsen U. Age and Infertility. 1986: 1389-1394.

Miyara F, Migne C, Dumont-Hassan M, Le Meur A, Cohen-Bacrie P, Aubriot FX, Glissant A, Nathan C, Douard S, Stanovici A*, et al.* Chromatin configuration and transcriptional control in human and mouse oocytes. *Mol Reprod Dev* 2003; **4**: 458-470.

Monniaux D. Driving folliculogenesis by the oocyte-somatic cell dialog: Lessons from genetic models. *Theriogenology* 2016; **1**: 41-53.

Monseur B, Murugappan G, Bentley J, Teng N, and Westphal L. Epigenetic clock measuring age acceleration via DNA methylation levels in blood is associated with decreased oocyte yield. *J Assist Reprod Genet* 2020; **5**: 1097-1103.

Morin SJ, Tao X, Marin D, Zhan Y, Landis J, Bedard J, Scott RT, and Seli E. DNA methylation-based age prediction and telomere length in white blood cells and cumulus cells of infertile women with normal or poor response to ovarian stimulation. *Aging* 2018; **12**.

Nielsen M. Nye kampagner skal få de unge til fødestuerne. Berlingske. 2015. Copenhagen, Denmark.

Niu L, Xu Z, and Taylor JA. RCP: a novel probe design bias correction method for Illumina Methylation BeadChip. *Bioinformatics* 2016; **17**: 2659-2663.

Nyboe Andersen A, Goossens V, Bhattacharya S, Ferraretti AP, Kupka MS, de Mouzon J, Nygren KG, European Ivf-monitoring Consortium ftESoHR, and Embryology. Assisted reproductive technology and intrauterine inseminations in Europe, 2005: results generated from European registers by ESHRE: ESHRE. The European IVF Monitoring Programme (EIM), for the European Society of Human Reproduction and Embryology (ESHRE). *Hum Reprod* 2009; **6**: 1267-1287.

O'Connell JF, Hawkes K, and Jones NGB. Grandmothering and the evolution of Homo erectus. *J. Hum. Evol.* 1999; **5**: 461-485.

OECD Family Database. Age of mothers at childbirth and age-specific fertility. 2018. OECD - Social Policy Division - Directorate of Employment, Labour and Social Affairs, http://www.oecd.org/els/family/database.htm, pp http://www.oecd.org/els/family/database.htm.

Okada M, Lee L, Maekawa R, Sato S, Kajimura T, Shinagawa M, Tamura I, Taketani T, Asada H, Tamura H*, et al.* Epigenetic Changes of the Cyp11a1 Promoter Region in Granulosa Cells Undergoing Luteinization During Ovulation in Female Rats. *Endocrinology* 2016; **9**: 3344-3354.

Oktay K, Briggs D, and Gosden RG. Ontogeny of Follicle-Stimulating Hormone Receptor Gene Expression in Isolated Human Ovarian Follicles 1. *J Clin Endocrinol Metab* 1997; **11**: 3748-3751.

Okuda K. Telomere Length in the Newborn. *Pediatric Research* 2002; **3**: 377-381.

Olesen MS, Starnawska A, Bybjerg-Grauholm J, Bielfeld AP, Agerholm I, Forman A, Overgaard MT, and Nyegaard M. Biological age of the endometrium using DNA methylation. *Reproduction* 2018; **2**: 167-172.

Olovnikov AM. Telomeres, telomerase, and aging: Origin of the theory. *Exp Gerontol* 1996; **4**: 443-448.

Olsen KW, Castillo-Fernandez J, Chan AC, Freiesleben NC, Zedeler A, Bungum M, Cardona A, Perry J, Skouby SO, Hoffmann ER*, et al.* Identification of a unique epigenetic profile in women with diminished ovarian reserve. *Fertil Steril* 2020a; **Submitted**.

Olsen KW, Castillo-Fernandez J, Zedeler A, Freiesleben NC, Bungum M, Chan AC, Cardona A, Perry JRB, Skouby SO, Borup R*, et al.* A distinctive epigenetic ageing profile in human granulosa cells. *Hum Reprod* 2020b; **In press**.

Olsen KW, Gruhn J, Hoffmann ER, and Grøndahl ML. Processing of human IVF/IVM oocytes for single cell RNA sequencing *Protocol Exchange* 2020c.

Olsen KW, Shukla V, Azad A, Skouby SO, Grøndahl ML, Hoffmann ER, and Borup R. Gene expression profile of human metaphase II oocytes in relation to age by single cell RNA sequencing. 2020d; **In preparation**

Ossewaarde ME, Bots ML, Verbeek AL, Peeters PH, van der Graaf Y, Grobbee DE, and van der Schouw YT. Age at menopause, cause-specific mortality and total life expectancy. *Epidemiology* 2005; **4**: 556-562.

Page SL and Hawley SR. Chromosome Choreography: The Meiotic Ballet. *Science* 2003; **5634)**: 785-789.

Pastore LM, Young SL, Baker VL, Karns LB, Williams CD, and Silverman LM. Elevated prevalence of 35-44 FMR1 trinucleotide repeats in women with diminished ovarian reserve. *Reprod Sci* 2012; **11**: 1226-1231.

Pastore LM, Young SL, Manichaikul A, Baker VL, Wang XQ, and Finkelstein JS. Distribution of the FMR1 gene in females by race/ethnicity: women with diminished ovarian reserve versus women with normal fertility (SWAN study). *Fertil Steril* 2017; **1**: 205-211 e201.

Pelosi E, Omari S, Michel M, Ding J, Amano T, Forabosco A, Schlessinger D, and Ottolenghi C. Constitutively active Foxo3 in oocytes preserves ovarian reserve in mice. *Nat Commun* 2013: 1843.

Persani L, Rossetti R, and Cacciatore C. Genes involved in human premature ovarian failure. *J Mol Endocrinol* 2010; **5**: 257-279.

Peters TJ, Buckley MJ, Statham AL, Pidsley R, Samaras K, V Lord R, Clark SJ, and Molloy PL. De novo identification of differentially methylated regions in the human genome. *Epigenetics and Chromatin* 2015; **1**: 1-16.

Phipson B, Maksimovic J, and Oshlack A. missMethyl: an R package for analysing methylation data from Illuminas HumanMethylation450 platform. *Bioinformatics* 2015; **2**: 286-288.

Pidsley R, Zotenko E, Peters TJ, Lawrence MG, Risbridger GP, Molloy P, Van Djik S, Muhlhausler B, Stirzaker C, and Clark SJ. Critical evaluation of the Illumina MethylationEPIC BeadChip microarray for whole-genome DNA methylation profiling. *Genome Biol* 2016; **1**: 208.

Pigny P, Merlen E, Robert Y, Cortet-Rudelli C, Decanter C, Jonard S, and Dewailly D. Elevated serum level of anti-mullerian hormone in patients with polycystic ovary syndrome: relationship to the ovarian follicle excess and to the follicular arrest. *J Clin Endocrinol Metab* 2003; **12**: 5957-5962.

Podfigurna-Stopa A, Czyzyk A, Grymowicz M, Smolarczyk R, Katulski K, Czajkowski K, and Meczekalski B. Premature ovarian insufficiency: the context of long-term effects. *J Endocrinol Invest* 2016; **9**: 983-990.

Pollack AZ, Rivers K, and Ahrens KA. Parity associated with telomere length among US reproductive age women. *Hum Reprod* 2018; **4**: 736-744.

Poulsen L, Bøtkjær L, Østrup O, Petersen K, Yding Andersen C, Grøndahl M, and Englund A. Two waves of transcriptomic changes in periovulatory human granulosa cells. *Human Reproduction* 2020; **In press**: 1-16.

Promega. ReliaPrep™ Large Volume HT gDNA Isolation System. Technical Manual. 2018.

Quach A, Levine ME, Tanaka T, Lu AT, Chen BH, Ferrucci L, Ritz B, Bandinelli S, Neuhouser ML, Beasley JM*, et al.* Epigenetic clock analysis of diet, exercise, education, and lifestyle factors. *Aging* 2017; **2**: 419-446.

R Core Team. A Language and Environment for Statistical Computing 2016.

Regan SLP, Knight PG, Yovich JL, Leung Y, Arfuso F, and Dharmarajan A. Granulosa Cell Apoptosis in the Ovarian Follicle-A Changing View. *Front Endocrinol (Lausanne)* 2018: 61.

Rhoads EE. Granulosa-cell Tumor of the Ovary; Report of Five Cases With Premature Menopause (Amenorrhea) and the Recurrence of Menstruation. *Am J Obstet Gynecol* 1946: 560-564.

Richardson SJ, Senikas V, and Nelson JF. Follicular depletion during the menopausal transition: Evidence for accelerated loss and ultimate exhaustion. *Journal of Clinical Endocrinology and Metabolism* 1987; **6**: 1231-1237.

Roetker NS, Pankow JS, Bressler J, Morrison AC, and Boerwinkle E. Prospective Study of Epigenetic Age Acceleration and Incidence of Cardiovascular Disease Outcomes in the ARIC Study (Atherosclerosis Risk in Communities). *Circ Genom Precis Med* 2018; **3**: e001937.

Rossello RA, Wang Z, Kizana E, Krebsbach PH, and Kohn DH. Cell communication and tissue engineering. *Commun. Integr. Biol.* 2009; **1**: 64-66.

Ryan CP, Hayes MG, Lee NR, McDade TW, Jones MJ, Kobor MS, Kuzawa CW, and Eisenberg DTA. Reproduction predicts shorter telomeres and epigenetic age acceleration among young adult women. *Sci Rep* 2018; **1**: 11100.

Raad G, Bazzi M, Tanios J, Mourad Y, Azouri J, Azouri J, and Fakih C. Optimization of The Cell Aggregates Method for Isolation and Purification of Human Granulosa Cells from Follicular Fluid. *Int J Fertil Steril* 2020; **4**: 339-345.

Saleh A, Kashir J, Thanassoulas A, Safieh-Garabedian B, Lai FA, and Nomikos M. Essential Role of Sperm-Specific PLC-Zeta in Egg Activation and Male Factor Infertility: An Update. *Front Cell Dev Biol* 2020: 28.

Sanders JL and Newman AB. Telomere length in epidemiology: a biomarker of aging, age-related disease, both, or neither? *Epidemiol Rev* 2013; **1**: 112-131.

Sankar A, Johansen JV, and Borup R. Single oocyte/embryo RNASeq data processing. *Protocol Exchange* 2020; **version 2**.

Santonocito M, Guglielmino MR, Vento M, Ragusa M, Barbagallo D, Borzi P, Casciano I, Scollo P, Romani M, Tatone C*, et al.* The apoptotic transcriptome of the human MII oocyte: characterization and age-related changes. *Apoptosis* 2013; **2**: 201-211.

Sehl ME, Henry JE, Storniolo AM, Ganz PA, and Horvath S. DNA methylation age is elevated in breast tissue of healthy women. *Breast Cancer Res Treat* 2017; **1**: 209-219.

Seifer DB and Merhi Z. Is AMH a regulator of follicular atresia? *J Assist Reprod Genet* 2014; **11**: 1403-1407.

Senapati S. Infertility: a marker of future health risk in women? *Fertil Steril* 2018; **5**: 783-789.
Sheikhha MH, Eftekhar M, and Kalantar SM. Investigating the association between polymorphism of follicle-stimulating hormone receptor gene and ovarian response in controlled ovarian hyperstimulation. *J Hum Reprod Sci* 2011; **2**: 86-90.
Shuster LT, Rhodes DJ, Gostout BS, Grossardt BR, and Rocca WA. Premature menopause or early menopause: long-term health consequences. *Maturitas* 2010; **2**: 161-166.
Siderakis M and Tarsounas M. Telomere regulation and function during meiosis. *Chromosome Research* 2007; **5**: 667-679.
Simon JA and Kingston RE. Mechanisms of polycomb gene silencing: knowns and unknowns. *Nat Rev Mol Cell Biol* 2009; **10**: 697-708.
Simpkin AJ, Howe LD, Tilling K, Gaunt TR, Lyttleton O, McArdle WL, Ring SM, Horvath S, Smith GD, and Relton CL. The epigenetic clock and physical development during childhood and adolescence: longitudinal analysis from a UK birth cohort. *Int J Epidemiol* 2017; **2**: 549-558.
Smith ZD, Chan MM, Humm KC, Karnik R, Mekhoubad S, Regev A, Eggan K, and Meissner A. DNA methylation dynamics of the human preimplantation embryo. *Nature* 2014; **7511**: 611-615.
Smith ZD, Chan MM, Mikkelsen TS, Gu H, Gnirke A, Regev A, and Meissner A. A unique regulatory phase of DNA methylation in the early mammalian embryo. *Nature* 2012; **7394**: 339-344.
Spiers H, Hannon E, Schalkwyk LC, Smith R, Wong CC, O'Donovan MC, Bray NJ, and Mill J. Methylomic trajectories across human fetal brain development. *Genome Res* 2015; **3**: 338-352.
Spilianakis CG, Lalioti MD, Town T, Lee GR, and Flavell RA. Interchromosomal associations between alternatively expressed loci. *Nature* 2005; **7042**: 637-645.
Spira A. The decline of fecundity with age. *Maturitas* 1988; **SUPPL. 1**: 15-22.
Statistics Denmark. Befolkningens udvikling 2016. 2016. https://www.dst.dk/da/Statistik/Publikationer/VisPub?cid=29443.
Statistics Denmark The register of 'FOD11: Average age of women given birth and new fathers' 2018. https://www.statbank.dk/FOD11.
Statistics Denmark. The register of 'FOD33: Age-specific fertility rates (single year), total fertility rates (aged 15-49), and gross and net reproduction rates' 2019. https://www.statbank.dk/statbank5a/SelectVarVal/Define.asp?Maintable=FOD33&PLanguage=1.
Statistics Denmark. FOD111: Average age of women given birth and new fathers by municipality. 2020. https://www.statbank.dk/statbank5a/SelectVarVal/Define.asp?Maintable=FOD111&PLanguage=1.
Sun W, Stegmann BJ, Henne M, Catherino WH, and Segars JH. A new approach to ovarian reserve testing. *Fertil Steril* 2008; **6**: 2196-2202.
Suzuki MM and Bird A. DNA methylation landscapes: provocative insights from epigenomics. *Nat Rev Genet* 2008; **6**: 465-476.
Sylvest R, Koert E, Vittrup I, Birch Petersen K, Nyboe Andersen A, Pinborg A, and Schmidt L. Status one year after fertility assessment and counselling in women of reproductive age-a qualitative study. *Ups J Med Sci* 2018; **4**: 264-270.
Sørensen NO, Marcussen S, Backhausen MG, Juhl M, Schmidt L, Tydén T, and Hegaard HK. Fertility awareness and attitudes towards parenthood among Danish university college students. *Reprod Health* 2016; **1**: 146.
te Velde ER and Pearson PL. The variability of female reproductive aging. *Hum Reprod Update* 2002; **2**: 141-154.
Templeton A, Morris JK, and W P. Factors that affect outcome of in vitro fertilisation treatment. *The Lancet* 1996: 1402–1406.
The Danish Fertility Society. Annual Report 2018: 'The results for 2018 are based on reports from public as well as private fertility clinics to the Danish Health Authority's IVF register'. 2019. https://fertilitetsselskab.dk/dataark-pr-aar/.

Thilagavathi J, Mishra SS, Kumar M, Vemprala K, Deka D, Dhadwal V, and Dada R. Analysis of telomere length in couples experiencing idiopathic recurrent pregnancy loss. *J Assist Reprod Genet* 2013; **6**: 793-798.

Torgerson DJ, Thomas RE, and Reid DM. Mothers and daughters menopausal ages: Is there a link? *Eur. J. Obstet. Gynecol. Reprod. Biol.* 1997; **1**: 63-66.

Townson DH and Combelles CMH. Ovarian Follicular Atresia, Basic Gynecology - Some
Related Issues. In Darwish, PA (ed). 2012. InTech, pp 43-74.

Treloar AE. Menstrual cyclicity and the pre-menopause. *Maturitas* 1981; **3-4**: 249-264.

Vassard D, Lallemant C, Nyboe Andersen A, Macklon N, and Schmidt L. A population-based survey on family intentions and fertility awareness in women and men in the United Kingdom and Denmark. *Ups J Med Sci* 2016; **4**: 244-251.

Vegetti W, Marozzi A, Manfredini E, Testa G, Alagna F, Nicolosi A, Caliari I, Taborelli M, Grazia M, Dalpra L*, et al.* Premature ovarian failure. *Mol Cell Endocrinol.* 2000; **1-2**: 53-57.

Wallace WH and Kelsey TW. Human ovarian reserve from conception to the menopause. *PLOS ONE* 2010; **1**: e8772.

Wang S, Zheng Y, Li J, Yu Y, Zhang W, Song M, Liu Z, Min Z, Hu H, Jing Y*, et al.* Single-Cell Transcriptomic Atlas of Primate Ovarian Aging. *Cell* 2020; **3**: 585-600 e519.

Wang TT, Ke ZH, Song Y, Chen LT, Chen XJ, Feng C, Zhang D, Zhang RJ, Wu YT, Zhang Y*, et al.* Identification of a mutation in GDF9 as a novel cause of diminished ovarian reserve in young women. *Hum Reprod* 2013; **9**: 2473-2481.

Wang TT, Wu YT, Dong MY, Sheng JZ, Leung PC, and Huang HF. G546A polymorphism of growth differentiation factor-9 contributes to the poor outcome of ovarian stimulation in women with diminished ovarian reserve. *Fertil Steril* 2010; **6**: 2490-2492.

Weenen C, Laven JSE, von Bergh ARM, Cranfield M, Groome NP, Visser JA, Kramer P, Fauser BCJM, and Themmen APN. Anti-Müllerian hormone expression pattern in the human ovary: Potential implications for initial and cyclic follicle recruitment. *Mol Hum Reprod* 2004; **2**: 77-83.

Weidner CI, Lin Q, Koch CM, Eisele L, Beier F, Ziegler P, Bauerschlag DO, Jöckel KH, Erbel R, Mühleisen TW*, et al.* Aging of blood can be tracked by DNA methylation changes at just three CpG sites. *Genome Biology* 2014; **2**: R24.

Welt CK, Smith PC, and Taylor AE. Evidence of early ovarian aging in fragile X premutation carriers. *J Clin Endocrinol Metab* 2004; **9**: 4569-4574.

Westergaard CG, Byskov AG, and Andersen CY. Morphometric characteristics of the primordial to primary follicle transition in the human ovary in relation to age. *Hum Reprod* 2007; **8**: 2225-2231.

Wilson GA, Dhami P, Feber A, Cortazar D, Suzuki Y, Schulz R, Schar P, and Beck S. Resources for methylome analysis suitable for gene knockout studies of potential epigenome modifiers. *Gigascience* 2012; **1**: 3.

Wissing ML, Kristensen SG, Andersen CY, Mikkelsen AL, Høst T, Borup R, and Grøndahl ML. Identification of new ovulation-related genes in humans by comparing the transcriptome of granulosa cells before and after ovulation triggering in the same controlled ovarian stimulation cycle. *Hum Reprod* 2014; **5**: 997-1010.

Wood J. Fecundity and natural fertility in humans. *Oxf Rev Reprod Biol* 1989: 61–109.

Xiao FH, He YH, Li QG, Wu H, Luo LH, and Kong QP. A genome-wide scan reveals important roles of DNA methylation in human longevity by regulating age-related disease genes. *PLOS ONE* 2015; **3**: e0120388.

Xu X, Chen X, Zhang X, Liu Y, Wang Z, Wang P, Du Y, Qin Y, and Chen ZJ. Impaired telomere length and telomerase activity in peripheral blood leukocytes and granulosa cells in patients with biochemical primary ovarian insufficiency. *Hum Reprod* 2017a; **1**: 201-207.

Xu Z, Langie SA, De Boever P, Taylor JA, and Niu L. RELIC: a novel dye-bias correction method for Illumina Methylation BeadChip. *BMC Genomics* 2017b; **1**: 4.

Xu Z, Niu L, Li L, and Taylor JA. ENmix: a novel background correction method for Illumina HumanMethylation450 BeadChip. *Nucleic Acids Res* 2016; **3**: e20.

Yu B, Russanova V, Gravina S, Hartley S, Mullikin J, Ignezweski A, Graham J, JH. S, DeCherney AH, and Howard B. DNA methylome and transcriptome sequencing in human ovarian granulosa cells links age-related changes in gene expression to gene body methylation and 3'-end GC density. *Oncotarget* 2015; **6**: 3627-3643.

Zelazowski MJ, Sandoval M, Paniker L, Hamilton HM, Han J, Gribbell MA, Kang R, and Cole F. Age-Dependent Alterations in Meiotic Recombination Cause Chromosome Segregation Errors in Spermatocytes. *Cell* 2017; **3**: 601-614 e613.

Zeng Y, Ni ZM, Liu SY, Gu X, Huang Q, Liu JA, and Wang Q. Parity and All-cause Mortality in Women and Men: A Dose-Response Meta-Analysis of Cohort Studies. *Sci Rep* 2016: 19351.

Zhang JJ, Liu X, Chen L, Zhang S, Zhang X, Hao C, and Miao YL. Advanced maternal age alters expression of maternal effect genes that are essential for human oocyte quality. *Aging* 2020; **4**: 3950-3961.

Zhou J, Peng X, and Mei S. Autophagy in Ovarian Follicular Development and Atresia. *Int J Biol Sci* 2019; **4**: 726-737.

Zymo Research. EZ DNA Methylation™ Kit. Instruction Manual: Ver. 1.2.6. 2019.

9. Appendices overview

Paper I: A distinctive epigenetic ageing profile in human granulosa cells.

Supplementary tables: https://figshare.com/s/82c3137d5b42e0a93121

Paper II: Identification of a unique epigenetic profile in women with diminished ovarian reserve.

Supplementary tables: https://figshare.com/s/a25352f38918b55d8ca7

Paper III: Gene expression profile of human metaphase II oocytes in relation to age by single cell RNA sequencing.

Supplementary tables: https://figshare.com/s/b8ff0c7f173c4ffa864e

Declarations of co-authorship

Paper I

A distinctive epigenetic ageing profile in human granulosa cells

A distinctive epigenetic ageing profile in human granulosa cells

K. W. Olsen[1,2,*,†], J. Castillo-Fernandez[3,†], A. Zedeler[4], N. C. Freiesleben[4,5], M. Bungum[6], A. C. Chan[2], A. Cardona[7], J. R. B. Perry[7], S. O. Skouby[1,8], R. Borup[2], E. R. Hoffmann[2], G. Kelsey[3,9], M. L. Grøndahl[1]

[1]Department of Obstetrics and Gynaecology, Department of Reproductive Medicine, Copenhagen University Hospital Herlev, Denmark
[2]DNRF Center for Chromosome Stability, Department of Cellular and Molecular Medicine, Faculty of Health and Medical Sciences, University of Copenhagen, Copenhagen, Denmark
[3]Epigenetics Programme, Babraham Institute, Cambridge, United Kingdom
[4] Department of Obstetrics and Gynaecology, The Fertility Clinic, Copenhagen University Hospital Hvidovre, Denmark
[5]VivaNeo Fertility Clinics, Stork IVF Clinic A/S, Copenhagen, Denmark.
[6]Reproductive Medicine Centre, Skåne University Hospital, Malmoe, Sweden.
[7]Medical Research Council Epidemiology Unit, University of Cambridge Addenbrooke's Hospital Cambridge, Cambridge, United Kingdom.
[8]Department of Clinical Medicine, Faculty of Health and Medical Sciences, University of Copenhagen, Copenhagen, Denmark.
[9]Centre for Trophoblast Research, University of Cambridge, Cambridge, United Kingdom.

*Correspondence address: kristina.wendelboe.olsen.01@regionh.dk, kristinawo@hotmail.com
[†]The authors consider that the first two authors should be regarded as joint First Authors.

Running title: Granulosa cell epigenetic ageing
Disclosure summary: The authors have nothing to disclose

STUDY QUESTION: Does women's age affect the DNA methylation (DNAm) profile differently in mural granulosa cells (MGC) from other somatic cells?
SUMMARY ANSWER: Accumulation of epimutations by age and a higher number of age-related differentially methylated regions (DMR) in MGC were found compared to leukocytes from the same woman, suggesting that the MGC have a distinctive epigenetic profile.
WHAT IS KNOWN ALREADY: The mechanisms underlying the decline in women's fertility from the mid-thirties remain to be fully elucidated. The DNAm age of many healthy tissues changes predictably with and follows chronological age, but DNAm age in some reproductive tissues has been shown to depart from chronological age (older: endometrium; younger: cumulus cells, spermatozoa).
STUDY DESIGN, SIZE, DURATION: This study is a multicenter cohort study based on retrospective analysis of prospectively collected data and material derived from healthy women undergoing IVF or ICSI treatment following ovarian stimulation with antagonist protocol. One hundred and nineteen women were included from September 2016 to June 2018 from four clinics in Denmark and Sweden.
PARTICIPANTS/MATERIALS, SETTING, METHODS: Blood samples were obtained from 118 healthy women with varying ovarian reserve status. MGC were collected from 63 of the 119 women by isolation from pooled follicles immediately after oocyte retrieval. DNA from leukocytes and MGC was extracted and analysed with a genome-wide methylation array. Data from the methylation array were processed using the ENmix package.
Subsequently, DNAm age was calculated using established and tailored age predictors and DMRs were analysed with the DMRcate package.
MAIN RESULTS AND ROLE OF CHANCE: Using established age predictors, DNAm age in MGC was found to be considerable younger and constant (average: 2.7 years) compared to chronological age (average: 33.9 years). A Granulosa Cell clock able to predict the age of both MGC (average: 32.4 years) and leukocytes (average: 38.8 years) was successfully developed. MGC differed from leukocytes in having a higher number

of epimutations (p = 0.003) but predicted telomere lengths unaffected by age (Pearson's correlation coefficient = -0.1, p = 0.47). DMRs were associated with age (age-DMRs) were identified in MGC (n = 335) and in leukocytes (n = 1) with a significant enrichment in MGC for genes involved in RNA processing (45 genes, $p = 3.96 \times 10^{-08}$) and gene expression (152 genes, $p = 2.3 \times 10^{-06}$). The top age-DMRs included the metastable epiallele *VTRNA2-1*, the DNAm regulator *ZFP57*, and the anti-Müllerian Hormone (*AMH*) gene. The apparent discordance between different epigenetic measures of age in MGC suggest that they reflect difference stages in the MGC lifecycle.

LIMITATIONS, REASONS FOR CAUTION: No gene expression data were available to associate with the epigenetic findings. The MGC are collected during ovarian stimulation which may influence DNAm, however no correlation between FSH dose and number of epimutations was found.

WIDER IMPLICATIONS OF THE FINDINGS: Our findings underline that the somatic compartment of the follicle follows a different methylation trajectory with age than other somatic cells. The higher number of epimutations and age-DMRs in MGC suggest that their function is affected by age.

STUDY FUNDING/COMPETING INTEREST(S): This project is part of ReproUnion collaborative study, co-financed by the European Union, Interreg V ÖKS, the Danish National Research Foundation, and the European Research Council. The authors declare no conflict of interest.

Keywords: DNA methylation / age / granulosa cells / reproduction / epigenetics

Introduction

The most important factor in determining female fertility potential is age. Most countries within the Organisation for Economic Co-operation and Development (OECD) have seen the average age of women at childbirth increase by between 2 and 5 years from 1970 to 2015 (OECD Family Database 2018). In Denmark in 2018, the average age for women giving birth was 31.0 years, while the age of first-time mothers was 29.3 years; in comparison, in 1968 the figures were 26.5 and 23.1 years, respectively (Statistics Denmark 2018). This implies an increasing challenge for female fertility followed by an increasing need of assisted reproduction, because both the quantity and quality (the competence to establish an ongoing pregnancy) of oocytes decline with advanced age (Franasiak et al. 2014). Children born after medically assisted reproduction in 2018 represented 9.8% of the Danish birth cohort (The Danish Fertility Society 2019). While life expectancy has increased substantially over the last century, timing of menopause as well as the age-related decline in reproductive potential have remained unchanged (Ceylan and Ozerdogan 2015; Baird et al. 2005), although some studies have indicated a small delay in the onset of menopause (Rödström et al. 2003; Van Noord et al. 1997).

During foetal life, oocytes arrested in the pro-phase of 1st meiosis are laid down in the ovary surrounded by one layer of pre-granulosa cells in the primordial follicles, which comprise the reproductive potential of the girl. In the primordial follicle, the pre-granulosa cells also remain in cell cycle arrest (Scalercio et al. 2015) for up to five decades until activation and subsequent folliculogenesis, a lengthy (six month) and highly complex process in which the follicles develop and mature. Upon activation, the pre-granulosa cells start proliferating and develop into an estimated 60 million mural granulosa cells (MGC) (McNatty et al. 1979) crucial for oestrogen production, ovulation of the matured oocyte in metaphase II, followed by luteinisation and corpus luteum formation (Dorrington et al. 1975). Follicular atresia affects all stages of folliculogenesis and only a limited number of the original 1-2 million oocytes present in the female ovary at birth remain when a woman reaches the age of 40 years. In addition to this depletion in the ovarian reserve of primordial follicles, the diminishing quality of oocytes including increase in aneuploidy (Franasiak et al. 2014) means that many women completely lose the ability to reproduce by the age of 40 years (Scheffer et al. 2003). The mechanisms involved in the age-associated increase in meiotic errors in

human oocytes remain to be fully elucidated. Several hypotheses for the reduced oocyte competence by age have been proposed; for example, the germline bottleneck theory of mutations in mitochondria, which considers that the most competent primordial follicles are selected and activated first, resulting in mitochondrial dysfunction, because of deleterious mutations in the remaining aged oocytes (Bergstrom and Pritchard 1998). The focus of the present study is the somatic cell compartments of the follicle: the cells that, by bidirectional communication with the oocytes, as well as by delivering nutrients to the oocyte, are crucial for oogenesis throughout folliculogenesis (Eppig 2001; Gilchrist et al. 2008). It has been suggested, based on data in Rhesus monkeys, that the capacity of pre-granulosa cells to repair double-stranded DNA breaks declines with increasing age (Zhang et al. 2015), as occurs in other somatic tissues with age. Whether granulosa cells age more rapidly than the rest of the body, thereby losing functionality and ability to support oocyte development, is not known.

Recently, it has been found that DNA methylation (DNAm) patterns can be used to predict chronological age with high accuracy. In 2013 Steve Horvath developed a multi-tissue age predictor (epigenetic clock), which is able to estimate age of most tissues and cell types with an accuracy of 3.6 years (Horvath 2013). The prediction is based on the weighted combination of methylation levels (methylation and demethylation) at 353 specific cytosine-phosphate-guanine (CpG) sites distributed across the genome. These CpG sites were selected out of 21,369 CpG sites measured with the Illumina 27K and 450K methylation array platforms and by analysing 7,844 non-cancer samples from 82 datasets containing 52 different cell and tissue types (Horvath 2013). The predicted age, referred to as DNAm age, is considered a biological measure of ageing. When the estimated DNAm age differs from the chronological age the term 'age acceleration' is used to describe faster or slower rates of ageing (Horvath 2013). Subsequently, several studies have found such deviations between the DNAm age and the chronological age in various tissue types and individuals (Sehl et al. 2017; Horvath et al. 2015b; Horvath et al. 2015a). One of the most interesting findings is that accelerated DNAm age in blood is associated with all-cause risk of mortality (Perna et al. 2016; Marioni et al. 2015). Since the development of the multi-tissue age predictor several more specialized epigenetic clocks have been developed with the aim of measuring different aspects of the ageing process (Levine et al. 2018; Weidner et al. 2014; Giuliani et al. 2016). Telomere length has for more than a decade been proposed to act as a biomarker for ageing (Sanders and Newman 2013) and possible relationship between female fertility and telomere length is debated (Kosebent et al. 2018). Recently, an estimator of telomere length based on DNAm data (DNAmTL) has been developed (Lu et al. 2019).

As the ability to reproduce is highly age-dependent in women, the above findings may have relevance in the understanding of ovarian ageing. A recent study by Morin et al. found that DNAm age of cumulus cells measured with Horvath's multi-tissue clock was substantially younger than chronological age regardless of the age and the response to ovarian stimulation of the women (Morin et al. 2018). The multi-tissue age predictor has been evaluated in other reproductive tissues, e.g., endometrium, in which the predicted age was significantly older compared with chronological age (Olesen et al. 2018), and spermatozoa, in which the predicted age was significantly younger than the chronological age (Horvath 2013). Moreover, DNAm age acceleration in leukocytes has been associated with reproductive life events such as menarche, puberty, and early menopause (Levine et al. 2016; Binder et al. 2018; Simpkin et al. 2017). However, the predictor has not been tested in the MGC, the cells supporting the oocytes during follicular growth and maturation, and which also produce the female sex hormones. Very few studies have investigated the DNAm profile of MGC, studies primarily focusing on differences in the methylome from women with polycystic ovarian syndrome (PCOS) (Qu et al. 2012; Pan et al. 2018; Sagvekar et al. 2019). MGC are available when oocytes are retrieved in treatments during ART. The aims of the present study were to: 1) assess the suitability of the multi-tissue DNAm age predictor and the DNAmTL predictor to MGC and leukocytes from women undergoing ART; 2) investigate if DNAm profiles of the two cell types

change with age and, if so, whether these changes are shared or tissue-specific.

Materials and Methods

Participants

This study is a multicentre cohort study based on retrospective analysis of prospectively collected data and material derived from healthy women undergoing IVF or ICSI treatment following controlled ovarian stimulation (COS) with GnRH antagonist protocol. Women receiving fertility treatment with either IVF or ICSI from September 2016 to January 2018 at four different clinics (Denmark: Herlev Hospital, Hvidovre Hospital, Stork IVF Clinic; Sweden: Skåne University Hospital) were invited to participate regardless of their age and anti-Müllerian hormone (AMH) level. They were primarily included during their first, second or third stimulation cycle. A total of 119 women were included in the study. Only women with no history of disease such as PCOS, severe endometriosis, dysregulated thyroid disease, severe comorbidity (insulin-dependent diabetes mellitus, non-insulin diabetes mellitus, gastrointestinal-, cardio-vascular-, pulmonary, liver or kidney disease) were asked to consider participation in the study. Seven participants were later diagnosed with PCOS as a secondary cause of infertility and were not excluded from the study.

Treatment protocol

The COS was initiated at day 2-3 of the menstrual cycle with recombinant FSH (Bemfola®; Gedeon Richter, Denmark. Gonal-f®; Merck-Serono, Denmark. Pergoveris®, Merck-Serono, Denmark) or urine derived human menopausal gonadotropin (Menopur®; Ferring Pharmaceuticals, Denmark) for 8-12 days, followed by the administration of a GnRH antagonist (Orgalutran®; MSD, Denmark). For the final follicle maturation and ovulation induction recombinant human chorionic gonadotropin (Ovitrelle®; Merck-Serono, Denmark) or a GnRH agonist (Gonapeptyl®; Ferring Pharmaceuticals, Denmark) was administrated when the leading follicles reached a diameter of >16 mm. Oocyte retrieval and collection of the MGC occurred 36 hours later.

Sample collection

Peripheral blood was collected (two 6 mL EDTA tubes) at one of the routine ultrasound scan visits in the clinics before the day of the oocyte retrieval. Within one hour after collection, the samples were centrifuged at 2000 g at 4 °C for 20 minutes dividing the blood into three sections: plasma, buffy coat and erythrocytes. The buffy coat containing the leukocytes was transferred to a cryovial (377267, Nunc™, Thermo Fisher Scientific™, Denmark) and stored at -80 °C until analysis. Plasma were divided into three cryovial tubes (377267, Nunc™, Thermo Fisher Scientific™, Denmark) and stored at -80 °C. The erythrocytes were discarded. MGC were isolated manually immediately after oocyte retrieval: granulosa cell aggregates, free of blood clots, were separated from the follicular fluid with a pipette and transferred to a 10 mL tube containing 3 mL washing solution (10% phosphate-buffered saline (AM9625, Invitrogen™, Thermo Fisher Scientific™, Denmark) + sterile water (1:10) + 1% polyvinyl alcohol (341584, Sigma-Aldrich, Denmark)). The MGC suspension was centrifuged at 300 g for 10 minutes and the sediment (the MGC) was isolated and transferred to a 0.2 mL tube (AB0620, Thermo Fisher Scientific™, USA), snap frozen in liquid nitrogen, and stored at -80 °C until analysis. At the time of isolation, the amount of MGC aggregates were noted (few, medium and numerous). Samples from 63 of the women were categorized medium and numerous and these were chosen for the analysis to ensure sufficient input of DNA.

DNA methylation analysis

DNA from the leukocytes (1 mL buffy coat) and MGC was isolated with the ReliaPrep™ Large Volume HT gDNA Isolation kit (A2751, Promega, Wisconsin, USA) according to the manufacturer's protocol. This was done using the Tecan Freedom EVO®-HSM Workstation. Genome-wide methylation levels were measured using the Illumina Infinium MethylationEPIC BeadChip (Illumina Inc., San Diego, CA) (Illumina 2015). Five hundred nanogram of DNA per sample were bisulfite treated by use of the Zymo EZ-96 DNA methylation kit (Zymo Research, Irvine, CA, USA). Thereafter, the samples were hybridized to the arrays (Infinium Methylation EPIC array) according

to the manufacturer's protocol. The DNA isolation and generation and management of the Illumina EPIC methylation array data was performed by the Human Genotyping Facility of the Genetic Laboratory of the Department of Internal Medicine, Erasmus MC, the Netherlands.

Methylome data processing

Illumina EPIC array data were processed using the ENmix package (Xu et al. 2016) in R (R Core Team 2016) to obtain methylation beta-values. Briefly, background correction was performed using the Exponential-Normal mixture distribution (ENmix) method using out-of-band type I probe intensities to model background noise (Xu et al. 2016), dye-bias correction was performed using the Regression on Logarithm of Internal Control probes (RELIC) method (Xu et al. 2017), and probe design bias adjustment was performed by implementing the Regression on Correlated Probes (RCP) method (Niu et al. 2016). Signals with a detection p-value > $1x10^{-6}$ and a number of beads < 3 were set to missing. Samples with missing data in > 5% of CpGs were excluded, as well as CpGs with missing data in > 5% of samples. Samples identified with outlier values in bisulfite intensity, total intensity, or beta-value distribution according to the ENmix quality control function were also excluded. Polymorphic (probes containing single nucleotide polymorphisms at the interrogated CpG site) and cross-hybridising probes (probes mapping to multiple regions of the genome) were filtered using the DMRcate package (Peters et al. 2015). Out of the 63 MGC samples, 59 remained for analysis. All 118 leukocyte samples passed quality control filters. These methylation beta-values were used for the analysis of DNAm aberrations.

Epigenetic ageing analysis

The online DNA Methylation Age Calculator (https://dnamage.genetics.ucla.edu/home) was used to estimate DNAm age. As recommended by the authors, noob normalization was performed in minfi (Aryee et al. 2014) to obtain beta-values. The MGC and leukocytes were analysed separately. Age acceleration difference was defined as the difference between DNAm age and chronological age, while age acceleration residuals as the residuals of DNAm age regressed on chronological age. An improved DNAm age predictor for MGC (Granulosa Cell clock) was developed by adding 27 MGC samples with normal AMH levels to a subset (n = 621) of the samples used to train the Skin & Blood clock (Levine et al. 2018; Horvath et al. 2018). Only studies with publicly available intensity data (*.IDAT) files were included in the training set of this predictor (GSE104471, GSE109042, GSE111223, GSE77136, and GSE80261). The Granulosa Cell clock was built following the methods described in the development of the Skin & Blood clock (Levine et al. 2018; Horvath et al. 2018). Briefly, a transformed version of chronological age, which has a logarithmic dependence until the age of 20 and linear dependence afterwards, was regressed on 452,567 CpG sites shared between the Illumina 450K and EPIC methylation arrays using an elastic regression model (10-fold cross validation to select lambda) that automatically selected 296 CpG sites. The predictor was tested on the remaining 32 MGC samples and the 118 leukocytes samples, which were not part of the training set.

Predicted telomere length analysis

Similar to the estimation of DNAm age the online DNA Methylation Age Calculator (https://dnamage.genetics.ucla.edu/home) was used to estimate DNAmTL. The predictor outputs a measure of leukocytes telomere length in which higher numbers indicate longer telomeres (Lu et al. 2019).

Accumulation of DNA methylation aberrations

DNAm aberrations, potential epimutations, were defined as outliers across all samples of the same tissue type (Gentilini et al. 2015). These outliers were defined as values greater than or less than three time the interquartile range from the upper or lower quartiles, respectively.

DMR analysis

Differentially methylated regions (DMR) analysis was performed using the DMRcate package (Peters et al. 2015) in R. Beta-values were converted to M-values and missing data were imputed to the mean across all samples of the same tissue type. False discovery rate (FDR) was set

at 10%. Gene ontology (GO) analysis was performed in R using the missMethyl package (Phipson et al. 2015) which accounts for the different number of probes per gene in the array.

Statistics

Difference between age groups were tested with one-way ANOVA. The number of epimutations in leukocytes and MGC were compared with Wilcoxon test. The age-DMR analysis was conducted with DMRcate (Peters et al. 2015). Enrichments were tested using Fisher's exact test. The accuracy of the different epigenetic clocks was measured by estimating Pearson's correlation coefficient, the median error defined as the median absolute difference between DNAm age and chronological age. All statistical analyses were performed in R and the value of $p < 0.05$ was considered statistically significant. The age of the women used in analysis referred to the time of the oocyte retrieval.

Ethics

All human materials were donated under approval from The Scientific Ethical Committee of the Capital Region, Denmark (ethical approval number: H-16027088) and the Danish Data Protection Agency (ID-nr.: HGH-2016_086) and conducted in accordance with the Helsinki Declaration II. All participants gave informed consent before the inclusion in the study.

Results

Participant characteristics

A total of 119 women were included in the study. Buffy coats were collected from each participant and 63 contributed additionally with donation of their MGC. Of note: one woman only participated with donation of her MGC. An overview of our participant population is presented in Table I (all) and Table SI (women donating MGC). Chronological age at the time of oocyte retrieval ranged from 25-44 years (average = 33.9 years). Based on the women's AMH level and the age-expected AMH level described by Lee and coworkers (Lee et al. 2012), the participants were categorized into ovarian reserve groups: diminished ovarian reserve (DOR) (under the 10th percentile), Normal (25th to 75th percentile), and High (above the 90th percentile). Women over 40 years were not categorized from their AMH level because it is well established that most of these women experience a diminished ovarian reserve (Liu et al. 2011; Klein and Sauer 2001).

Prediction of the DNAm age

DNAm age was analysed with the multi-tissue age predictor developed by Steve Horvath (Horvath 2013). A significant correlation between the DNAm age and the chronological age in leukocytes was confirmed (Pearson's correlation coefficient (cor) = 0.79; $p = 2.2\text{x}10^{-26}$) (Figure S1A). The predicted mean age was 35.0 years compared with an average chronological age of 33.9. In contrast, no significant correlation was present between DNAm age and chronological age in the MGC (cor = 0.16, $p = 0.21$). The DNAm age of MGC was substantially lower than the chronological age of the women with an average age of 6.8 years (Figure S1). To further explore DNAm age, we applied an alternative age estimator: the Skin & Blood clock (Levine et al. 2018; Horvath et al. 2018), in which cells with the same primary origin as MGC are well represented. The age predicted by the 391 CpG sites that comprise this clock was consistent with the women's chronological age in leukocytes (average = 33.0 years; cor = 0.92; $p = 4.0\text{x}10^{-48}$), but the DNAm age was still substantially younger in the MGC (Figure 1A), with an average age of 2.7 years. However, using the Skin & Blood clock a minor correlation with age in MGC was found (cor = 0.30; $p = 0.02$) (Figure 1A); in addition, there was a weak correlation between MGC and leukocytes (cor = 0.23; $p = 0.086$; Figure 1B). The predicted DNAm age was younger whether the MGC were derived from women with low ovarian reserve (women with DOR or age > 40 years) or from women with normal or high ovarian reserve (Figure 1A). Adjusting for AMH levels or the ovarian stimulation regimens did not change the age acceleration.

We then looked at the association between age acceleration difference and chronological age (Figure 1C and 1D). The age acceleration difference was small in leukocytes (median = -1.04; range = -6.32 to 4.77) and showed a positive correlation with chronological age (cor = 0.41; $p = 0.001$); in contrast, in MGC the difference was large in absolute values (median = -29.96; range = -41.54 to

-22.99), was negative, and increased in magnitude with age (cor = -0.99; $p = 2.4x10^{-47}$; Figure 1C). As expected from the latter observation, we found a negative correlation (cor = -0.42, $p = 0.001$) in the age acceleration differences between leukocytes and MGC (Figure 1D).

A Granulosa Cell clock

Due to the poor correlation in DNAm and chronological age for MCGs, we decided to improve the Skin & Blood epigenetic age estimator by incorporating 27 of our MGC samples in a training set (which we name the Granulosa Cell clock). The Granulosa Cell clock we developed consists of 296 CpG sites (Table SII). Figure 2A shows the prediction of DNAm age of the remaining 32 MGC samples that were not used in the training set; the Granulosa Cell clock yielded an improved correlation of 0.47 ($p = 0.006$). When applying the Granulosa Cell clock to our leukocyte data a good correlation was found (cor = 0.85, $p = 4.3x10^{-34}$). Figure S2A shows the intersection between the Skin & Blood clock and the Granulosa Cells clock (37 CpGs). The genomic distribution of the clock type specific CpG sites – 354 CpGs in the Skin & Blood clock, and 259 CpGs in the Granulosa Cell clock – is shown in Figure S2B. When comparing the mean DNAm levels of each CpG across all samples between leukocytes and MGC it is evident that the DNAm levels of the CpG sites in the Granulosa Cell clock are shared between the two tissues, whereas those in the Skin & Blood clock are not (Figure S2C).

Predicted telomere length

Telomere length is another biomarker of ageing that can be predicted from DNAm profiles.
DNAmTL was calculated for both cell types. In leukocytes telomere length was negatively correlated with age (cor = -0.62, $p = 4.0x10^{-14}$) (Figure 3A), while in MGC telomere length was shorter and unaffected by age (cor = -0.1, $p = 0.47$) (Figure 3B).

Epimutations

As another measure of ageing we used the accumulation of errors in DNAm (here defined as epimutations). We observed that epimutations increased exponentially with advanced maternal age in both tissues. However, the rate of increase was higher in MGC (Figure 4A). Overall, epimutations were more frequent in MGC (paired samples Wilcoxon test; $p = 0.003$) compared with leukocytes of the same women (Figure 4B). We found no association between the total dose of FSH and the number of epimutations (leukocytes: cor = 0.14, $p = 0.54$, MGC: cor = 0.32, $p = 0.053$). Epimutated sites showed a moderate enrichment in intergenic regions (odds ratio (OR) = 1.18; $p = 1.1x10^{-171}$) and depletion close to promoter regions (0-200 base pair (bp) upstream of the transcription start site) (OR = 0.71; $p = 1.4x10^{-264}$).

Epigenome-wide association study

To further study the relationship between ageing and DNAm we conducted an epigenome-wide association study (EWAS) of chronological age. Due to limited sample size we were underpowered to detect genome-wide significant signals ($p < 5x10^{-8}$) at single CpG site resolution (power = 0.00, effect size=0.15) (Figure S3). In order to increase the statistical power to detect differences we conducted the identification of DMRs in the extremes of our sample (women under 30 years old (n = 19) and women above 40 (n= 6); only one woman with PCOS as her secondary diagnosis was in those age groups and included in this analysis, which however did not affect the result (data not shown)). A total of 335 DMRs associated with age (age-DMRs) were identified in MGC and only one in leukocytes (Table SIII). The most significant signal in MGC was identified at the metastable-epiallele vault RNA 2-1 (*VTRNA2-1)*, where a gain of methylation was observed that was significant in MGC but not leukocytes (Figure 5 and Figure S4). The second most significant signal was found in the *AMH* gene where a gain of methylation in the gene body was observed in MGC (Table SIII, full list; Table II, selected genes). Out of the 335 age-DMRs, 311 showed a loss of methylation with age, while only 24 gained methylation. Age-DMRs were enriched in promoters (0-200 bp upstream of the transcription start site) (Fisher's exact test; OR = 3.32; $p = 7.1x10^{-122}$). Gene ontology (GO) analysis of the genes associated with the 335 age-DMRs revealed an enrichment for ribonucleic acid (RNA) processing ($p = 3.96x10^{-08}$) and gene expression ($p = 2.3x10^{-06}$)

(Table SIV). In addition, we tested for enrichment in gene lists related to reproduction and granulosa cell expression profiles (Table SV). We tested for enrichment in genes involved in female reproductive system disease and infertility (https://gemma.msl.ubc.ca/phenotypes.html) (Zoubarev et al. 2012), genes expressed in granulosa cells after ovulation induction (Grøndahl et al. 2012), and genes expressed in granulosa cells prior to hCG (Wissing et al. 2014). Only genes involved in Female Reproductive System Disease showed an over-representation (p = 0.006). As a negative control to ensure we were not observing a spurious signal, we also tested a random gene list with a similar number of genes (disease by infectious disease), which showed no significant enrichment (p = 0.16).

Discussion

Our data clearly demonstrate that MGC from the human ovary have a distinctive epigenetic ageing profile compared with blood collected from the same woman. To our knowledge these data show that MGCs have the largest error predicated by the multi-tissue DNAm clock. As expected, we found a significant correlation between DNAm age and chronological age in leukocytes with both the multi-tissue age predictor (Horvath 2013) and the Skin & Blood clock (Horvath et al. 2018). The MGC, on the other hand, showed no or limited correlation with chronological age which, together with their substantially younger DNAm age, suggests that MGC age epigenetically differently and independently from other somatic cells in the body. Not surprisingly, these results are consistent with findings in cumulus cells, which showed an average DNAm age, based on the multi-tissue age predictor, of 9.3 years regardless of the chronological age of the women (comparison of two age groups; young (32.8 years) vs. old (41.9 years)) (Morin et al. 2018). We conclude that ageing of the somatic cells in the ovary affects different DNAm sites than the sites found in other tissue types. Although the association was limited, our results indicate that women with a young DNAm age of their leukocytes also have a younger DNAm age in their MGC. We further demonstrated that the magnitude of the age acceleration differences of the MGC gradually elevated with advanced age. This may partially be explained by the limited correlation with chronological age and the reduced range in the DNAm age estimates.

The multi-tissue age predictor did not perform well in the MGC, which could be explained by the lack of MGC in the training data set during the development of the multi-tissue age predictor. However, the predictor has previously been shown to provide accurate estimates of chronological age for tissues not represented in the training data (e.g. oesophagus, jejunum, pancreas, spleen) (Horvath 2013). Intriguingly, the Skin & Blood clock also lacks MGC in its training set but was able to show at least a weak correlation with chronological age. A plausible explanation could be that the tissues used to train this clock were closer in origin to MGC. The Skin & Blood clock was designed having in mind its performance in fibroblasts and other cell types/tissues used in *ex vivo* studies, such as keratinocytes, buccal cells, endothelial cells, lymphoblastoid cells, skin, blood, and saliva. Cells of mesodermal origin, as MGC are (Sawyer et al. 2002), are well represented in this clock. By improving the Skin & Blood clock with the development of the Granulosa Cell clock we were able to detect a correlation between DNAm age and chronological age in MGC. However, the DNAm age was somewhat over-estimated when applying the Granulosa Cell clock to our leukocyte data, which again suggests that MGC are epigenetically different from other somatic cells. The Granulosa Cell clock could be capturing a fraction of mitotic ageing which explains why leukocytes with a history of more cell divisions show a higher DNAm age. In addition, the genomic distribution of the CpG content of the two clocks differs, primarily in the proportion of CpGs in islands (28% vs. 38%) and open sea, defined as isolated CpGs located >4 kb from a CpG island, (38% vs. 26%). Even though the Skin & Blood clock and the Granulosa Cell clock only have 37 CpG sites in common, the Granulosa cell clock performed well in both cell types, suggesting that the 354 CpG sites included in the Skin & Blood clock are not exclusive to the ageing process of somatic cells. We observed an enrichment in CpG islands in the intersected CpG sites compared with background (all sites in the array). From studies in other tissues it is known that gains of methylation at CpG island promoters are observed in age-DMRs (Bell et al. 2016; Teschendorff et al. 2010; Rakyan

et al. 2010). Methylation acquisition with age at promoters of genes, such as the well replicated fatty acid elongase 2 gene (*ELOVL2)* (Sawyer et al. 2002), might be shared across all cell types, and that is why we observe this enrichment at the intersected CpG sites.

To further explore the ageing process, we calculated the DNAmTL. Shorter telomere length has been shown to correlate with advanced age in other cell types (Shammas 2011). The expected correlation between chronological age and DNAmTL was found in the leukocytes; however, we found that the DNAmTL of MGC was shorter and unaffected by age, which may reflect that the DNAmTL predictor was trained in blood and fails to predict the telomere length in MGC. Interestingly, Morin et al. found the opposite in cumulus cells, where cumulus cells have a longer relative telomere length than white blood cells from women pursuing ART treatment (Morin et al. 2018). However, the study had actual measures and not estimates from DNAm profiles. Granulosa cells proliferate rapidly throughout the late phase of folliculogenesis (from 30 pre-granulosa cells in the primordial follicle (Westergaard et al. 2007) to around 60 million in the ovulatory follicle (Gougeon 1996; Hirshfield 1985)). It has been suggested that granulosa cells have shorter telomere length, despite the presence of active telomerase which functions to restore shortened telomeres (Kosebent et al. 2018). The microenvironment of granulosa cells contains oestrogens reported to influence telomerase activity (Bayne et al. 2011) as well as other agents with potential influence on telomere length (Kosebent et al. 2018). Since MGC are unique cells in terms of their many years or decades of quiescence followed by an accelerated mitotic activity, they may represent another aspect of ageing than other cells. We already know that compromised repair of DNA double strand breaks is associated with accelerated loss of ovarian follicles and accumulation of double strand breaks in human oocytes (Titus et al. 2013), and that the capacity of pre-granulosa cells to repair double strand breaks declines with increasing age (Zhang et al. 2015) in non-human primates, suggesting that also the MGC are affected by advanced age.

DNAm age and predicted telomere length can be used as a prediction of chronological age or as a reflection of biological ageing, however they are not a measure of the actual ageing process and might reflect different aspects of ageing. Therefore, as a third approach to study ageing in MGC we investigated the frequency of epimutations, which are not restricted only to a limited subset of CpGs in the array. The notion that epimutations accumulate during the lifetime first gained prominence from the epigenetic divergence observed in identical twins; during early life, twins were indistinguishable at sites assayed for DNAm, but became divergent at older ages (Fraga et al. 2005). More recent studies examining methylation in peripheral blood from infants to centenarians have reported an exponential increase in epimutations with age (Gentilini et al. 2015). We also observed that the number of epimutations in MGC increases substantially with advancing age. We found a significantly higher frequency of epimutations in intergenic regions of the genome, which makes us speculate that promotor regions, which are often more conserved, are partially more protected from these types of events. However, the number of epimutations was significantly greater in MGC compared to leukocytes. This may due to hormonal exposure of these cells during COS and investigating epimutations in MGC from a natural cycle would remove the potential confound of COS. However, women treated with high dose of FSH did not have a higher number of epimutations compared with women treated with a low dose of FSH, suggesting that the relatively short time of hormone exposure does not influence the epigenetics in mature follicles. Still, it remains unknown when during folliculogenesis the epimutations occur.

Finally, EWAS data revealed 335 DMRs when comparing MGC from young (< 30 years) and reproductively older women (≥ 40 years). These age-DMRs were not observed in leukocytes from the same participants or generally reported in other tissues (Day et al. 2013), suggesting a different ageing process in MGC. Interestingly, the comparison in leukocytes identified only one age-DMR, which may suggest that more drastic changes with age occur in MGC as a potential reflection of the loss of function in the ovarian follicle (the competence of the oocyte) with increasing age. The age-DMR found in the leukocytes was in the *REC8* meiotic recombination protein gene, which

encodes the REC8 protein involved in the meiotic cohesin complex that binds sister chromatids (Parisi et al. 1999). Decreased level of REC8 in dictyate stage oocytes (before resumption of meiosis) in women ≥40 years has been suggested to partly explain the high frequency of aneuploidy found in oocytes from women with advanced maternal age (Tsutsumi et al. 2014). Interestingly, *REC8* has been added to the list of candidate genes for premature ovarian insufficiency (POI), as a mutation was found in blood from two women diagnosed with POI (Bouilly et al. 2016).

Furthermore, changes in the DNAm of *REC8* in leukocytes were recently suggested to be a biomarker for cancer risk (Bartlett et al. 2019). Whether *REC8* DNAm in leucocytes relates to female fertility and general health is unclear and needs further exploration before drawing any conclusions.

The most significant signal we identified in MGC was at the *VTRNA2-1* epiallele, which exhibited a gain of methylation. Even though this is a metastable epiallele with a methylation level that varies between individuals but generally considered to be shared across tissues from the same individual (Silver et al. 2015), we only observed this signal in MGC and not in leukocytes, again suggesting that MGC differ from other somatic cell types. Another significant signal observed was increased methylation in the zinc finger protein 57 homolog (*ZFP57)* gene, which is a significant factor in DNAm maintenance and has been linked with metastable epiallele methylation (Kessler et al. 2018). The possible functional significance of this finding is unclear at this stage; recently, ovarian dysfunction after prenatal exposure to insecticide has been connected to altered expression of downstream *ZFP57* target genes in the adult mouse ovary (Legoff et al. 2019).

GO analysis of the MGC age-DMRs revealed enrichment in pathways related to gene transcription. Studies in other somatic cells have suggested a global deregulation of gene expression with age and also a decrease in the amount of processed messenger RNA (mRNA) in aged cells (Sawyer et al. 2002). Our results suggest that MGC are not the exception and might be experiencing a similar effect on mRNA processing at a relatively early age. Interestingly, the second most significant signal we found was in the *AMH* gene, with increased methylation in the gene body. AMH is produced by the granulosa cells of small growing follicles and plays a key role in folliculogenesis (Rajpert-De Meyts et al. 1999). The expression of AMH (both mRNA and protein) in human granulosa cells wanes with increasing size of the human follicle (Grøndahl et al. 2011; Kristensen et al. 2017) reaching a stable low level in MGC isolated from pre-ovulatory follicles before ovulation induction and at oocyte retrieval (Wissing et al. 2014). The primary factors regulating AMH expression in granulosa cells are oocyte derived factors: growth differentiation factor 9 (GDF9) and bone morphogenetic protein 15 (BMP15), as well as FSH (Roy et al. 2018). As methylation of gene bodies primarily has been correlated with increased expression (Jjingo et al. 2012), our finding suggests an age-related higher expression of AMH in the pre-ovulatory follicle which may reflect an altered communication between the oocyte and granulosa cells. These findings are supported by Yu et al., who found age-related changes in the *AMH* gene in human granulosa cells (Yu et al. 2015). It had been shown that the concentration of GDF9 in the follicular fluid decreases with increasing age of women, indicating an alteration in the secretion of oocyte specific factors with age (Han et al. 2011). Other genes associated with age-DMRs in MGC were placenta growth factor (*PGF*), growth hormone secretagogue receptor (*GHSR*) and growth hormone receptor (*GHR*); all reported to be involved in folliculogenesis. PGF is expressed by MGC and is required for ovulation, luteinization and follicular angiogenesis in primates (Bender et al. 2018), and GHSR in mice has been shown to be activated in response to stress resulting in a reduced number of primordial follicles (Natale et al. 2019). Furthermore, a recent study showed a lower number of GHR in MGC in reproductive older women compared with younger women (Regan et al. 2018). Our findings thus support and extend an association between age and these genes in the ovarian follicle. However, whether the changes are causative (as expected for promotor methylation) or a consequence (as in gene-body methylation) of changes in gene expression is unknown and needs further investigation. Due to a limited number of cells from the MGC collection we were not able to perform a gene expression analysis to evaluate

whether the epigenetic findings are correlated with the changes in gene expression in the MGC.

With the comparison of two somatic cell types, our findings suggest that MGC age differently to non-ovarian somatic cells in the human body. MGC play a pivotal role in folliculogenesis and in the interaction with the oocyte, so further knowledge about ageing of the MGC might give us important insights into ageing of the oocyte itself. How can we reconcile the seemingly discordant effects we observe in MGC in DNAm age prediction, estimated telomere length and age-related increase in epimutations? One possibility is that these outcomes are associated with different aspects of ageing and the unique biology of MGCs and the ovarian follicle. For instance, MGCs may experience a similar, fixed process of proliferation and expansion once the follicle is activated irrespective of when during the woman's life course it occurs. In contrast, with increasing age, the length of time that the follicle has remained in the dormant state increases. Therefore, if telomere length and predicted DNAm age are properties very much associated with mitotic events, these parameters will be similar whatever the chronological age of the donor. The increase in epimutations we observe with age in MGCs might therefore indicate that these DNAm aberrations are accumulating mostly in the period of extended follicle dormancy. One potential consequence is that the epigenetic fidelity of ovarian somatic cells at the time of follicular recruitment in older women is impaired.

More studies are needed to establish whether our Granulosa Cell clock or epimutation detection could be used to detect premature reproductive ageing in women and to investigate whether the clock is also applicable to cumulus cell or other cells of the human ovary.

Although invasive, this knowledge could potentially give us a tool to determine an individual's pace of reproductive ageing, thereby giving women a better chance to plan the best time for pregnancy.

Author's roles

KWO, MLG and RB designed and initiated the study. KWO, AZ, NlCF and MB were involved in patient recruitment and sample collection. KWO, JCF, MLG and GK were involved in the analysis and interpretation of data and participated in writing and finalizing the manuscript. JCF and AC performed the bioinformatic analysis and JCF prepared the figures and supplementary tables with input from KWO. KWO prepared Table I, Table II and Table SI. JRBP contributed to the analysis of the data. ACC provisioned the study material. ERH, RB and SOS participated in finalizing the manuscript. All authors reviewed the manuscript and accepted the final version.

Acknowledgement

We thank all participating women for their willingness to participate in the study. We also want to express our gratitude to all nurses and embryologists, who were involved in the patient recruitment and material sampling at Herlev Hospital, Hvidovre Hospital, Skåne University Hospital and Stork IVF Clinic A/S.

Funding

The study is part of the ReproUnion program funding a PhD position for KWO. ReproUnion was supported by the Interreg program for Øresund-Kattegat-Skagerak, which was supported by EU funds, Capital region of Denmark, Region Zealand, Region Skåne and Ferring Pharmaceutical Company, Department of Gynaecology-Obstetrics at Herlev-Gentofte Hospital, Denmark and the Danish National Research Foundation (DNRF). Center for Chromosome Stability (DNRF115) have also supported the project financially. Work in GK's group was supported by grants from the UK Biotechnology and Biological Sciences Research Council (BBS/E/B/000C0423) and Medical Research Council (MR/S000437/1). RB was supported by the European Research Council (ERC grant 724718-ReCAP), ACC and ERH by the Novo Nordisk Foundation Young Investigator Award (NNF15OC0016662).

Conflict of interest

The authors declare no conflict or competing interests.

References

Aryee MJ, Jaffe AE, Corrada-Bravo H, Ladd-Acosta C, Feinberg AP, Hansen KD, and Irizarry RA.

Minfi: A flexible and comprehensive Bioconductor package for the analysis of Infinium DNA methylation microarrays. *Bioinformatics* 2014; **10**: 1363-1369.

Baird DT, Collins J, Egozcue J, Evers LH, Gianaroli L, Leridon H, Sunde A, Templeton A, Van Steirteghem A, Cohen J*, et al.* Fertility and ageing. *Hum Reprod Update* 2005; **3**: 261-276.

Bartlett AH, Liang JW, Sandoval-Sierra JV, Fowke JH, Simonsick EM, Johnson KC, and Mozhui K. Longitudinal study of leukocyte DNA methylation and biomarkers for cancer risk in older adults. *Biomark Res* 2019; **10**: 1-13.

Bayne S, Li H, Jones ME, Pinto AR, van Sinderen M, Drummond A, Simpson ER, and Liu JP. Estrogen deficiency reversibly induces telomere shortening in mouse granulosa cells and ovarian aging in vivo. *Protein Cell* 2011; **4**: 333-346.

Bell CG, Xia Y, Yuan W, Gao F, Ward K, Roos L, Mangino M, Hysi PG, Bell J, Wang J*, et al.* Novel regional age-associated DNA methylation changes within human common disease-associated loci. *Genome Biol.* 2016; **1**: 193.

Bender HR, Trau HA, and Duffy DM. Placental Growth Factor Is Required for Ovulation, Luteinization, and Angiogenesis in Primate Ovulatory Follicles. *Endocrinology* 2018; **2**: 710-722.

Bergstrom CT and Pritchard J. Germline bottlenecks and the evolutionary maintenance of mitochondrial genomes. *Genetics* 1998; **4**: 2135-2146.

Binder AM, Corvalan C, Mericq V, Pereira A, Santos JL, Horvath S, Shepherd J, and Michels KB. Faster ticking rate of the epigenetic clock is associated with faster pubertal development in girls. *Epigenetics* 2018; **1**: 85-94.

Bouilly J, Beau I, Barraud S, Bernard V, Azibi K, Fagart J, Fèvre A, Todeschini AL, Veitia RA, Beldjord C*, et al.* Identification of Multiple Gene Mutations Accounts for a new Genetic Architecture of Primary Ovarian Insufficiency. *J Clin Endocrinol Metab* 2016; **12**: 4541-4550.

Ceylan B and Ozerdogan N. Factors affecting age of onset of menopause and determination of quality of life in menopause. *Turk J Obstet Gynecol* 2015; **1**: 43-49.

Day K, Waite LL, Thalacker-Mercer A, West A, Bamman MM, Brooks JD, Myers RM, and Absher D. Differential DNA methylation with age displays both common and dynamic features across human tissues that are influenced by CpG landscape. *Genome Biol.* 2013; **9**: 1-19.

Dorrington JH, Moon YS, and Armstrong DT. Estradiol-17beta biosynthesis in cultured granulosa cells from hypophysectomized immature rats; stimulation by follicle-stimulating hormone. *Endocrinology* 1975; **5**: 1328–1331.

Eppig JJ. Oocyte control of ovarian follicular development and function in mammals. *Reproduction* 2001; **6**: 829-838.

Fraga MF, Ballestar E, Paz MF, Ropero S, Setien F, Ballestar ML, Heine-Suner D, Cigudosa JC, Urioste M, Benitez J*, et al.* Epigenetic differences arise during the lifetime of monozygotic twins. *Proc Natl Acad Sci U S A* 2005; **30**: 10604-10609.

Franasiak JM, Forman EJ, Hong KH, Werner MD, Upham KM, Treff NR, and Scott Jr. RT. The nature of aneuploidy with increasing age of the female partner: a review of 15,169 consecutive trophectoderm biopsies evaluated with comprehensive chromosomal screening. *Fertil Steril* 2014; **3**: 656-663.

Gentilini D, Garagnani P, Pisoni S, Bacalini MG, Calzari L, Mari D, Vitale G, Franceschi C, and Di Blasio AM. Stochastic epigenetic mutations (DNA methylation) increase exponentially in human aging and correlate with X chromosome inactivation skewing in females. *Aging* 2015; **8**: 568-578.

Gilchrist RB, Lane M, and Thompson JG. Oocyte-secreted factors: regulators of cumulus cell function and oocyte quality. *Hum Reprod Update* 2008; **2**: 159-177.

Giuliani C, Cilli E, Bacalini MG, Pirazzini C, Sazzini M, Gruppioni G, Franceschi C, Garagnani P, and Luiselli D. Inferring chronological age from DNA methylation patterns of human teeth. *Am J Phys Anthropol* 2016; **4**: 585-595.

Gougeon A. Regulation of Ovarian Follicular Development in Primates: Facts and Hypotheses. *Endocrine Reviews* 1996; **2**: 121-155.

Grøndahl ML, Andersen CY, Bogstad J, Borgbo T, Boujida VH, and Borup R. Specific genes are selectively expressed between cumulus and

granulosa cells from individual human pre-ovulatory follicles. *Mol Hum Reprod* 2012; **12**: 572-584.

Grøndahl ML, Nielsen ME, Dal Canto MB, Fadini R, Rasmussen IA, Westergaard LG, Kristensen SG, and Yding Andersen C. Anti-Mullerian hormone remains highly expressed in human cumulus cells during the final stages of folliculogenesis. *Reprod Biomed Online* 2011; **4**: 389-398.

Han M, Park SB, and Park BJ. Lower growth factor expression in follicular fluid undergone in-vitro fertilization. *Clin Exp Reprod Med* 2011; **4**: 210-215.

Hirshfield A. Comparison of Granulosa Cell Proliferation in Small Follicles of Hypophysectomized, Prepubertal, and Mature Rats. *Biol. Reprod.* 1985; **4**: 979-987

Horvath S. DNA methylation age of human tissues and cell types. *Genome Biol.* 2013; **10**.

Horvath S, Mah V, Lu AT, Woo JS, Choi OW, Jasinska AJ, Riancho JA, Tung S, Coles NS, Braun J*, et al.* The cerebellum ages slowly according to the epigenetic clock. *Aging* 2015a; **5**: 294-306.

Horvath S, Oshima J, Martin GM, Lu AT, Quach A, Cohen H, Felton S, Matsuyama M, Lowe D, Kabacik S*, et al.* Epigenetic clock for skin and blood cells applied to Hutchinson Gilford Progeria Syndrome and ex vivo studies. *Aging* 2018; **7**: 1758-1775.

Horvath S, Pirazzini C, Bacalini MG, Gentilini D, Di Blasio AM, Delledonne M, Mari D, Arosio B, Monti D, Passarino G*, et al.* Decreased epigenetic age of PBMCs from Italian semisupercentenarians and their offspring. *Aging* 2015b; **12**: 1159-1170.

Illumina. Infinium® HD Assay Methylation Protocol Guide. 2015.

Jjingo D, Conley AB, Yi SV, Lunyak VV, and Jordan IK. On the presence and role of human gene-body DNA methylation. *Oncotarget* 2012; **4**: 462-474.

Kessler N, Waterland R, Prentice A, and Silver M. Establishment of environmentally sensitive DNA methylation states in the very early human embryo. *SCI ADV* 2018; **7**: eaat2624.

Klein J and Sauer MV. Assessing fertility in women of advanced reproductive age. *Am J Obstet Gynecol* 2001; **3**: 758-770.

Kosebent EG, Uysal F, and Ozturk S. Telomere length and telomerase activity during folliculogenesis in mammals. *J Reprod Dev* 2018; **6**: 477-484.

Kristensen SG, Mamsen LS, Jeppesen JV, Bøtkjær JA, Pors SE, Borgbo T, Ernst E, Macklon KT, and Andersen CY. Hallmarks of Human Small Antral Follicle Development: Implications for Regulation of Ovarian Steroidogenesis and Selection of the Dominant Follicle. *Front Endocrinol (Lausanne)* 2017; **376**: 1-10.

Lee JE, Park DS, Kim M-L, Yoon BS, Song T, Kim MK, Seong SJ, and Kim Y-J. Age-related distribution of anti-Müllerian hormone levels in 2,879 Korean women with regular menstruation. *Korean J of Obstet Gynecol.* 2012; **12**: 920.

Legoff L, Dali O, D'Cruz SC, Suglia A, Gely-Pernot A, Hemery C, Kernanec PY, Demmouche A, Kervarrec C, Tevosian S*, et al.* Ovarian dysfunction following prenatal exposure to an insecticide, chlordecone, associates with altered epigenetic features. *Epigenetics Chromatin* 2019; **1**: 29.

Levine ME, Lu AT, Chen BH, Hernandez DG, Singleton AB, Ferrucci L, Bandinelli S, Salfati E, Manson JE, Quach A*, et al.* Menopause accelerates biological aging. *Proc Natl Acad Sci U S A* 2016; **33**: 9327-9332.

Levine ME, Lu AT, Quach A, Chen BH, Assimes TL, Bandinelli S, Hou L, Baccarelli AA, Stewart JD, Li Y*, et al.* An epigenetic biomarker of aging for lifespan and healthspan. *Aging* 2018; **4**: 573-591.

Liu K, Case A, Cheung AP, Sierra S, AlAsiri S, Carranza-Mamane B, Case A, Dwyer C, Graham J, Havelock J*, et al.* Advanced Reproductive Age and Fertility. *J Obstet Gynaecol Can* 2011; **11**: 1165-1175.

Lu AT, Seeboth A, Tsai P-C, Sun D, Quach A, Reiner AP, Kooperberg C, Ferrucci L, Hou L, Baccarelli AA*, et al.* DNA methylation-based estimator of telomere length. *Aging* 2019.

Marioni RE, Shah S, McRae AF, Chen BH, Colicino E, Harris SE, Gibson J, Henders AK, Redmond P, Cox SR*, et al.* DNA methylation age of blood predicts all-cause mortality in later life. *Genome Biol* 2015: 25.

McNatty K, Smith D, Makris A, Osathanondh R, and Ryan K. The Microenvironment of the

Human Antral Follicle: Interrelationships among the Steroid Levels in Antral Fluid, the Population of Granulosa Cells, and the Status of the Oocyte in Vivo and in Vitro. *J. Clin. Endocrinol. Metab.* 1979; **66**: 851–860.

Morin SJ, Tao X, Marin D, Zhan Y, Landis J, Bedard J, Scott RT, and Seli E. DNA methylation-based age prediction and telomere length in white blood cells and cumulus cells of infertile women with normal or poor response to ovarian stimulation. *Aging* 2018; **12**.

Natale MRD, Soch A, Ziko I, De Luca SN, Spencer SJ, and Sominsky L. Chronic predator stress in female mice reduces primordial follicle numbers: implications for the role of ghrelin. *J Endocrinol* 2019; **3**: 201-219.

Niu L, Xu Z, and Taylor JA. RCP: a novel probe design bias correction method for Illumina Methylation BeadChip. *Bioinformatics* 2016; **17**: 2659-2663.

OECD Family Database. Age of mothers at childbirth and age-specific fertility. 2018. http://www.oecd.org/els/family/database.htm .

Olesen MS, Starnawska A, Bybjerg-Grauholm J, Bielfeld AP, Agerholm I, Forman A, Overgaard MT, and Nyegaard M. Biological age of the endometrium using DNA methylation. *Reproduction* 2018; **2**: 167-172.

Pan JX, Tan YJ, Wang FF, Hou NN, Xiang YQ, Zhang JY, Liu Y, Qu F, Meng Q, Xu J*, et al.* Aberrant expression and DNA methylation of lipid metabolism genes in PCOS: a new insight into its pathogenesis. *Clin Epigenetics* 2018: 6.

Parisi S, McKay MJ, Molnar M, Thompson MA, van der Spek PJ, van Drunen-Schoenmaker E, Kanaar R, Lehmann E, Hoeijmakers JHJ, and Kohli J. Rec8p, a Meiotic Recombination and Sister Chromatid Cohesion Phosphoprotein of the Rad21p Family Conserved from Fission Yeast to Humans. *Mol Cell Biol.* 1999; **5**: 3515-3528.

Perna L, Zhang Y, Mons U, Holleczek B, Saum KU, and Brenner H. Epigenetic age acceleration predicts cancer, cardiovascular, and all-cause mortality in a German case cohort. *Clin Epigenetics* 2016; **64**: 1-7.

Peters TJ, Buckley MJ, Statham AL, Pidsley R, Samaras K, V Lord R, Clark SJ, and Molloy PL. De novo identification of differentially methylated regions in the human genome. *Epigenetics and Chromatin* 2015; **1**: 1-16.

Phipson B, Maksimovic J, and Oshlack A. missMethyl: an R package for analysing methylation data from Illuminas HumanMethylation450 platform. *Bioinformatics* 2015; **2**: 286-288.

Qu F, Wang FF, Yin R, Ding GL, El-Prince M, Gao Q, Shi BW, Pan HH, Huang YT, Jin M*, et al.* A molecular mechanism underlying ovarian dysfunction of polycystic ovary syndrome: hyperandrogenism induces epigenetic alterations in the granulosa cells. *J Mol Med (Berl)* 2012; **8**: 911-923.

R Core Team. A Language and Environment for Statistical Computing 2016.

Rajpert-De Meyts E, Jørgensen N, Græm N, Müller J, Cate RL, and Skakkebæk NE. Expression of anti-Mullerian hormone during normal and pathological gonadal development: Association with differentiation of Sertoli and granulosa cells. *J. Clin. Enocrinol. Metab.* 1999; **10**: 3836-3844.

Rakyan VK, Down TA, Maslau S, Andrew T, Yang TP, Beyan H, Whittaker P, McCann OT, Finer S, Valdes AM*, et al.* Human aging-associated DNA hypermethylation occurs preferentially at bivalent chromatin domains. *Genome Res* 2010; **4**: 434-439.

Regan SLP, Knight PG, Yovich JL, Arfuso F, and Dharmarajan A. Growth hormone during in vitro fertilization in older women modulates the density of receptors in granulosa cells, with improved pregnancy outcomes. *Fertil Steril* 2018; **7**: 1298-1310.

Roy S, Gandra D, Seger C, Biswas A, Kushnir VA, Gleicher N, Kumar TR, and Sen A. Oocyte-Derived Factors (GDF9 and BMP15) and FSH Regulate AMH Expression Via Modulation of H3K27AC in Granulosa Cells. *Endocrinology* 2018; **9**: 3433-3445.

Rödström K, Bengtsson C, Milsom I, Lissner L, Sundh V, and Bjoürkelund C. Evidence for a secular trend in menopausal age: a population study of women in Gothenburg. *Menopause* 2003; **6**: 538-543.

Sagvekar P, Kumar P, Mangoli V, Desai S, and Mukherjee S. DNA methylome profiling of granulosa cells reveals altered methylation in genes regulating vital ovarian functions in

polycystic ovary syndrome. *Clin Epigenetics* 2019; **1**: 61.

Sanders JL and Newman AB. Telomere length in epidemiology: a biomarker of aging, age-related disease, both, or neither? *Epidemiol Rev* 2013: 112-131.

Sawyer HR, Smith P, Heath DA, Juengel JL, Wakefield SJ, and McNatty KP. Formation of Ovarian Follicles During Fetal Development in Sheep. *Biol. Reprod.* 2002; **4**: 1134-1150.

Scalercio SR, Brito AB, Domingues SF, Santos RR, and Amorim CA. Immunolocalization of growth, inhibitory, and proliferative factors involved in initial ovarian folliculogenesis from adult common squirrel monkey (Saimiri collinsi). *Reprod Sci* 2015; **1**: 68-74.

Scheffer GJ, Broekmans FJM, Looman CWN, Blankenstein M, Fauser BCJM, DeJong FH, and Te Velde ER. The number of antral follicles in normal women with proven fertility is the best reflection of reproductive age. *Hum Reprod* 2003; **4**: 700-706.

Sehl ME, Henry JE, Storniolo AM, Ganz PA, and Horvath S. DNA methylation age is elevated in breast tissue of healthy women. *Breast Cancer Res Treat* 2017; **1**: 209-219.

Shammas MA. Telomeres, lifestyle, cancer, and aging. *Curr Opin Clin Nutr Metab Care* 2011; **1**: 28-34.

Silver MJ, Kessler NJ, Hennig BJ, Dominguez-Salas P, Laritsky E, Baker MS, Coarfa C, Hernandez-Vargas H, Castelino JM, Routledge MN*, et al.* Independent genomewide screens identify the tumor suppressor VTRNA2-1 as a human epiallele responsive to periconceptional environment. *Genome Biol* 2015; **118**: 1-14.

Simpkin AJ, Howe LD, Tilling K, Gaunt TR, Lyttleton O, McArdle WL, Ring SM, Horvath S, Smith GD, and Relton CL. The epigenetic clock and physical development during childhood and adolescence: longitudinal analysis from a UK birth cohort. *Int J Epidemiol* 2017; **2**: 549-558.

Statistics Denmark The register of 'FOD11: Average age of women given birth and new fathers' 2018. https://www.statbank.dk/FOD11.

Teschendorff AE, Menon U, Gentry-Maharaj A, Ramus SJ, Weisenberger DJ, Shen H, Campan M, Noushmehr H, Bell CG, Maxwell AP*, et al.* Age-dependent DNA methylation of genes that are suppressed in stem cells is a hallmark of cancer. *Genome Res* 2010; **4**: 440-446.

The Danish Fertility Society. Annual Report 2018: 'The results for 2018 are based on reports from public as well as private fertility clinics to the Danish Health Authority's IVF register'. 2019. https://fertilitetsselskab.dk/dataark-pr-aar/.

Titus S, Li F, Stobezki R, Akula K, Unsal E, Jeong K, Dickler M, Robson M, Moy F, Goswami S*, et al.* Impairment of BRCA1-related DNA double-strand break repair leads to ovarian aging in mice and humans. *Sci Transl Med* 2013; **172**: 172ra121.

Tsutsumi M, Fujiwara R, Nishizawa H, Ito M, Kogo H, Inagaki H, Ohye T, Kato T, Fujii T, and Kurahashi H. Age-related decrease of meiotic cohesins in human oocytes. *PLOS ONE* 2014; **5**: e96710.

Van Noord PAH, Boersma H, Dubas JS, Te Velde E, and Dorland M. Age at natural menopause in a population-based screening cohort: The role of menarche, fecundity, and lifestyle factors. *Fertil Steril* 1997; **1**: 95-102.

Weidner CI, Lin Q, Koch CM, Eisele L, Beier F, Ziegler P, Bauerschlag DO, Jockel K-H, Erbel R, Muhleisen TW*, et al.* Aging of blood can be tracked by DNA methylation changes at just three CpG sites. *Genome Biol* 2014; **2**: R24.

Westergaard CG, Byskov AG, and Andersen CY. Morphometric characteristics of the primordial to primary follicle transition in the human ovary in relation to age. *Hum Reprod* 2007; **8**: 2225-2231.

Wissing ML, Kristensen SG, Andersen CY, Mikkelsen AL, Høst T, Borup R, and Grøndahl ML. Identification of new ovulation-related genes in humans by comparing the transcriptome of granulosa cells before and after ovulation triggering in the same controlled ovarian stimulation cycle. *Hum Reprod* 2014; **5**: 997-1010.

Xu Z, Langie SA, De Boever P, Taylor JA, and Niu L. RELIC: a novel dye-bias correction method for Illumina Methylation BeadChip. *BMC Genomics* 2017; **1**: 4.

Xu Z, Niu L, Li L, and Taylor JA. ENmix: a novel background correction method for Illumina HumanMethylation450 BeadChip. *Nucleic Acids Res* 2016; **3**: e20.

Yu B, Russanova V, Gravina S, Hartley S, Mullikin J, Ignezweski A, Graham J, JH. S, DeCherney AH, and Howard B. DNA methylome and transcriptome sequencing in human ovarian granulosa cells links age-related changes in gene expression to gene body methylation and 3'-end GC density. *Oncotarget* 2015; **6**: 3627-3643.

Zhang D, Zhang X, Zeng M, Yuan J, Liu M, Yin Y, Wu X, Keefe DL, and Liu L. Increased DNA damage and repair deficiency in granulosa cells are associated with ovarian aging in rhesus monkey. *J Assist Reprod Genet* 2015; **7**: 1069-1078.

Zoubarev A, Hamer KM, Keshav KD, McCarthy EL, Santos JR, Van Rossum T, McDonald C, Hall A, Wan X, Lim R*, et al.* Gemma: a resource for the reuse, sharing and meta-analysis of expression profiling data. *Bioinformatics* 2012; **17**: 2272-2273.

Table I Demographic and clinical characteristics of the participant population divided into four age groups.

	Age groups					
	Demographic & Clinical Characteristics					
	25-29 years	30-34 years	35-39 years	40-44 years	Overall	One-way ANOVA *p*-value
Number [MGC[1]]	27 [20]	35 [19]	47 [18]	10 [6]	119 [63]	-
Age at oocyte retrieval	27.5 ± 1.2	32.1 ± 1.4	37.3 ± 1.5	41.7 ± 1.4	33.9 ± 4.7	$2.2x10^{-16}$
BMI (kg/m^2)	24.3 ± 4.2	24.5 ± 4.1	24.1 ± 3.5	24.2 ± 2.5	24.3 ± 3.8	0.977
AMH[2] (pmol/L)	27.5 ± 20.1 (2.2-86)	30.6 ± 22.3 (0.6-94)	18.8 ± 19.1 (0.2-68)	10.3 ± 16.2 (0.3-55)	23.5 ± 20.9 (0.2-94)	0.008
Ovarian reserve category						
- DOR[3]						
- Normal	5	5	13	-	23	-
- High	17	20	22	-	59	-
- 40-44 years	5	10	12	-	27	-
	-	-	-	10	10	-
Primary cause of infertility						
- Male factor						
- Female factor	9	13	12	-	34	-
- Unexplained	6	9	3	10	28	-
- Other causes*	12	11	16	-	39	-
	-	2	16	-	18	-
FSH (IU/L)	6.4 ± 2.4	5.7 ± 3.9	10.0 ± 8.8	8.0 ± 2.4	7.8 ± 6.4	0.017
LH (IU/L)	5.7 ± 4.7	5.5 ± 3.1	8.9 ± 9.5	6.5 ± 2.0	7.1 ± 6.9	0.195
LH/FSH ratio	1.1 ± 1.1	1.2 ± 0.6	1.0 ± 0.8	0.9 ± 0.5	1.04 ± 0.8	0.639
Prolactin (IU/L)	263 ± 135	325 ± 125	303 ± 142	236 ± 122	295 ± 135	0.195
TSH[4] (IU/L)**	1.5 ± 0.6	1.8 ± 0.8	1.8 ± 0.9	1.5 ± 0.5	1.7 ± 0.8	0.340
	Cycle Characteristics					
No. of oocytes	9.7 ± 3.8	10.0 ± 6.5	6.3 ± 4.3	6.8 ± 5.3	8.1 ± 5.3	0.004
No. of 2PN[5] zygotes	5.7 ± 2.9	5.4 ± 4.2	3.1 ± 2.8	3.7 ± 4.1	4.4 ± 3.6	0.006
No. of clinically usable embryos	3.8 ± 2.5	3.2 ± 2.8	1.3 ± 1.8	2 ± 1.4	2.5 ± 2.4	$5.9x10^{-05}$
Utilization rate***	0.7 ± 0.3	0.6 ± 0.3	0.5 ± 0.4	0.7 ± 0.3	0.6 ± 0.3	0.027

Mean ± standard deviation (range).
*Single women and women with a female partner.
**This is baseline measurement. In case of TSH > 2.5 IU/L with +/- thyreoidea peroxidase (TPO) antibodies, regulation to < 2.5 IU/L or 2.5-4.0 without TPO antibodies was ensured before treatment start following the Danish Fertility Society's Guideline.
*** No. of clinically useable embryos/no. of 2PN zygotes.

[1] Mural granulosa cells
[2] Anti-Müllerian hormone
[3] Diminished ovarian reserve
[4] Thyroid-stimulating hormone
[5] Two pronuclear

Table II Age-DMRs of selected genes.

Gene name	Gene symbol	Chromosome	DMR[6] width	No. of CpG's[7]	Min. FDR[8]	Stouffer	Mean beta fold change
Vault RNA 2-1	*VTRNA2-1*	5	1756	17	$3.4x10^{-34}$	$3.6x10^{-6}$	0.1832
Anti-Mullerian hormone	*AMH*	19	2954	16	$3.8x10^{-19}$	$4.1x10^{-5}$	-0.0994
Zinc finger protein 57	*ZFP57*	6	924	21	$2.5x10^{-25}$	$4.5x10^{-4}$	-0.1794
Glyceraldehyde-3-phosphate dehydrogenase	*GAPDH*	12	285	2	$2.6x10^{-15}$	0.0104	-0.0791
Aquaporin 2	*AQP2*	12	771	10	$6.4x10^{-21}$	0.0121	-0.0662
Growth hormone receptor	*GHR*	5	108	2	$1.6x10^{-7}$	0.0390	-0.0556
Placental growth factor	*PGF*	14	304	6	$7.8x10^{-8}$	0.1999	-0.0084
Cytochrome P450 family 26 subfamily A member 1	*CYP26A1*	10	173	6	$1.1x10^{-7}$	0.2170	-0.0156
Estrogen receptor 1	*ESR1*	6	44	2	$2.5x10^{-7}$	0.3760	-0.0501
Growth hormone secretagogue receptor	*GHSR*	3	336	9	$1.4x10^{-7}$	0.7644	-0.0145

[6] Differentially methylated regions
[7] Cytosine-phosphate-guanine
[8] False discovery rate

Figure 1

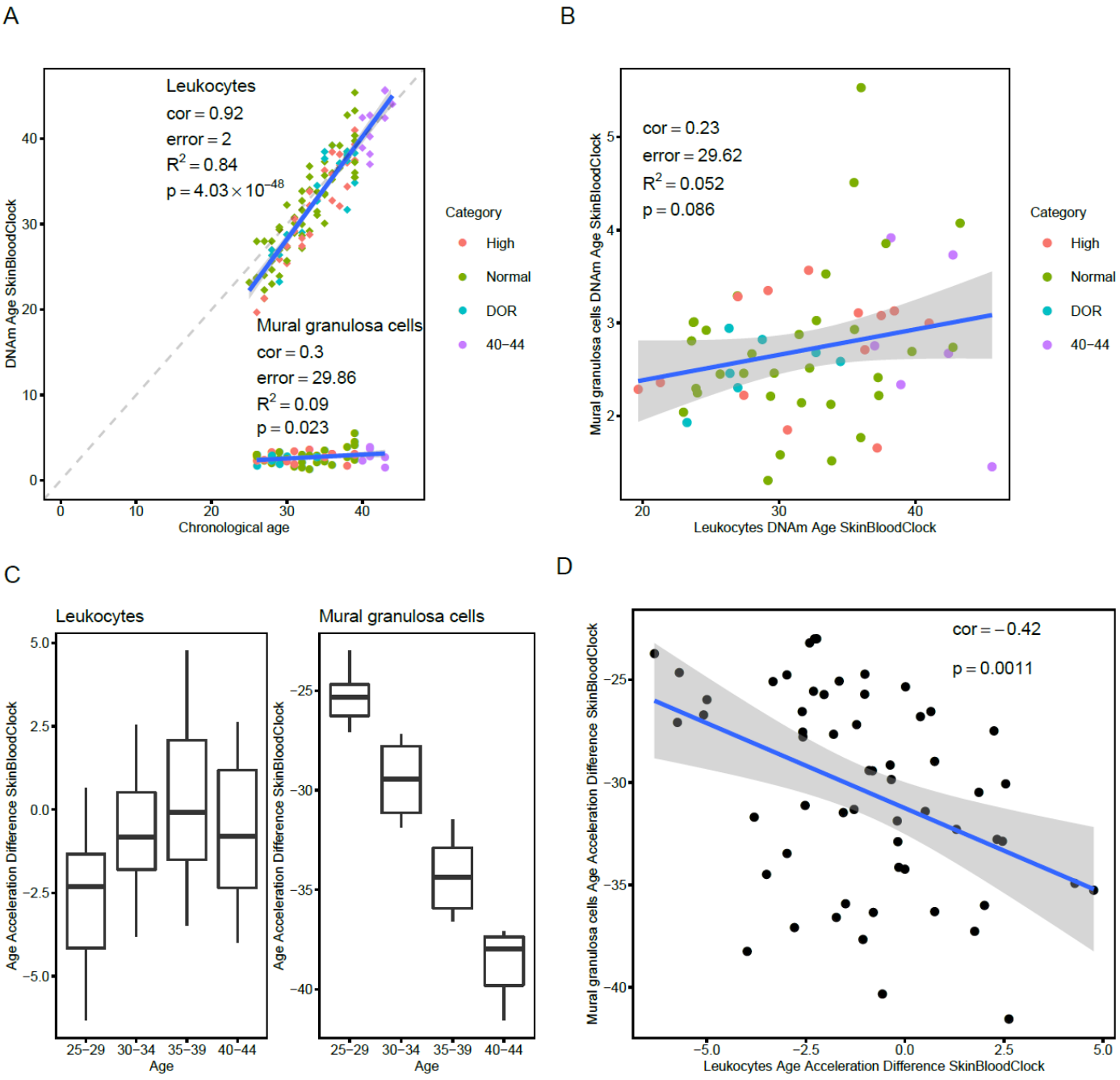

Figure 1 Epigenetic age in mural granulosa cells and leukocytes. (**A**) DNAm age in granulosa cells (n = 59) and leukocytes (n = 118) using Horvath's Skin & Blood clock. Dashed line indicates a perfect prediction (y = x). The participants are divided into groups regarding their ovarian reserve status, indicated with colours: blue = diminished ovarian reserve (DOR), green = Normal, red = High, purple = 40-44 years. (**B**) Scatter plot illustrating the correlation between the DNAm age of leukocytes and granulosa cells collected from the same individual. (**C**) Box plots of the age acceleration differences in the two cell types. The women are divided into age groups (25-29, 30-34, 35-39 and 40-44 years). The age acceleration difference magnitudes are greatest in the oldest age group in the granulosa cells (max(absolute values) = 41.55). The leukocytes exhibit a different pattern with only a slight age acceleration difference (max(absolute values) = 6.32). (**D**) Scatter plot showing the association of age acceleration differences between the two cell types (correlation (cor) = -0.42, *p* = 0.001).

Figure 2

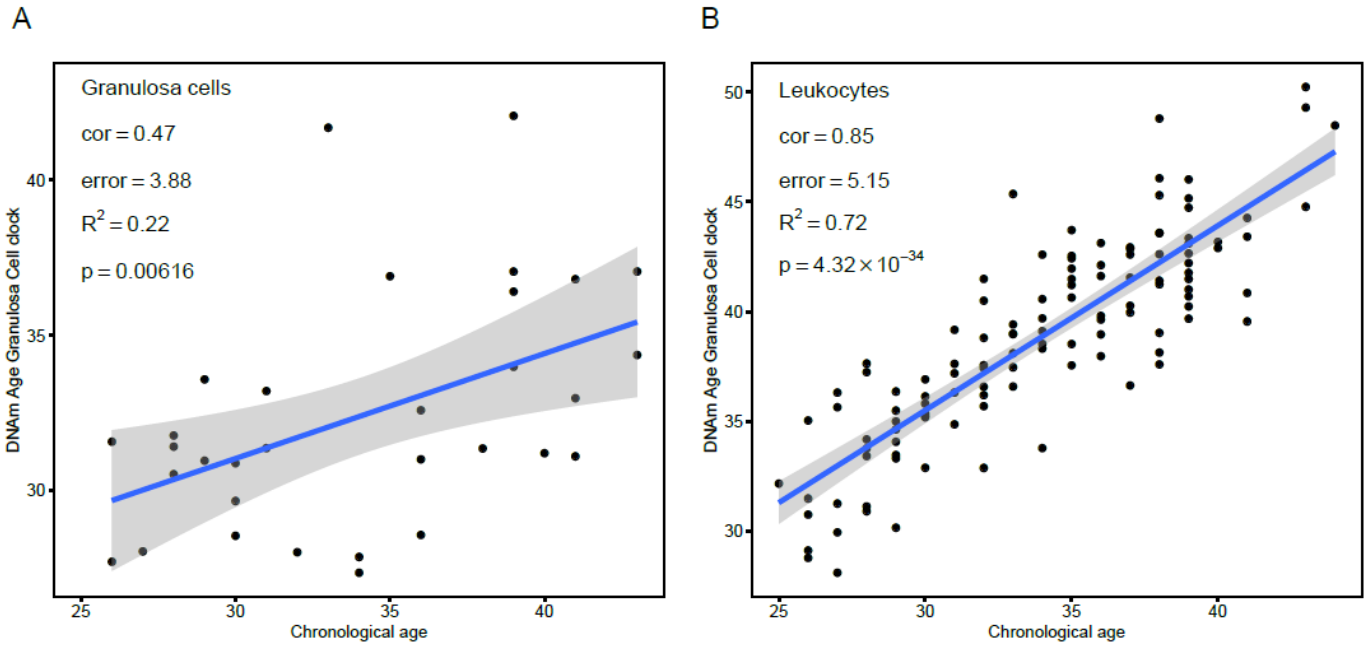

Figure 2 The Granulosa Cell clock. A novel Granulosa Cell clock was developed including 296 cytosine-phosphate-guanine (CpG) sites. (**A**) Scatter plot showing the correlation between chronological age and DNAm age in mural granulosa cells (MGC) calculated with the Granulosa Cell clock. (**B**) Scatter plot showing the Granulosa Cells clock applied to leukocytes. Note that the clock over-estimates the age in leukocytes (error = 5.15 years).

Figure 3

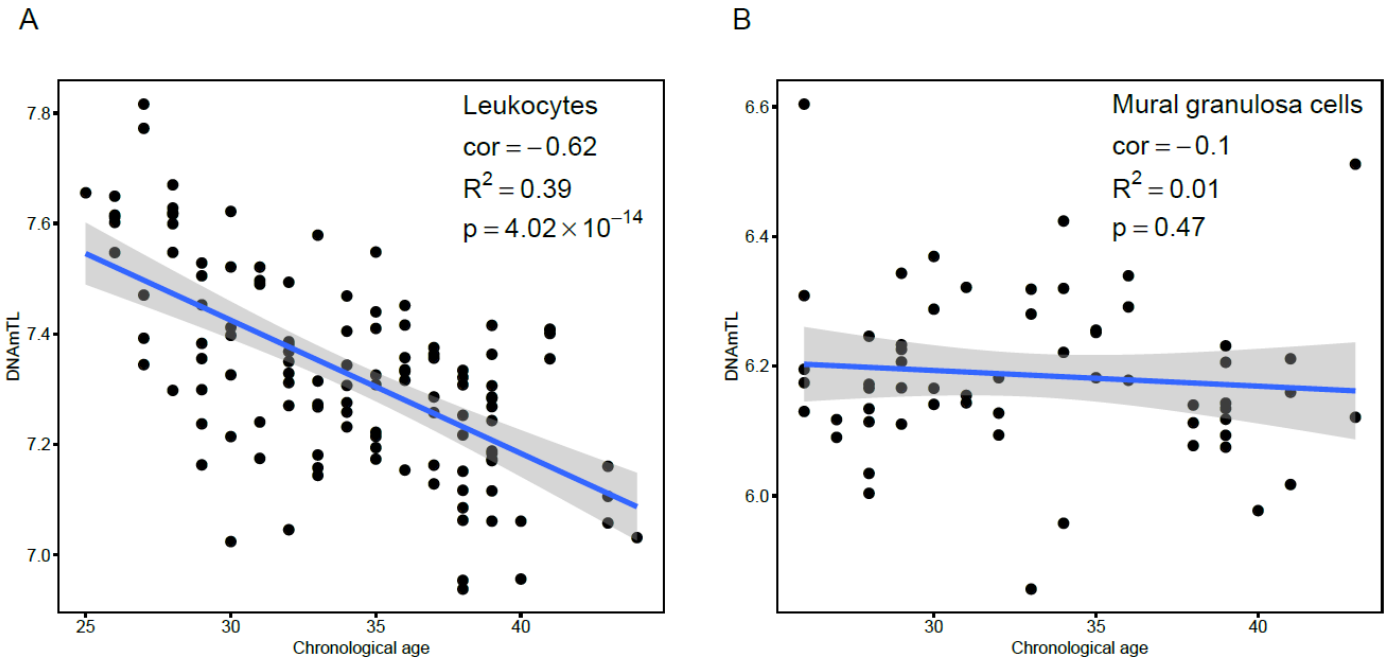

Figure 3 Predicted telomere length in mural granulosa cells and leukocytes. The predicted telomere length (DNAmTL) in relation to age. Scatter plots indicating the Pearson's correlation coefficient (cor) between predicted telomere length and age in leukocytes (**A**) and MGC (**B**).

Figure 4

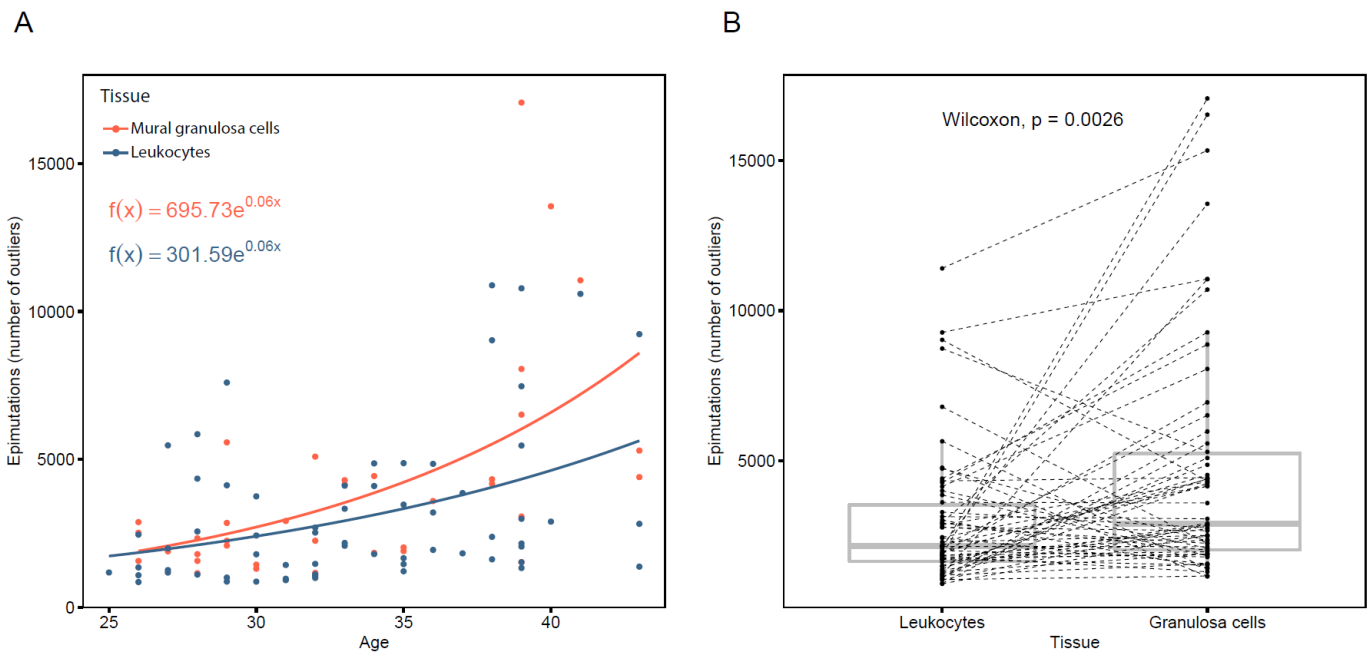

Figure 4 Epimutations in mural granulosa cells and leukocytes. Epimutations (number of outliers) in relation to age. (**A**) Scatterplot indicated the number of epimutations as a function of age in MGC (red) and leukocytes (blue), with exponential lines of best fit. (**B**) Comparison of epimutations in paired MGC and leukocyte samples; boxes represent the interquartile range, with the media values depicted by the horizontal bar; Wilcoxon test, *p* = 0.003 (mean of differences = 1,693.5).

Figure 5

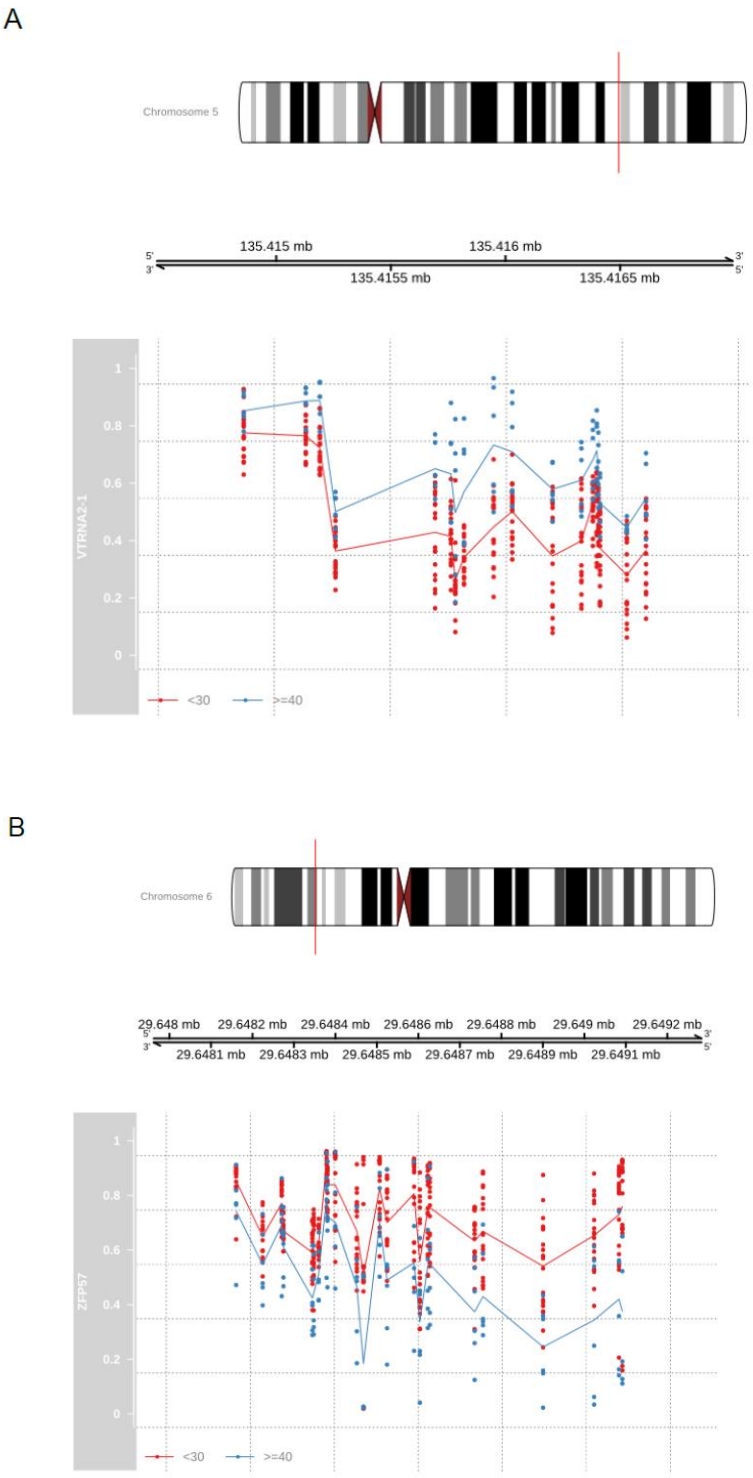

Figure 5 Epialleles in mural granulosa cells from women <30 years and ≥40 years of age. (**A**) EWAS of chronological age in MGC, illustrated by the most significant signal (Stouffer = 3.62×10^{-6}) detected at the meta-stable epiallele *VTRNA2-1* in chromosome 5. Methylation at CpGs within *VTRNA2-1* comparing values in young (< 30 years; red) and older women (≥ 40 years; blue); mean beta fold change = 0.18. (**B**) Another significant signal (Stouffer = 4.5×10^{-4}) also located in a putative meta-stable epiallele was observed in *ZFP57* on chromosome 6, where women under 30 years showed on average greater methylation levels (mean beta fold change = -0.18). The unit of the chromosome length measurements are mega base (mb).

SUPPLEMENTARY

Table SI Demographic and clinical characteristics of the participant population of the women donated mural granulosa cells.

	Age groups					
	Demographic & Clinical Characteristics					
	25-29 years	30-34 years	35-39 years	40-44 years	Overall	One-way ANOVA *p*-value
Number	20	19	18	6	63	-
Age at oocyte retrieval	27.7 ± 1.2	32.1 ± 1.4	37.6 ± 1.6	41.5 ± 1.2	33.1 ± 4.9	$2.2x10^{-16}$
BMI (kg/m^2)	24.0 ± 3.8	24.0 ± 3.9	24.1 ± 3.4	23.9 ± 2.8	24.0 ± 3.6	0.998
AMH (pmol/L)	26.2 ± 21.5 (2.2-86)	30.0 ± 22.1 (4.6-75)	25.5 ± 20.5 (2.1-68)	13.6 ± 20.5 (0.3-55)	25.9 ± 21.3 (0.3-86)	0.446
Ovarian reserve category						
- DOR[1]	5	3	1	-	9	-
- Normal	12	12	10	-	34	-
- High	3	4	7	-	14	-
- 40-44 years	-	-	-	6	6	-
Primary cause of infertility						
- Male factor	8	9	2	-	19	-
- Female factor	6	6	2	6	20	-
- Unexplained	6	3	8	-	17	-
- Other causes*	-	1	6	-	7	-
FSH (IU/L)	6.3 ± 2.3	4.9 ± 2.2	7.3 ± 4.0	8.1 ± 2.2	6.3 ± 3.0	0.070
LH (IU/L)	6.4 ± 5.1	6.2 ± 3.6	6.7 ± 6.3	7.3 ± 2.0	6.5 ± 4.8	0.983
LH/FSH ratio	1.2 ± 1.2	1.4 ± 0.7	1.0 ± 0.8	1.0 ± 0.5	1.2 ± 0.9	0.705
Prolactin (IU/L)	275 ± 130	335 ± 125	278 ± 145	262 ± 130	293 ± 133	0.449
TSH (IU/L)**	1.4 ± 0.6	1.9 ± 0.7	2.0 ± 1.1	1.7 ± 0.5	1.8 ± 0.8	0.127
	Cycle Characteristics					
No. of oocytes	10.1 ± 3.8	12.1 ± 6.9	7.3 ± 5.2	8.2 ± 6.6	9.7 ± 5.8	0.072
No. of 2PN[2] zygotes	5.8 ± 2.9	6.5 ± 4.0	3.7 ± 3.7	4.2 ± 5.4	5.3 ± 3.9	0.134
No. of clinically usable embryos	3.9 ± 2.5	3.7 ± 2.9	1.9 ± 2.3	2.0 ± 1.8	3.1 ± 2.6	0.050
Utilization rate***	0.7 ± 0.2	0.6 ± 0.3	0.6 ± 0.4	0.7 ± 0.4	0.6 ± 0.3	0.613

Mean ± standard deviation (range).
*Single women and women with a female partner.
*This is baseline measurement. In case of TSH > 2.5 IU/L with +/- thyreoidea peroxidase (TPO) antibodies, regulation to < 2.5 IU/L or 2.5-4.0 without TPO antibodies was ensured before treatment start following the Danish Fertility Society's Guideline.
*** No. of clinically useable embryos/no. of 2PN zygotes.

[1] Diminished ovarian reserve
[2] Two pronuclear

Figure S1

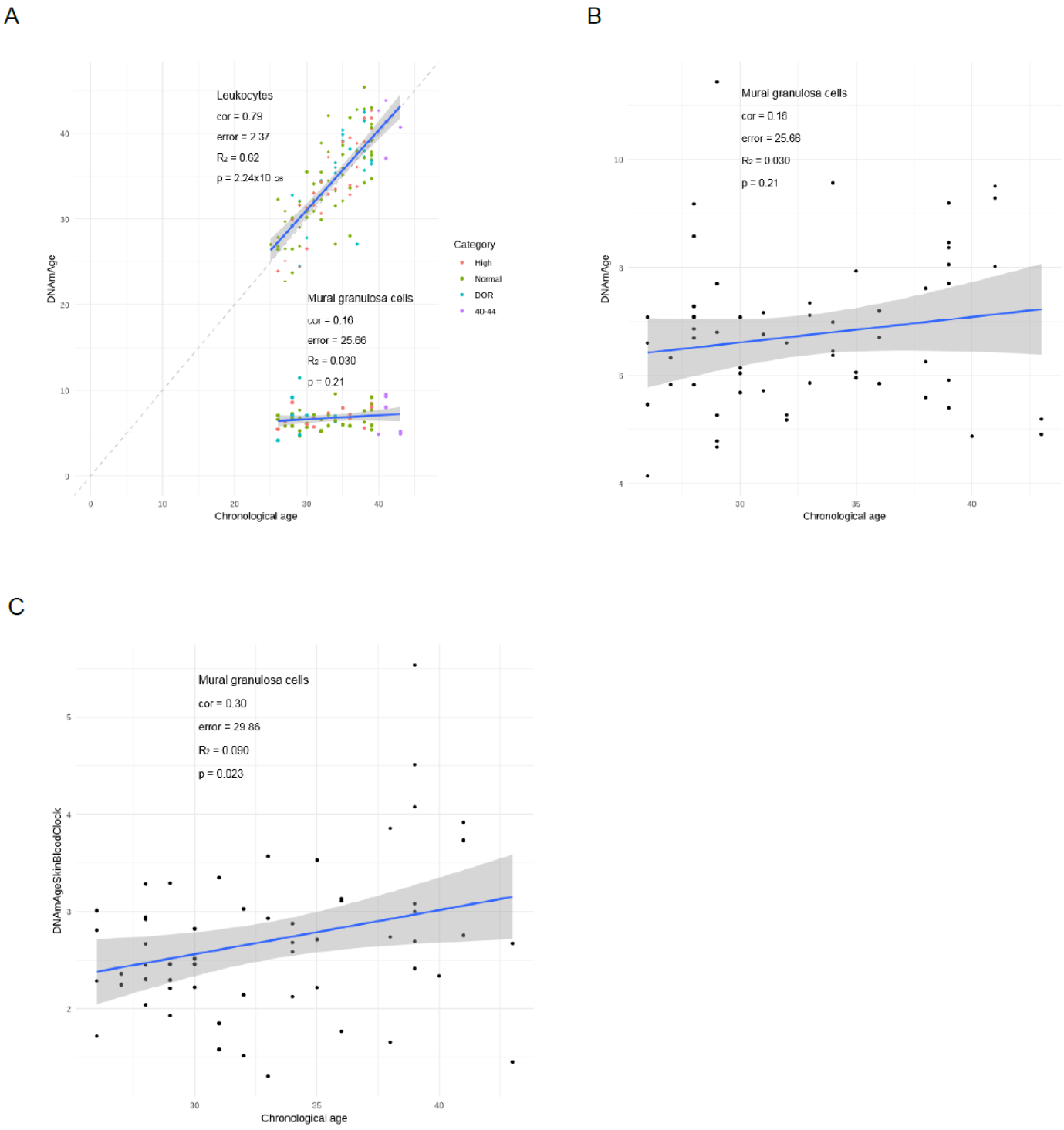

Figure S1 Choice of epigenetic clock. (**A**) Scatter plot showing the correlation between DNAm age and chronological age in leukocytes and MGC calculated with the multi-tissue age predictor. Leukocytes are correlated with chronological age (Pearson's correlation coefficient (cor) = 0.79, $p = 2.2x10^{26}$). (**B**) The DNAm age in mural granulosa cells (MGC) calculated with the multi-tissue age predictor and the Skin & Blood clock. There is no significant age-correlation between the DNAm (multi-tissue age predictor) and chronological age (cor = 0.16, error = 25.7 years, $p = 0.21$) and only a slight correlation using the Skin & Blood clock (cor = 0.3, error = 29.9 years, $p = 0.02$). DOR = Diminished ovarian reserve.

Figure S2

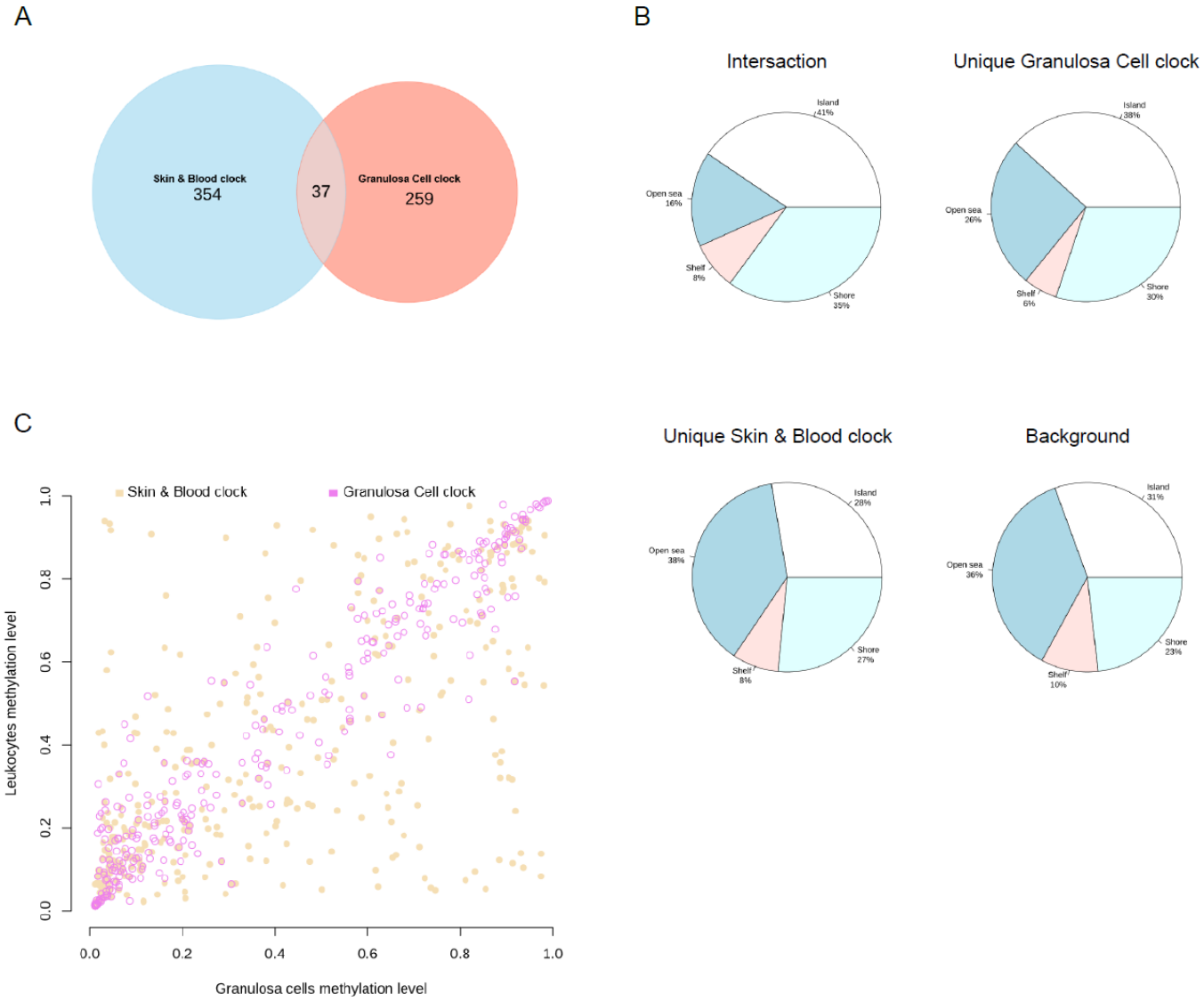

Figure S2 The development of the Granulosa Cell clock. (**A**) Venn diagram indicating the intersection between the CpGs in the Skin & Blood clock and the CpGs in the Granulosa Cell clock. (**B**) Distribution in relation to CpG islands of the intersected CpGs, unique Granulosa Cells clock CpGs, unique Skin & Blood Clock CpGs, and background CpGs. (**C**) Comparison of the mean methylation values across all the samples in both leukocytes (pink) and MGC (yellow) with the two clocks.

Figure S3

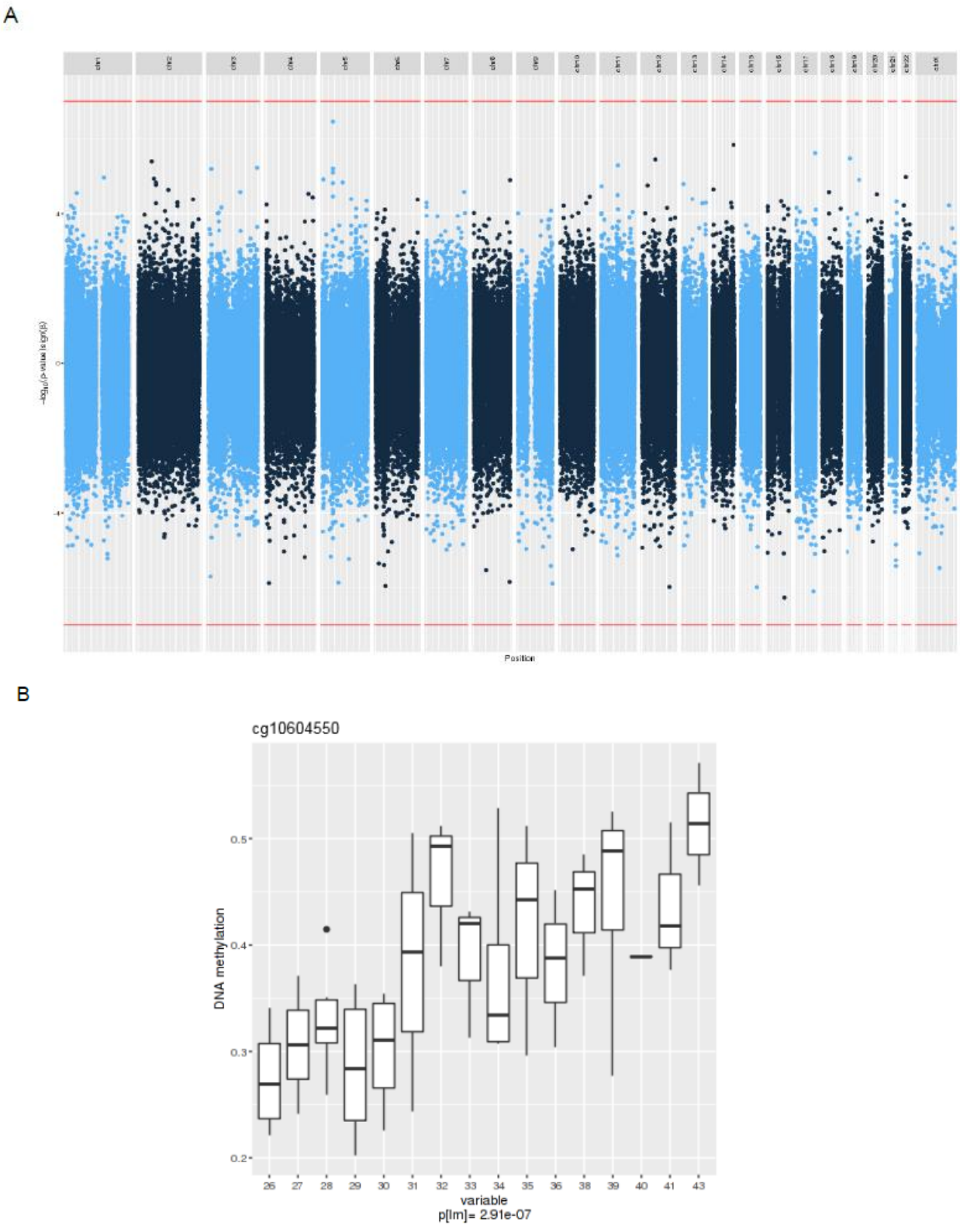

Figure S3 Epigenome-wide association study. (**A**) Manhattan plot showing the absence of genome-wide significant signals at single CpG site resolution. Because of limited sample size, the analysis is underpowered at single CpG resolution. (**B**) The figure shows the top CpG site (cg10604550) associated with age (p = 2.9x10^{-07}), although the association does not survive correction for multiple testing.

Figure S4

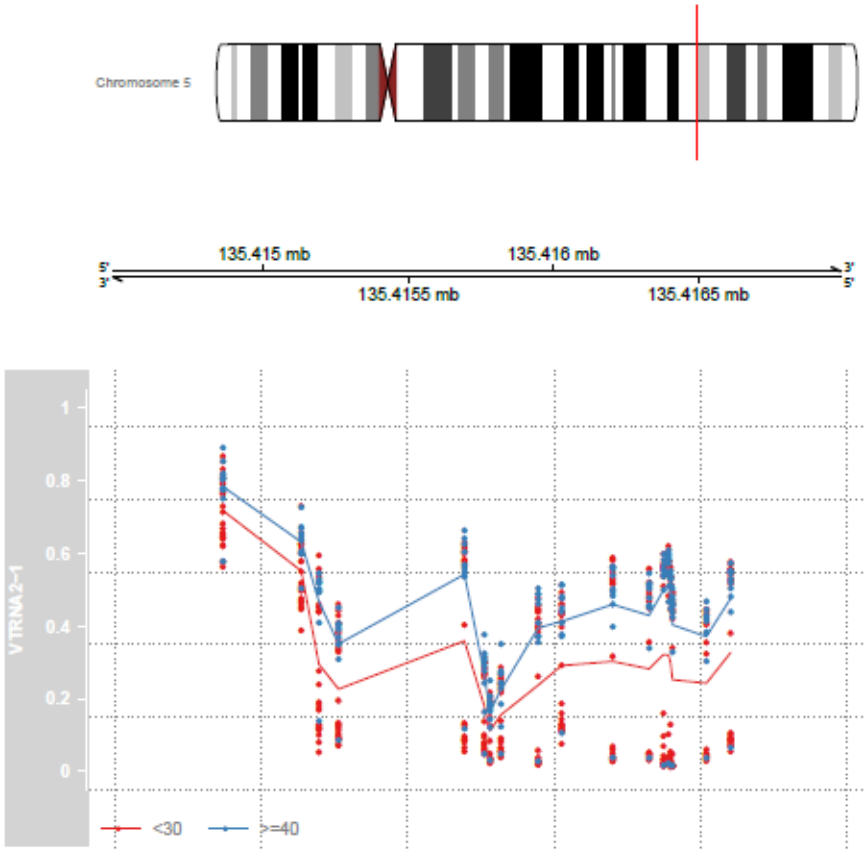

Figure S4 Epialleles in leukocytes. EWAS of chronological age in leukocytes, illustrated by the meta-stable epiallele *VTRNA2-1* in chromosome 5. Methylation at CpGs within *VTRNA2-1* comparing values in young (< 30 years; red) and older women (≥ 40 years; blue). Although women above 40 years show a slight gain in methylation compared to women under 30, the difference is not significant at an false discovery rate (FDR) of 10%, in contrast to in MGC (see Figure 5).

Paper I

Supplementary tables can be retrieved via this link:

https://figshare.com/s/82c3137d5b42e0a93121

Paper II

Identification of a unique epigenetic profile in women with diminished ovarian reserve

Identification of a unique epigenetic profile in women with diminished ovarian reserve

K. W. Olsen[a,b], J. Castillo-Fernandez[c], A. C. Chan[b], N. C. Freiesleben[d,e], A. Zedeler[d], M. Bungum[f], A. Cardona[g,h], J. R. B. Perry[g], S. O. Skouby[a], E. R. Hoffmann[b], G. Kelsey[c,i], M. L. Grøndahl[a]

[a]Department of Obstetrics and Gynaecology, Department of Reproductive Medicine, Copenhagen University Hospital Herlev, Denmark. [b]DNRF Center for Chromosome Stability, Department of Cellular and Molecular Medicine, Faculty of Health and Medical Sciences, University of Copenhagen, Copenhagen, Denmark. [c]Epigenetics Programme, Babraham Institute, Cambridge, United Kingdom. [d]Department of Obstetrics and Gynaecology, The Fertility Clinic, Copenhagen University Hospital Hvidovre, Denmark. [e]VivaNeo Fertility Clinics, Stork IVF Clinic A/S, Copenhagen, Denmark. [f]Reproductive Medicine Centre, Skåne University Hospital, Malmoe, Sweden. [g]Medical Research Council Epidemiology Unit, University of Cambridge Addenbrooke's Hospital Cambridge, Cambridge, United Kingdom. [h]Department of Genetics, University of Cambridge, Cambridge, United Kingdom. [i]Centre for Trophoblast Research, University of Cambridge, Cambridge, United Kingdom.

Objective: To investigate whether epigenetic profiles of mural granulosa cells (MGC) and leukocytes from women with diminished ovarian reserve (DOR) differ from women with normal or high ovarian reserve.
Design: Prospectively collected material from a multicenter cohort of women undergoing fertility treatment.
Setting: Private and university-based facilities for clinical services and research.
Patients: 119 women were included. Blood samples and MGC were collected from women with varying age and ovarian reserve status (Anti Müllerian Hormone (AMH) level).
Interventions: None.
Main outcome measure (s): Measures of epigenetic aging rates from whole genome methylation array data, i.e., DNA methylation variability, age acceleration, DNAmTL, and accumulation of epimutations.
Results: Comparison of DOR or high ovarian reserve samples to controls (normal ovarian reserve) showed differential methylation variability between DOR and normal samples at 4,199 CpGs in MGC, and 447 between high and normal (FDR < 0.05). Variable sites in MGC from DOR were enriched in regions marked with the repressive histone modification H3K27me3, and also included genes involved in folliculogenesis, such as *IGF2* and *AMH*. Regardless of ovarian reserve, very few signals were detected in leukocytes and no overlaps with those in MGC were found. Furthermore, we found a higher number of epimutations in MGC from women with DOR (Kruskal-Wallis test; $p = 0.008$, difference in means = 3,485).
Conclusion: The somatic cells of human ovarian follicles have a distinctive epigenetic profile in women with DOR. The changes resemble those of premature aging. Ovarian reserve status was not reflected in the leucocytes epigenetic profile.

Keywords: DNA methylation, ovarian reserve, granulosa cells, reproduction, epigenetics

CONFLICT OF INTEREST AND FUNDING
The authors have no conflict of interest.
This work was supported by the ReproUnion Program, co-financed by the European Union, Interreg V ÖKS, Capital region of Denmark, Region Zealand, Region Skåne and Ferring Pharmaceutical Company.
Furthermore, the study was supported by the Department of Gynaecology-Obstetrics at Herlev-Gentofte Hospital, Denmark and the Danish National Research Foundation (DNRF). Center for Chromosome Stability (DNRF115) at the University of Copenhagen have also supported the project financially. ACC and ERH was supported by the Novo Nordisk Foundation Young Investigator Award (NNF15OC0016662). JCF and GK was supported by grants from the UK Biotechnology and Biological Sciences Research Council (BBS/E/B/000C0425) and Medical Research Council (MR/S000437/1). The funders did not have any role in study design; in the collection, analysis, and interpretation of data; in the writing of the report; and in the decision to submit the article for publication.

KWO and JCF should be considered similar in author order.
Corresponding author: Kristina Wendelboe Olsen, MSc, Fertilitetsklinikken, Rigshospitalet, Blegdamsvej 9, 2100 København, Denmark.
kristina.wendelboe.olsen@regionh.dk, kristinawo@hotmail.com, + 45 40 41 17 44.

INTRODUCTION

As women age, they experience a decline in their fecundity (the ability to produce offspring), which ultimately terminates in the menopause around the age of 51 years (1-3). Age-related infertility one of the greatest challenges in human reproduction, even with assisted reproductive technologies (ART) the live birth rate in women ≥ 40 years is only 3.2% per treatment cycle (4). However, some women experience loss of fertility prematurely and are characterized as having (pathological) diminished ovarian reserve (DOR) (5).

The human ovary contains non-growing follicles (primordial follicles) that develop around week twenty of gestation (6). At birth, a baby girl has on average 1 million primordial follicles, the number declines with increasing age such that at menopause only approximately one thousand follicles remain (7). Most follicles degrade during atresia, an apoptotic breakdown, which regulates the number of ovulating follicles during a women's reproductive life (8). For women with DOR it is unclear whether the postnatal pool of primordial follicles is reduced from the beginning or the rate of the atretic breakdown is accelerated (5). On the other hand, their oocytes have the same quality (rate of aneuploidies) as other women of the same age (9, 10). Anti-Müllerian hormone (AMH) is a serum biomarker for the number of primordial follicles in the ovary (ovarian reserve) and used to tailor and predict outcomes of controlled ovarian stimulation (COS) in women undergoing fertility treatment (11). AMH is produced by the granulosa cells in the small antral follicles (12). As with the number of primordial follicles, the level of AMH declines with age (13).

A woman's reproductive lifespan has previously been shown to be positively correlated with telomere length in white blood cells (14). Telomere length is a known biomarker for biological aging and, recently, a DNA methylation telomere length estimator (DNAmTL) was developed using DNA methylation data. It is based on 140 cytosine-phosphate-guanine (CpG) sites and functions as a biomarker of cell replication but also as a marker of age-related pathologies associated with telomere length (15). In the last decade, data from DNA methylation arrays have underpinned development of the multi-tissue age predictor (16), and subsequently also more specialized epigenetic clocks, making it possible to investigate biological aging, age-related disease and overall mortality (17-21).

There is limited knowledge about the epigenetics of ovarian follicle cells and how they differ from other somatic cells in the body. Recently, a distinctive DNA methylation profile was described in granulosa lutein cells from women diagnosed with polycystic ovary syndrome (PCOS) (22). One hundred and six differentially methylated CpG sites associated with 88 genes were found, many of which are known to be related to PCOS and ovarian function. The observed epigenetic changes were suggested to contribute to the ovarian defect found in PCOS (22).

The aims of the present study were to: 1) investigate if DNA methylation profiles of leukocytes and mural granulosa cells (MGC) differ between women with different ovarian reserve and, if so, investigate whether these changes are shared or tissue-specific; and 2) investigate if the magnitude of a woman's ovarian reserve is reflected in the DNA methylation age (DNAm age) and the DNAmTL of the two cell types.

MATERIAL & METHODS

Participants and Sample Collection

Informed consent was obtained from participants before inclusion to the study. A total of 119 women receiving vitro fertilization (IVF) or intracytoplasmic sperm injection (ICSI) treatment following COS with gonadotrophin-releasing hormone (GnRH) antagonist protocol and with no history of disease were asked to consider participation in the study. A detailed treatment protocol has recently been described in Olsen *et al.* (23). After inclusion seven participants were diagnosed with PCOS as a secondary cause of infertility but were retained in the study. The study protocol was approved by The Scientific Ethical Committee of the Capital Region, Denmark (ethical approval number: H-16027088) and the Danish Data Protection Agency (ID-nr.: HGH-2016_086). The

study was conducted in accordance with the Helsinki Declaration II.

A comprehensive description of the handling and processing of the blood and MGC has recently been described by Olsen *et al*. (23).

Epigenetic Aging Analysis and Predicted Telomere Length

The DNA methylation analysis were performed as previously described in Olsen *et al*. (23).

Our recently published Granulosa Cell clock (23) and the online DNA Methylation Age Calculator (https://dnamage.genetics.ucla.edu/home) were used to estimate DNAm age. MGC and leukocytes were analysed separately and for the obtainment of β-values, noob-normalization was performed in minfi (24). Age acceleration difference was defined as the difference between DNAm age and chronological age. Age acceleration residuals were defined as the residuals of DNAm age regressed on chronological age.

The online DNA Methylation Age Calculator (https://dnamage.genetics.ucla.edu/home) was used to estimate DNAmTL. Higher numbers in the predictor outputs indicate longer telomeres as described by Lu and colleagues (15).

Differential DNA Methylation Variations

Differential variability at each CpG site was tested using the missMethyl package (25) in R (R Core Team 2016). β-values were converted to M-values and missing data were imputed to the mean across all samples of the same tissue type. False discovery rate (FDR) was set at 5%. Gene ontology analyses were performed with the same package accounting for the different number of probes per gene in the array. To identify regions harbouring multiple neighbouring CpG sites showing evidence of differential variability we used the DMRcate package (DMR: differential methylated regions) in R (26) allowing for at least two consecutive CpG sites.

Analysis of Epimutations

As described recently in Olsen *et al*., outlier methylation values (greater than or less than three time the interquartile range from the upper or lower quartiles, respectively) at each CpG site across all samples were used to define epimutations (23). The frequencies of epimutations per sample were used for analysis.

Statistical Analysis

The difference between ovarian reserve groups was tested with one-way ANOVA. Age acceleration, DNAmTL, and number of epimutations were compared with Kruskal-Wallis test. Linear regression was used to test for the association between DNAmTL and AMH level.

All statistical analyses were performed in R (26). The value of $p < 0.05$ was considered statistically significant. FDR was set at 5%.

The subgrouping of the women used in the analyses was based on data from Lee and colleagues (27) with the lowest age-related AMH level (5th and 10th percentiles) in the 'DOR' category, the medium age-related AMH level (25th to 75th percentile) in the 'normal' category and with the largest age-related AMH level in the 'high' category (> 90th percentile).

In the age acceleration and DNAmTL analysis, adjustment for age were performed.

RESULTS

Participants Characteristics

In the present study 119 women were included (118 buffy coats and 63 MGC samples), which are the same cohort as described in Olsen *et al*. (23). Participants were divided into three ovarian reserve subgroups; DOR, normal and high. AMH levels ranged from 0.2 to 94 pmol/L (mean = 23.5 pmol/L). Age was defined as the woman's age on the day of oocyte retrieval and ranged from 25 to 44 years (mean = 33.9 years).

Besides the significant difference in the AMH level, follicle stimulating hormone (FSH) level, luteinizing hormone (LH)/FSH ratio, the numbers of oocytes retrieved, fertilized oocytes, and useable embryos were significant different between the groups ($p < 0.05$). The utilization rate was the same for the three subgroups (Table I).

An overview of the participants' clinical and demographic characteristics is shown in Table I and Suppl. Table I (women donating MGC).

Epigenetic Age is not Accelerated in Women with Diminished Ovarian Reserve

DNAm age was estimated for the three subgroups of women using the Granulosa Cell clock

(23) (Figure S1A and S1B) and the Skin & Blood clock (28) (Figure S1C and S1D). For both age predictors and tissue types no association between age acceleration (residuals) and ovarian reserve was found. However, a suggestive trend toward lower age acceleration with higher AMH levels was observed in the leukocytes for both clocks (Figure S1A and S1C).

Predicted Telomere Length

Replicative senescence and telomere length are considered biomarkers of aging and have been developed as an estimator of age (DNAmTL), we plotted the DNAmTL in leukocytes and MGC against the AMH level of the women (Figure 1). We found no association between the DNAmTL and the AMH level either in leukocytes (p = 0.61) (Figure 1A) or in MGC (p = 0.75) (Figure 1B) when adjusting for chronological age. However, the age adjusted DNAmTL values were found to be significantly higher in the DOR group compared with the normal group (leukocytes: p = 0.008; MGC: p = 0.0001) or high group (Leukocytes: p = 0.028; MGC: p = 0.013) (Figure 1C and 1D). When comparing the unadjusted DNAmTL values between ovarian reserve groups the difference between the DOR group and the other two was observed in MGC (Normal: p = 0.0001; High: p = 0.0073) (Figure S2G) but not in leukocytes (Normal: p = 0.42; High: p = 0.54) (Figure S2F). When plotting the unadjusted values of DNAmTL against the AMH level once again we do not observe an association neither in leukocytes (p = 0.083) (Figure S2A) nor in MGC (p = 0.83) (Figure S2B). However, stratifying the samples by ovarian reserve category in leukocytes shows significant associations in normal and high AMH samples (p = 6.26×10^{-5} and 0.025, respectively) (Figure S2D and E), indicating that the linear relationship between AMH level and DNAmTL only exists within categories but not across them.

Differential Variability in DNA Methylation

We sought to identify differentially methylated positions associated with AMH levels or ovarian reserve category. Due to a limited sample size we were underpowered to detect genome-wide significant signals with a moderate effect size (p < 5×10^{-8}, power = 0.00, effect size = 0.15) (Figure S3). To further study the relationship between the ovarian reserve and DNA methylation we performed a differential DNA methylation variability analysis by comparing DOR or high ovarian reserve samples to normal controls (Suppl. tables V-IX). Differential variability between DOR and normal samples was observed at 4,199 CpGs in MGC, but only 447 between high and normal (FDR < 0.05). Regardless of the ovarian reserve status, very few signals were detected in the leukocytes and no overlaps with the signals in MGC were found. The Manhattan plots in figures 2A and 2C (DOR vs. normal) and 2B and 2D (high vs. normal) illustrate the differential DNA methylation variability in the two ovarian reserve categories across the genome in leukocytes and MGC, respectively. Both DOR and high ovarian reserve samples showed mostly increased variability at these CpGs compared to controls. Using publicly available Chromatin Immunoprecipitation Sequencing (ChIP-sequencing) data for different histone marks profiled in ovarian tissue, we found that the variable CpGs in MGC from DOR were enriched in regions marked with H3K27me3 (trimethylation at lysine 27 of histone H3) (Figure 23E), an epigenetic modification associated with inactive gene promotors. Similarly, variable CpGs in the high AMH group were enriched for regions of weak transcription (Figure 2F). Gene ontology analysis of genes associated with the variable CpGs in DOR revealed an enrichment for categories related to, among others, cell-to-cell adhesion, while no enriched categories were found for the genes associated with variable methylation in high AMH samples (Suppl. Table III, IV). Subsequently, the identified single CpGs were used to call regions of differential variability. A total number of 692 regions were found in DOR women (Suppl. Table V, selected genes: Table III), but only 76 regions were found in women with a high AMH level (Suppl. Table VI). Two examples of DNA methylation variability are shown in figure 4; insulin growth factor 2 (*IGF2)* (Figure 42G) and *AMH* (Figure 2H). Table SI shows differential DNA methylation variability regions in DOR MGC of selected genes.

Epimutations

Further to the observed DNA methylation variability, we also looked at the number of epimutations in the two cell types for the three groups of women (Figure 5). We observed that there

is no significant difference in the number of epimutations between the three ovarian reserve groups in leukocytes, but found that epimutations were significantly more frequent in MGC from women with DOR compared with women with a normal ovarian reserve (Kruskal-Wallis test; p = 0.0079) or from women with a high ovarian reserve (Kruskal-Wallis test; p = 0.072). Epimutated sites showed a moderate enrichment in intergenic regions (OR = 1.18; $p = 1.1 \times 10^{-171}$) and depletion close to promoter regions (0-200 bp upstream of the transcription start site) (OR = 0.71; $p = 1.4 \times 10^{-264}$) for all samples (23), but were more frequent in the DOR samples.

DISCUSSION

This is to our knowledge the first study describing the epigenetic differences between healthy women with different ovarian reserve. Our data clearly demonstrate that the MGC – which provide crucial support to the growing oocyte – of women with DOR have a different epigenetic profile than those of women with a normal, age-adjusted ovarian reserve. Their MGCs are characterized by having a higher number of epimutations and greater DNA methylation variability, together with longer DNAmTL. These effects, except longer DNAmTL, are not found in leukocytes from the same women. Interestingly, no age acceleration was observed in DOR as compared to control. This distinctive epigenetic profile found in women with DOR might give some explanation of why these women often are reproductively challenged compared to women with a normal ovarian reserve.

The subgroups of women included in this study only differ significantly in parameters related to their ovarian reserve status (AMH, FSH, number of retrieved oocytes, etc.). The utilization rate for all groups are unchanged, the data confirming previous findings that women with DOR have the same quality of oocytes as age-matched women (9, 10).

We have recently presented the performance of the well-known multi-tissue epigenetic clock (16) in leukocytes and MGC, showing that DNA methylation changes with age in MGCs do not correlate with chronological age (23). In the present study, we found no significant differences between age acceleration and the ovarian reserve subgroups, but we found a trend in the leukocytes, indicating that women with high AMH levels have a younger DNAm age than women with lower AMH levels. However, a larger study group is needed to validate these findings.

Although we did not find any significant association between the DNAmTL and AMH levels as a continuous variable, the DNAmTL predictor was able to capture differences in the DOR group unrelated to chronological age, showing higher values of DNAmTL, and longer estimated telomeres, in the DOR group for both leukocytes and MGC. Previous findings showed a significantly reduced telomere length in leukocytes and MGC in women with premature ovarian insufficiency (29). It is possible that dysregulation of telomere length is a hallmark in cells from women with POI or DOR, perhaps accelerated by genetic variants in DNA repair pathways that participate in maintenance of telomeres (30, 31). This could give rise to both longer and shorter telomeres (32).

The variable CpGs found in the DOR group in MGC overlapped with sites of H3K27me3 enrichment, including bivalent domains, which is a chromatin modification associated with heritable gene silencing (33). Studies in granulosa cells from rats have shown that enhancer of zeste homolog 2 (EZH2), which induces H3K27me3 deposition, is decreased after human chorionic gonadotropin (hCG) stimulation (34) and after ovulation (35). This suggests that H3K27me3 is decreased causing the chromatin to loosen up, which might allow DNA methylation and gene activation to occur (34). If a similar change is induced by hCG/LH in human granulosa cells, the observed variable methylation of H3K27me3 may suggest altered response to ovulation induction in women with DOR. However, functional studies are required to investigate this hypothesis.

An increasing variability in DNA methylation has been observed with increasing age, and a model in which variability is a by-product of the aging process itself exists (36). Our results show greater DNA methylation variability in MGC of the DOR group, which may indicate a distinct rate of ovarian aging in these women. The enhanced variability in DNA methylation may be associated with a functional effect on the MGC. In support of this possibility, we found overlap between several differential variable CpG sites with genes presented in the female reproduction gene list

(https://gemma.msl.ubc.ca/phenotypes.html) (37)) (data not shown).

Interestingly, increased variability is seen at genes involved in folliculogenesis, such as *IGF2* and *AMH*, both of which play essential roles in folliculogenesis. IGF2 promotes proliferation and differentiation of the MGC in response to FSH (38). IGF2 is synthesized in theca cells by small antral follicles and by the MGC in the large ovulatory follicles (39), and acts in a paracrine fashion in granulosa cells in the small antral follicles (39). Moreover, it has recently been shown that IGF2 is increased with increasing follicle size and peaks in large preovulatory follicles (40). The higher variability in the *AMH* gene in MGC in women with DOR is intriguing as AMH is suggested as a candidate to gate-keeper of the initial recruitment of primordial follicles (41). Whether the higher variability in the MGC in mature follicle reflects a potential altered expression and function in early folliculogenesis and recruitment remains to be investigated. The central role of AMH in the later phase of folliculogenesis and its relationship with FSH, androgens and estrogen has mainly been investigated and described in women with PCOS (42). If the role of AMH in the later phase of folliculogenesis is involved in pathophysiology in DOR remains to by elucidated.

Genes in the variable regions were, among others, associated with the gene ontology category cell-to-cell adhesion, which may influence the close interaction between the MGC and their function in folliculogenesis in women with DOR. Furthermore, glucuronidation, an enzyme reaction process catalysed by uridine diphosphate glucuronosyltransferases as a part of the metabolic pathway, was another enriched category in the variable regions of DOR MGCs. Glucuronide metabolites have previously been identified as indices of ovarian function (43, 44). In the ovary, 5α-reduced C_{19} steroid glucuronides have been found in follicular fluid (45), suggesting that the ovary is a site for glucuronidation and steroid glucuronidation is an important intracrine pathway involved in termination of steroid signaling (46).

A recent study focusing on the DNAm profile in granulosa lutein cells from women with PCOS found 106 differentially methylated CpG sites, associated with 88 genes, between PCOS and control subjects, including genes known to be related to PCOS and ovarian function (22). We found only one gene overlap (metastasis suppressor 1 (MTSS1)) between this gene list and the lists of the present study, suggesting distinct profiles related to high AMH and PCOS.

Epimutations are here defined as DNA methylation outliers, which are suggested to represent epigenetic defects that accumulate with aging (47). We found that the number of epimutations in MGC from the DOR group was significantly elevated compared to the normal and high group. This is similar to the numbers we recently found in women above the age of 40 years (23). Epimutations across age and ovarian reserve status occur at the same genomic locations but are more frequent in women with DOR and with advanced maternal age. These findings suggest that the MGC of women with DOR, even though they do not have an older DNAm age, appear epigenetically like women with advanced maternal age (23). It also correlates with the reduced fertility potential found in women with DOR and women with advanced maternal age. Recently, Fan and colleagues found that apoptosis is increased in MGC from women with DOR (48), which could be a result of the increased number of epimutations resulting from a poorly regulated establishment or maintenance of DNA methylation. Even though in evolutionary terms, genetic variability makes the genome able to adapt to new environments (49), an increased number of epimutations are also found in diseases such as cancer (50, 51), α-thalassaemia (52) and cardiovascular disease (53). Thus, we speculate whether the unstable methylome in the MGC causes an epigenetic dysfunction resulting in the poor ovarian reserve found in the DOR women.

With our epigenetic profiling of MGC, and with further research of cells of the human ovarian follicle, we might in the future be able to develop a diagnostic and/or prognostic biomarker for premature DOR or use the (reversible) DNA methylation as a therapeutic target for treatment in women at risk of premature loss of fertility.

ACKNOWLEDGEMENTS

The authors thank the staff at participating clinics and the women participating in the study, without whom this research would not be possible. Thanks to Sofie Lindgren Christiansen, PhD and Jane Alrø

Bøtkjær, PhD for performing preliminary test runs in the laboratory.

DATA AVAILABLE ON REQUEST

The data underlying this article will be shared on reasonable request to the corresponding author.

REFERENCES

1. Treloar AE. Menstrual cyclicity and the pre-menopause. Maturitas 1981;3:249-64.
2. te Velde ER, Pearson PL. The variability of female reproductive aging. Hum Reprod Update 2002;8:141-54.
3. Depmann M, Broer SL, van der Schouw YT, Tehrani FR, Eijkemans MJ, Mol BW *et al.* Can we predict age at natural menopause using ovarian reserve tests or mother's age at menopause? A systematic literature review. Menopause 2016;23:224-32.
4. Aflatoonian A, Eftekhar M, Mohammadian F, Yousefnejad F. Outcome of assisted reproductive technology in women aged 40 years and older. Iranian Journal of Reproductive Medicine 2011;9:281-4.
5. Pastore LM, Christianson MS, Stelling J, Kearns WG, Segars JH. Reproductive ovarian testing and the alphabet soup of diagnoses: DOR, POI, POF, POR, and FOR. J Assist Reprod Genet 2018;35:17-23.
6. Wallace WH, Kelsey TW. Human ovarian reserve from conception to the menopause. PLoS One 2010;5:e8772.
7. Faddy MJ, Gosden RG, Gougeon A, Richardson SJ, Nelson JF. Accelerated disappearance of ovarian follicles in mid-life: implications for forecasting menopause. Hum Reprod 1992;7:1342-6.
8. Gougeon A, Chainy GB. Morphometric studies of small follicles in ovaries of women at different ages. J Reprod Fert 1987;81:433-42.
9. Abdalla H, Thum MY. An elevated basal FSH reflects a quantitative rather than qualitative decline of the ovarian reserve. Hum Reprod 2004;19:893-8.
10. Guerif F, Lemseffer M, Couet M, Gervereau O, Ract V, Royere D. Serum antimullerian hormone is not predictive of oocyte quality in vitro fertilization. Ann Endocrinol (Paris) 2009;70:230-4.
11. Rooij IAJV, Broekmans FJM, Te Velde ER, Fauser BCJM, Bancsi LFJMM, Jong FHD *et al.* Serum anti-Müllerian hormone levels : a novel measure of ovarian reserve. Hum Reprod 2002;17:3065-71.
12. Weenen C, Laven JSE, von Bergh ARM, Cranfield M, Groome NP, Visser JA *et al.* Anti-Müllerian hormone expression pattern in the human ovary: Potential implications for initial and cyclic follicle recruitment. Mol Hum Reprod 2004;10:77-83.
13. de Kat AC, van der Schouw YT, Eijkemans MJ, Herber-Gast GC, Visser JA, Verschuren WM *et al.* Back to the basics of ovarian aging: a population-based study on longitudinal anti-Mullerian hormone decline. BMC Med 2016;14:151.
14. Aydos SE, Elhan AH, Tukun A. Is telomere length one of the determinants of reproductive life span? Arch Gynecol Obstet 2005;272:113-6.
15. Lu AT, Seeboth A, Tsai P-C, Sun D, Quach A, Reiner AP *et al.* DNA methylation-based estimator of telomere length. Aging 2019;11.
16. Horvath S. DNA methylation age of human tissues and cell types. Genome Biol 2013;14:R115.
17. Weidner CI, Lin Q, Koch CM, Eisele L, Beier F, Ziegler P *et al.* Aging of blood can be tracked by DNA methylation changes at just three CpG sites. Genome Biology 2014;15:R24.
18. Giuliani C, Cilli E, Bacalini MG, Pirazzini C, Sazzini M, Gruppioni G *et al.* Inferring chronological age from DNA methylation patterns of human teeth. Am J Phys Anthropol 2016;159:585-95.
19. Levine ME, Lu AT, Quach A, Chen BH, Assimes TL, Bandinelli S *et al.* An epigenetic biomarker of aging for lifespan and healthspan. Aging 2018;10:573-91.
20. Marioni RE, Shah S, McRae AF, Chen BH, Colicino E, Harris SE *et al.* DNA methylation age of blood predicts all-cause mortality in later life. Genome Biol 2015;16:25.
21. Perna L, Zhang Y, Mons U, Holleczek B, Saum KU, Brenner H. Epigenetic age acceleration predicts cancer, cardiovascular, and all-cause mortality in

a German case cohort. Clin Epigenetics 2016;8:1-7.
22. Makrinou E, Drong AW, Christopoulos G, Lerner A, Chapa-Chorda I, Karaderi T *et al.* Genome-wide methylation profiling in granulosa lutein cells of women with polycystic ovary syndrome (PCOS). Mol Cell Endocrinol 2019:110611.
23. Olsen KW, Castillo-Fernandez J, Zedeler A, Freiesleben NC, Bungum M, Chan AC *et al.* A distinctive epigenetic ageing profile in human granulosa cells. Hum Reprod 2020.
24. Aryee MJ, Jaffe AE, Corrada-Bravo H, Ladd-Acosta C, Feinberg AP, Hansen KD *et al.* Minfi: A flexible and comprehensive Bioconductor package for the analysis of Infinium DNA methylation microarrays. Bioinformatics 2014;30:1363-9.
25. Phipson B, Maksimovic J, Oshlack A. missMethyl: an R package for analysing methylation data from Illuminas HumanMethylation450 platform. Bioinformatics 2015;32:286-8.
26. R Core Team. A Language and Environment for Statistical Computing In, 2016.
27. Lee JE, Park DS, Kim M-L, Yoon BS, Song T, Kim MK *et al.* Age-related distribution of anti-Müllerian hormone levels in 2,879 Korean women with regular menstruation. Korean J of Obstet Gynecol 2012;55:920.
28. Horvath S, Oshima J, Martin GM, Lu AT, Quach A, Cohen H *et al.* Epigenetic clock for skin and blood cells applied to Hutchinson Gilford Progeria Syndrome and ex vivo studies. Aging 2018;10:1758-75.
29. Xu X, Chen X, Zhang X, Liu Y, Wang Z, Wang P *et al.* Impaired telomere length and telomerase activity in peripheral blood leukocytes and granulosa cells in patients with biochemical primary ovarian insufficiency. Hum Reprod 2017;32:201-7.
30. Day FR, Ruth KS, Thompson DJ, Lunetta KL, Pervjakova N, Chasman DI *et al.* Large-scale genomic analyses link reproductive aging to hypothalamic signaling, breast cancer susceptibility and BRCA1-mediated DNA repair. Nat Genet 2015;47:1294-303.
31. Thompson DJ, Genovese G, Halvardson J, Ulirsch JC, Wright DJ, Terao C *et al.* Genetic predisposition to mosaic Y chromosome loss in blood. Nature 2019;575:652-7.
32. Cesare AJ, Reddel RR. Alternative Lengthening of Telomeres in Mammalian Cells. In: Tomoska L, Nosek J, eds. Origin and Evolution of Telomeres: Landes Bioscience, 2008.
33. Simon JA, Kingston RE. Mechanisms of polycomb gene silencing: knowns and unknowns. Nat Rev Mol Cell Biol 2009;10:697-708.
34. Okada M, Lee L, Maekawa R, Sato S, Kajimura T, Shinagawa M *et al.* Epigenetic Changes of the Cyp11a1 Promoter Region in Granulosa Cells Undergoing Luteinization During Ovulation in Female Rats. Endocrinology 2016;157:3344-54.
35. Maekawa R, Lee L, Okada M, Asada H, Shinagawa M, Tamura I *et al.* Changes in gene expression of histone modification enzymes in rat granulosa cells undergoing luteinization during ovulation. J Ovarian Res 2016;9:15.
36. Jones MJ, Goodman SJ, Kobor MS. DNA methylation and healthy human aging. Aging Cell 2015;14:924-32.
37. Zoubarev A, Hamer KM, Keshav KD, McCarthy EL, Santos JR, Van Rossum T *et al.* Gemma: a resource for the reuse, sharing and meta-analysis of expression profiling data. Bioinformatics 2012;28:2272-3.
38. Baumgarten SC, Convissar SM, Zamah AM, Fierro MA, Winston NJ, Scoccia B *et al.* FSH Regulates IGF-2 Expression in Human Granulosa Cells in an AKT-Dependent Manner. J Clin Endocrinol Metab 2015;100:E1046-55.
39. el-Roeiy A, Chen X, Roberts VJ, LeRoith D, Roberts J, C. T., Yen SS. Expression of insulin-like growth factor-I (IGF-I) and IGF-II and the IGF-I, IGF-II, and insulin receptor genes and localization of the gene products in the human ovary. J Clin Endocrinol Metab 1993;77:1411-8.
40. Bøtkjær JA, Pors SE, Petersen TS, Kristensen SG, Jeppesen JV, Oxvig C *et al.* Transcription profile of the insulin-like growth factor signaling pathway during human ovarian follicular development. J Assist Reprod Genet 2019;36:889-903.
41. Durlinger AL, Visser JA, Themmen APN. Regulation of ovarian function: the role of anti-Mullerian hormone. Reproduction 2002;124:601-9.
42. Dewailly D, Robin G, Peigne M, Decanter C, Pigny P, Catteau-Jonard S. Interactions between androgens, FSH, anti-Mullerian hormone and estradiol during folliculogenesis in the human

normal and polycystic ovary. Hum Reprod Update 2016;22:709-24.
43. Collins WP, Collins PO, Kilpatrick MJ, Manning PA, Pike JM, Tyler JP. The concentrations of urinary oestrone-3-glucuronide, LH and pregnanediol-3alpha-glucuronide as indices of ovarian function. Acta endocrinologica 1979;90:336-48.
44. Sachdev R, Von Hagen S, Kamnani A, Santoro N. Persistent pregnanediol glucuronide secretion after gonadotrophin suppression indicates adrenal source of progesterone in premature ovarian failure. Hum Reprod 1998;13:2061-3.
45. Prévost J, Brochu M, Bélanger A, Lambert R. Conjugated and Unconjugated C-21, C-19 and C-18 Steroid Concentrations in Human Follicular Fluid From Hyperstimulated Follicles. Gynecol Endocrinol 1987;1.
46. Albert C, Barbier O, Vallée M, Beaudry G, Bélanger A, Hum DW. Distribution of uridine diphosphate-glucuronosyltransferase (UGT) expression and activity in cynomolgus monkey tissues: Evidence for differential expression of steroid-conjugating UGT enzymes in steroid target tissues. Endocrinology 2000;141:2472-80.
47. Holliday R. The Inheritance of Epigenetic Defects. Science 1987;238: 163-70.
48. Fan Y, Chang Y, Wei L, Chen J, Li J, Goldsmith S *et al.* Apoptosis of mural granulosa cells is increased in women with diminished ovarian reserve. J Assist Reprod Genet 2019;36:1225-35.
49. Doerfler W, Böhm P. DNA Methylation: Development Genetic Disease and Cancer Springer-Verlag Berlin Heidelberg, 2006.
50. Feinberg AP, Vogelstein B. Hypomethylation distinguishes genes of some human cancers from their normal counterparts. Nature 1983;301:89-92.
51. Feinberg AP, Tycko B. The history of cancer epigenetics. Nature Reviews Cancer 2004;4:143-53.
52. Tufarelli C, Sloane Stanley JA, Garrick D, Sharpe JA, Ayyub H, Wood WG *et al.* Transcription of antisense RNA leading to gene silencing and methylation as a novel cause of human genetic disease. Nature Genetics 2003;34:157-65.
53. Ying AK, Hassanain HH, Roos CM, Smiraglia DJ, Issa JPJ, Michler RE *et al.* Methylation of the estrogen receptor-α gene promoter is selectively increased in proliferating human aortic smooth muscle cells. Cardiovasc Res 2000;46:172-9.

Table I Clinical and demographic characteristics of the participating women.

	Ovarian reserve groups Clinical and Demographic Characteristics				
	DOR	Normal	High	Overall	One-way ANOVA p-value
Number [MGC]	28 [11]	63 [37]	28 [15]	119 [63]	-
Age at OPU (years)	35.5 ± 4.7	33.2 ± 4.8	33.8 ± 4.2	33.9 ± 4.7	0.09
BMI (kg/m^2)	24.3 ± 3.3	24.1 ± 3.9	24.5 ± 4.0	24.3 ± 3.8	0.90
AMH (pmol/L)	3.1 ± 1.7	18.5 ± 8.8	55.1 ± 14.3	23.5 ± 20.9	2.2x10^{-16}
Primary cause of infertility - Male factor - Female factor - Unexplained - Other causes*	 8 12 2 6	 20 7 27 9	 6 9 10 3	 34 28 39 18	 - - - -
FSH (IU/L)	11.5 ± 10.9	6.7 ± 3.0	5.9 ± 2.3	7.8 ± 6.4	0.001
LH (IU/L)	8.2 ± 9.9	6.3 ± 5.9	7.6 ± 4.6	7.1 ± 6.9	0.51
LH/FSH ratio	0.7 ± 0.6	0.97 ± 0.6	1.7 ± 1.1	1.04 ± 0.8	0.0002
Prolactin (IU/L)	258 ± 111	314 ± 141	283 ± 136	295 ± 135	0.23
TSH (IU/L)**	1.5 ± 0.6	1.7 ± 0.9	1.7 ± 0.7	1.7 ± 0.8	0.46
Total FSH dose (IU)	2879 ± 3.6	1697 ± 834	1684 ± 748	1853 ± 970	0.0001
Stimulation duration (days)	9.2 ± 3.9	9.1 ± 2.4	10. 6 ± 2.5	9.5 ± 2.7	0.0502
Cycle Characteristics					
No. of oocytes	4.6 ± 2.4	8.7 ± 5.0	10.4 ± 6.2	8.1 ± 5.3	0.002
No. of 2PN zygotes	2.5 ± 2.1	4.4 ± 3.2	5.6 ± 4.1	4.2 ± 3.4	0.002
No. of clinically usable embryos	0.6 ± 1.2	2.5 ± 2.4	3.5 ± 3.0	2.3 ± 2.5	5.2x10^{-5}
Utilization rate***	0.5 ± 0.4	0.6 ± 0.3	0.6 ± 0.3	0.6 ± 0.3	0.26

Mean ± standard deviation.

*Single women and women with a female partner.

**This is baseline measurement. In case of TSH > 2.5 IU/L with +/- thyreoidea peroxidase (TPO) antibodies, regulation to < 2.5 IU/L or 2.5-4.0 without TPO antibodies was ensured before treatment start following the Danish Fertility Society's Guideline.

*** No. of clinically useable embryos/no. of 2PN zygotes.

Figure 1

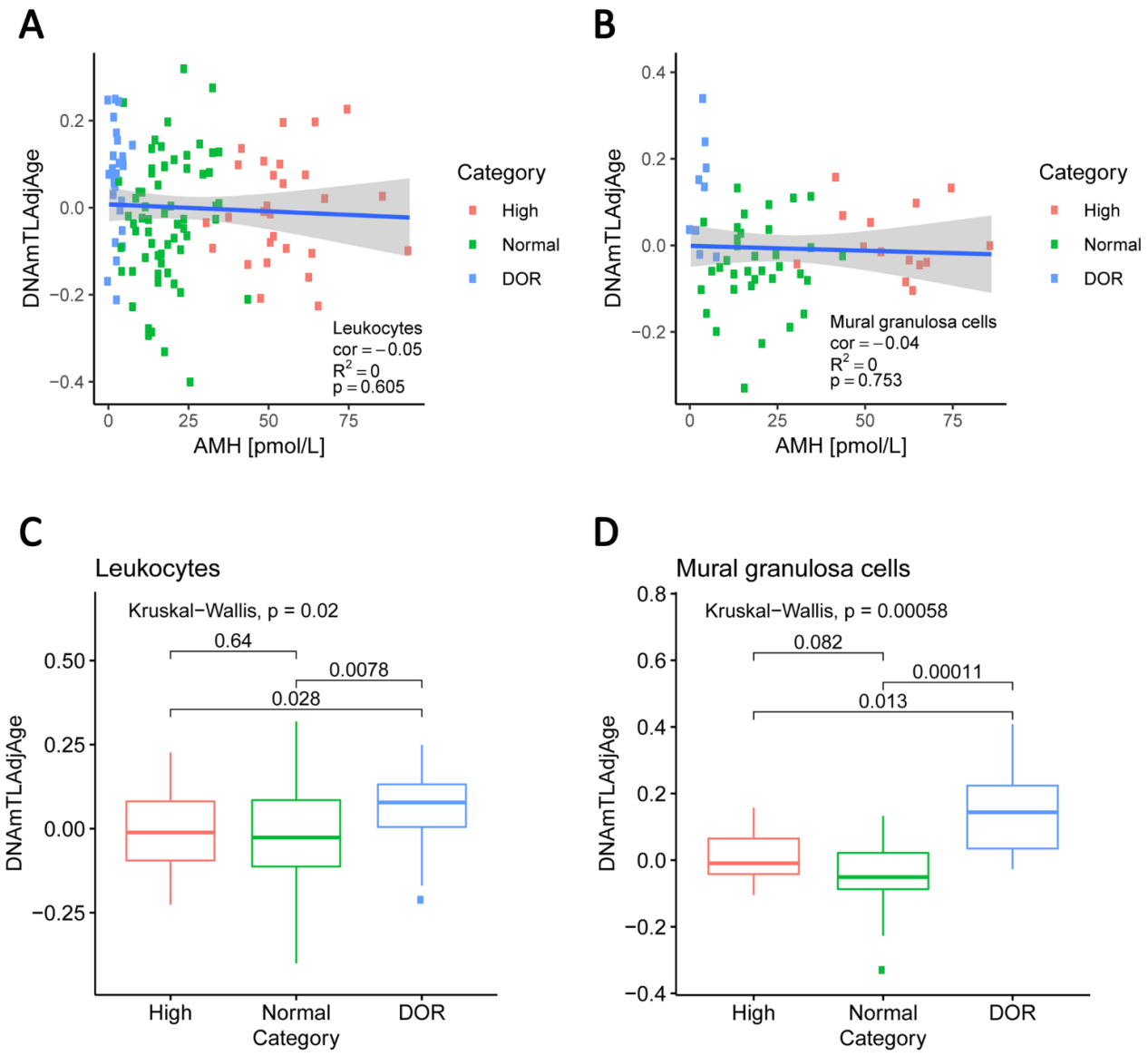

Figure 1. Predicted telomere length (DNAmTL) in relation to AMH level and ovarian reserve in leukocytes and mural granulosa cells. The women are divided into groups regarding their ovarian reserve status, indicated with colours: red (high), green (normal) and blue (diminished ovarian reserve (DOR)). Scatter plots indicating the correlation (cor) between predicted telomere length adjusted for age in (**A**) leukocytes (cor = -0.05, *p* = 0.605) and (**B**) mural granulosa cells (MGC) (cor = -0.04, *p* = 0.753). (**C** and **D**) Boxplot of DNAmTL values adjusted for age in the three ovarian reserve subgroups. The DNAmTL value is higher in the DOR group in both (**C**) leukocytes (Kruskal-Wallis: *p* = 0.02) and (**D**) MGC (Kruskal-Wallis: *p* = 0.00058).

Figure 2

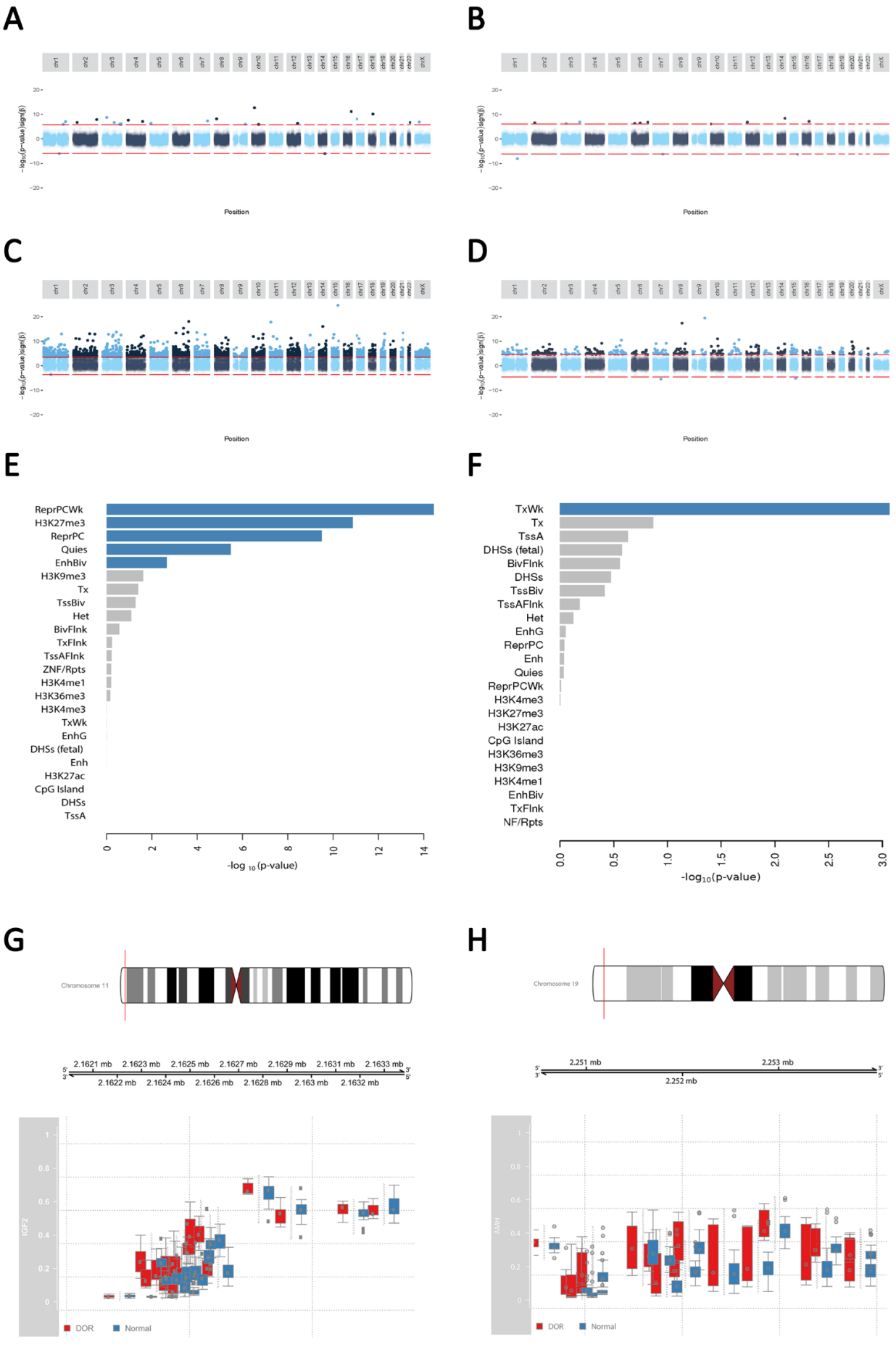
A
B
C
D
Position
E
ReprPCWk
H3K27me3
ReprPC
Quies
EnhBiv
H3K9me3
Tx
TssBiv
Het
BivFlnk
TxFlnk
TssAFlnk
ZNF/Rpts
H3K4me1
H3K36me3
H3K4me3
TxWk
EnhG
DHSs (fetal)
Enh
H3K27ac
CpG Island
DHSs
TssA
-log 10 (p-value)
F
TxWk
Tx
TssA
DHSs (fetal)
BivFlnk
DHSs
TssBiv
TssAFlnk
Het
EnhG
ReprPC
Enh
Quies
ReprPCWk
H3K4me3
H3K27me3
H3K27ac
CpG Island
H3K36me3
H3K9me3
H3K4me1
EnhBiv
TxFlnk
NF/Rpts
-log10(p-value)
G
Chromosome 11
2.1621 mb
2.1623 mb
2.1625 mb
2.1627 mb
2.1629 mb
2.1631 mb
2.1633 mb
2.1622 mb
2.1624 mb
2.1626 mb
2.1628 mb
2.163 mb
2.1632 mb
IGF2
DOR
Normal
H
Chromosome 19
2.251 mb
2.253 mb
2.252 mb
AMH
DOR
Normal

Figure 2

Figure 2. Differential variability in DNA methylation in leukocytes and mural granulosa cells between women with different ovarian reserve. (**A**, **B**, **C** and **D**) Manhattan plots of *p*-values from the differential variability test of DNA methylation. Each point represents a CpG with the chromosomal position along the x-axis and the negative logarithm of the associated *p*-value on the y-axis. Red lines represent the significant level of FDR = 0.05. (**A** and **B**) Few signals are found in the variability of the DNA methylation in leukocytes between the ovarian reserve subgroups. (**C**) A great variability is found in the diminished ovarian reserve (DOR) group in the mural granulosa cells (MGC). (**D**) An increased variability is also found in the group with high AMH levels. (**E**) Blue bars indicate regions with chromatin states or chromatin marks in which CpGs with high variability are enriched, e.g. H3K27me3 in the DOR category. (**F**) Only one category is significantly enriched in the high group; TxWk. TssA, Active transcription start site; TssAFlnk, Flanking Tss; TxFlnk, Transcribed at gene 5' and 3'; Tx, Strong transcription; TxWk, Weak transcription; EnhG, Genic enhancers; Enh, Enhancers; ZNF/Rpts, ZNF genes & repeats; Het, Heterochromatin; TssBiv, Bivalent/Poised Tss; BivFlnk, Flanking Bivalent Tss/Enh; EnhBiv, Bivalent Enhancer; ReprPC, Repressed PolyComb; ReprPCWk, Weak Repressed PolyComb; Quies, Quiescent. A greater methylation variation in the CpGs of (**G**) *IGF2* and (**H**) *AMH* in mural granulosa cells in women with diminished ovarian reserve (DOR) compared with women with the normal ovarian reserve

Figure 3

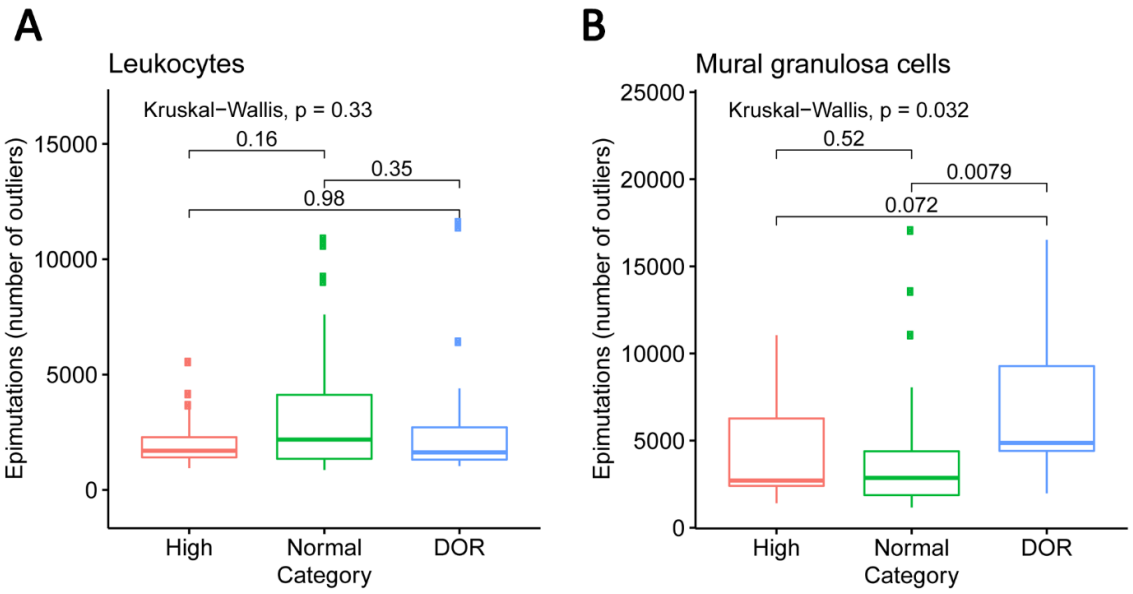

Figure 3 Frequency of epimutations. Epimutations (number of outliers) in relation to ovarian reserve. (**A**) The number of epimutations in leukocytes from women with a high ovarian reserve or diminished ovarian reserve (DOR) are non-significantly different from the normal ovarian reserve (high: $p = 0.16$, DOR: $p = 0.35$). (**B**) The boxplot shows a significantly higher number of epimutations in MGC from women with DOR compared with women with a normal ovarian reserve ($p = 0.008$).

SUPPLEMENTARY

Table SI Differential DNA methylation variability regions in mural granulosa cells of selected genes when comparing women with diminished ovarian reserve to women with a normal ovarian reserve.

Gene name	Gene symbol	Chromosome	Width of the region	No. of CpGs	Minimum FDR	Stouffer
Tripeptidyl-peptidase 1	*TPP1*	11	224	4	1.15×10^{-9}	0.0081
Folate Receptor 1	*FOLR1*	11	211	2	9.77×10^{-5}	0.0145
Inhibin Subunit Beta B	*INHBB*	2	284	3	2.47×10^{-5}	0.0198
Anti-Müllerian hormone	*AMH*	19	2432	12	2.82×10^{-5}	0.0670
Telomere Maintenance 2	*TELO2*	16	240	4	2.11×10^{-5}	0.1873
B-Cell Translocation Gene 4	*BTG4*	11	754	6	3.82×10^{-6}	0.7350
Insulin-like growth factor 2	*IGF2*	11	964	18	4.58×10^{-5}	0.9575
Imprinted maternally expressed transcript	*H19*	11	865	20	8.29×10^{-7}	0.9575
Vimentin	*VIM*	10	608	9	8.83×10^{-12}	0.9795
CD82 Molecule	*CD82*	11	37	2	0.00012	0.1882
Catechol-O-Methyltransferase	*COMT*	22	138	3	1.85×10^{-5}	0.0606
Histone Deacetylase 2	*HDAC2*	6	466	2	2.56×10^{-11}	0.0009
Homeobox D11	*HOXD11*	2	763	2	1.69×10^{-5}	0.0751
O-6-Methylguanine-DNA Methyltransferase	*MGMT*	10	517	13	5.15×10^{-5}	0.9289
Neurofilament Medium	*NEFM*	8	30	3	3.00×10^{-5}	0.4366
Notch Receptor 4	*NOTCH4*	6	815	14	1.02×10^{-6}	0.5935
Nuclear Receptor Subfamily 3 Group C Member 2	*NR3C2*	4	396	4	7.55×10^{-9}	0.3359
Ovarian Cancer-Associated Gene 2 Protein	*OVCA2*	17	1159	6	8.07×10^{-13}	0.5370
Paired box 2	*PAX2*	10	1225	7	4.89×10^{-8}	0.0251
Platelet Derived Growth Factor Receptor Alpha	*PDGFRA*	4	382	6	7.31×10^{-8}	0.2126
Semaphorin 3F	*SEMA3F*	3	1239	7	3.11×10^{-8}	0.1136
Solute Carrier Family 39 Member 4	*SLC39A4*	8	1550	9	6.15×10^{-15}	0.0538
Tumor Associated Calcium Signal Transducer 2	*TACSTD2*	1	1129	12	1.89×10^{-11}	0.0230
Transgelin	*TAGLN*	11	629	9	3.13×10^{-6}	0.0816
Wnt Family Member 5B	*WNT5B*	12	412	8	5.71×10^{-7}	0.0225

Table SII Clinical and demographic characteristics of the women donating mural granulosa cells.

	Ovarian reserve group				
	DOR	Normal	High	Overall	One-way ANOVA p-value
Number of women*	10	35	14	59	-
Age at OPU (years)	32.2 ± 5.8	33.0 ± 5.0	33.6 ± 4.8	33.0 ± 5.0	0.81
BMI (kg/m^2)	23.4 ± 3.5	24.2 ± 3.7	24.1 ± 3.6	24.0 ± 3.6	0.84
AMH (pmol/L)	4.0 ± 2.0	19.6 ± 10.0	58.8 ± 14.3	26.2 ± 21.3	$2.2x10^{-16}$
Primary cause of infertility					
- Male factor	4	13	1	18	-
- Female factor	6	5	7	18	-
- Unexplained	-	13	4	17	-
- Other causes**	-	4	2	6	-
FSH (IU/L)	6.6 ± 3.3	6.5 ± 3.2	5.2 ± 2.6	6.3 ± 3.1	0.46
LH (IU/L)	5.2 ± 2.5	6.3 ± 4.7	10.1 ± 5.8	6.9 ± 4.8	0.099
LH/FSH ratio	0.7 ± 0.4	1.0 ± 0.5	2.5 ± 1.0	1.3 ± 0.9	$1.7x10^{-5}$
Prolactin (IU/L)	295 ± 124	289 ± 129	297 ± 162	292 ± 134	0.98
TSH (IU/L)***	1.3 ± 0.6	1.8 ± 0.9	1.9 ± 0.8	1.8 ± 0.9	0.19
Total FSH dose (IU)	2419 ± 1113	1783 ± 948	1779 ± 727	1878 ± 937	0.21
Stimulation duration	9.3 ± 3.2	9.2 ± 2.5	11.1 ± 2.7	9.7 ± 2.8	0.11
Cycle Characteristics					
No. of oocytes	6.6 ± 2.0	9.5 ± 5.1	11.9 ± 6.5	9.5 ± 5.5	0.16
No. of 2PN zygotes	4.1 ± 2.9	4.7 ± 3.2	5.7 ± 4.1	4.8 ± 3.5	0.73
No. of clinically usable embryos	1.6 ± 1.8	3.1 ± 2.5	4.7 ± 3.3	3.1 ± 2.7	0.03
Utilization rate****	0.5 ± 0.3	0.6 ± 0.3	0.7 ± 0.2	0.6 ± 0.3	0.53

Mean ± standard deviation.

*Only samples, who passed the quality control test are included.

**Single women and women with a female partner.

***This is baseline measurement. In case of TSH > 2.5 IU/L with +/- thyreoidea peroxidase (TPO) antibodies, regulation to < 2.5 IU/L or 2.5-4.0 without TPO antibodies was ensured before treatment start following the Danish Fertility Society's Guideline.

**** No. of clinically useable embryos/no. of 2PN zygotes.

Figure S1

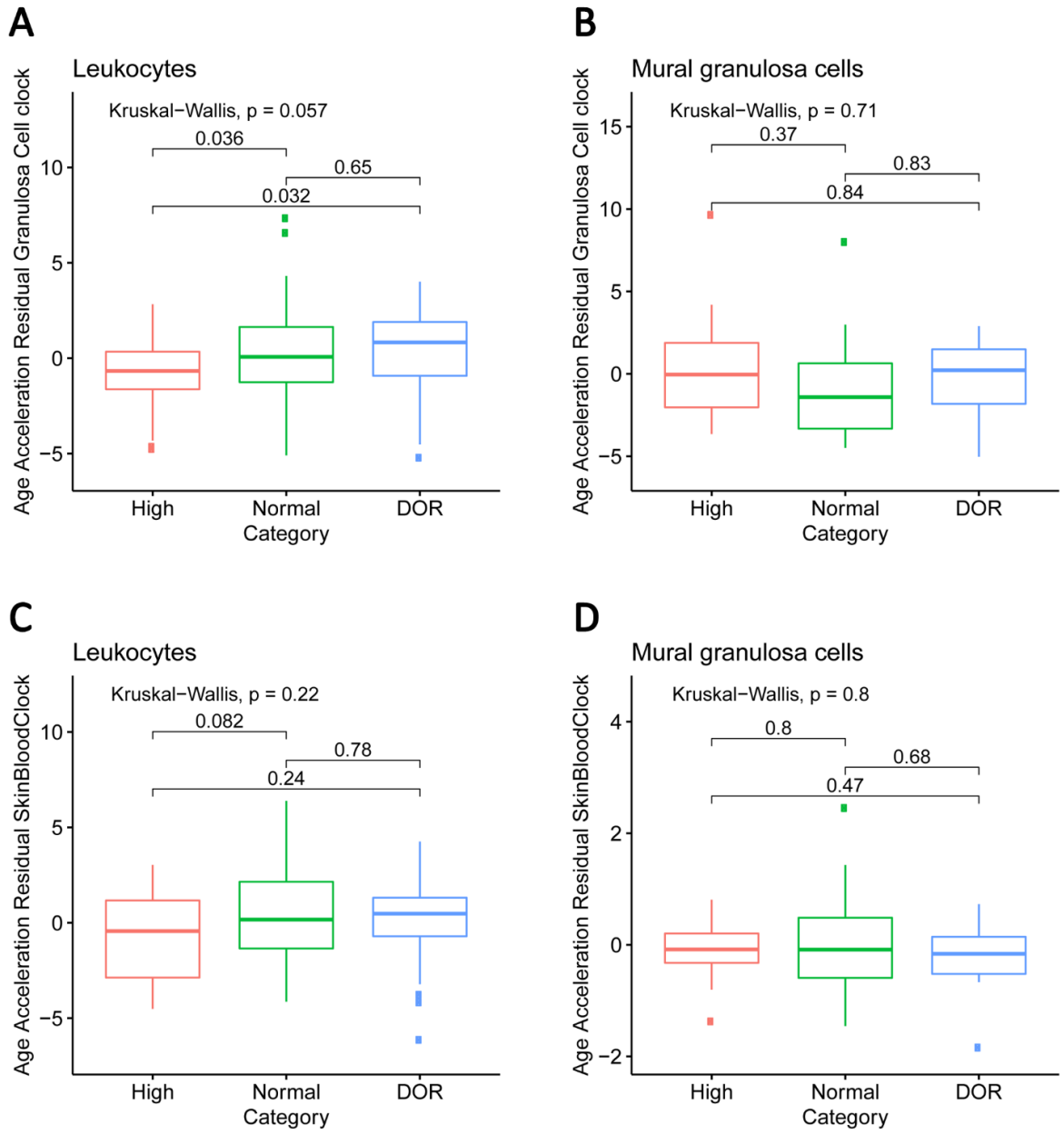

Figure S1. Age acceleration in leukocytes and mural granulosa cells in women with diverse ovarian reserve. Age acceleration in leukocytes (n = 118) and in mural granulosa cells (MGC (n =63)) using the Granulosa cell clock and the Skin & Blood clock (adjusted for age). The women are divided into groups regarding their ovarian reserve status, indicated with colours: red (high), green (normal) and blue (diminished ovarian reserve (DOR)). (**A**) A suggestive trend showing lower age acceleration with high AMH level in leukocytes (Kruskal-Wallis: $p = 0.057$). (**B**) No association between age acceleration and ovarian reserve was found in MGC (Kruskal-Wallis: $p = 0.71$). (**C**) A similar trend is found in the leukocytes using the Skin & Blood clock, however less noticeable (Kruskal-Wallis: $p = 0.22$). (**D**) Again, no association found in the MGC (Kruskal-Wallis: $p = 0.8$).

Figure S2

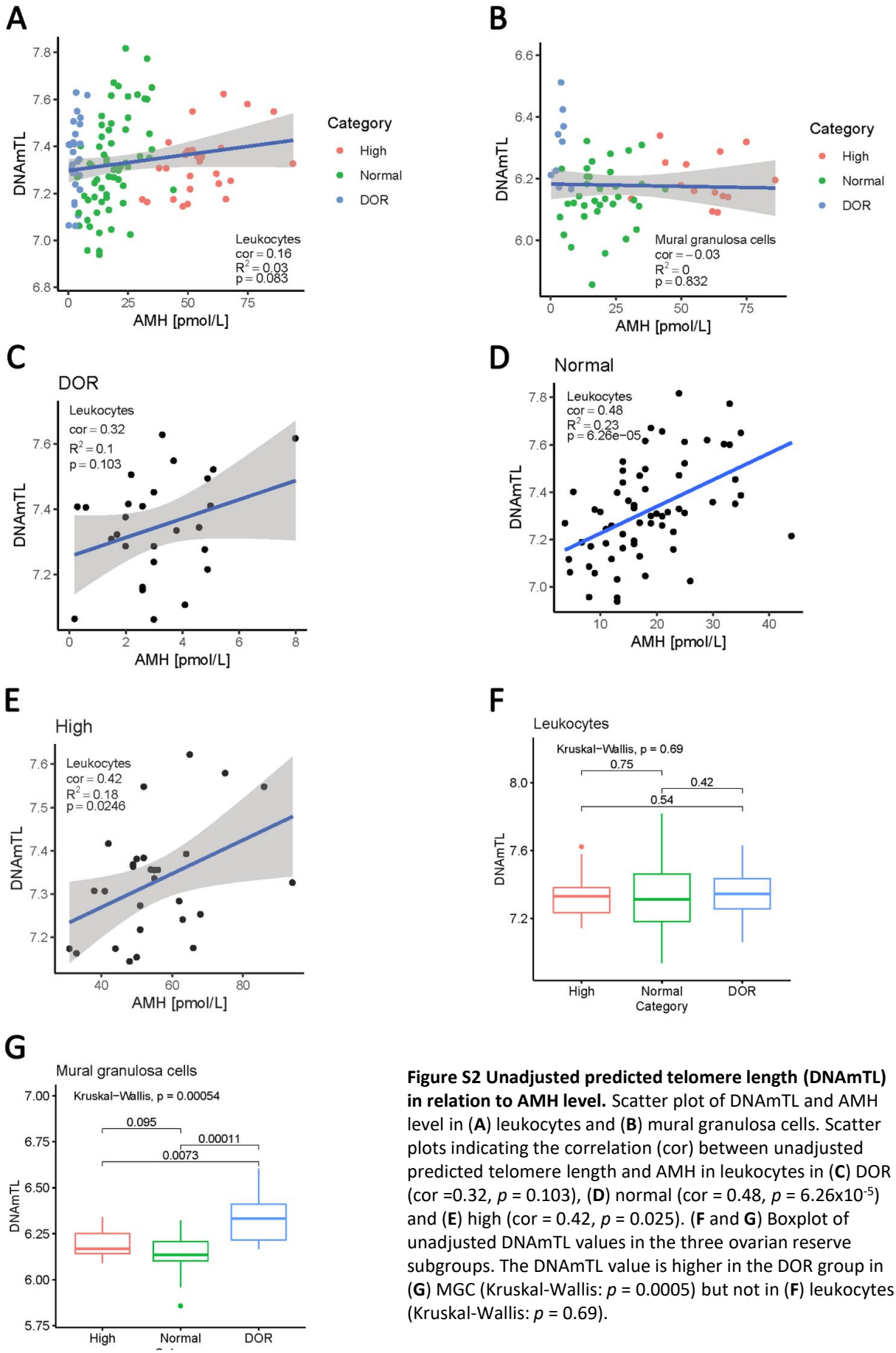

Figure S2 Unadjusted predicted telomere length (DNAmTL) in relation to AMH level. Scatter plot of DNAmTL and AMH level in (**A**) leukocytes and (**B**) mural granulosa cells. Scatter plots indicating the correlation (cor) between unadjusted predicted telomere length and AMH in leukocytes in (**C**) DOR (cor =0.32, p = 0.103), (**D**) normal (cor = 0.48, p = 6.26×10^{-5}) and (**E**) high (cor = 0.42, p = 0.025). (**F** and **G**) Boxplot of unadjusted DNAmTL values in the three ovarian reserve subgroups. The DNAmTL value is higher in the DOR group in (**G**) MGC (Kruskal-Wallis: p = 0.0005) but not in (**F**) leukocytes (Kruskal-Wallis: p = 0.69).

Figure S3

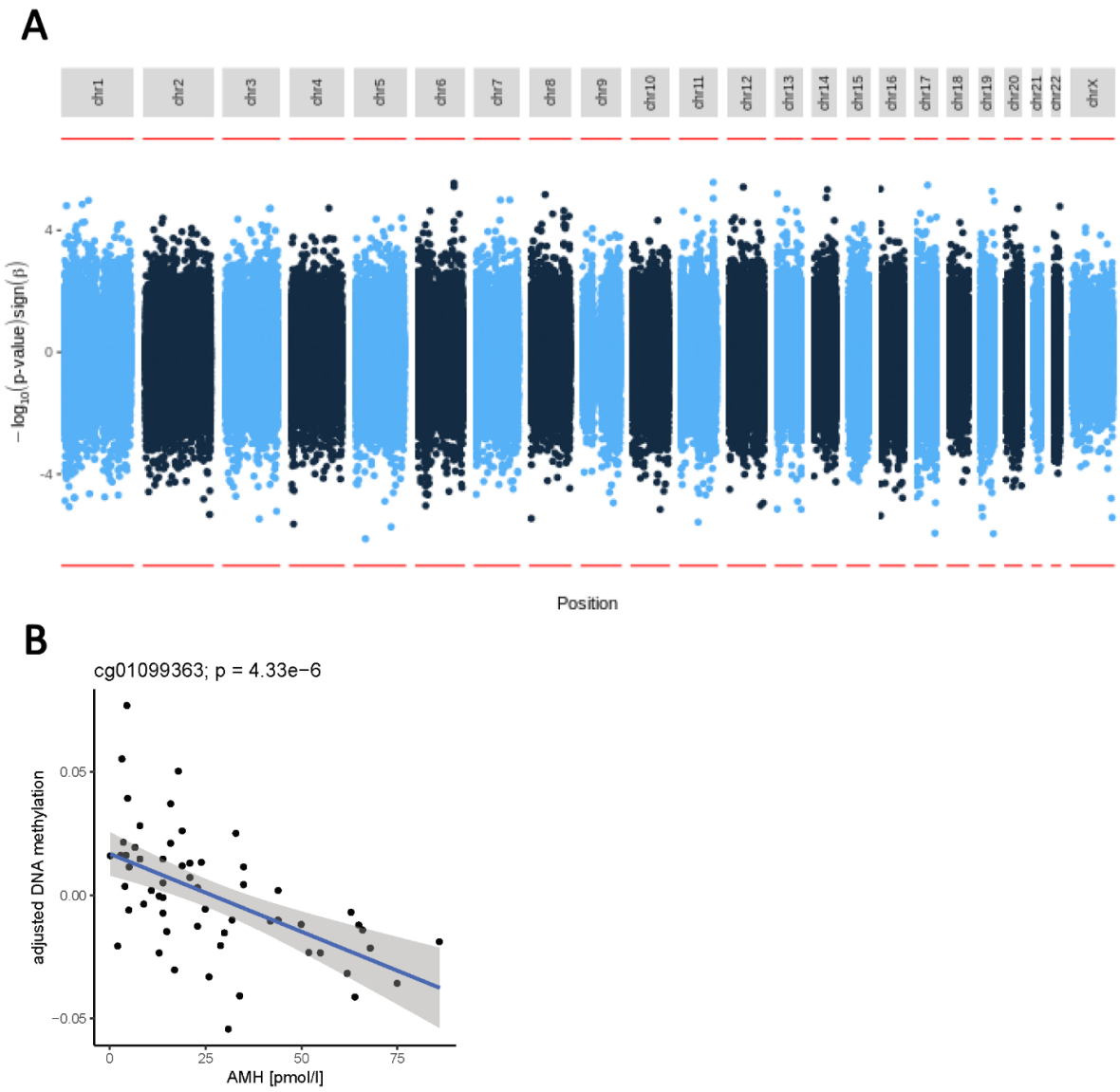

Figure S3 Epigenome-wide association of DNA methylation with AMH levels. (**A**) Manhattan plot showing the absence of genome-wide significant signals at single CpG site resolution in mural granulosa cells in women with different AMH levels. Because of limited sample size, the analysis is underpowered at single CpG resolution. (**B**) Scatter plot of the top CpG hit associated with AMH level.

Paper II

Supplementary tables can be retrieved via this link:

https://figshare.com/s/a25352f38918b55d8ca7

Paper III

Gene expression profile of human metaphase II oocytes
in relation to age by single cell RNA sequencing

Gene expression profile of human metaphase II oocytes in relation to age by single cell RNA sequencing

K. W. Olsen[1,2,*], V. Shukla[2], A. Azad[2], S. O. Skouby[1,3], M. L. Grøndahl[1], E. R. Hoffmann[2], R. Borup[2]

[1]Department of Obstetrics and Gynaecology, Department of Reproductive Medicine, Copenhagen University Hospital Herlev, Denmark. [2]DNRF Center for Chromosome Stability, Department of Cellular and Molecular Medicine, Faculty of Health and Medical Sciences, University of Copenhagen, Copenhagen, Denmark. [3]Department of Clinical Medicine, Faculty of Health and Medical Sciences, University of Copenhagen, Copenhagen, Denmark.
*Corresponding address: kristina.wendelboe.olsen.01@regionh.dk, 0000-0002-3902-200X
Running title: Gene expression profile of ageing oocytes
Disclosure summary: The authors have nothing to disclose

The competence of the human oocyte to establish a pregnancy declines with advanced reproductive age. To investigate the effect of age on gene expression in two age groups of metaphase II (MII) oocytes, we used single cell RNA sequencing. The oocytes used, in this pilot study, were obtained from women undergoing IVF/ICSI treatment from September to November 2016 (eight oocytes from younger (< 35 years) and three oocytes from older (≥ 35 years) women). We identified 315 differentially expressed genes in the MII oocytes between the two age groups. Gene function enrichment analysis showed that genes downregulated in the older MII oocytes (n = 187) mainly were involved in cell cycle, mitotic cell cycle, cell cycle process, microtubule-based process, and mitotic nuclear division, which confirm previous findings. On the other hand, genes upregulated (n = 128) were involved in mitochondrial organization, oxidative phosphorylation, ATP metabolic process and inner mitochondrial membrane organization, which are novel findings in MII oocytes from women with advanced reproductive age. These preliminary results may contribute to increasing the knowledge about the molecular mechanisms involved in ovarian ageing.

Keywords: gene expression; human oocyte; ovarian ageing; RNA sequencing, metaphase II

INTRODUCTION

A woman's reproductive capacity depends on the quantity and quality of the oocytes in the ovary. With increasing age, both the quantity of the ovarian follicles as well as the quality of the oocytes decrease due to follicular atresia and chromosomal aneuploidies, respectively (Vollenhoven and Hunt 2018). Medically assisted reproduction (MAR) has been improved in the last decades; however, it only provides limited help to pregnancy outcomes in women of advances reproductive age (Liu *et al.* 2011; Wennberg *et al.* 2016; Shirasuna and Iwata 2017). Oocyte donations programmes have revealed that recipients with advanced reproductive age have the same pregnancy potential as the young women donating the oocytes (Navot *et al.* 1991) underlining that the age-induced decline in oocyte competence is the main challenge.

The human oocytes are unique cells; during foetal life they are laid down in primordial follicles in the ovary, arrested in prophase of the first meiotic division, and complete meiosis in adulthood, having potentially cell cycles up to 5 decades long. Upon activation, the primordial follicle and the enclosed immature oocyte starts to grow to develop into an

ovulating follicle 6-12 month later, extruding a metaphase II (MII) oocyte, the largest cell of the body. During folliculogenesis and oogenesis, the oocytes stockpile organelles, proteins and mRNA to orchestrate all the events of 1st and 2nd meiotic divisions and early embryonic development until the new genome takes over (Gosden and Lee 2010; Gosden 2002).

Human oocytes are extraordinary error-prone when they divide their chromosomes. DNA replication occurs in oocytes in foetal life followed by the formation of cohesion holding the sister chromatids together (Greaney *et al.* 2018). The chromosome segregation, however, occurs during final oocyte maturation and the cohesion molecules have to be sustained for many decades to avoid errors. The meiosis and oocyte maturation process are complex, and many proteins are involved as topoisomerase II (TOPII), spindle assembly checkpoint (SAC), maturation promoting factor (MPF) (Arroyo *et al.* 2020; Adhikari and Liu 2014; Marston and Wassmann 2017; Li *et al.* 2013).

A depletion of the ovarian follicles during reproductive senescence is occurring with apoptosis of the oocytes and the surrounding follicle cells (Hussein 2005). Mitochondria are essential in cell survival and apoptosis (Tait and Green 2010) and play a central role in this follicular atresia (May-Panloup *et al.* 2016). Mitochondria produce energy by oxidative phosphorylation required for all cellular processes (May-Panloup *et al.* 2016). The mitochondrial DNA (mtDNA) is transmitted to the embryo almost exclusively from the oocyte. Paternal mtDNA will be eliminated and the maternal mitochondrial plays therefore a central role in embryonic development (May-Panloup *et al.* 2016).

Previous studies have shown that age affects the gene expression profile of the oocytes. Grøndahl et al. found changes in the gene expression profile when comparing MII oocytes from young and reproductive elder women (Grøndahl *et al.* 2010). This includes genes involved in the cell cycle signalling pathway, spindle checkpoint regulation, DNA stability, and chromosome segregation (Grøndahl *et al.* 2010). Differences in the single cell gene expression profile of MII oocytes have also been found in women with endometriosis when compared with healthy oocyte donors (Ferrero *et al.* 2019). Differentially expressed mRNAs and non-coding RNAs were found in MII oocytes when comparing oocytes from women with different ages and ovarian reserve (antral follicular count) (Barragan *et al.* 2017), whereas Smits et al. found no difference in the gene expression with increasing reproductive age in germinal vesicle (GV) oocytes (Smits *et al.* 2018). Further studies are needed to elucidate when during the folliculogenesis the difference in competence by increasing women's age is introduced and the mechanisms leading to the increase in aneuploidy by increasing age.

Two newly published studies of transcriptome profiles of single human MII oocytes between two age groups of women showed differences in gene expression between young and older oocytes (Barone *et al.* 2020; Zhang *et al.* 2020). Zhang and co-workers identified *TOP2B* as a key gene affected by advanced age and a knockdown mouse model confirmed that it affects the quality of the oocyte and the early embryo by a developmental arrest in the 2-cell stage with *TOP2B* mRNA levels decreased in the MII mice oocytes (Zhang *et al.* 2020).

Another recent study using single cell RNA sequencing (scRNA-seq) found differences in gene expression in two age groups of GV oocytes from mice (Zhang *et al.* 2019). They found that mitochondrial dysfunction and endoplasmic reticulum stress are likely to be involved in oocyte ageing (Zhang *et al.* 2019).

It is technically challenging to study the gene expression profile in single oocytes, and *in vivo* matured oocytes from women undergoing fertility treatment are a limited resource for both practical and ethical reasons. Therefore, limited knowledge exists about the age-related changes in the gene expression in the *in vivo* matured human oocytes at single cell level. With this study, we investigate the gene expression profile in MII oocytes from healthy women analysed by scRNA-seq. The study aimed to identify and investigate differentially expressed genes in human MII oocytes collected from women of young and advanced reproductive age.

MATERIALS AND METHODS

This study was performed as a collaboration within ReproUnion (www.reprounion.eu), the oocytes collected from the Fertility Clinic at the Copenhagen University Hospital, Herlev, the

sequencing performed at Biotech Research & Innovation Centre (BRIC) at the University of Copenhagen and the scRNA-seq libraries and bioinformatical analysis performed at Center for Chromosome Stability at the University of Copenhagen.

STUDY POPULATION

Eleven women between the age of 26 and 38 years were included in the study. The women were all undergoing *in vitro* fertilization (IVF) or intracytoplasmic sperm injection (ICSI) treatment at the time of the collection of the oocyte. Due to ethical reasons only women with more than eight oocytes retrieved were included in the study.

The study is a prospective cohort study with retrospective analysis. The oocytes were collected from September 2016 to November 2016. Only healthy women treated with gonadotropin-releasing hormone (GnRH) antagonist protocol for the controlled ovarian stimulation were invited to the study. In agreement to participating a consent form was signed after receiving oral and written information and at least 24 hours of considerations.

TREATMENT PROTOCOL

The women were treated according to the clinic's guidelines starting at day two or three of the women's menstrual cycle with recombinant follicle-stimulating hormone (rFSH) for eight to twelve days (six women were treated with Bemfola®; Gedeon Richter, Denmark and four women with Gonal-f®; Merck-Serono, Denmark). One woman was treated with urine derived human menopausal gonadotropin (Menopur®; Ferring Pharmaceuticals, Denmark). In addition, the women were treated with GnRH antagonist (Orgalutran®; MSD, Denmark) and with an ovulation trigger before oocyte retrieval with recombinant human chorionic gonadotropin (rhCG) (Ovitrelle®; Merck-Serono, Denmark).

SAMPLE COLLECTION AND PROCESSING OF HUMAN OOCYTES

The procedures have previously been described in *Protocol Exchange (Olsen et al. 2020)*. Briefly, oocytes were collected immediately after oocyte retrieval. The cumulus cells were removed enzymatically with hyaluronidase (cat. no. 15115001, SynVitro™ Hyadase, Origio, Denmark) and subsequently washed twice in a washing solution (10% phosphate-buffered saline (cat. no. AM9625, Invitrogen™, Thermo Fisher Scientific™, Denmark). The oocytes were then checked for nuclear maturation and morphology, and retrospectively, only MII oocytes were chosen for further scRNA-seq analysis. The zona pellucida was removed with Tyrode's solution (10605000A, Acidified Tyrodes Solution, Origio, Denmark), and the zona-free oocyte washed and transferred with 2 µl washing solution to a 0.2 ml collection tube (cat. no. AB0620, Thermo Fisher Scientific™, USA). Lastly, the tubed oocyte was flash frozen in liquid nitrogen and store at -80 °C until analysis.

cDNA SYNTHESIS

RNA was extracted and cDNA synthesis from eleven MII oocytes was done using SMART-Seq v4 Ultra Low Input RNA Kit (cat. no. 634894, TaKaRa, CA, USA). The oocytes were lysed, and first strand was synthesized with a 3' SMART-Seq CDS Primer II A and SMART-Seq v4 Oligonucleotide. cDNA was amplified with PCR for 15 cycles. AMPure XP beads (cat. no. A63880, Beckman Coulter, IN, USA) were used for the purification of the cDNA. The cDNA was quantified at Qubit High Sensitivity Platform (cat. no. Q33216, Qubit® 3.0 Fluorometer, Thermo Fisher Scientific™, Denmark).

LIBRARY CONSTRUCTIONS

Libraries were generated with 0.2 ng/µl of amplified cDNA using the Nextera XT DNA Library (cat. no. FC-131-1024, Illumina, CA, USA) according to manufactory's protocol. The libraries were purified with AMPure XP beads (cat. no. A63880, Beckman Coulter, IN, USA), quantified by at the Qubit Fluorometer with the high sensitivity assay (cat. no. Q32851, Thermo Fisher Scientific™, Denmark). After a successful qubit measurement, the libraries were quantified with high sensitivity DNA Bioanalyzer (cat. no. 5067-4626, Agilent Technologies, CA, USA) before 1.5 pM of the pooled library were loaded on Illumina NextSeq550 (Illumina, CA, USA) for sequencing to generate 75 base pair reads. The sequencing was performed using a NextSEq550 at the Biotech Research & Innovation Centre (BRIC), University at Copenhagen, Copenhagen, Denmark.

PROCESSING OF SINGLE CELL RNA SEQUENCING DATA

The processing of scRNA-seq data are based on the protocol from Sankar et al. (Sankar *et al.* 2020).

We transformed the per-cycle base call (BCL) file output from the sequencing run of 11 human MII oocytes into per-read FASTQ files using the bcl2fastq2 Conversion Software v2.19 from Illumina. The samples libraries were multiplexed across four sequencing lanes and the FastQ files from each of the four lanes were concatenated to generate one set of paired fastq files per sample.

We performed sample QC and filtering of reads to remove low quality reads, adaptor sequences and low quality bases with trimmomatic version 0.36 (Chen *et al.* 2017) in two steps using ILLUMINACLIP://Trimmomatic-0.36/adapters/NexteraPE-PE.fa:2:30:10 SLIDINGWINDOW:4:20 CROP:72 HEADCROP:10 MINLEN:40 followed by and extra trim of headbases with HEADCROP:10.

Subsequent to filtering, we used the remaining paired reads for alignment by hisat2 (Bolger *et al.* 2014) to the human genome GeneCode v.27 release with the paired GenCode v.27 gtf file containing gene annotations using: $HISAT2 -p 22 --dta -x .gencode.v27 -1 R1.fastq -2 R2.fastq -S sample.sam (Pertea *et al.* 2016). The resulting sam files were sorted, indexed and transformed to bam files using samtools (Li *et al.* 2009). QC measures of aligned reads were generated using picard metrics (https://slowkow.github.io/picardmetrics) and the CollectRnaSeqMetrics tool from picard tools (http://broadinstitute.github.io/picard). We filtered the bam files for mitochondrial reads and Stringtie was applied to merge and assemble reference guided transcripts for gene level quantifications of raw counts, and transcripts per million (TPM) (Pertea *et al.* 2016) of 56,607 reference genes (including 19,722 protein coding, 14,368 lncRNA and 1,877 miRNA).

DOWN-SAMPLING ANALYSIS

Downsamling normalization of scRNA samples to count-depth = 7,690,504 (minimum depth of scRNA seq samples in the project) was performed iteratively on the 11 bam files based on samtools view –s sampling integrated with gene expression summarization using stringtie and parsing of count data and TPM data into annotated expression matrices.

DIFFERENTIAL EXPRESSION ANALYSIS

The 11 samples were grouped according to age with 8 samples < 35 years and 3 samples above 36 years of age. 30,711 (54.25%) of the 56,607 reference genes with null read counts were not included in the analysis, but the features were included in the result files with fold-change and p-values set to NA.

The expression of the 25,896 remaining genes with counts above zero were analyzed using the R software (R Core Team 2016), Bioconductor (Gentleman *et al.* 2004) packages including DESeq2 (Love *et al.* 2014) and the SARTools packages (Varet *et al.* 2016).

Rlog transformation of count data to log2 scale was performed and the differential analyses was carried out according to the DESeq2 dispersion model (Love *et al.* 2014) with a gene being differentially expressed if Benjamini-Hochberg adjusted p-values < 0.05 and FC > 1.5.

PRINCIPAL COMPONENT ANALYSIS AND HIRERARCHICAL CLUSTERING

To assess the heterogeneity of the 315 differentially expressed genes we performed hierarchical clustering and PCA based on the TPM (transcript per million) values of the 11 human MII samples. We applied the prcomp function in the R stats package to perform the PCA analysis and the heatmap.2 function in the gplots package to perform the hierarchical clustering and generate the heatmap of relative gene expression (z-scores) using Euclidean distance and the ward.2D clustering method.

FUNCTIONAL ENRICHMENT

Reactome pathways and gene ontology gene sets of biological function from the Molecular Signatures Database (https://www.gsea-msigdb.org/gsea, Broad Institute, San Diego, CA, USA) were used to test for significantly enriched pathways and biological functions in the 315 differentially expressed genes. Functional enrichments were determined by the one-sided version of Fisher's exact test, p < 0.001 (q-value < 0.05) (Boyle *et al.* 2004), as implemented in ClusterProfiler R package (Yu *et al.* 2012). Integration of fold change difference of genes in selected enriched pathways was performed using the pathview package in R.

ETHICS

In Denmark, the national health programme covers up to three completed ART cycles in the public fertility clinics for infertile women ≤ 41 years. In the study we compensated the donation of an oocyte with an additional treatment cycle if pregnancy was not achieved within the normal offer.

The study was conducted in accordance with the Helsinki Declaration II and approved by the Scientific Ethical Committee of the Capital Region, Denmark (ethical approval number: H-16027088) and the Danish Data Protection Agency (ID-nr.: HGH-2016_086). All participants provided informed consent.

RESULTS

PARTICIPANTS CHARACTERISTICS

A total of 11 MII oocytes were included in this study. Oocytes were only donated from women who had more than eight oocytes retrieved. The participants were divided into two age groups of young reproductive age (26-34 years) and advanced reproductive age (37-38 years). The baseline characteristics of the women are found in Table I. The two age groups were comparable, besides the expected age-related parameters as age, FSH, prolactin and the number of oocytes retrieved.

THE TRANSCRIPTOME OF HUMAN MII OOCYTES

Single-cell RNA sequencing method was performed to analyse the differences in gene expression between MII oocytes from women of young reproductive age (< 35 years) and advanced reproductive age (> 35 years). In total we found 315 genes were differentially expressed in the MII oocytes between the two age groups (Figure 1A, suppl. Table I). Of the 315 genes, 187 genes were downregulated (suppl. Table II), and 128 genes were upregulated (suppl. Table III) in MII oocytes from women of advanced reproductive age compared to oocytes from women of young age.

GENE ONTOLOGY ENRICHMENT ANALYSIS OF DIFFERENTIALLY EXPRESSED GENES

Figure 1A shows a hierarchical cluster of the 315 differentially expressed genes within the two age groups, downregulated differentially expressed genes are blue and upregulated genes are red. The PCA plot of the differentially expressed genes (Figure 1B) displays the greatest variance of the samples (56.6%) on the x-axis, while the variance between samples only counts for 9.2% at the y-axis. The 187 differentially expressed genes which are downregulated in women with advanced reproductive age, are among others associated with cell cycle, mitotic cell cycle, cell cycle process, microtubule-based process and mitotic nuclear division (Figure 2, Figure 3, Table II + III and suppl. Table IV + V). The 128 differentially expressed genes that were upregulated in the older MII oocytes were on the other hand associated with mitochondrial organization, oxidative phosphorylation, ATP metabolic process and inner mitochondrial membrane organization (Figure 2, Figure 3, Table II + III and suppl. Table IV + V).

Figure 4 shows the functional group network of the GO analysis, with the size of the cycle correlating with the number of genes. This show a significant number of the differentially expressed genes being involved in oxidative phosphorylation and inner mitochondrial membrane organisation (Table II and suppl. Table IV).

PATHWAY ANALYSIS WITH GENES INVOLVED IN OXIDATIV PHOSPHORYLATION AND CELL CYCLE

The oxidative phosphorylation is the most significant pathway with differentially expressed genes upregulated in MII oocytes from women with advanced reproductive age. A Kyoto Encyclopedia of Genes and Genomes (KEGG) analysis of the differentially expressed genes are shown in Figure 5. Genes marked in red are upregulated in MII oocytes from women with advanced reproductive age. This include genes coding for the subunits of complex I, IV and V in the mitochondrial respiratory chain.

The most significant pathway of differentially expressed genes downregulated in the older MII oocytes are cell cycle (Figure 6, suppl. Table II). The differentially expressed genes marked with green are downregulated and one differentially gene (*CDC25B/C*) are upregulated. Gene affected are e.g. *MAD2*, *Cyclin A/B* and *PCNA.*

DISCUSSION

The underlying mechanisms of oocyte quality reduction due to ovarian ageing are still not well understood. Our preliminary results revealed at single cell level that gene expression profiling of MII

oocytes differs between young and advanced reproductive age. Genes involved in oxidative phosphorylation, mitochondrial processes, and generation of metabolites were found to be upregulated in MII oocytes from women of advanced reproductive age, while genes involved in cell cycle, mitosis, and microtubules organization were less expressed in these women compared to the oocytes from women of young age.

Even though, the age difference between the young and older MII oocytes was less than ten years we observed a strong difference in the hierarchical cluster of the differentially expressed genes between the two groups, indicating that major changes in the gene expression are occurring in the mid-thirties. This might reflect the drastic decrease in the oocyte quality found in women from the mid of their late thirties (Gruhn *et al.* 2019; Hassold and Hunt 2001). The differentially expressed genes downregulated are involved in processes of cell cycles (e.g. *CDC20*, *MAD2L1*, *CCNB1*), mitotic nuclear division (e.g. *CHEK1*) and chromosome segregation (e.g. *CDC20*, *CENPH*, *KIF4A*). We found a functional overlap, but no gene overlap, with a previous study using microarray (Grøndahl *et al.* 2010). However, both the present data and the data from the microarray reveal functional impacts that may explain why oocytes from women of advanced reproductive age have a higher number of aneuploidies and thereby a decreased quality. The cellular processes involved in meiotic cell division and chromosomes segregation are not optimal in the older oocytes. This difference was not previously found in GV oocytes obtained after oocyte retrieval (Smits *et al.* 2018), which could suggest that the age-related decline in oocyte quality are occurring during oocyte maturation and meiosis. However, it might seem unlikely that all transcriptional alterations in the older MII oocytes are occurring during the final maturation process. More research is therefore needed to investigate these theories.

Downregulation of *CDC20* in MII oocytes from women of advanced reproductive age is consistent with findings in mice, as mice with low *CDC20* expression had a high frequency of chromosome segregation errors resulting in aneuploidies (Jin *et al.* 2010). Likewise, loss of KIF4A is associated with age-related aneuploidies in mice due to spindle defects and chromosome misalignments (Tang *et al.* 2018). The *CHEK1* gene codes for the important CHEK1 protein involved in S and G2 phase of cell cycle checkpoints. Inhibition of CHEK1 increases replication stress and DNA damage and can ultimately lead to cell death (Oo *et al.* 2018). The downregulation of *CHEK1* in the older MII oocytes may affect the oocytes from women of advanced reproductive age resulting in a poor ovarian reserve and quality of the oocytes.

The differentially expressed genes upregulated in the MII oocytes from women of advanced reproductive age are involved in mitochondrial processes (e.g. *TIMM10*, *NDUFB3*), oxidative phosphorylation (e.g. *NDUFS5*, *NDUFA3*) and energy production (e.g. *ATP5H*). Mitochondria generate ATP through oxidative phosphorylation and are present in a high number in the oocytes to overcome the high demand of energy at the beginning of embryonic development (Dumollard *et al.* 2007). Previous studies have shown that mitochondrial dysfunction is associated with ovarian ageing (Bentov *et al.* 2011), why we therefore speculate that the upregulation of genes involved in the mitochondrial energy production is a manifest of how the oocytes compensate for the decline in the oocyte quality occurring with advanced reproductive age. In contrast, Zhang et *al.* found that genes involved in mitochondrial function including oxidative phosphorylation and ATP production pathway were significantly downregulated in GV oocytes of 32-week-old mice compared to 5-week-old mice (Zhang *et al.* 2019). However, it may reflect the difference in both species and oocyte maturity, since the MII oocytes we included originated from antral follicles that managed to respond to the FSH and LH signal and develop into mature ovulating follicles.

All participating women had more than eight oocytes retrieved, which indicates that they have a high quantity of follicles in their ovaries, despite some were of advanced reproductive age. The gene expression differences found in the MII oocytes are therefore likely to reflect the differences in the quality of the oocytes. Unfortunately, we have a very small sample size, but recent studies from Barone et al. and Zhang et al. are consistent with our findings (Barone *et al.* 2020; Zhang *et al.* 2020). They also suggest that the differences in gene expression are higher with age above 40 years (Zhang *et al.* 2020).

CONCLUSION

In this small pilot study, we found a significant difference in the gene expression profile of MII oocytes from women with advanced reproductive age compared to women of young reproductive age. We found 315 differentially expressed genes, that were either down- or upregulated in MII oocytes from women of advanced reproductive age. The differentially expressed genes were found to be involved in mitochondria function, oxidative phosphorylation, cell cycle, and mitosis.

FUTURE PERSPECTIVES

This study showed that the gene expression of genes involved in cell cycle and energy production are affected by women's age. Future studies with a larger number of oocytes and a broader age-range are needed to confirm our findings. Furthermore, a proof-of-concept study could be performed by inhibiting specific proteins that potential could result in chromosome errors to more precisely find therapeutic targets to improve the chromosome quality in women with advanced reproductive age. By identifying mechanisms that can affect the human oocytes directly, it may become possible to improve the genetic quality of oocytes and their resulting embryos.

AUTHOR'S ROLE

KWO, MLG, RB, and ERH designed at initiated the study. KWO were involved in patient recruitment and sample collection. VS generated the mRNA libraries. RB and AA developed the bioinformatic pipeline. KWO, MLG, ERH, and RB were involved in the analysis and interpretation of data. KWO wrote the manuscript and prepared table I. RB prepared the figures, the tables, and contributed to the writing of the manuscript. MLG, ERH supervised the project. VS, RB, MLG, and ERH participated in finalizing the manuscript. All authors reviewed the manuscript and accepted the final version.

DATA AND CODE AVAILABILITY

Scripts used for processing and analysis of the scRNA-seq data are shared on reasonable request to the corresponding author.

ACKNOWLEDGEMENT

We want to thank all the women, who were willing to donate one oocyte to research during the sensitive time of fertility treatment. We also want to thank all the staff at Herlev Hospital, who were involved in the patient recruitment and material sampling.

FUNDING

The project was funded by the ReproUnion, supported by the Interreg program for Øresund-Kattegat-Skagerak by EU funds, Capital region of Denmark, Region Zealand, Region Skåne and Ferring Pharmaceutical Company. Furthermore, the project was supported financially by the Department of Gynaecology-Obstetrics at Herlev-Gentofte Hospital, Denmark and the Danish National Research Foundation (DNRF). Center for Chromosome Stability (DNRF115). The study was also supported by the European Research Council (ERC grant 724718-ReCAP) and by the Novo Nordisk Foundation Young Investigator Award (NNF15OC0016662).

CONFLICT OF INTEREST

The authors have nothing to disclose.

REFERENCES

Adhikari D and Liu K. The regulation of maturation promoting factor during prophase I arrest and meiotic entry in mammalian oocytes. *Mol Cell Endocrinol* 2014; **1**: 480-487.

Arroyo A, Kim B, and Yeh J. Luteinizing Hormone Action in Human Oocyte Maturation and Quality: Signaling Pathways, Regulation, and Clinical Impact. *Reprod Sci* 2020.

Barone S, Sarogni P, Valli R, Pallotta MM, Silvia G, Frattini A, Khan AW, Rapalini E, Parri C, and Musio A. Chromosome Missegregation in Single Human Oocytes Is Related to the Age and Gene Expression Profile. *Int J Mol Sci* 2020; **6**.

Barragan M, Pons J, Ferrer-Vaquer A, Cornet-Bartolome D, Schweitzer A, Hubbard J, Auer H, Rodolosse A, and Vassena R. The transcriptome of human oocytes is related to age and ovarian reserve. *Mol Hum Reprod* 2017; **8**: 535-548.

Bentov Y, Yavorska T, Esfandiari N, Jurisicova A, and Casper RF. The contribution of mitochondrial

function to reproductive aging. *J Assist Reprod Genet* 2011; **9**: 773-783.

Bolger AM, Lohse M, and Usadel B. Trimmomatic: a flexible trimmer for Illumina sequence data. *Bioinformatics* 2014; **15**: 2114-2120.

Boyle EI, Weng S, Gollub J, Jin H, Botstein D, Cherry JM, and Sherlock G. GO::TermFinder--open source software for accessing Gene Ontology information and finding significantly enriched Gene Ontology terms associated with a list of genes. *Bioinformatics* 2004; **18**: 3710-3715.

Chen S, Huang T, Zhou Y, Han Y, Xu M, and Gu J. AfterQC: automatic filtering, trimming, error removing and quality control for fastq data. *BMC Bioinformatics* 2017; **Suppl 3**: 80.

Dumollard R, Ward Z, Carroll J, and Duchen MR. Regulation of Redox Metabolism in the Mouse Oocyte and Embryo. *Development* 2007; **3**: 455-465.

Ferrero H, Corachan A, Aguilar A, Quinonero A, Carbajo-Garcia MC, Alama P, Tejera A, Taboas E, Munoz E, Pellicer A*, et al.* Single-cell RNA sequencing of oocytes from ovarian endometriosis patients reveals a differential transcriptomic profile associated with lower quality. *Hum Reprod* 2019; **7**: 1302-1312.

Gentleman RC, Carey VJ, Bates DM, Bolstad B, Dettling M, Dudoit S, Ellis B, Gautier L, Ge Y, Gentry J*, et al.* Bioconductor: open software development for computational biology and bioinformatics. *Genome Biology* 2004; **10**: R80.

Gosden R and Lee B. Portrait of an oocyte: our obscure origin. *J Clin Invest* 2010; **4**: 973-983.

Gosden RG. Oogenesis as a foundation for embryogenesis. *Mol Cell Endocrinol* 2002; **2**: 149-153.

Greaney J, Wei Z, and Homer H. Regulation of chromosome segregation in oocytes and the cellular basis for female meiotic errors. *Hum Reprod Update* 2018; **2**: 135-161.

Gruhn JR, Zielinska AP, Shukla V, Blanshard R, Capalbo A, Cimadomo D, Nikiforov D, Chan ACH, Newnham LJ, Vogel I*, et al.* Chromosome errors in human eggs shape natural fertility over reproductive life span. *Science* 2019; **6460**: 1466-1469.

Grøndahl ML, Yding Andersen C, Bogstad J, Nielsen FC, Meinertz H, and Borup R. Gene expression profiles of single human mature oocytes in relation to age. *Hum Reprod* 2010; **4**: 957-968.

Hassold T and Hunt P. To err (meiotically) is human: the genesis of human aneuploidy. *Nature reviews. Genetics* 2001; **4**: 280-291.

Hussein MR. Apoptosis in the Ovary: Molecular Mechanisms. *Hum Reprod Update* 2005; **2**: 162-177.

Jin F, Hamada M, Malureanu L, Jeganathan KB, Zhou W, Morbeck DE, and van Deursen JM. Cdc20 is critical for meiosis I and fertility of female mice. *PLoS Genet* 2010; **9**: e1001147.

Li H, Handsaker B, Wysoker A, Fennell T, Ruan J, Homer N, Marth G, Abecasis G, Durbin R, and Genome Project Data Processing S. The Sequence Alignment/Map format and SAMtools. *Bioinformatics* 2009; **16**: 2078-2079.

Li XM, Yu C, Wang ZW, Zhang YL, Liu XM, Zhou D, Sun QY, and Fan HY. DNA topoisomerase II is dispensable for oocyte meiotic resumption but is essential for meiotic chromosome condensation and separation in mice. *Biol Reprod* 2013; **5**: 118.

Liu K, Case A, Cheung AP, Sierra S, AlAsiri S, Carranza-Mamane B, Case A, Dwyer C, Graham J, Havelock J*, et al.* Advanced Reproductive Age and Fertility. *J Obstet Gynaecol Can* 2011; **11**: 1165-1175.

Love MI, Huber W, and Anders S. Moderated estimation of fold change and dispersion for RNA-seq data with DESeq2. *Genome Biol* 2014; **12**: 550.

Marston AL and Wassmann K. Multiple Duties for Spindle Assembly Checkpoint Kinases in Meiosis. *Front Cell Dev Biol* 2017: 109.

May-Panloup P, Boucret L, Chao de la Barca JM, Desquiret-Dumas V, Ferre-L'Hotellier V, Moriniere C, Descamps P, Procaccio V, and Reynier P. Ovarian ageing: the role of mitochondria in oocytes and follicles. *Hum Reprod Update* 2016; **6**: 725-743.

Navot D, Bergh RA, Williams MA, Garrisi GJ, Guzman I, Sandler B, and Grunfeld L. Poor oocyte quality rather than implantation failure as a cause of age-related decline in female fertility. *The Lancet* 1991; **8754**: 1375-1377.

Olsen KW, Gruhn J, Hoffmann ER, and Grøndahl ML. Processing of human IVF/IVM oocytes for single cell RNA sequencing *Protocol Exchange* 2020.

Oo ZY, Stevenson AJ, Proctor M, Daignault SM, Walpole S, Lanagan C, Chen J, Skalamera D, Spoerri L, Ainger SA*, et al.* Endogenous

Replication Stress Marks Melanomas Sensitive to CHEK1 Inhibitors In Vivo. *Clin Cancer Res* 2018; **12**: 2901-2912.

Pertea M, Kim D, Pertea GM, Leek JT, and Salzberg SL. Transcript-level expression analysis of RNA-seq experiments with HISAT, StringTie and Ballgown. *Nat Protoc* 2016; **9**: 1650-1667.

R Core Team. A Language and Environment for Statistical Computing 2016.

Sankar A, Johansen JV, and Borup R. Single oocyte/embryo RNASeq data processing. *Protocol Exchange* 2020; **version 2**.

Shirasuna K and Iwata H. Effect of aging on the female reproductive function. *Contracept Reprod Med* 2017: 23.

Smits MAJ, Wong KM, Mantikou E, Korver CM, Jongejan A, Breit TM, Goddijn M, Mastenbroek S, and Repping S. Age-related gene expression profiles of immature human oocytes. *Mol Hum Reprod* 2018; **10**: 469-477.

Tait SWG and Green DR. Mitochondria and Cell Death: Outer Membrane Permeabilization and Beyond. *Nat Rev Mol Cell Biol* 2010; **9**: 621–632.

Tang F, Pan MH, Lu Y, Wan X, Zhang Y, and Sun SC. Involvement of Kif4a in Spindle Formation and Chromosome Segregation in Mouse Oocytes. *Aging Dis* 2018; **4**: 623-633.

Varet H, Brillet-Gueguen L, Coppee JY, and Dillies MA. SARTools: A DESeq2- and EdgeR-Based R Pipeline for Comprehensive Differential Analysis of RNA-Seq Data. *PLOS ONE* 2016; **6**: e0157022.

Vollenhoven B and Hunt S. Ovarian ageing and the impact on female fertility. *F1000Res* 2018.

Wennberg AL, Opdahl S, Bergh C, Aaris Henningsen AK, Gissler M, Romundstad LB, Pinborg A, Tiitinen A, Skjaerven R, and Wennerholm UB. Effect of maternal age on maternal and neonatal outcomes after assisted reproductive technology. *Fertil Steril* 2016; **5**: 1142-1149 e1114.

Yu G, Wang LG, Han Y, and He QY. clusterProfiler: an R package for comparing biological themes among gene clusters. *OMICS* 2012; **5**: 284-287.

Zhang JJ, Liu X, Chen L, Zhang S, Zhang X, Hao C, and Miao YL. Advanced maternal age alters expression of maternal effect genes that are essential for human oocyte quality. *Aging* 2020; **4**: 3950-3961.

Zhang T, Xi Q, Wang D, Li J, Wang M, Li D, Zhu L, and Jin L. Mitochondrial dysfunction and endoplasmic reticulum stress involved in oocyte aging: an analysis using single-cell RNA-sequencing of mouse oocytes. *J Ovarian Res* 2019; **1**: 53.

Table I Demographic and clinical characteristics of the study population.

	Young reproductive age	Advanced reproductive age	All	One-way ANOVA
Number	8	3	11	-
Age at oocyte retrieval (years)	30.1 ± 3.3	37.7 ± 0.6	32.2 ± 4.5	0.0039
BMI (kg/m^2)	23.0 ± 3.4	26.5 ± 0.7	23.8 ± 3.4	0.218
Primary cause of infertility				
- Female factor	1	-	1	-
- Male factor	2	-	2	-
- Unexplained	5	1	6	-
- Other causes*	-	2	2	-
AMH[1] (pmol/L)	25.5 ± 7.6	17 ± 6.9	23.2 ± 8.1	0.1257
FSH (IU/L)	4.8 ± 1.3	6.8 ± 1.7	5.3 ± 1.6	0.0743
LH[2] (IU/L)	5.5 ± 3.0	4.8 ± 0.6	5.3 ± 2.6	0.74
FSH/LH ratio	0.8 ± 0.7	0.8 ± 0.1	0.8 ± 0.6	0.2058
Prolactin (IU/L)	371 ± 157	148 ± 58.6	310 ± 170	0.046
TSH[3] (IU/L)	2.0 ± 0.7	1.6 ± 0.6	1.9 ± 0.6	0.3809
Stimulation drug				
- Gonal-f®	2	2	4	-
- Bemfola®	5	1	6	-
- Menopur®	1	-	1	-
FSH dose (IU)	1434 ± 303	2025 ± 1120	1595 ± 626	0.1742
Stimulation duration (days)	9.1 ± 1.0	8.7 ± 2.1	9.0 ± 1.3	0.6188
No. of oocytes	14 ± 2.7	9.7 ± 1.2	12.8 ± 3.1	0.0289
Utilization rate	0.6 ± 0.2	0.4	0.5 ± 0.2	0.547

Mean ± standard deviation.

*Single women and women with a female partner.

[1] Anti-Müllerian hormone

[2] Luteinizing hormone

[3] Thyroid stimulating hormone

Figure 1

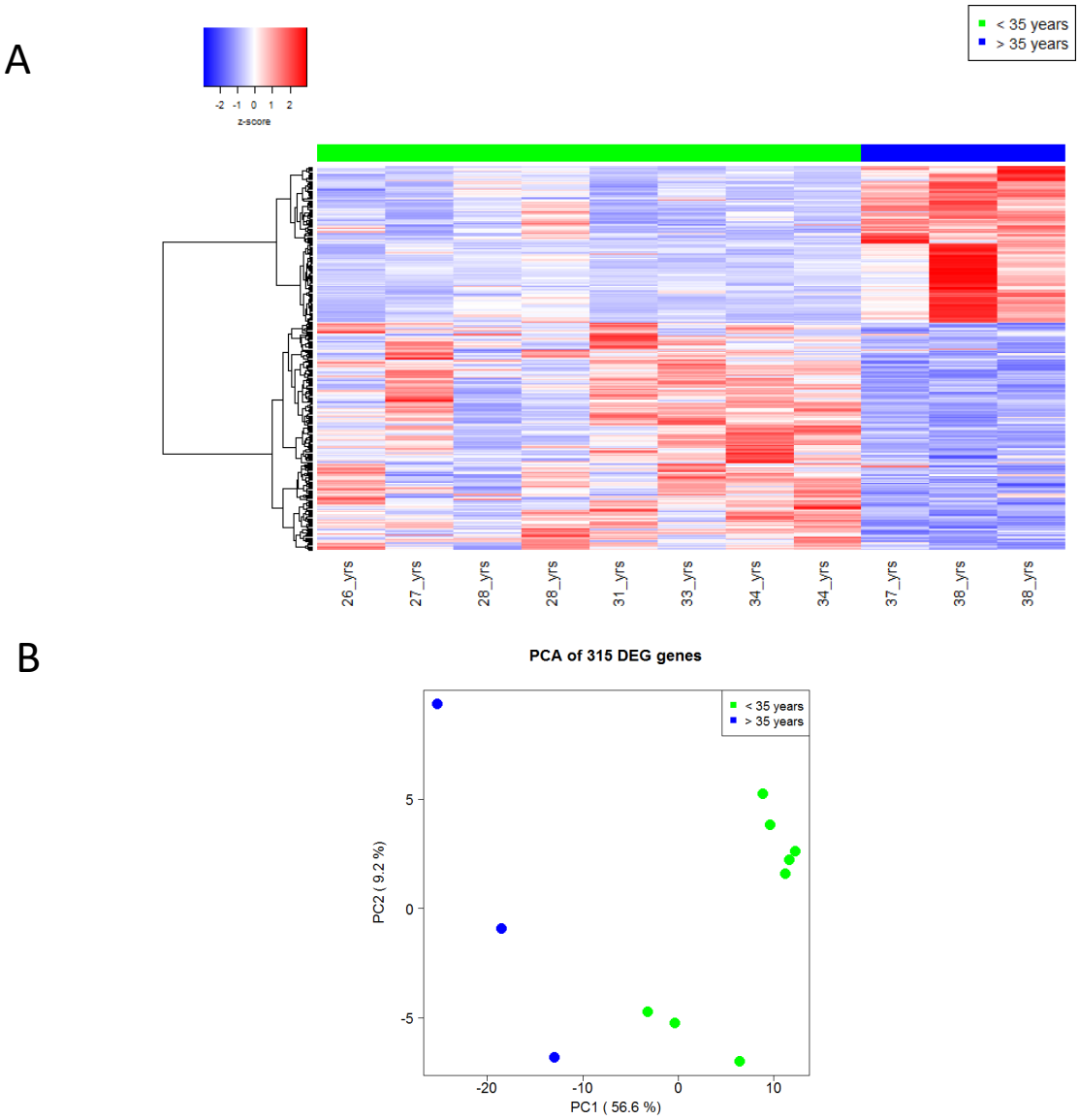

Figure 1 Hierarchical cluster of 315 differentially expressed genes (DEGs) and principal component analysis (PCA-plot) of young (26-34 years, n = 8) and older (37-38 years, n = 3) metaphase II (MII) oocytes. (**A**) Hierarchical cluster of DEGs using Euclidean distance and ward.D2 as clustering method. The colour represent the standardized mean gene expression level (Z-score) of 11 metaphase II (MII) oocytes from women of young (green) and advanced (blue) maternal age. The z-score represents standard deviations from the mean (white) from downregulation (blue) to upregulation (red).
The upper colour bar represent the 11 samples (columns) and the left panel show the hierarchical cluster of the 315 differentially expressed genes (rows) between the young (< 35 years) and advanced (> 36 years) maternal age group (BH adjusted *p*-value < 0.05). The heatmap shows genes that are upregulated in women with advanced maternal age in red (Z-score > 0) and genes down regulated are represented in blue (Z-score < 0). (**B**) PCA-plot of DEGs. PCA-plot displays summarised data of 315 DEGs in 11 metaphase II (MII) oocytes samples. Women of young maternal age are represented in green and women of advanced maternal age are represented in blue. In general, variances between the two age groups on the x-axis (principal component 1, PC1) separated the data the most (56.6%). Variances on y-axis were lower with 9.2% (principal component 2, PC2).

Figure 2

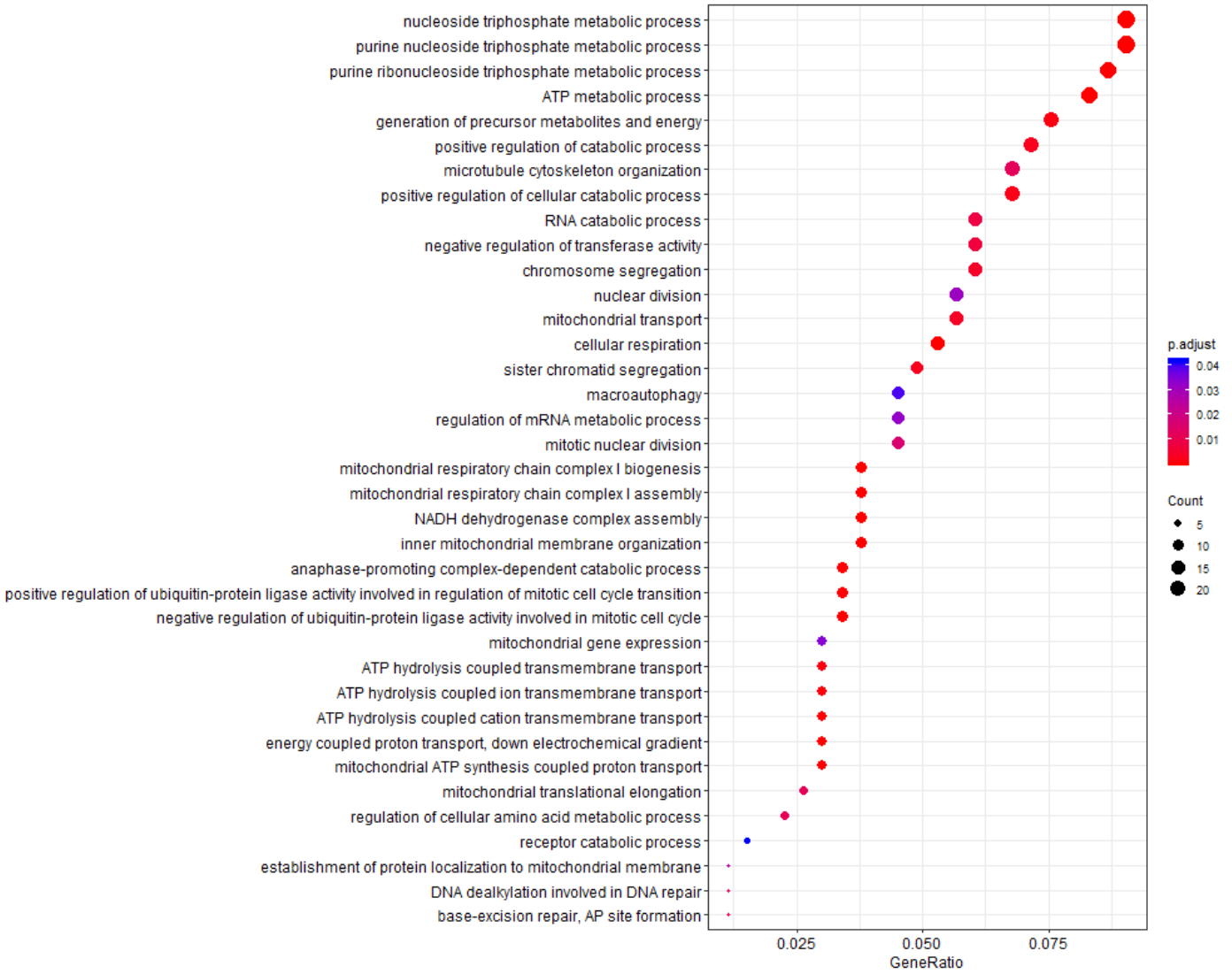

Figure 2 Pathway enrichment analysis of 315 differential expressed genes. Kyoto Encyclopedia of Genes and Genomes (KEGG) analysis of the differential expressed genes between young and older MII oocytes. KEGG enrichment analysis carried out by overrepresentation analysis based on the hypergeometric distribution (one-sided Fisher's exact test). The vertical axis is the pathways and the horizontal axis is the gene ratio. GeneRatio: the ratio of differentially expressed genes to the all genes that were annotated in the pathway. The size of balls represents gene numbers and colour represents adjusted *p*-value.

Figure 3

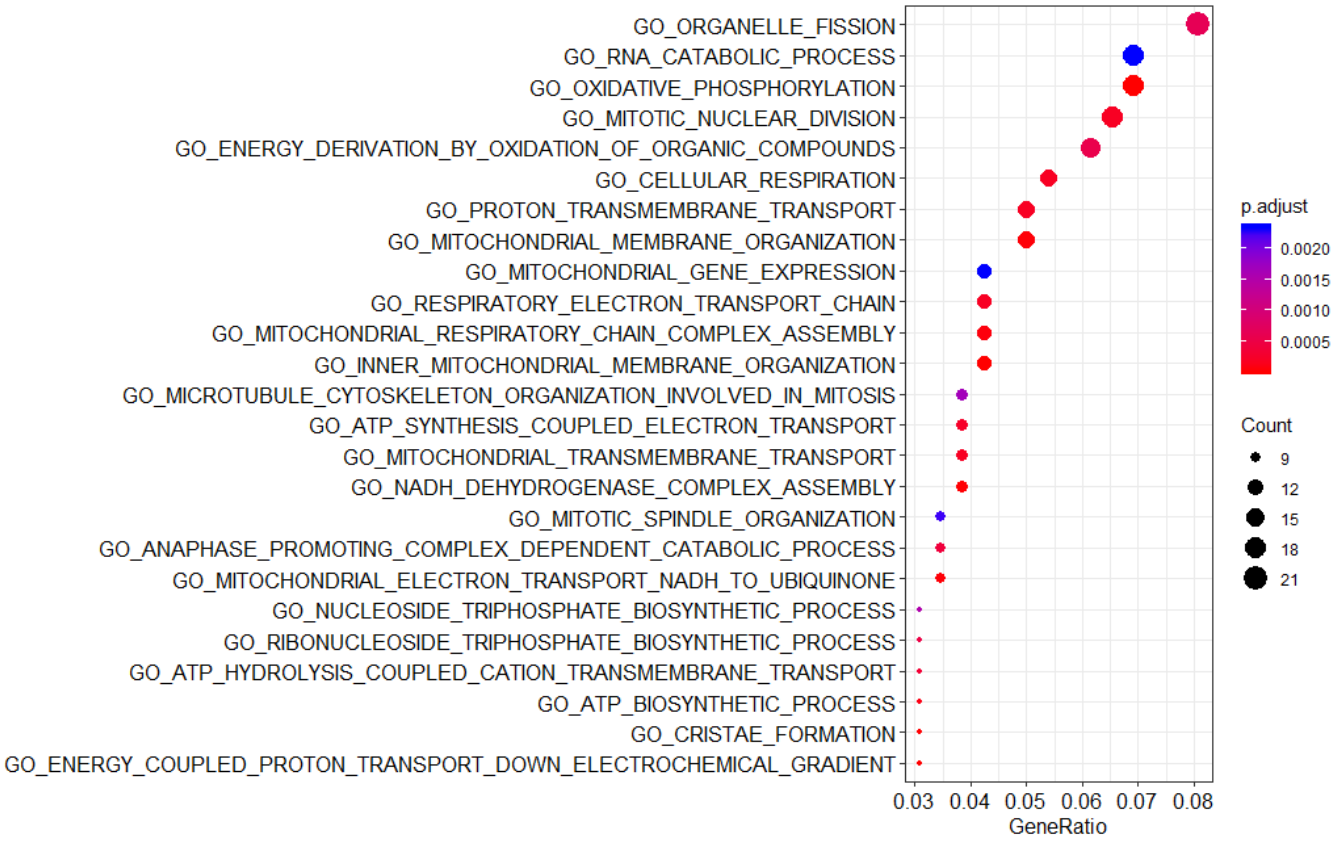

Figure 3 Gene Ontology (GO) of biological processes with differential expressed genes (collapsed terms). The 25 most significant GO terms extracted by GO enrichment analysis and KEGG enrichment analysis carried out by overrepresentation analysis based on the hypergeometric distribution (one-sided Fisher's exact test).The vertical axis is the GO terms and the horizontal axis is the gene ratio. GeneRatio: the ratio of differentially expressed genes to the all genes that were annotated in the pathway. The size of balls represents gene numbers and colour represents adjusted *p*-value.

Figure 4

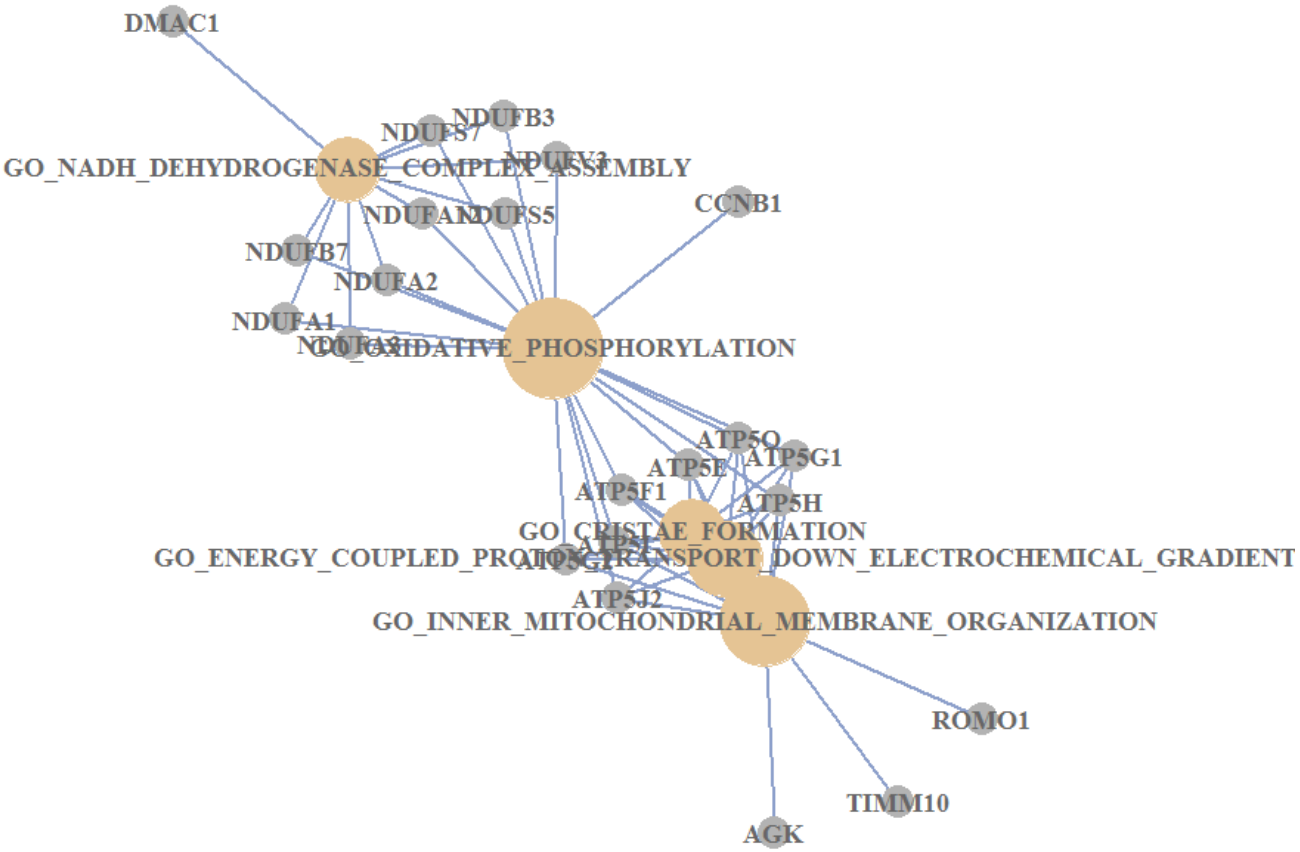

Figure 4 Functionally grouped network of gene ontology (GO) enrichment analysis of differential expressed genes. Functional enrichment analysis was performed for all DEGs. The plot show the enrichment map network of the organized enriched terms based on the output from overrepresentation analysis (one-sided Fisher's exact test). The differential expressed gene were enriched in e.g. oxidative phosphorylation, mitochondrial membrane organisation and NADH dehydrogenase complex assembly. The size of each circle is correlated to the number of genes. The colours of the circle represent the biological function (yellow) and the involved genes (grey). The blue lines represent the functional network.

Figure 5

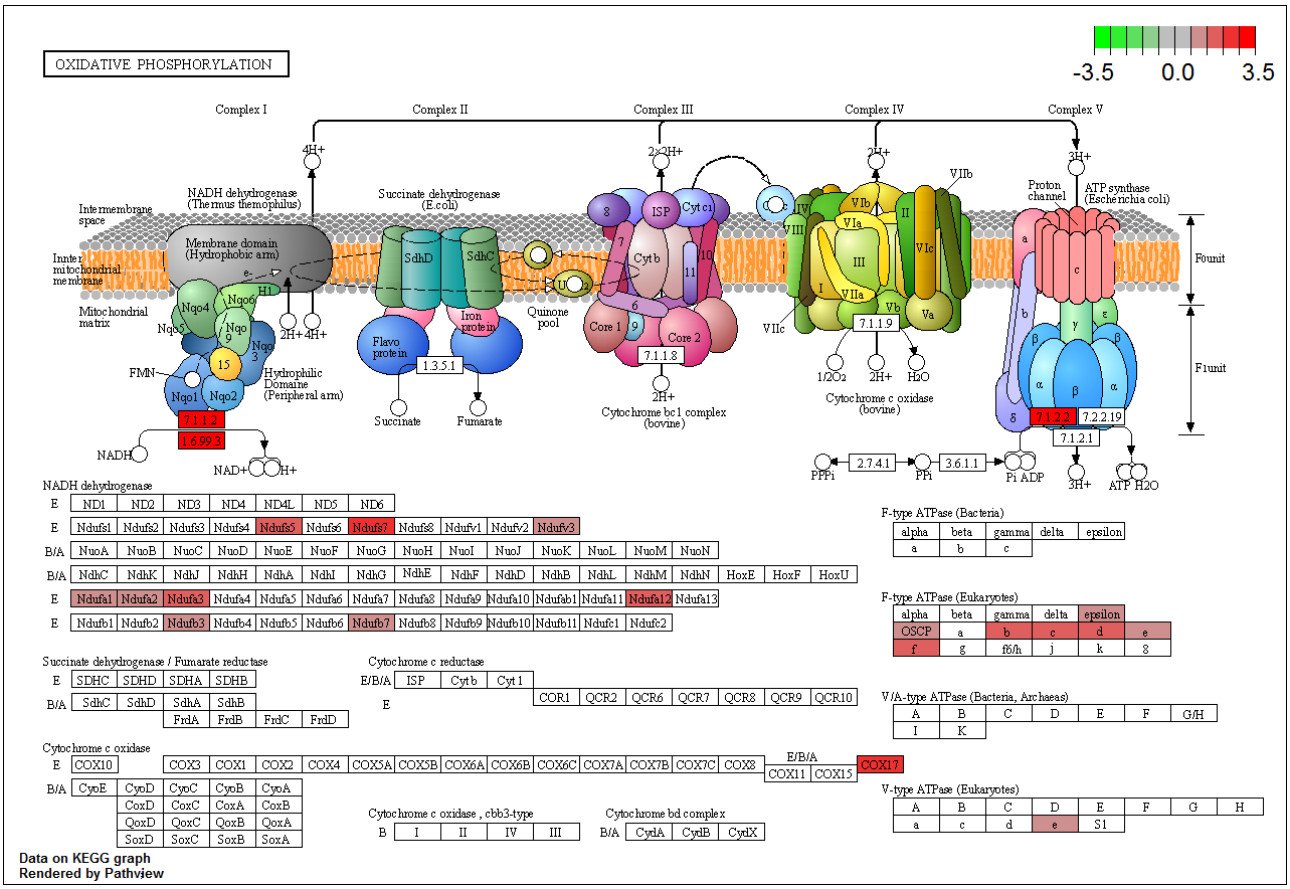

Figure 6 KEGG pathways analysis with differential expressed genes upregulated in metaphase (MII) oocytes from women of advanced maternal age. The upper part of the figure shows the respiratory chain complexes of oxidative phosphorylation pathway and the lower portion represents the genes as rectangles. The genes in red are upregulated in MII oocytes from women of advanced maternal age. The colour intensities represent how much they are upregulated compared to the MII oocytes from women of young maternal age.

Figure 6

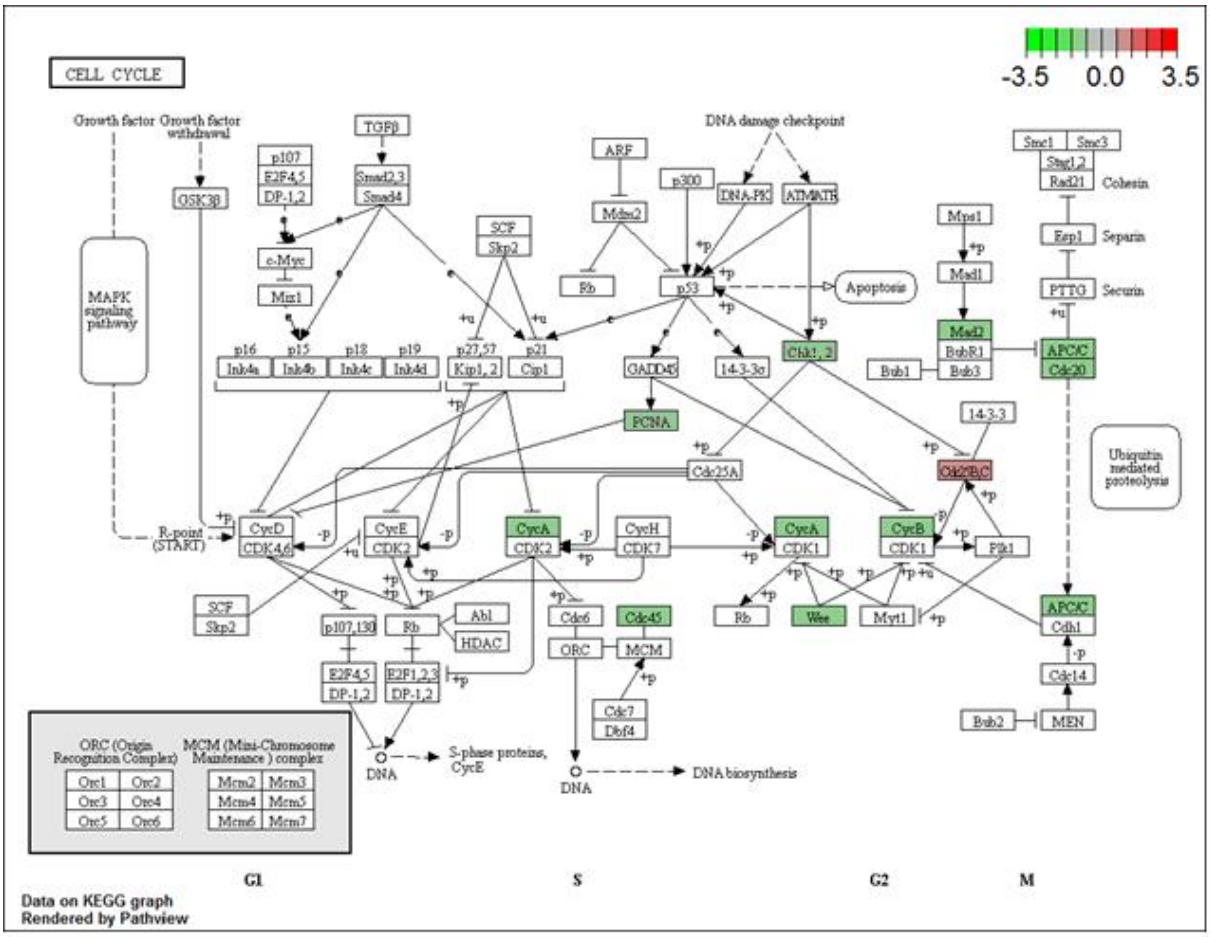

Figure 7 KEGG pathways analysis with differential expressed genes involved in cell cycle. The coloured boxes are genes in the pathway that are differentially expressed. Genes marked with green colour is for values below 0, it means for genes with a log2FC < 0 (downregulated in older metaphase II (MII) oocytes) and genes are red with a log2FC > 0 (upregulated in older MII oocytes). Grey colour indicate genes with no differences between the two age groups.

Table II

Gene ontology enrichment analysis	Gene ratio	P-values	Genes involved
A. Highly enriched GO terms			
Purine nucleoside triphosphate metabolic process	24/265	4.56E-11	NDUFS5/ATP5I/ATP5J2/NDUFA3/NDUFA12/NDUFB3/NDUFA1/ATP5H/NDUFS7/ATP5G2/NDUFB7/ATP5O/ATP5F1/ATP5G1/NDUFV3/NDUFA2/ATP5E/NUP160/NUDT15/MFN1/NADK/NUP35/TIGAR/CCNB1
Nucleoside triphosphate metabolic process	24/265	1.61E-10	NDUFS5/ATP5I/ATP5J2/NDUFA3/NDUFA12/NDUFB3/NDUFA1/ATP5H/NDUFS7/ATP5G2/NDUFB7/ATP5O/ATP5F1/ATP5G1/NDUFV3/NDUFA2/ATP5E/NUP160/NUDT15/MFN1/NADK/NUP35/TIGAR/CCNB1
Purine ribonucleoside triphosphate metabolic process	23/265	1.73E-10	NDUFS5/ATP5I/ATP5J2/NDUFA3/NDUFA12/NDUFB3/NDUFA1/ATP5H/NDUFS7/ATP5G2/NDUFB7/ATP5O/ATP5F1/ATP5G1/NDUFV3/NDUFA2/ATP5E/NUP160/MFN1/NADK/NUP35/TIGAR/CCNB1
Ribonucleoside triphosphate metabolic process	23/265	2.41E-10	NDUFS5/ATP5I/ATP5J2/NDUFA3/NDUFA12/NDUFB3/NDUFA1/ATP5H/NDUFS7/ATP5G2/NDUFB7/ATP5O/ATP5F1/ATP5G1/NDUFV3/NDUFA2/ATP5E/NUP160/MFN1/NADK/NUP35/TIGAR/CCNB1
ATP metabolic process	22/265	1.32E-10	NDUFS5/ATP5I/ATP5J2/NDUFA3/NDUFA12/NDUFB3/NDUFA1/ATP5H/NDUFS7/ATP5G2/NDUFB7/ATP5O/ATP5F1/ATP5G1/NDUFV3/NDUFA2/ATP5E/NUP160/NADK/NUP35/TIGAR/CCNB1
Purine ribonucleoside monophosphate metabolic process	22/265	2.41E-09	NDUFS5/ATP5I/ATP5J2/NDUFA3/NDUFA12/NDUFB3/NDUFA1/ATP5H/NDUFS7/ATP5G2/NDUFB7/ATP5O/ATP5F1/ATP5G1/NDUFV3/NDUFA2/ATP5E/NUP160/NADK/NUP35/TIGAR/CCNB1
Purine nucleoside monophosphate metabolic process	22/265	2.56E-09	NDUFS5/ATP5I/ATP5J2/NDUFA3/NDUFA12/NDUFB3/NDUFA1/ATP5H/NDUFS7/ATP5G2/NDUFB7/ATP5O/ATP5F1/ATP5G1/NDUFV3/NDUFA2/ATP5E/NUP160/NADK/NUP35/TIGAR/CCNB1
Ribonucleoside monophosphate metabolic process	22/265	4.86E-09	NDUFS5/ATP5I/ATP5J2/NDUFA3/NDUFA12/NDUFB3/NDUFA1/ATP5H/NDUFS7/ATP5G2/NDUFB7/ATP5O/ATP5F1/ATP5G1/NDUFV3/NDUFA2/ATP5E/NUP160/NADK/NUP35/TIGAR/CCNB1
Nucleoside monophosphate metabolic process	22/265	1.12E-08	NDUFS5/ATP5I/ATP5J2/NDUFA3/NDUFA12/NDUFB3/NDUFA1/ATP5H/NDUFS7/ATP5G2/NDUFB7/ATP5O/ATP5F1/ATP5G1/NDUFV3/NDUFA2/ATP5E/NUP160/NADK/NUP35/TIGAR/CCNB1
Generation of precursor metabolites and energy	20/265	2.36E-05	COX17/NDUFS5/NDUFA3/NDUFA12/NDUFB3/NDUFA1/NDUFS7/GYG1/PDHA1/NDUFB7/NDUFV3/NDUFA2/NUP160/FASTKD1/ETFA/PNPT1/NUP35/TIGAR/CCNB1/UGDH
B. Selected Pathways			
Microtubule cytoskeleton organization	18/265	0.000352536	DYNLT1/CHMP2A/SLC16A1/KATNA1/PKHD1/BORA/DNAH3/DNAAF2/CHEK1/GAS2L3/MZT1/DOCK7/CKAP5/CCNB1/KIF4A/UVRAG/TUBG2/CDC20
Chromosome segregation	16/265	8.68E-05	CHMP2A/NUP160/ZWINT/CENPH/SMC2/CDCA2/MAD2L1/CDC27/TERB1/CKAP5/NUF2/CCNB1/KIF4A/UVRAG/CDC20/UBE2C
Mitochondrial transport	15/265	7.83E-05	TIMM10/ATP5I/ATP5J2/ATP5H/ATP5G2/ATP5O/DYNLT1/PSMB7/PDCD5/ATP5F1/ATP5G1/ATP5E/AGK/PNPT1/ACTL6A
Nuclear chromosome segregation	14/265	0.000196436	CHMP2A/NUP160/ZWINT/CENPH/SMC2/MAD2L1/CDC27/TERB1/CKAP5/NUF2/CCNB1/KIF4A/CDC20/UBE2C
Sister chromatid segregation	13/265	5.45E-05	CHMP2A/NUP160/ZWINT/CENPH/SMC2/MAD2L1/CDC27/CKAP5/NUF2/CCNB1/KIF4A/CDC20/UBE2C
Electron transport chain	12/265	1.19E-05	NDUFS5/NDUFA3/NDUFA12/NDUFB3/NDUFA1/NDUFS7/NDUFB7/NDUFV3/NDUFA2/ETFA/CCNB1/UGDH
Oxidative phosphorylation	10/265	4.63E-06	NDUFS5/NDUFA3/NDUFA12/NDUFB3/NDUFA1/NDUFS7/NDUFB7/NDUFV3/NDUFA2/CCNB1

Table III

Pathway name	Gene ratio	P-values	Genes involved
A. Highly enriched pathways			
The citric acid (TCA) cycle and respiratory electron transport	20/178	5,98E+02	NDUFS5/ATP5I/ATP5J2/NDUFA3/NDUFA12/NDUFB3/NDUFA1/ATP5H/NDUFS7/PDHA1/ATP5G2/NDUFB7/ATP5O/ATP5F1/ATP5G1/NDUFV3/NDUFA2/ATP5E/SLC16A1/ETFA
Cell Cycle Checkpoints	19/178	5,12E+07	PSMB7/PSMD10/RPA1/NUP160/PSMD9/PSMD1/ZWINT/CCNA2/CENPH/RMI1/CHEK1/MAD2L1/CDC27/CKAP5/NUF2/CCNB1/CDC45/CDC20/UBE2C
Infectious disease	19/178	2,65E+09	ELOB/POLR2L/RPL34/RPL36AL/POLR2I/PSMB7/CHMP2A/RPL32/CD9/RPS26/PSMD10/AP2S1/NUP160/PSMD9/PSMD1/GTF2E1/SH3KBP1/TAF7/NUP35
Respiratory electron transport, ATP synthesis by chemiosmotic coupling, and heat production by uncoupling proteins.	18/178	2,07E+02	NDUFS5/ATP5I/ATP5J2/NDUFA3/NDUFA12/NDUFB3/NDUFA1/ATP5H/NDUFS7/ATP5G2/NDUFB7/ATP5O/ATP5F1/ATP5G1/NDUFV3/NDUFA2/ATP5E/ETFA
M Phase	18/178	0.000125358974078914	PSMB7/PSMD10/NUP160/PSMD9/PSMD1/ZWINT/CENPH/SMC2/MZT1/MAD2L1/CDC27/NUP35/CKAP5/NUF2/CCNB1/TUBG2/CDC20/UBE2C
Transcriptional Regulation by TP53	17/178	0.000160007951945829	ELOB/POLR2L/POLR2I/RRAGC/RPA1/CASP6/CCNA2/RMI1/RNF34/CHEK1/TAF7/TIGAR/CCNB1/TTC5/PCNA/BANP/SLC38A9
Metabolism of amino acids and derivatives	14/178	0.00362328449405566	ARG2/RPL34/RPL36AL/PDHA1/PSMB7/RPL32/RPS26/PSMD10/PSMD9/AIMP2/PSMD1/ACAT1/OAZ1/HIBADH
Separation of Sister Chromatids	13/178	2,10E+08	PSMB7/PSMD10/NUP160/PSMD9/PSMD1/ZWINT/CENPH/MAD2L1/CDC27/CKAP5/NUF2/CDC20/UBE2C
Mitotic Anaphase	13/178	3,79E+09	PSMB7/PSMD10/NUP160/PSMD9/PSMD1/ZWINT/CENPH/MAD2L1/CDC27/CKAP5/NUF2/CDC20/UBE2C
Mitotic Metaphase and Anaphase	13/178	3,99E+09	PSMB7/PSMD10/NUP160/PSMD9/PSMD1/ZWINT/CENPH/MAD2L1/CDC27/CKAP5/NUF2/CDC20/UBE2C
DNA Repair	13/178	0.00276583768347038	POLR2L/ALKBH5/POLR2I/MGMT/RPA1/MPG/CCNA2/RMI1/CHEK1/MBD4/OGG1/ACTL6A/PCNA
B. Selected Pathways			
Regulation of mitotic cell cycle	10/178	1,75E+08	PSMB7/PSMD10/PSMD9/PSMD1/CCNA2/MAD2L1/CDC27/CCNB1/CDC20/UBE2C
Mitotic Spindle Checkpoint	9/178	0.000114938166283639	NUP160/ZWINT/CENPH/MAD2L1/CDC27/CKAP5/NUF2/CDC20/UBE2C
DNA Replication	8/178	0.000481184469737087	PSMB7/PSMD10/RPA1/PSMD9/PSMD1/CCNA2/CDC45/PCNA
Mitochondrial biogenesis	8/178	0.000200154305434043	ATP5I/ATP5J2/ATP5H/ATP5G2/ATP5O/ATP5F1/ATP5G1/ATP5E
Resolution of Sister Chromatid Cohesion	8/178	0.00139655909039166	NUP160/ZWINT/CENPH/MAD2L1/CKAP5/NUF2/CCNB1/CDC20

Paper III

Supplementary tables can be retrieved via this link:

https://figshare.com/s/b8ff0c7f173c4ffa864e

PHD-THESIS
DECLARATION OF CO-AUTHORSHIP

The declaration is for PhD students and must be completed for each conjointly authored article. Please note that if a manuscript or published paper has ten or less co-authors, all co-authors must sign the declaration of co-authorship. If it has more than ten co-authors, declarations of co-authorship from the corresponding author(s), the senior author and the principal supervisor (if relevant) are a minimum requirement.

1. Declaration by	
Name of PhD student	Kristina Wendelboe Olsen
E-mail	kristina.wendelboe.olsen.01@regionh.dk, kwo@sund.ku.dk, kristinawo@hotmail.com
Name of principal supervisor	Sven Olaf Skouby
Title of the PhD thesis	Epigenetic and gene expression profiling of the human ovarian follicles with the significance of age and ovarian reserve

2. The declaration applies to the following article	
Title of article	A distinctive epigenetic ageing profile in human granulosa cells
Article status	
Published ☐ Date:	Accepted for publication ☑ Date: 17.03.2020
Manuscript submitted ☐ Date:	Manuscript not submitted ☐
If the article is published or accepted for publication, please state the name of journal, year, volume, page and DOI (if you have the information).	Accepted for publication with minor revision in Human Reproduction, 10.02.2020

3. The PhD student's contribution to the article ***(please use the scale A-F as benchmark)*** Benchmark scale of the PhD-student's contribution to the article **A**. Has essentially done all the work (> 90 %) **B**. Has done most of the work (60-90 %) **C**. Has contributed considerably (30-60 %) **D.** Has contributed (10-30 %) **E.** No or little contribution (<10 %) **F.** Not relevant	**A, B, C, D, E, F**
1. Formulation/identification of the scientific problem	C
2. Development of the key methods	F
3. Planning of the experiments and methodology design and development	B
4. Conducting the experimental work/clinical studies/data collection/obtaining access to data	B
5. Conducting the analysis of data	C
6. Interpretation of the results	B
7. Writing of the first draft of the manuscript	A
8. Finalisation of the manuscript and submission	B

Provide a short description of the PhD student´s specific contribution to the article.[i]
The PhD student has contributed to the design of the study, written the protocol and applied to the relevant authorities for approval to conduct study. Moreover, has she initiated and coordinated the recruitment of participants on the four different clinics and collected a large number of the biological samples. The PhD student has also contributed to the analysis and interpretation of the data and writing the first draft of the manuscript. Furthermore, has she contributed and coordinated the finalization of the manuscript.

4. Material from another thesis / dissertation[ii]	
Does the article contain work which has also formed part of another thesis, e.g. master's thesis, PhD thesis or doctoral dissertation (the PhD student's or another person's)?	Yes: ☐ No: ☒
If yes, please state name of the author and title of thesis / dissertation.	
If the article is part of another author's academic degree, please describe the PhD student's and the author's contributions to the article so that the individual contributions are clearly distinguishable from one another.	

5. Signatures of the co-authors[iii]

	Date	Name	Title	Signature
1.	25/5 20	Marie Louise Grøndahl	DMSc	
2.		Sven Olaf Skouby	Professor	
3.		Juan Castillo-Fernandez	PhD	
4.				
5.				
6.				
7.				
8.				
9.				
10.				

6. Signature of the principal supervisor

I solemnly declare that the information provided in this declaration is accurate to the best of my knowledge.
Date: 22/05/2020
Principal supervisor: Sven O. Skouby

7. Signature of the PhD student

I solemnly declare that the information provided in this declaration is accurate to the best of my knowledge.
Date: 22/5 2020
PhD student: Kristina Wendelboe Olsen

GRADUATE SCHOOL OF HEALTH AND MEDICAL SCIENCES
UNIVERSITY OF COPENHAGEN

PHD-THESIS
DECLARATION OF CO-AUTHORSHIP

The declaration is for PhD students and must be completed for each conjointly authored article. Please note that if a manuscript or published paper has ten or less co-authors, all co-authors must sign the declaration of co-authorship. If it has more than ten co-authors, declarations of co-authorship from the corresponding author(s), the senior author and the principal supervisor (if relevant) are a minimum requirement.

1. Declaration by	
Name of PhD student	Kristina Wendelboe Olsen
E-mail	kristina.wendelboe.olsen.01@regionh.dk, kwo@sund.ku.dk, kristinawo@hotmail.com
Name of principal supervisor	Sven Olaf Skouby
Title of the PhD thesis	Epigenetic and gene expression profiling of the human ovarian follicles with the significance of age and ovarian reserve

2. The declaration applies to the following article	
Title of article	Identification of a unique epigenetic profile in women with diminished ovarian reserve.
Article status	
Published ☐ Date:	Accepted for publication ☐ Date:
Manuscript submitted ☑ Date: 20.05.2020	Manuscript not submitted ☐
If the article is published or accepted for publication, please state the name of journal, year, volume, page and DOI (if you have the information).	Manuscript submitted to Fertility and Sterility

3. The PhD student's contribution to the article ***(please use the scale A-F as benchmark)*** Benchmark scale of the PhD-student's contribution to the article **A**. Has essentially done all the work (> 90 %) **B**. Has done most of the work (60-90 %) **C**. Has contributed considerably (30-60 %) **D.** Has contributed (10-30 %) **E.** No or little contribution (<10 %) **F.** Not relevant	**A, B, C, D, E, F**
1. Formulation/identification of the scientific problem	C
2. Development of the key methods	F
3. Planning of the experiments and methodology design and development	B
4. Conducting the experimental work/clinical studies/data collection/obtaining access to data	B
5. Conducting the analysis of data	C
6. Interpretation of the results	B
7. Writing of the first draft of the manuscript	A
8. Finalisation of the manuscript and submission	B

Provide a short description of the PhD student´s specific contribution to the article.[i]
The PhD student has contributed to the design of the study, written the protocol and applied to the relevant authorities for approval to conduct study. Moreover, has she initiated and coordinated the recruitment of participants on the four different clinics and collected a large number of the biological samples. The PhD student has also contributed to the analysis and interpretation of the data and writing the first draft of the manuscript. Furthermore, has she contributed and coordinated the finalization of the manuscript.

4. Material from another thesis / dissertation[ii]	
Does the article contain work which has also formed part of another thesis, e.g. master's thesis, PhD thesis or doctoral dissertation (the PhD student's or another person's)?	Yes: ☐ No: ☒
If yes, please state name of the author and title of thesis / dissertation.	
If the article is part of another author's academic degree, please describe the PhD student's and the author's contributions to the article so that the individual contributions are clearly distinguishable from one another.	

5. Signatures of the co-authors[iii]

	Date	Name	Title	Signature
1.	25/5 20	Marie Louise Grøndahl	DMSc	
2.		Sven Olaf Skouby	Professor	
3.		Juan Castillo-Fernandez	PhD	
4.				
5.				
6.				
7.				
8.				
9.				
10.				

6. Signature of the principal supervisor

I solemnly declare that the information provided in this declaration is accurate to the best of my knowledge.
Date: 22/05/2020
Principal supervisor: Sven O. Skouby

7. Signature of the PhD student

I solemnly declare that the information provided in this declaration is accurate to the best of my knowledge.
Date: 22/5 2020
PhD student: Kristina Wendelboe Olsen

GRADUATE SCHOOL OF HEALTH AND MEDICAL SCIENCES
UNIVERSITY OF COPENHAGEN

PHD-THESIS
DECLARATION OF CO-AUTHORSHIP

The declaration is for PhD students and must be completed for each conjointly authored article. Please note that if a manuscript or published paper has ten or less co-authors, all co-authors must sign the declaration of co-authorship. If it has more than ten co-authors, declarations of co-authorship from the corresponding author(s), the senior author and the principal supervisor (if relevant) are a minimum requirement.

1. Declaration by	
Name of PhD student	Kristina Wendelboe Olsen
E-mail	kristina.wendelboe.olsen.01@regionh.dk, kwo@sund.ku.dk, kristinawo@hotmail.com
Name of principal supervisor	Sven O. Skouby
Title of the PhD thesis	Epigenetic and gene expression profiling of the human ovarian follicles with the significance of age and ovarian reserve

2. The declaration applies to the following article	
Title of article	Gene expression profile of human metaphase II oocytes in relation to age by single cell RNA sequencing
Article status	
Published ☐ Date:	Accepted for publication ☐ Date:
Manuscript submitted ☐ Date:	Manuscript not submitted ☒
If the article is published or accepted for publication, please state the name of journal, year, volume, page and DOI (if you have the information).	

3. The PhD student's contribution to the article ***(please use the scale A-F as benchmark)*** Benchmark scale of the PhD-student's contribution to the article **A.** Has essentially done all the work (> 90 %) **B.** Has done most of the work (60-90 %) **C.** Has contributed considerably (30-60 %) **D.** Has contributed (10-30 %) **E.** No or little contribution (<10 %) **F.** Not relevant	**A, B, C, D, E, F**
1. Formulation/identification of the scientific problem	C
2. Development of the key methods	F
3. Planning of the experiments and methodology design and development	C
4. Conducting the experimental work/clinical studies/data collection/obtaining access to data	B
5. Conducting the analysis of data	C
6. Interpretation of the results	B
7. Writing of the first draft of the manuscript	A
8. Finalisation of the manuscript and submission	B
Provide a short description of the PhD student´s specific contribution to the article.[i] The PhD student has contributed to the design and initiation of the study, written the protocol and and applied to the relevant authorities for approval to conduct study. Moreover, has she initiated and coordinated the recruitment of participants and collected the oocytes used in this study. The PhD student has also contributed to the analysis and interpretation of the data and writing the first draft of the manuscript. Furthermore, has she contributed and coordinated the finalization of the manuscript.	

4. Material from another thesis / dissertation[ii]	
Does the article contain work which has also formed part of another thesis, e.g. master's thesis, PhD thesis or doctoral dissertation (the PhD student's or another person's)?	Yes: ☐ No: ☒
If yes, please state name of the author and title of thesis / dissertation.	
If the article is part of another author's academic degree, please describe the PhD student´s and the author´s contributions to the article so that the individual contributions are clearly distinguishable from one another.	

5. Signatures of the co-authors[iii]

	Date	Name	Title	Signature
1.	27/05/20	Vallari Shukla	PhD	
2.	27/5/20	Ajuna Azad	MSc	
3.	26/05/20	Sven O. Skouby	Professor	
4.	25/5 20	Marie Louise Grøndahl	DMSc	
5.	207052 020	Eva R. Hoffmann	Professor	
6.	26/5-20	Rehanna Borup	PhD	
7.				
8.				
9.				
10.				

6. Signature of the principal supervisor

I solemnly declare that the information provided in this declaration is accurate to the best of my knowledge.
Date: 26/05/2020
Principal supervisor: Sven O. Skouby

7. Signature of the PhD student

I solemnly declare that the information provided in this declaration is accurate to the best of my knowledge.
Date: 27/05 - 2020
PhD student: Kristina Wendelboe Olsen

Please learn more about responsible conduct of research on the Faculty of Health and Medical Sciences' website.

---

[i] This can be supplemented with an additional letter if needed.

[ii] Please see Ministerial Order on the PhD Programme at the Universities and Certain Higher Artistic Educational Institutions (PhD Order) § 12 (4):

"Any articles included in the thesis may be written in cooperation with others, provided that each of the co-authors submits a written declaration stating the PhD student's or the author's contribution to the work."

[iii] If more signatures are needed please add an extra sheet.